



**Biogasoline from Catalytic Cracking of Wood-Derived Oil Over
Nano Catalyst**

Abdulrahim Saad

**A Thesis Submitted in Fulfillment of the Requirements for the
Degree of Doctor of Philosophy in Chemical Engineering
Prince of Songkla University**

2015

Copyright of Prince of Songkla University



**Biogasoline from Catalytic Cracking of Wood-Derived Oil Over
Nano Catalyst**

Abdulrahim Saad

**A Thesis Submitted in Fulfillment of the Requirements for the
Degree of Doctor of Philosophy in Chemical Engineering**

Prince of Songkla University

2015

Copyright of Prince of Songkla University

Thesis Title Biogasoline from Catalytic Cracking of Wood-Derived Oil Over
 Nano Catalyst
 Author Mr. Abdulrahim Saad
 Major Program Chemical Engineering

Major Advisor

.....
 (Assoc. Prof. Dr. Sukritthira Ratanawilai)

Co-advisor

.....
 (Assoc. Prof. Dr. Chakrit Tongurai)

Examining Committee :

.....Chairperson
 (Assoc. Prof. Dr. Penjit Srinophakun)

.....Committee
 (Assoc. Prof. Dr. Sukritthira Ratanawilai)

.....Committee
 (Assoc. Prof. Dr. Chakrit Tongurai)

.....Committee
 (Assoc. Prof. Dr. Sutham Sukmanee)

.....Committee
 (Assoc. Prof. Dr. Pakamas Chetpattananondh)

The Graduate School, Prince of Songkla University, has approved this thesis as fulfillment of the requirements for the Doctor of Engineering Degree in Chemical Engineering.

.....
 (Assoc. Prof. Dr. Teerapol Srichana)
 Dean of Graduate School

This is to certify that the work here submitted is the result of the candidate's own investigations. Due acknowledgement has been made of any assistance received.

.....Signature
(Assoc. Prof. Dr. Sukritthira Ratanawilai)
Major Advisor

.....Signature
(Chakrit Tongurai)
Co-advisor (If any)

.....Signature
(Mr. Abdulrahim Saad)
Candidate

I hereby certify that this work has not been accepted in substance for any degree, and is not being currently submitted in candidature for any degree.

.....Signature

(Mr. Abdulrahim Saad)

Candidate

Thesis Title	Biogasoline from Catalytic Cracking of Wood- Derived Oil Over Nano Catalyst
Author	Mr. Abdulrahim Saad
Major Program	Chemical Engineering
Academic Year	2015

ABSTRACT

The aim of this thesis was to study the viability of upgrading wood derived oils to generate biogasoline and to gain a fundamental understanding of the operating conditions of the process by using a commercial zeolite catalyst compared with a prepared nanocrystalline zeolite catalyst. Zeolite catalysts have been exploited for producing renewable fuels suitable for gasoline applications.

In this study, experimental studies were carried out on the conversion of rubberwood derived liquids obtained as a by-product during the pyrolysis of wood in charcoal manufacturing to produce organic liquid products (OLP) where the interested fraction was the gasoline portion, particularly gasoline-range aromatics (benzene, toluene, ethylbenzene, and xylenes; BTEX), which have potential fuel applications due to their high octane rating appropriate for blending gasoline. The experiments were conducted in a dual reactor using an ordinary commercial HZSM-5 catalyst and a nanocrystalline HZSM-5 catalyst.

The crude pyrolysis liquids derived from rubberwood included aqueous phase and settled tar. The settled tar was separated by decantation as a first fraction and labelled as pyrolysis tar (PT). The aqueous phase was treated to remove water by evaporation and the concentrated liquid was then named pyrolysis oil (PO) as a second fraction. The pyrolysis oil (PO) itself was fractionated into two fractions by a conventional vacuum distillation. The two fractions were labelled as

the light fraction (LF) and the heavy fraction (HF). The four fractions were physiochemically characterized showing that the light fraction had a very high water content (60 wt%) and acetic acid; therefore it was ignored from the upgrading experiments.

Upgrading experiments of the three fractions were conducted at atmospheric pressure in the dual reactor system, operated in the temperature range of 400 to 600 °C with a catalyst weight of 1 to 5 g and a nitrogen flow rate of 3 to 10 mL/min. 15 g for each fraction were introduced into the first reactor at the rate of 1.4 g/min. The products from the second reactor were cooled (collected in an ice-cooled flask) and separated into liquid and gaseous products. The liquid product was obtained in the form of immiscible layers, i.e., an organic layer and an aqueous layer.

Upgrading studies were first carried out with the pyrolysis oil using the commercial HZSM-5 catalyst. The results showed that the maximum yield of organic liquid product (OLP) was 13.6 wt%, which was achieved at 511 °C, a catalyst weight of 3.2 g, and an N₂ flow rate of 3 mL/min. The maximum percentage of gasoline aromatics (BTEX) was about 27 wt% obtained at 595 °C, a catalyst weight of 5 g, and an N₂ flow rate of 3 mL/min .

The catalytic upgrading was also conducted with the pyrolysis tar (PT) fraction using the commercial HZSM-5 catalyst. The maximum yield of OLP was about 28.33 wt%, achieved at 536 °C and a catalyst weight of 3.5 g. the OLP exhibited a higher percentage of BTEX aromatics with a maximum value of about 54 wt%, obtained at 575 °C with a catalyst weight of 5 g.

The heavy fraction was very viscous; therefore 5% of ethanol was added to the sample prior to feed in the reactor. The heavy fraction (HF) with a 5% of ethanol was also upgraded with the

commercial catalyst. The OLP from the HF obtained a very low yield compared to the previous fractions. The maximum yield obtained at 400 °C and a catalyst weight of 5 g was about 11 wt%. Correspondingly, the maximum percentage of BTEX aromatics was about 38 wt%, obtained at 600 °C and a catalyst weight of 5 g.

Regarding the gasoline aromatics; from the GCMS analysis it was interestingly found that other aromatic compound beside the BTEX were produced having high octane ratings such as naphthalene, methyl-naphthalene, indan, etc.

The catalytic upgrading of the three fractions was carried out using nanocrystalline HZSM-5 zeolite prepared following the hydrothermal method. The experiments were conducted in the dual reactor with the same optimal conditions (For the maximum yields of OLP and the maximum percentages of BTEX aromatics in OLPs) of the commercial catalysts experiments for each fraction, i.e., temperature, catalyst weight and N₂ flowrate.

The effect of the optimal operating parameters on the OLP yields and percentages of aromatics were studied over the pyrolysis oil, heavy fraction and pyrolysis tar. It was found that the OLPs obtained from the three fractions exhibited higher yields with the nano catalyst, whereas the ordinary catalyst exhibited little lower yields. Correspondingly, higher aromatic percentages of about 33 wt%, 51 wt% and 51.26 wt% were displayed from the nano catalyst for the pyrolysis oil, heavy fraction and tar respectively, whereas the commercial catalyst displayed little lower aromatics percentages i.e., 30 wt%, 49 wt% and 48 wt% for the pyrolysis oil, heavy fraction and tar respectively. In addition, the CHNO analysis of the OLPs obtained by using the nano catalyst showed a high decrease of oxygen about 2 wt%, 4 wt% and 3.5 wt% for the upgraded pyrolysis oil, heavy fraction and tar respectively, whereas

the commercial catalyst exhibited about 15 wt%, 16 wt% and 5 wt% for the pyrolysis oil, heavy fraction and tar respectively.

ACKNOWLEDGEMENT

I greatly acknowledge the financial assistance from Prince of Songkla University in the form of graduate scholarship and also the financial support for performing the experimental work in this study.

I wish to express my appreciation and gratitude to Dr. Sukritthira Ratanawilai for being my primary and proficient feedback; also for her encouragement, guidance and supervision throughout my study. Her door was always opened and she had always taken the time to discuss all issues, ranging from study to personal. She created a good working atmosphere and gave me the freedom to perform my laboratory experiments, and for this I am very much grateful to her.

Big thanks also go to my Co-adviser, Dr. Chakrit Tongurai for providing the guidance and suggestions which helped my work to be much more thorough.

I would also like to thank Dr. Juntima Chungsiriporn for her assistance and cooperation by supplying the raw material that I used in my study, and by giving the opportunity to visit Phatthalung province where the raw material is widely produced.

I express my appreciation to all the staffs of chemical engineering department for maintaining friendly and cordial atmosphere, with special mention of Dr. Pakamas Chetpattananondh, Dr. Kulchanat Prasertsit, Dr. Suratsawadee Kungsanant and Dr. Nattawan Kladkaew for their useful discussions and suggestions throughout my regular progress reports.

I would like to highlight a particular appreciation on Mrs. Janya Intamane and her energetic technical staff; Mr. Somkid Geenapong, Ms. Pornpimon Sansook, Mr. Tanakorn Kiatkwanboot, Mr. Sorn Jiaraboot and Ms. Jutarat Kantakapan for their assistance in performing experiments and analysis, with special appreciation to Mr. Somkid who used to fix and follow up running of my lab during the struggles with some experimental facilities. Also I have to thank Mrs. Rattaya Musikkasem and Ms. Amonrat Wihakarat for their patience and for their assistance in processing the official documents.

I deem it a privilege to acknowledge and express regards to the chairperson and members of examining committee. Assoc. Prof. Dr. Penjit

Srinophakun, department of chemical engineering, Kasetsart University. Assoc. Prof. Dr. Sukritthira Ratanawilai, Assoc. Prof. Dr. Chakrit Tongurai, Assoc. Prof. Dr. Sutham Sukmanee and Assoc. Prof. Dr. Pakamas Chetpattananondh from the department of chemical engineering, Prince of Songkla University.

The scientists of the scientific equipment centre also deserve special gratitude for their assistance in performing some of the tests reported in this study.

Finally, heartfelt thanks must be directed toward my family, who has been a continuous source of encouragement and support. I would like to deeply thank my mother, brothers and sisters for their unconditional concern. Similarly, the family of my institution; industrial research & consultancy centre deserves special recognition and appreciation for their concerns.

Abdulrahim Saad

Contents

	Page
1. Introduction	1
1.1 Rational/ Problem statement.....	1
1.2 Overview of the research work.....	4
2. Theoretical background and literature review	7
2.1 Upgrading routes for converting pyrolysis oils to fuels.....	7
2.1.1 Catalytic upgrading by hydrodeoxygenation process.....	8
2.1.2 Catalytic upgrading by zeolite cracking process.....	14
2.1.2.1 Advantages of using zeolite catalysts.....	14
2.1.2.2 Process conditions.....	14
2.1.2.3 HZSM-5 catalyst.....	15
2.1.2.3.1 Shape selectivity and acidity.....	16
2.1.2.3.2 Synthesis and characterization of HZSM-5 catalyst.....	19
2.1.2.3.2.1 Synthesis of HZSM-5.....	19
2.1.2.3.2.2 Nano-crystalline zeolite.....	20
2.1.2.3.2.3 Characterization of HZSM-5.....	21
2.1.2.4 Catalyst deactivation.....	22
2.1.2.5 Reaction pathways on pyrolysis oil upgrading.....	23
2.2 Prospect of catalytic upgrading of pyrolysis oils to gasoline.....	28
2.2.1 Catalytic fast pyrolysis (CFP).....	28
2.2.2 Hydrodeoxygenation (HDO).....	29
2.2.3 Integrated hydropyrolysis and hydroconversion process (IH ²).....	31
3. Objectives	34
4. Results and discussion	35
4.1 Fractionation and characterisation of the pyrolysis liquids derived from rubberwood.....	35
4.2 Catalytic cracking of pyrolysis oil derived from rubberwood to produce gasoline-range aromatics.....	37
4.2.1 Characterization of the commercial zeolite catalyst.....	38
4.2.1.1 X-ray diffraction (XRD) analysis.....	38
4.2.1.2 Scanning Electron Microscopy (SEM).....	39

Contents (continued)

4.2.1.3 Fourier-Transform Infrared (FTIR).....	39
4.2.2 Chemical composition of the OLP identified by GC–MS.....	40
4.2.3 Thermal cracking of the pyrolysis oil.....	41
4.3 Catalytic conversion of pyrolysis tar to produce green gasoline-range aromatics.....	44
4.3.1 Chemical composition of the organic liquid products identified by GC–MS.....	44
4.3.2 Thermal cracking of the pyrolysis tar.....	45
4.4 Comparative Study for Catalytic Conversion of Pyrolysis Oil and Tar Derived from Rubberwood to Produce Green Gasoline-Range Aromatics...	48
4.5 Catalytic conversion of heavy fraction of the pyrolysis oil to generate gasoline-range aromatics.....	48
4.5.1 Product distribution.....	49
4.5.2 Content of gasoline-range aromatics.....	50
4.5.3 Optimization.....	51
4.6 Catalytic conversion of the three fractions over prepared nanocrystalline HZSM-5 zeolite and compared with the commercial catalyst.....	54
4.6.1 X-ray diffraction (XRD) analysis.....	55
4.6.2 Scanning Electron Microscopy (SEM).....	57
4.6.3 Fourier-Transform Infrared (FTIR).....	58
4.6.4 OLP yields and the percentages of aromatics.....	58
4.6.5 Chemical composition of the organic liquid products identified by GC–MS.....	60
4.6.6 The elemental compositions (CHN-O) of the organic liquid products....	67
5. Concluding remarks	69
6. References	72
7. Appendices	81
Appendix A: Characterisation of liquid derived from pyrolysis process of charcoal production in south of Thailand.....	81

Contents (continued)

Appendix B: Catalytic cracking of pyrolysis oil derived from rubberwood to produce green gasoline components.....	90
Appendix C: Catalytic conversion of pyrolysis tar to produce green gasoline-range aromatics.....	109
Appendix D: Comparative study for catalytic conversion of pyrolysis oil and tar derived from rubberwood to produce green gasoline-range aromatics.....	119
Appendix E: Research octane number (RON) and Motor octane number (MON) of pure compounds.....	148
Appendix F: determination of chloride in the heavy fraction.....	149
Appendix G: Sherrer's equation used for estimating the crystal size.....	150
Appendix H: Fourier-Transform Infrared (FTIR).....	152
Appendix I: GC-FID analysis.....	154
Appendix J: GC-MS Analyses.....	156
Appendix K: CHN-O Analyses.....	161
8. Vitae.....	162

List of Tables

Tables	Page
1. Comparison between pyrolysis oil and crude oil.....	4
2. Catalyzed HDO using metal sulphides.....	13
3. Physical Characteristics of the Pyrolysis oil, light fraction and heavy fraction	35
4. Chemical composition at the optimum condition of the highest percentage of gasoline fraction (pyrolysis oil).....	41
5. Chemical composition at the optimum condition of the highest OLP yield ((pyrolysis oil).....	43
6. Comparison between thermal and catalytic cracking of the pyrolysis oil using three different conditions.....	44
7. Chemical composition at the optimum condition of the highest percentage of gasoline fraction (pyrolysis tar).....	46
8. Chemical composition at the optimum condition of the highest OLP yield (pyrolysis tar).....	47
9. Comparison between thermal and catalytic cracking of the pyrolysis tar using three different conditions.....	48
10. Overall Product Distribution (wt% of the feed) for the 15 experimental runs...	50
11. Composition of Gasoline Aromatics in the OLP.....	51
12. Predicted and Experimental Results at Optimum Conditions.....	54
13. Gasoline Aromatics Content in OLP at Optimum Conditions.....	54
14. Compositions of BTEX aromatics in the OLP for the three fractions using prepared nanocrystalline and commercial catalysts.....	59
15. Experimental results at optimum conditions for the three fractions using prepared nanocrystalline and commercial catalyst.....	59
16. OLP composition of the pyrolysis oil at the optimum condition of the highest percentage of gasoline fraction.....	61
17. OLP composition of the heavy fraction at the optimum condition of the highest percentage of gasoline fraction.....	62
18. OLP composition of the pyrolysis tar at the optimum condition of the highest percentage of gasoline fraction.....	63

List of Tables (continued)

19. OLP composition of the pyrolysis oil at the optimum condition of the highest OLP yield.....	64
20. OLP composition of the heavy fraction at the optimum condition of the highest OLP yield.....	65
21. OLP composition of the pyrolysis tar at the optimum condition of the highest OLP yield.....	66

List of Figures

Figure	Page
1. Biomass resources converted to bioenergy carriers.....	1
2. Principle of a Fast Pyrolysis Process.....	3
3. Overview of the research work.....	4
4. Flow diagram for conversion of biomass to bio-fuels.....	7
5. Reactions accompanying catalytic upgrading of pyrolysis oil upgrading.....	9
6. Mechanism of HDO over transition metal catalysts.....	10
7. Suggested mechanism of HDO of 2-ethylphenol over a Co-MoS ₂ catalyst.....	12
8. Secondary building units (SBU's) of zeolite structure and their symbols.....	16
9. Skeletal diagram of the (100) face of HZSM-5. (b) HZSM-5 Channel structure.....	16
10. Schematic representation of shape selectivity in zeolite channels.....	18
11. Bronsted and lewis acid sites on zeolite.....	19
12. XRD pattern of a pure crystalline HZSM-5.....	22
13. Proposed reaction pathways for the conversion of pyrolysis oil over HZSM-5 zeolite.....	24
14. Proposed reaction pathway for the conversion of acids and esters.....	25
15. Proposed reaction pathway for the conversion of alcohols.....	26
16. Proposed reaction pathway for the conversion of aldehydes and ketones.....	27
17. Proposed reaction pathway for the conversion of phenols.....	27
18. Experimental setup of the fluidized bed reactor system.....	30
19. HDO process illustrating the overall production route from biomass to fuels, i.e., gasoline, kerosene, diesel and fuel oil.....	32
20. Overall process flow of the IH ² system.....	33
21. Conventional vacuum distillation assembly.....	37
22. Distributions and classification of the components.....	37
23. Dual reactor setup.....	38
24. . XRD pattern of HZSM-5 catalyst.....	39
25. SEM image for HZSM-5 catalyst.....	39

List of Figures (continued)

26. FFT-IR spectra of pyridine adsorbed in a commercial HZSM-5 after pyridine adsorption and evacuation at 150 °C.....	40
27. Experimental results versus predicted values of (a) OLP yield and (b) gasoline aromatics (%) in OLP.....	52
28. Surface plot of: (A) OLP yield and (B) gasoline aromatics (%) in OLP as functions of catalyst weight and reactor temperature.....	53
29. Preparation of nanocrystalline H-ZSM-5 using hydrothermal method.....	56
30. XRD pattern of nanocrystalline HZSM-5.....	57
31. SEM image for nanocrystalline HZSM-5.....	57
32. FFT-IR spectra of pyridine adsorbed in a nanocrystalline HZSM-5 after pyridine adsorption and evacuation at 150 °C.....	58
33. Elemental composition of the three fractions upgraded with nano-catalyst and ordinary catalyst compared the same fractions before upgrading.....	68
34. Oxygen content of the three fractions upgraded with nano-catalyst and ordinary catalyst compared the same fractions before upgrading.....	69

List of Publication and Proceeding (If Possible)

Abdulrahim Saad, Sukritthira Ratanawilai. "Characterisation of liquid derived from pyrolysis process of charcoal production in south of Thailand." *Iranica Journal of Energy and Environment*, 2014, 5(2):184-191.

Abdulrahim Saad, Sukritthira Ratanawilai, and Chakrit Tongurai. "Catalytic Cracking of Pyrolysis Oil Derived from Rubberwood to Produce Green Gasoline Components." *BioResources*, 2015, 10 (2): 3224-3241.

Abdulrahim Saad, Sukritthira Ratanawilai, and Chakrit Tongurai. "Catalytic Conversion of Pyrolysis Tar to Produce Green Gasoline-range Aromatics." *Energy Procedia*, 2015, 79: 471–479 .International Conference on Alternative Energy in Developing Countries and Emerging Economies-May 2015.

Abdulrahim Saad, Sukritthira Ratanawilai, and Chakrit Tongurai. "Comparative Study for Catalytic Conversion of Pyrolysis Oil and Tar Derived from Rubberwood to Produce Green Gasoline-Range Aromatics." This manuscript has been submitted to the journal of "Biomass and Bioenergy ", Elsevier.

1. Introduction

1.1 Rational/ Problem statement

Energy from fossil fuel sources constitutes an important part in transportation and industrialization. However, the consumption of energy is increasing, mainly in the transportation sector, because of population growth [1, 2]. It is believed that the intensive demand of fossil fuels has created global problems, which have led scientists to look for new alternative sources; as at present, fuels mainly derived from crude oil while crude oil is depleting [3-5]. Substantial research is pursued in order to explore renewable fuels to substitute diesel and gasoline. The appropriate ones must be similar, to a great extent, to the conventional fuels, with low emissions of greenhouse gases (GHG) such as CO₂, N₂O and CH₄, which arise from conventional fuel combustion. Biomass resources as readily available and renewable sources of energy will play an increasingly vital role in the future [6, 7]. Figure 1 exhibits the potential of biomass to be transformed to energy and other bioproducts [8].

Fuels derived from biomass considered as approaching fuels of future and are considered environmentally friendly [6, 9]. First generation biofuels refer to bioethanol and biodiesel made from sugar, starch, and vegetable oil. To date, such biofuels have been widely produced across several countries and continents, notably Brazil, South America, Europe, and the United States [10, 11]; however, they have been produced from raw materials in competition with food and feed industries, giving rise to ethical and political concerns. Therefore, it is very important to be able to produce biofuels from other biomass sources that do not influence food supply, such as wood. Considering the paths of second generation biofuels, much research has currently been focused on converting biomass to liquid route via syngas to produce higher alcohols or methanol to produce hydrocarbons [12-15]. It has been reported that, zeolite cracking and hydrodeoxygenation (HDO) are preferred among the other biomass processing routes, and the competitiveness of these routes is achieved due to a reasonable feasibility when pyrolysis oil is used as platform chemical, indicating that zeolite cracking and HDO constitute economical routes for the generation of second generation bio-fuels in the future [16-19].

Since zeolite cracking and HDO depend on the pyrolysis oil as platform chemical; it would be an interesting aspect to discuss the production, application and physiochemical properties of pyrolysis oil. Pyrolysis oil is defined as the liquid condensate of the vapors from the process of biomass pyrolysis. The synonyms of

pyrolysis oil involves pyrolysis liquids, bio-crude oil, pyrolysis oils, liquid smoke, wood distillates wood liquids and pyroligneous acid [20]. Amongst our study, the terms pyrolysis liquids, pyrolysis oil and pyroligneous liquid will be used.

Pyrolysis oils are produced from different agricultural and forest waste materials such as rice hulls, wheat straw, rice straw, peanut hulls, switchgrass and wood being the most abundant raw material for pyrolysis oil production [20]. In Thailand, particularly the peninsular area in the south, rubber tree is planted extensively, being a very important source for wood as potential feedstocks for pyrolysis oil production.

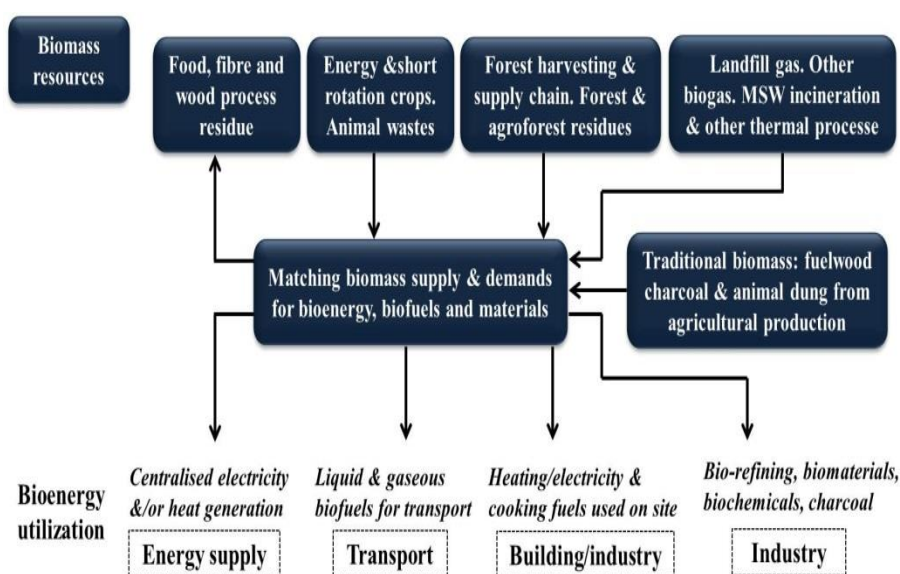


Figure 1. Biomass resources converted to bioenergy carriers [8]

Pyrolysis process is defined as the thermal degradation of biomass without oxygen at temperatures ranging from 300 °C to 600 °C. As a consequence, charcoal (solid), pyrolysis oil (liquid), and gas will be produced. The main pyrolysis reaction is:



The conventional pyrolysis, called slow pyrolysis, is associated mainly with high production of charcoal, in which the biomass (usually wood) is heated under a slow heating rate in temperatures between 300 °C and 400 °C. In contrast, fast pyrolysis is associated with high yield of oil at high heating rates to temperatures around 500 °C, with very short residence times, followed by rapid cooling of the vapors (Figure 2) [21].

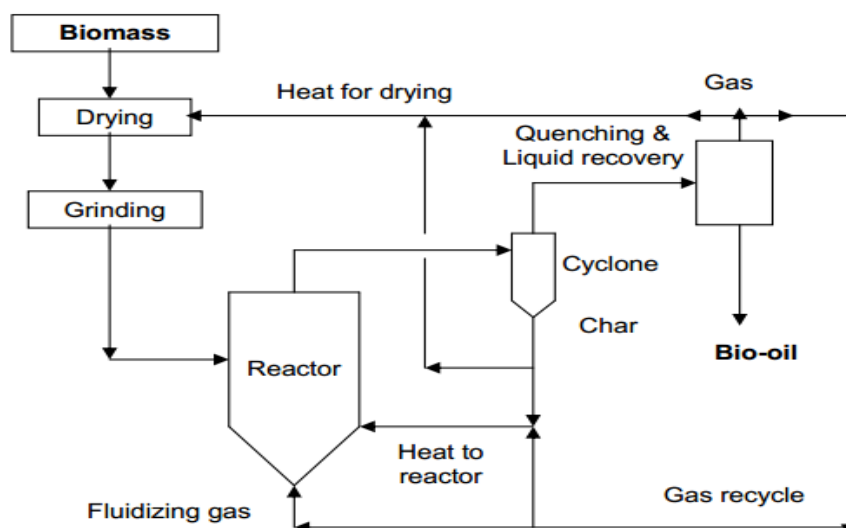


Figure 2. Principle of a Fast Pyrolysis Process [21]

At present, the technology of fast pyrolysis is preferred and widely applied to produce pyrolysis oils. It is considered as the most feasible route [12, 22, 23]. The pyrolysis oil is known to be viscous with a dark brownish color. It is a multicomponent mixture comprised of more than 300 oxygenated constituents such as alcohols, acids, steroids, aldehydes, phenolics, esters, ketones and derived basically from fragmentation and depolymerisation reactions of the biomass building blocks. The composition of pyrolysis oil depends on the biomass feed and process condition as well [20, 24]. The physical properties of the pyrolysis oil result from its chemical composition, which is significantly different from that of crude oil as shown in Table 1.

The direct use of pyrolysis oils as high grade fuels might be limited due to some inferior characteristics such as thermal instability, high oxygen content, poor heating value and high viscosity. As a consequence, before the pyrolysis oil can be used it would be necessary to upgrade it to improve its quality by reducing the oxygen content.

The upgrading process essentially involves the conversion of oxygen-rich compounds into hydrocarbons that are consistent with the traditional fuels. Upgrading of pyrolysis oils has been developed by several techniques such as catalytic cracking and hydrodeoxygenation [20, 24-26].

Catalytic cracking is preferred due to its significant advantages over hydrotreating, i.e., it doesn't require hydrogen, operates at atmospheric pressure, and has a lower operating cost [27].

Table 1. Comparison between pyrolysis oil and crude oil [16, 24, 25]

Physical property	Pyrolysis oil	Crude oil
Specific gravity	1.05-1.25	0.86
pH	2.8-3.8	-
HHV (MJ/kg)	16-19	44
Viscosity (at 50 °C) (cP)	40-100	180
Ash	0.2	0.1
Water content (wt%)	15-30	0.1
Elemental composition (wt%)		
C	55-65	83-86
H	5-7	11-14
O	28-40	<1
S	<0.05	<4
N	0.4	<1

Recent work on catalytic upgrading of pyrolysis oils have shown that a variety of hydrocarbons can be formed when H-ZSM-5 zeolite is used as a catalyst, and it has been proven to be the most effective catalyst for the production of gasoline range hydrocarbons, because it promotes deoxygenation reactions due to its shape selectivity and strong acidity [28-30].

Presently, the concern of producing biogasoline, particularly gasoline-range hydrocarbons from pyrolysis oils, has been arousing attention. A handful of previous studies have demonstrated that pyrolysis oils derived from different biomass sources could be converted to gasoline hydrocarbons by catalytic cracking over HZSM-5 catalysts.

1.2 Overview of the research work

In this work, a crude pyrolysis liquid was obtained from local suppliers in Phatthalung Province. The pyrolysis liquid is derived as a by-product during the manufacture of charcoal from rubber wood. This liquid is divided after a certain time, into aqueous and oily layer. The former (pyroligneous liquid), more accurately called wood vinegar, is used extensively in agriculture in plant growth and protection. The pyroligneous liquid was concentrated to a liquid, labelled as pyrolysis oil (the first fraction). The pyrolysis oil was then fractionated into two fractions by vacuum distillation; light fraction and heavy fraction. Additionally, the oily layer (more accurately

called pyrolysis tar) from the crude pyrolysis liquid was separated by decantation. Thus in this work, the catalytic cracking of three fractions (pyrolysis oil, heavy fraction and tar) was investigated, and their viability for producing gasoline-range aromatics was studied, showing that pyrolysis tar has the highest yield among the other fractions. The experiments were conducted in a dual reactor using two kinds of zeolite catalysts; commercial HZSM-5 catalyst and nanocrystalline HZSM-5 catalyst. The effect of operating conditions on the yield of organic liquid product (OLP) and the percentage of gasoline-range aromatics in the OLP were investigated. The optimum operating conditions were analyzed using design of experiments (DOE) and response surface methodology (RSM). RSM statistically explores the interactions between one or more than one response variables and some explanatory variables. It uses an arrangement of designed experiments to attain an optimized response. Figure 3 illustrates the overview of the research work.

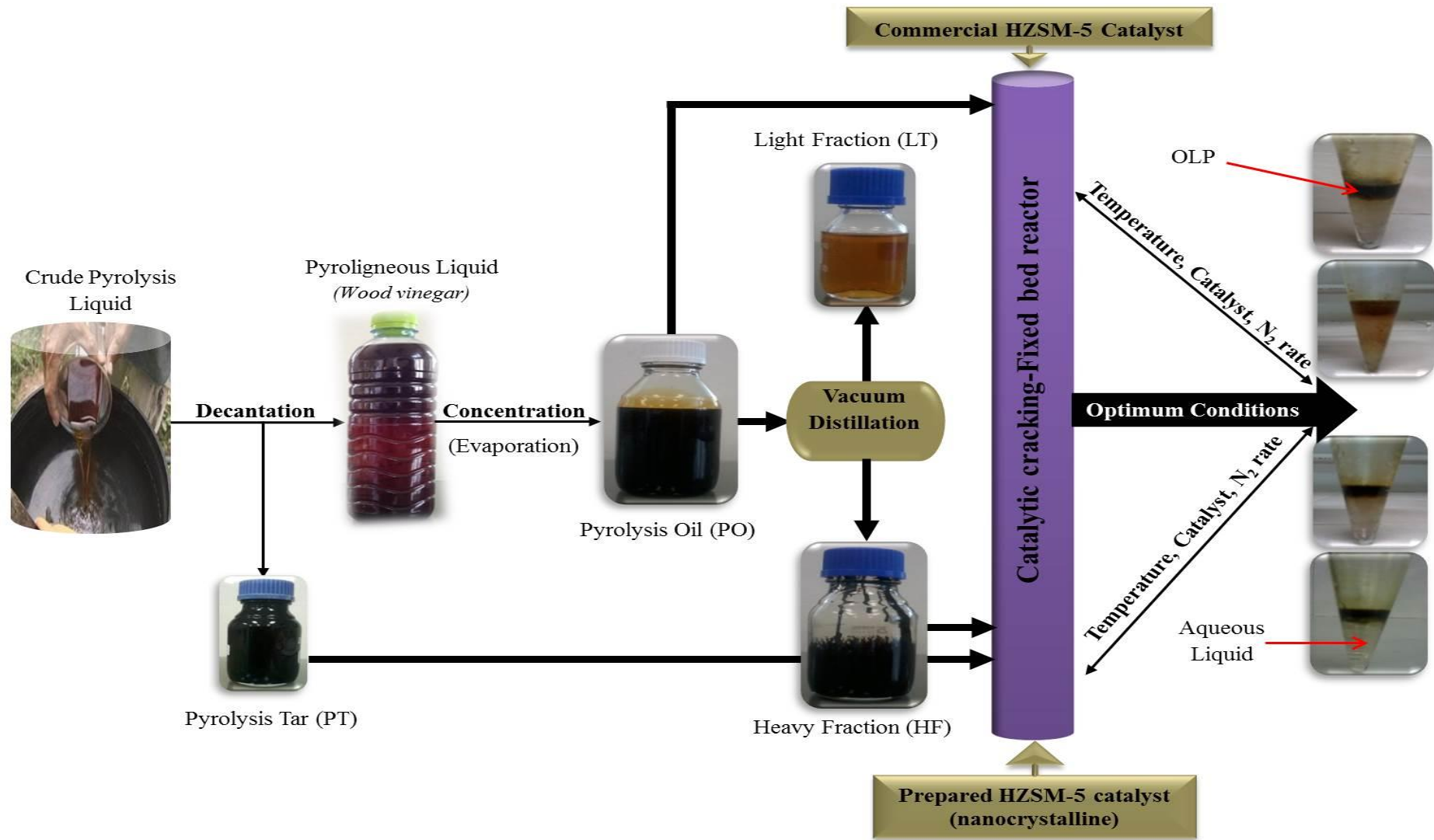


Figure 3. Overview of the research work

2. Theoretical background and literature review

2.1 Upgrading routes for converting pyrolysis oils to fuels

The conversion of biomass to pyrolysis oils was described in the previous section. They have been identified as the most reasonable alternative fuels that can be generated from biomass materials with low cost. It was noted that these oils are not able to be used as transport fuels, but can be used as direct firing of boilers and also for turbine and diesel applications [31], meaning that their final applications are limited due to some undesirable properties such as high viscosities, high oxygen contents, low hydrogen to carbon (H/C) ratios, high water content, high acidity, low heating value and instability.

In order for the pyrolysis oils to be valuable as transportation fuels, they must be upgraded by pursuing a chemical conversion to develop their volatility and thermal stability by increasing and reducing the viscosity via deoxygenation and reduction of molecular weight. The routes used for upgrading pyrolysis oils are depicted in Figure 4.

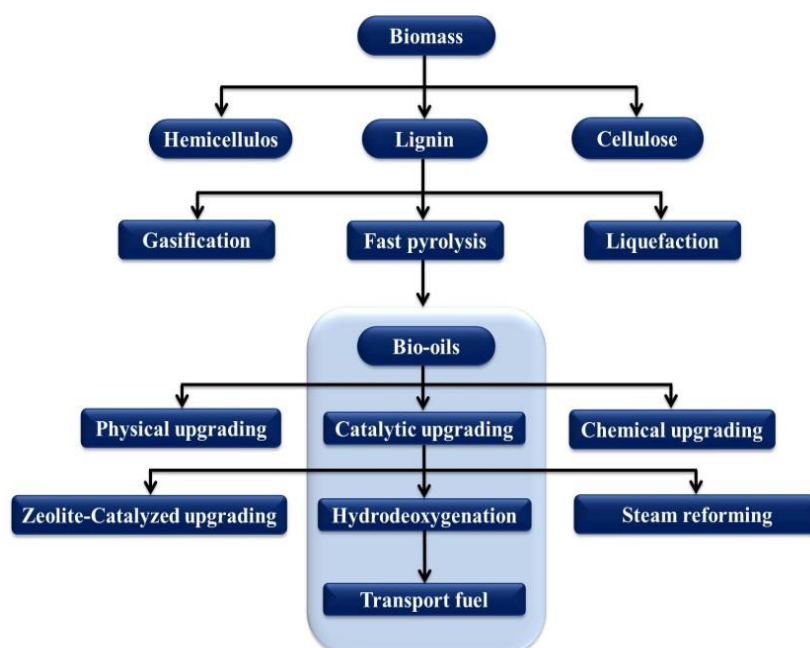


Figure 4. Flow diagram for conversion of biomass to bio-fuels [32]

A series of upgrading work have been studied with the purpose of producing volatile hydrocarbon-rich liquid products that might be used as fuel. There are two key routes to generate hydrocarbon fuels from pyrolysis oils, which considered as 2nd generation fuels in the coming prospect. These routes are; catalytic cracking and hydrodeoxygenation (HDO),

which are denoted to as catalytic upgrading of pyrolysis oil. Both routes have some advantages and disadvantages, but still not economically developed on a large scale [33].

The catalytic upgrading of pyrolysis oils involved a very complicated network of reactions because of their oil complex nature and content. Reactions such as cracking, decarboxylation, decarbonylation, hydrogenation, hydrodeoxygenation, hydrocracking and polymerization were stated to occur for both HDO and zeolite cracking [34-36]. Figure 5 represents some examples of these reactions.

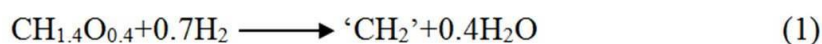
In this review the catalytic upgrading of pyrolysis oils using the tow processes are described. Part of this section is dedicated to the aspects of processing conditions, reaction mechanisms, choice of catalyst and deactivation mechanisms. From these concerns, we will give an overview to the two routes relatively to each other.

2.1.1 Catalytic upgrading by hydrodeoxygenation process

Most of previous work on hydrodeoxygenation route focused on biomass-derived oils as feed. The original work with this process was the effort to produce gasoline from the liquefaction oil derived from wood at the Albany Biomass Liquefaction Pilot Plant. The treated liquefaction oil was more deoxygenated as compared to the fast pyrolysis oil, giving a good specification of thermal stability and required less hydrogenation to produce gasoline [37].

Hydrodeoxygenation (HDO) includes reactions with hydrogen, which produce hydrocarbons and water. It was adopted from catalytic hydroprocessing of the conventional hydrodesulfurization (HDS) in petroleum refining, which is used in the removal of sulfur from organic compounds [27, 38, 39]. During Hydrodeoxygenation, the oxygen is converted to H₂O which is environmentally friendly, however in HDS process, oxygen is converted to H₂S. Both HDO and HDS require hydrogen in the process.

The reactions corresponding to Figure 5 are related to HDO; however HDO is the key reaction occurring during the process, therefore, it can be generally written as follows:



Where 'CH₂' denotes an indefinite hydrocarbon. In the conceptual reaction, water is formed and therefor at least two liquid layers will appear as product, i.e., an organic layer and an aqueous layer. The existence of immiscible layers has been stated, which occurred because of the organic compounds formation having lower densities, therefore the light fraction

separates on top of the water [29, 40]. Nevertheless, the complete deoxygenation shown in Eq. 1 is rarely attained, so a product with oxygen-containing compounds is often formed.

With respect to operating conditions, a high H₂ pressure (as high as 100–200 bar) is required to achieve high HDO conversion. In addition, a high temperature (295–395 °C) is also needed as reported previously [29, 41, 42].

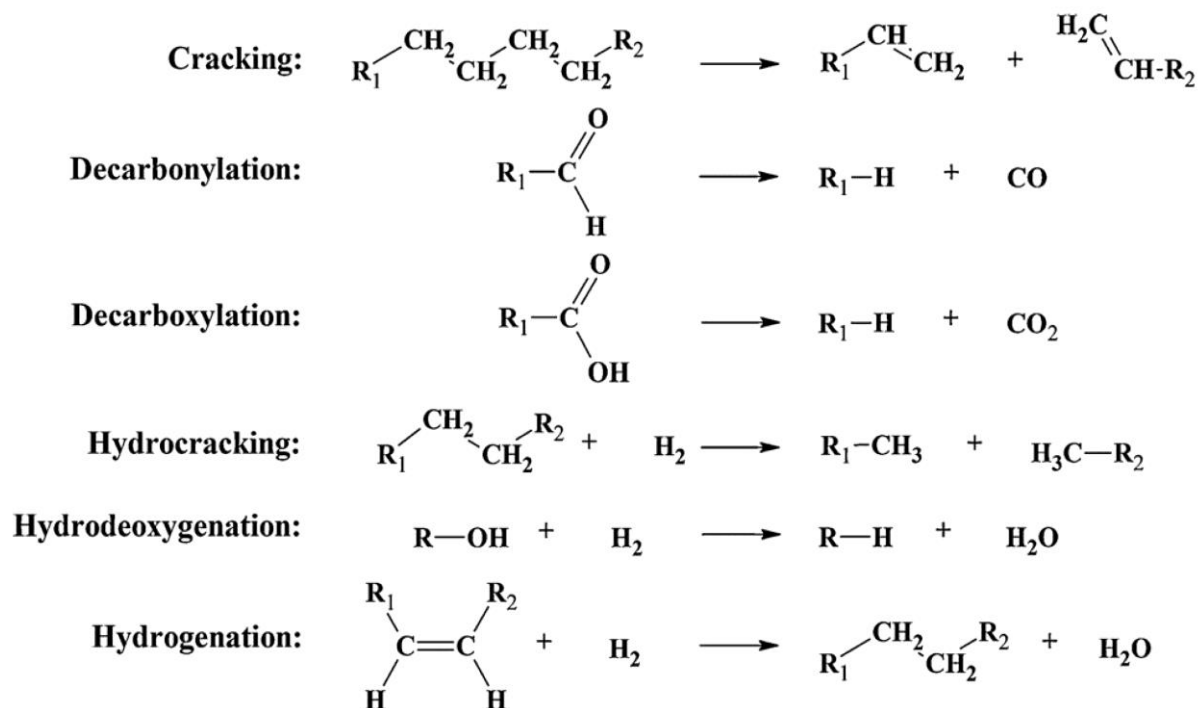


Figure 5. Reactions accompanying catalytic upgrading of pyrolysis oil upgrading [29]

Another operating pressure in patent literature was reported in the range of 10 to 120 bar [43, 44]. It has been described that the high pressure enhances the hydrogen to dissolve in the oil so that it can be highly existed in the surface of catalyst, which leads to an increase in reaction rate and decrease in coking as well [40, 45].

2.1.1.1 Catalysts and reaction mechanisms

The catalysts that are active to accelerate the Hydrodeoxygenation reactions involve noble metals, metal sulphide, metal carbides, metal nitrides and metal phosphides supported on metal oxides or carbon, but noble metals such as platinum are so expensive in spite of their high activity for HDO reactions [36, 46, 47]. Generally, these catalysts are suitable for the HDO process and well known for deoxygenating biomass-derived liquids. They are tested mostly for refining petroleum products however; more studies are needed to develop their function for both deoxygenizing and isomerizing, considering their cost by using non-noble transition metals.

As shown in Table 2 a variety of different catalysts for conversion of biomass derived oils via HDO process, has been investigated. In the following paragraph, they will be discussed as metal catalysts, metal sulphides, metal phosphides and metal nitrides.

I. Metal catalysts

The metallic catalysts have been used by using transition metal catalysts and they have been tested to upgrade biomass derived oils. These catalysts have usually a bi-functional activity, denotes two aspects; the activation of oxygenated compound, which can be attained using a transition metal oxide form, usually supplemented with the support, and that must combine with viability of donating hydrogen to oxygenated compounds, that would take place on the transition metals, which can possibly activate H_2 [48-51]. Figure 6 demonstrates the combined mechanism, where the adsorption of the oxygenated compound and its activation are clarified.

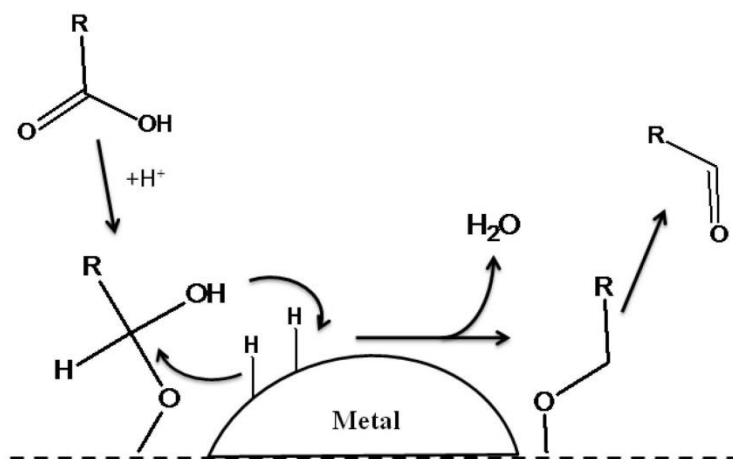


Figure 6. Mechanism of HDO over transition metal catalysts [51]

A competing reaction between hydrogenation and HDO of aromatic rings is generally occurred in the upgrading reactions. Metals comprising nickel, iron, cobalt, palladium, rhodium, ruthenium, iridium and platinum are active. As such, an attempt was made for the hydrodeoxygenation of guaiacol using iron supported on (Fe/SiO_2) [52]. A good selectivity of aromatics was observed as it produced toluene, xylene and benzene with less aromatic ring hydrogenation. A study by Gutierrez et al. [53] reported the activity of Pd, Rh and Pt supported on ZrO_2 for HDO of guaiacol. It was found that the apparent activity decreased as:



II. Metal sulphides catalysts

Metal sulphides were one of the most widely catalysts that used to remove sulfur and nitrogen from petroleum in the traditional hydroprocessing technology. In these catalysts, cobalt or nickel works as promoters, donating electrons to the molybdenum atoms, which makes the bond between molybdenum and sulphur weak and thereby a sulphur vacancy site. The sites considered as the active sites in hydrodesulfurization (HDS) and hydrodeoxygenation (HDO) reactions [22, 32, 38, 54]. As can be summarized in Table 2 there are some results characterizing the HDO catalysed by metal sulphides.

III. Metal phosphides catalyst

The standard catalysts for removing nitrogen and sulphur from petroleum are sulfided CoMo and NiMo and can also be used for the elimination of oxygen, particularly in biomass-derived oils; however, these catalysts have relatively low HDO conversions. Therefore, it was clear that new catalysts are needed. The transition metal phosphides were also used for petroleum hydroprocessing and considered potential substitutes for the CoMo and NiMo sulfided materials as new candidates for pyrolysis oils upgrading. Some authors [55] reported that these catalysts have relatively higher activities and HDO conversions as compared with the sulfided CoMo/Al₂O₃ catalysts, which undergo rapid deactivation.

IV. Metal nitrides catalyst

The catalysts of metal nitrides have also been studied for hydrodeoxygenation, and they have potential advantages in resisting oxidation, they can be simply prepared and have low cost. A few works was reported on metal nitrides, using catalysts such as γ -Mo₂N, β -Mo₂N, molybdenum metals or molybdenum-containing compounds like MoO₂. The catalysts showed higher yield of deoxygenated compounds [56, 57].

Due to structures' complexity of the biomass-derived oils and their variabilities, only little information is available characterizing the reaction mechanism of biomass oils hydroprocessing. In the process of hydrodeoxygenation, oxygen is eliminated as water, carbon dioxide, carbon monoxide and few others via different reactions.

Richard et al. [47] proposed a reaction mechanism by studying 2-ethylphenol hydrodeoxygenation on MoS₂ catalysts (Figure 7). The oxygen of the molecule is adsorbed on the MoS₂ slab edge, initiating the compound. The species of S-H will be also presented along the catalyst's edge. The species are generated from the H₂ in the feed.

This allows proton donation from the sulfur to the attached molecule that forms a carbocation. This undertakes direct C-O bond cleavage, to form the deoxygenated compound, and hereafter oxygen which is removed as water.

Throughout the prolonged operation, it can be noticed that the activity of the catalyst was decreased because of its transformation from a sulphide form to an oxide form. However avoiding this, can be done by feeding H_2S to the system which will stabilize the catalyst by regenerate the sulphide sites.

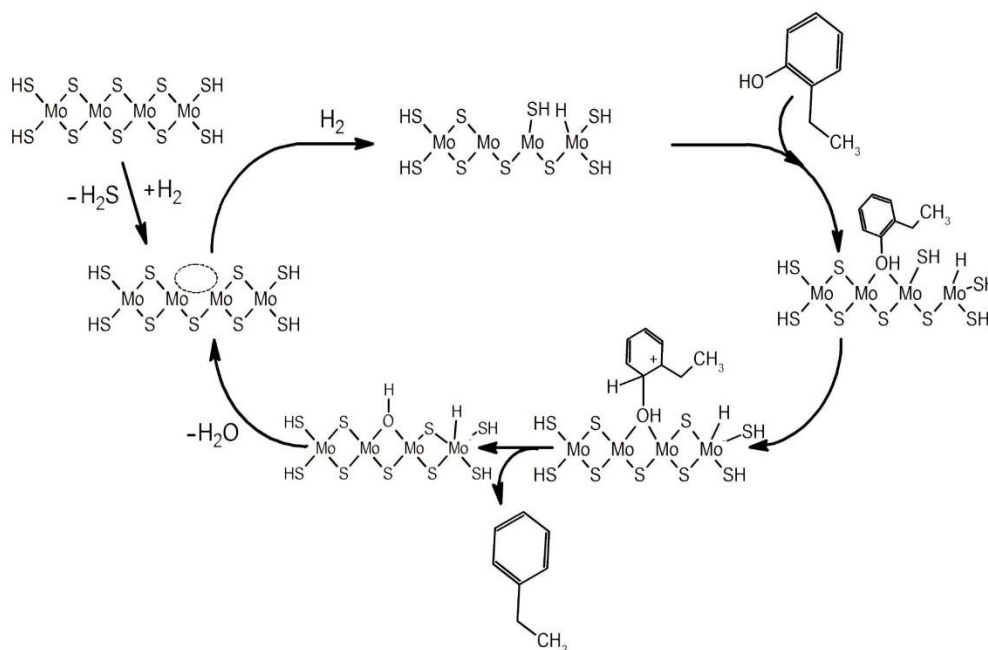


Figure 7. Suggested mechanism of HDO of 2-ethylphenol over a Co-MoS₂ catalyst [51]

Table 2. Catalyzed HDO using metal sulphides [51]

Catalyst	Support	Reactor configuration	Operating conditions				Lignin-derived compounds
			T (K)	P (bar)	T (h)	WHSV (h ⁻¹)	
CoMoWS	SBA-15	Fixed bed	583	30	0.84–4.17	24.5	ANI
CoMoWS	SBA-16	Fixed bed	583	30	0.84–4.17	24.5	ANI
CoMoS	—	Fixed bed	573	40	—	—	GUA
CoMoS	—	Batch	673	50	1	—	GUA
CoMoS	—	Batch	553	70	—	—	GUA
CoMoS	—	Batch	573	50	3.34	—	4MP
CoMoS	g-Al ₂ O ₃	Fixed bed	573	40	—	—	GUA
CoMoS	g-Al ₂ O ₃	Batch	523	75	0.08–5	—	Ph
CoMoS	g-Al ₂ O ₃	Flow reactor	523	15	—	—	Ph
CoMoS	g-Al ₂ O ₃	Batch	523	75	2	—	Ph
CoMoS	Al ₂ O ₃	Fixed bed	573	40	—	—	GUA
CoMoS	Al ₂ O ₃	Trickle bed	573	40	—	—	GUA
CoMoS	Al ₂ O ₃	Batch	573	80	1–5	—	GUA
CoMoS	Al ₂ O ₃	Batch	573	50	—	—	GUA
CoMoS	Al ₂ O ₃	Batch	573	50	—	—	ANI
CoMoS	Al ₂ O ₃	Fixed bed	573	28.5	—	—	Ph
CoMoS	Al ₂ O ₃	Batch	573	50	4	—	Ph
CoMoS	TiO ₂	Fixed bed	573	40	—	—	GUA
CoMoS	ZrO ₂	Fixed bed	573	40	—	—	GUA
CoMoS	C	Batch	553	70	2	—	GUA
NiMoS	—	Batch	400–700	50	1	—	GUA
NiMoS	—	Parr	623	28	1	—	Ph
NiMoS	g-Al ₂ O ₃	Batch	523	75	0.08–5	—	Ph
NiMoS	g-Al ₂ O ₃	Flow reactor	523	15	—	—	Ph
NiMoS	g-Al ₂ O ₃	Batch	523	75	2	—	Ph
NiMoS	g-Al ₂ O ₃	Batch	723	28	1	—	CAT
NiMoS	g-Al ₂ O ₃	Batch	723	28	1	—	GUA
NiMoS	g-Al ₂ O ₃	Batch	723	28	1	—	Syr
MoS ₂	—	Fixed bed	573	40	—	—	GUA
MoS ₂	—	Fixed bed	573	50	—	1	ANI
MoS ₂	—	Batch	623	44	5	—	4MP
MoS ₂	—	Parr	623	28	1	—	Ph
MoS ₂	C	Batch	573	50	4.17	—	GUA
MoS ₂	g-Al ₂ O ₃	Fixed bed	573	40	—	—	GUA
MoS ₂	g-Al ₂ O ₃	Fixed bed	573	50	—	2	ANI

(T= temperature; P = pressure; t = time; WHSV = weight hourly space velocity)

2.1.2 Catalytic upgrading by zeolite cracking process

Zeolites are common catalysts widely used in fluid catalytic cracking (FCC) process. This process can be applied to biomass derived oils to upgrade them to hydrocarbon fuels, where the zeolites are also used. However, HDO in this manner seems more developed than zeolite cracking, because developing HDO has been adopted to a great extent from the process of hydrodesulfurization, yet zeolite cracking cannot be generalized in the same degree from FCC [27, 39, 59].

2.1.2.1 Advantages of using zeolite catalysts

Despite the fact that both zeolite and hydrodeoxygenation catalysts have the ability to act as effective catalysts in cracking process, the zeolite catalysts offer some advantages over the hydrotreating catalysts. The advantages can be addressed as in the following point [60, 61]:

- Zeolite catalysts have the ability to provide a definite distribution of product, whereas hydrotreating catalysts cannot, because of the shape selectivity of zeolite catalysts.
- Large and low molecular weight compounds produced from wood pyrolysis can react effectively on zeolite catalysts. However, hydrodeoxygenation can be attained effectively only when large compounds such as phenolic compounds are in high concentration, as the low molecular weight mixtures are not thermally stable in the hydrotreating conditions.
- In hydrodeoxygenation, the sulfiding of hydrotreating catalyst by adding sulfur to the feed is necessary to enhance the catalyst activity, however this process is avoided in case zeolite catalysts.

2.1.2.2 Process conditions

Upgrading of biomass derived oils is basically influenced by temperature, catalysts, space velocities, reactor types and arrangement of reactors. The reactions shown in Figure 5 occur in principal; however the cracking reactions are the principal ones. In the process of zeolite cracking, biomass derived oils are transformed to three phases; oil, aqueous, and gaseous product. The reaction temperatures used in the process typically ranged from 300 to 600 °C [27, 45, 62, 63].

Sharma et al. [64] investigated the effect of temperature on HZSM-5 catalyst to upgrade pyrolysis oil derived from aspen wood in a fixed bed reactor in a range of temperature between 370–410 °C. As the temperature increased the produced organic liquid

decrease and the gas yield increased. This is because of the reaction rate which occurs at high temperatures, producing smaller compounds.

Zeolite cracking process, in contrast to the HDO doesn't require hydrogen so it might be able to be processed at atmospheric pressure, yet it must be conducted at high residence time [65], so that a satisfying deoxygenation degree can be ensured.

2.1.2.3 HZSM-5 catalyst

Zeolites in general are porous crystalline consisting of Al, Si, and O atoms with a composition of AlO_4 and SiO_4 tetrahedra that form a three-dimensional network. The oxygen atom is the linked point in the structure. The structures of zeolites have been found to occur in 8 sub units as shown in Figure 8. These units are termed as secondary building units (SBU's) [66].

Zeolites own a quite uniform structure and a narrow pore size distribution with a high pore volume. The high pore volume makes it suitable for use as adsorber, and its narrow pore size distribution makes it capable for use as molecular sieve. Furthermore, zeolite catalysts have the ability to exchange ions which makes them applied in different industrial applications such as reforming, cracking, isomerization and alkylation [66, 67].

In our study, an interest is being paid to HZSM-5; a vital catalyst of the zeolite family which is basically used to transform long chain hydrocarbons to more valuable compounds, such as aromatics hydrocarbons. HZSM-5 zeolite was initially synthesised by Mobil in 1972 and has been industrially produced since long time. It is one of the most important molecular sieve catalysis materials and considered as a highly porous material. Throughout its structure there is an intersecting two dimensional pore structure which formed by 5 oxygens in unit ring (5-membered oxygen ring).

The microporous material is formed from the connection of the ten secondary building units as depicted in Figure 9 which shows the skeletal diagram of (100) face of ZSM-5 and its channel structure [61,68, 69].

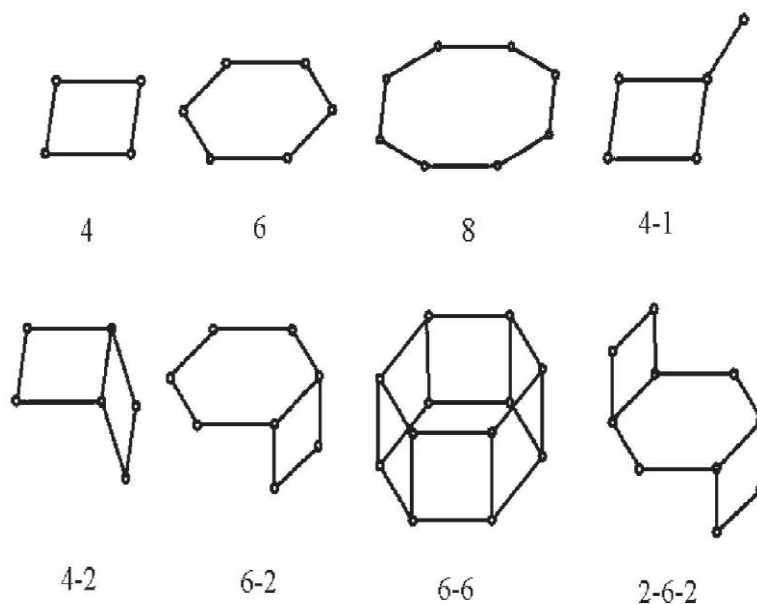


Figure 8. Secondary building units (SBU's) of zeolite structure and their symbols [67]

In the following, shape selectivity and acidity; synthesis and characterization; reaction pathways on pyrolysis oil upgrading; deactivation of the zeolite catalyst are described.

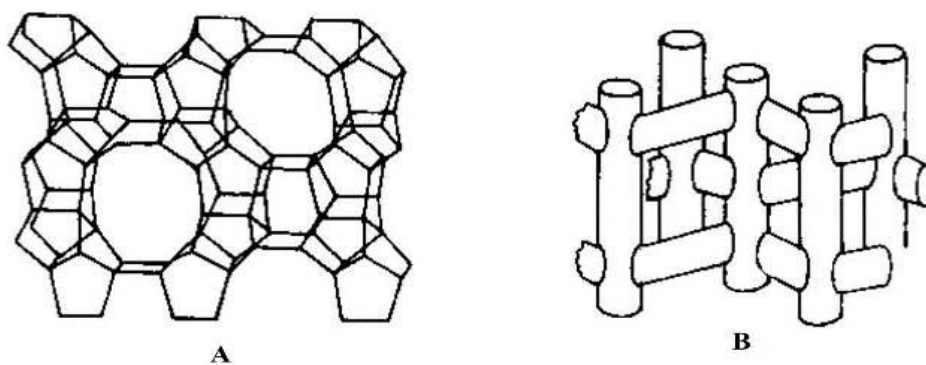


Figure 9. (A) Skeletal diagram of the (100) face of HZSM-5. (B) HZSM-5 Channel structure [70]

2.1.2.3.1 Shape selectivity and acidity

The zeolite framework structure and the presence of acid sites control and identify the reactivity and selectivity of zeolites. The shape selectivity which describes the selectivity of zeolites can either be functioned by reactant selectivity, product selectivity or

transition state selectivity. On other hand, the Bronsted and Lewis acid models describe the acidity of the catalyst. In this section, all these features are described.

-Reactant selectivity

The reactant shape selectivity was stated initially by Weisz and Frilette [70], where reactant selectivity takes place when the access of certain reactant molecules are suppressed to diffuse through the catalyst pores due to the large size, whereas other molecules (smaller size) can diffuse and react. This type of selectivity is shown in Figure 10 (a).

-Product selectivity

The product shape selectivity was also first reported by Weisz and Frilette [71], which applies to product molecules, formed in the zeolite and cannot escape quickly from the zeolites pores due to steric considerations. This type of selectivity is shown in Figure 10 (b).

-Transition state selectivity

The definition of transition state selectivity was expanded by Csicsery [71]. This selectivity type is a kinetic effect occurs around the active sites when the configuration of a potential transition state for a certain reaction mechanism is spatially restricted and thus just few reaction pathways are viable. This is depicted in Figure 10 (c).

-The acidity of zeolite

The fundamental of acidity of solid catalysts is of essential importance in different aspects linked to the applications of solid surfaces, particularly for catalytic processes. In chemical industry, more to the point, petrochemical reactions, zeolite catalyst play a major role in reactions such as cracking, polymerization, isomerization and disproportionation. Such reactions were assumed to occur via carbenium ions compounds. It was predicted that the strength of an acid site in zeolite occurs disparity of charges among silicon and aluminium atoms in the framework; as a consequence, the atoms of aluminium are capable to make active acid sites [61, 66]. In the next paragraph, origin and characteristics of these sites will be discussed.

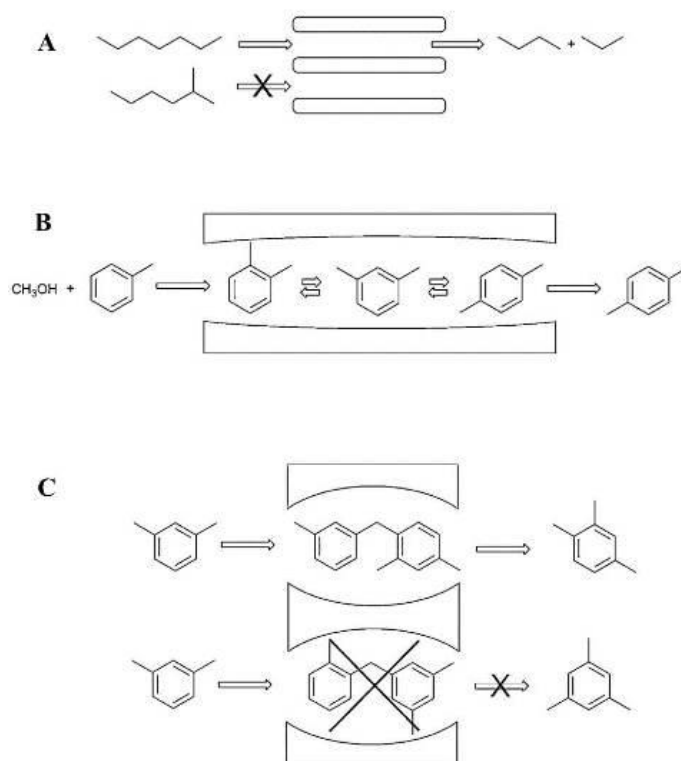


Figure 10. Schematic representation of shape selectivity in zeolite channels; (A) Reactant selectivity, (B) Product selectivity, (C) Transition state selectivity [71]

-Bronsted Acidity

In Brønsted's view, the acid is defined as a proton donor, while the base is the proton acceptor. The acidity of proton donor arises when the cations balancing the framework anionic charge are protons (H^+). The conceptual theory is that when an acid and a base react together, the acid creates its conjugate base, and the base creates its conjugate acid through the exchange of the hydrogen cation (proton). Bronsted acid sites are described in Figure 11 (B). Even though, the activity phenomenon of Bronsted acid on the surface is still not completely understood, the Bronsted acid sites are suggested to be the main reason for the high activity of most zeolites [73].

-Lewis Acidity

Lewis acid sites are suggested to be formed from the dehydration of Bronsted acid sites. Nevertheless their role is still not completely understood, the initial cracking of bulky molecular weight compounds are believed to arise on Lewis acid sites. With the formation of Lewis acid sites, protons are lost as water. Figure 11 (A) shows Lewis acid sites in zeolites.

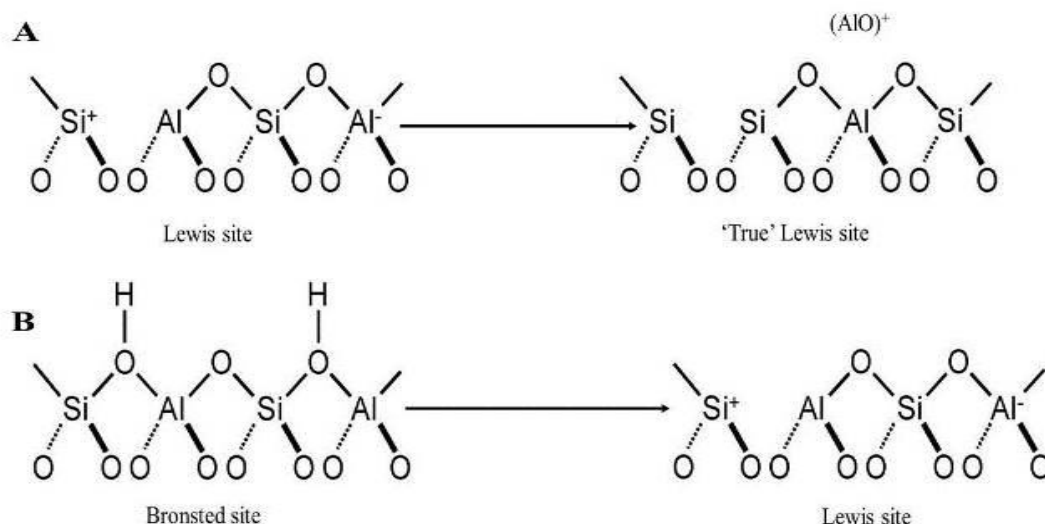


Figure 11. Bronsted and lewis acid sites on zeolite [74]

2.1.2.3.2 Synthesis and characterization of HZSM-5 catalyst

2.1.2.3.2.1 Synthesis of HZSM-5

Several zeolites such as mordenite, stilbite and analcime naturally occur. However, some of them have also been prepared. Several interesting zeolites that can be industrially used (e.g. ZSM-5) are synthetic without a natural complement. Zeolites synthesis is generally carried out under hydrothermal conditions where the sources of silica and alumina with an exchangeable cation are dissolved in water under high pH conditions generated by OH^- ion concentrations. Crystallization of the zeolite from the created inhomogeneous gel is affected by heating the resulting gel for a period of time. The final framework composition of the zeolite is determined by controlling the $SiO_2:Al_2O_3$ ratio in the gel. The source of silica is soluble silicates and their hydrates which are widely used (e.g. sodium metasilicate pentahydrate and silica sols). The aluminium source is metal aluminates (e.g. sodium aluminate) and for the source of exchangeable cations, alkali metals and alkaline earth metals are usually used. Formation of the exact zeolite required structure is affected by the correct concentrations of reagents, temperature, pressure and time. Tetrapropylammonium (TPA) is an important template to synthesize HZSM-5 zeolite [75]. It is used to form the crystal structure of the zeolite conferring to the procedure of Mobil Oil Co. [76].

The synthesis mixture is usually prepared by combining tetrapropylammonium bromide, sodium silicate, sodium aluminate, sodium chloride and sodium hydroxide. A templating role is provided by tetrapropylammonium bromide during nucleation and crystallization. After crystallization, tetrapropylammonium ions occluded in the structure are

removed by calcining the dried product form crystallization between 450 to 550 °C. This method produces Na-ZSM-5, where is reacted with exact concentration of HCl solution (ion exchange) to produce HZSM-5 [77].

2.1.2.3.2.2 Nano-crystalline zeolite

Conventional zeolites are industrially synthesised with micro-sized crystals. During the last decade, there have been efforts to reduce the size of zeolites from micron to nanometer size i.e., zeolites with crystals less than 100 nm. A significant change would be expected in the nanosized properties relative to the conventional molecular sieves, particularly in the fields of membranes, microelectronics, sensing and other applications [78].

The decrease of zeolite crystals from the micrometer scale to the nanometer would improve the properties of zeolites such as decreased diffusion path lengths and increased surface area, and this is expected to be very important in catalytic reactions. When the crystal size is reduced below 100 nm, the external surface area of the zeolite dramatically increases achieving zeolites with over 25% of the total surface area on the external surface [79].

Numerous studies have developed synthetic methods to prepare different zeolite structures in the nanosize range, such as silicalite, ZSM-5, mordenite, Beta and faujasite. The nanosized zeolites are generally prepared by using clear precursor solutions with an excess of organic templates. The zeolites here are often called colloidal molecular sieves when they are present as discrete particles in solution. This system needs fast nucleation with minimum aggregation of the particles during the entire process of crystallization [80]. Preparing zeolite crystals in nanoscale, the precursor systems must have a high degree of supersaturation, as the supersaturation would outcome in high rates of nucleation, a large amount of nuclei, and therefore in the smallest sizes of particle [78].

Nano crystalline ZSM- 5 was synthesized as reported by Van Grieken et al [81]. The synthetic method involved a template molecule, e.g. tetrapropylammonium hydroxide acts as an organic structure-directing agent; aluminum isopropoxide as alumina source; tetraethylorthosilicate as silica source. The aluminum isopropoxide was added gradually to a precooled solution of tetrapropylammonium hydroxide and stirred at 0 °C attaining a clear solution and then adding tetraethylorthosilicate drop wise. The mixtures were stirred vigorously and the solution was then left at room temperature for 41 h to hydrolyze the tetraethylorthosilicate completely. The gel occurred was then evaporated at 80 °C to get a concentrated gel. The concentrated gel was then charged into a Teflon-lined

stainless-steel autoclave to crystallize the solution hydrothermally for 48 h at 170 °C. The solid product was isolated using centrifugation.

Unfortunately, the use of organic templates such as tetrapropylammonium hydroxide makes the process of synthesising nanocrystalline zeolites very expensive. Furthermore, the yield is mostly low, and hardly exceeds a few percent.

2.1.2.3.2.3 Characterization of HZSM-5

Identification and characterization of zeolite catalysts can be made by a number of methods focused on two main areas; structure and acidity. For structure characterization, X-ray diffraction analysis and scanning electron microscopy are used, whereas in acidity characterization, temperature programmed adsorption and desorption studies (TPA/D) and/ or infrared spectroscopy (IR) are used. X-ray diffraction (XRD), scanning electron microscopy (SEM), infrared spectroscopy (IR), and temperature programmed adsorption and desorption studies (TPA/D) are discussed in the following.

I. X-ray Powder Diffraction

This method is used a measurement of zeolites structure to fingerprint them. XRD identify the crystal phase where the x-ray irradiation of the zeolite powder is undertaken delivering a scattering from the regular array of atoms and ions in the structure. According to the Bragg equation $n\lambda=2d\sin\theta$, the symmetry of framework and non-framework of the zeolite composition can be attained producing a diagnostic fingerprint of 2d spacing [65]. Figure 12 represents a typical pattern of HZSM-5 which appeared in literature [81].

II. Scanning Electron Microscopy (SEM)

SEM is used to characterise the morphology of the crystal and is taken for a direct measurement of the crystal size [66].

III. Infrared (IR) Spectroscopy

It is used for identification of both acid sites and carried out by locating bands which absorbed by a sample in the region of infrared. The measurement of hydroxyl (OH) groups on the surface of the catalyst is made to identify the acid site. Bronsted and Lewis acids can be identified by this method; IR indicated that ZSM-5 has two stretching bands, one at a wavelength 3720 cm^{-1} identified as silanol SiOH groups and the other 3605 cm^{-1} and identified as A1-0-(H)-Si bridge [66].

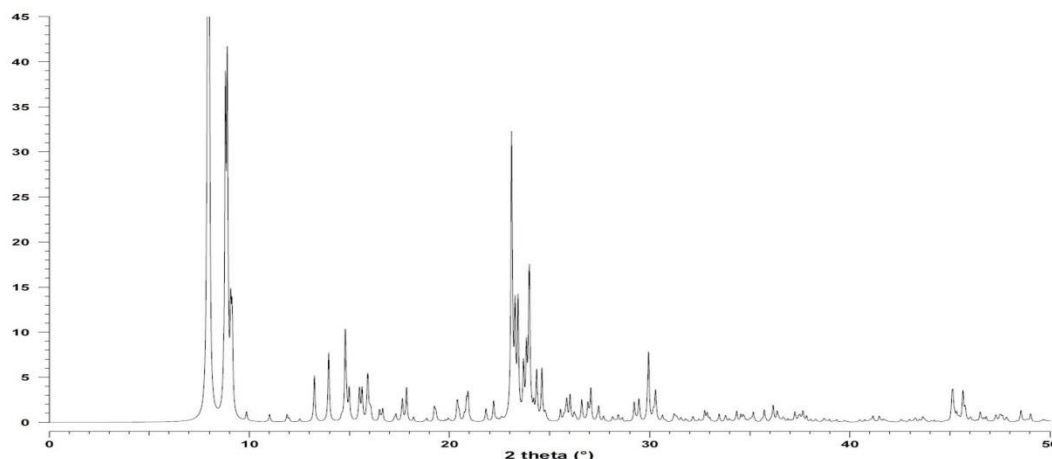


Figure 12. XRD pattern of a pure crystalline HZSM-5 [82]

IV. Temperature Programmed Adsorption and Desorption

Temperature programmed adsorption and desorption is a method most frequently used for identification of zeolite acidity. It comprises the quantitative measurement of gases amount, i.e., ammonia and pyridine, as the basic probe molecules that can be adsorbed on the surface at different temperatures. For example, the adsorption of pyridine coupled with IR spectroscopy has been utilized for identifying Lewis and Bronsted acidity on ZSM-5 catalyst. The pyridine ion (Bronsted-bound pyridine) created a stretching vibration at ca. 1560 cm^{-1} , while 1450 cm^{-1} is due to coordinated pyridine (Lewis-bound) [65].

2.1.2.4 Catalyst deactivation

As for HDO, the loss of catalyst activity occurs due to accumulation of coke. The deactivation of catalyst considered as an insidious problem in zeolite cracking, where carbon formed primarily by polymerization and condensation reactions resulting in pores blockage in the zeolites [83, 84]. The formation of precursors throughout the processing pyrolysis oil over HZSM-5 was investigated by Guo et al. [84] who found that the reason for deactivation was the initial build-up of the compounds with the high molecular weight, principally composed of aromatic buildings. The portions created in the inner zeolite part cause the catalyst deactivation. It was also investigated that acid sites can play a vital role in the formation of carbon on the catalysts as studied by Huang et al. [84].

Briefly, it can be apparently said that reactions of carbon forming are influenced by the presence of acid sites presented on the catalyst achieving poly-aromatic

species. Therefore, acid sites are considered as vital portion of the mechanism for deactivating mechanisms and the deoxygenating reactions.

Finally, activation of zeolite catalysts by regeneration has been investigated by Vitolo et al. [85]. The continued regeneration of the zeolite was undertaken by heating the spent catalyst after washing with acetone in the presence of air in a furnace at 500 °C for 12 h. The coke deposits from the zeolite were easily removed at these conditions.

2.1.2.5 Reaction pathways on pyrolysis oil upgrading

In zeolite cracking, the reaction pathways are based on different of reactions that could convert the hydrocarbons to smaller fragments. The elimination of oxygen occurs due to decarboxylation, dehydration and decarbonylation reactions [29]. HZSM-5 as the most frequently used catalyst has been inspected for the cracking process of pyrolysis oil. Thus, Adjaye and co-workers [35] conducted a significant study using HZSM-5 catalysts to convert the compounds of pyrolysis oil and suggesting the major reaction pathways as depicted in Figure 13. They proposed that, a part of the heavy oxygenated organics with the high molecular weight compounds is cracked to light organics (step 4). Additionally, as in (step 5), some of these heavy organics deposit on the surface of the catalyst forming tar and coke due to polymerization. On the other hand, the light organics undertake different reactions (step 6), i.e., deoxygenation, cracking and oligomerization to produce water, carbon oxides and olefins. The light organic contains different compounds of acids, alcohols, esters, ethers, ketones and phenols which can be converted to various hydrocarbons over the HZSM-5 catalyst. The main deoxygenation route observed in the study was dehydration. The process of cracking produces different carbon fragments; the latter were transformed to a mixture of C₂-C₆ olefins by Oligomerization reactions. The C₂-C₆ olefins then produce benzene through a series of aromatization reactions and produce also various aromatic hydrocarbons by alkylation and isomerization reactions (step7). However, as shown in (step 8), some of the hydrocarbons (aromatics) formed coke via polymerization.

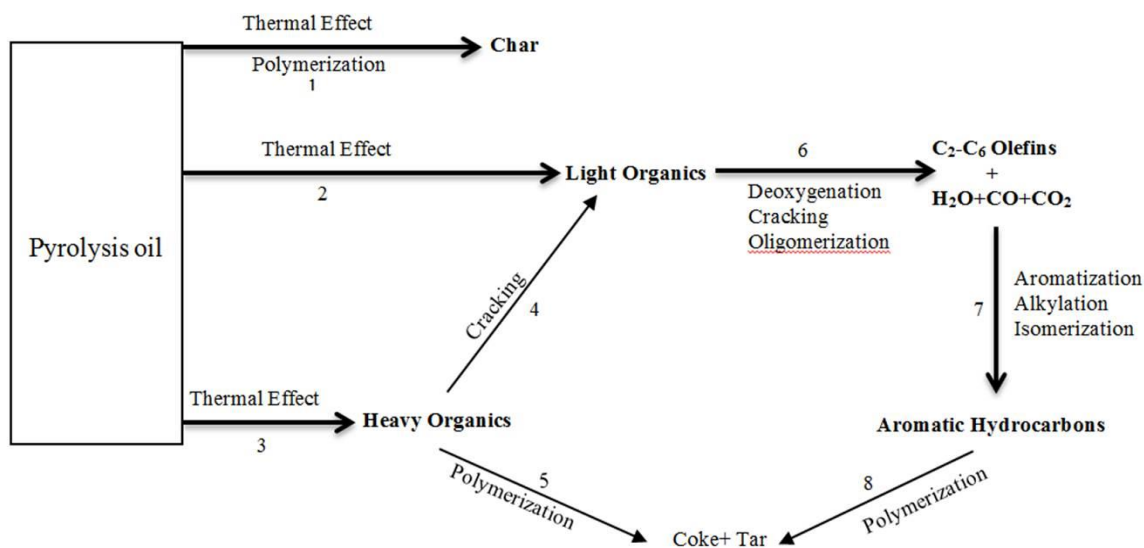


Figure 13. Proposed reaction pathways for the conversion of pyrolysis oil over HZSM-5 zeolite adapted from Adjaye et al. [35]

Model compounds were very useful to understand more the reaction steps included in the HZSM-5 conversion of the pyrolysis oils. The reactions pathways and mechanism are usually performed by using model compounds. The conversion of model pyrolysis oil compounds over HZSM-5 catalysts and the investigation of the major pathways have been reported previously to define appropriate operating conditions which can improve or suppress specific reactions. Also when using different reaction pathways or models to predict the same product distribution in catalytic processes, the model compounds reactions can be efficiently used to differentiate between the rival models. An extensive study was done by Adjaye and Gayubo et al [34, 86]. They selected some acids, esters, alcohols, aldehyde, ketones, ethers and phenols as model compounds to represent the components of the pyrolysis oil. In their study, they observed that upgrading of pyrolysis oil was complex and included a number of reactions such as deoxygenation, cracking, oligomerization, cyclization, isomerization, condensation and polymerization. Methyl acetate and propanoic acid were used as the model compounds of the acids and esters. They were converted mainly to coke, gases, water, aliphatic and aromatic hydrocarbons as shown in the reaction pathway (Figure 14). From this scheme it was proposed that two major routes occurred, which include decarboxylation (step 1), deoxygenation, condensation, cracking, aromatization and polymerization (steps 2-5).

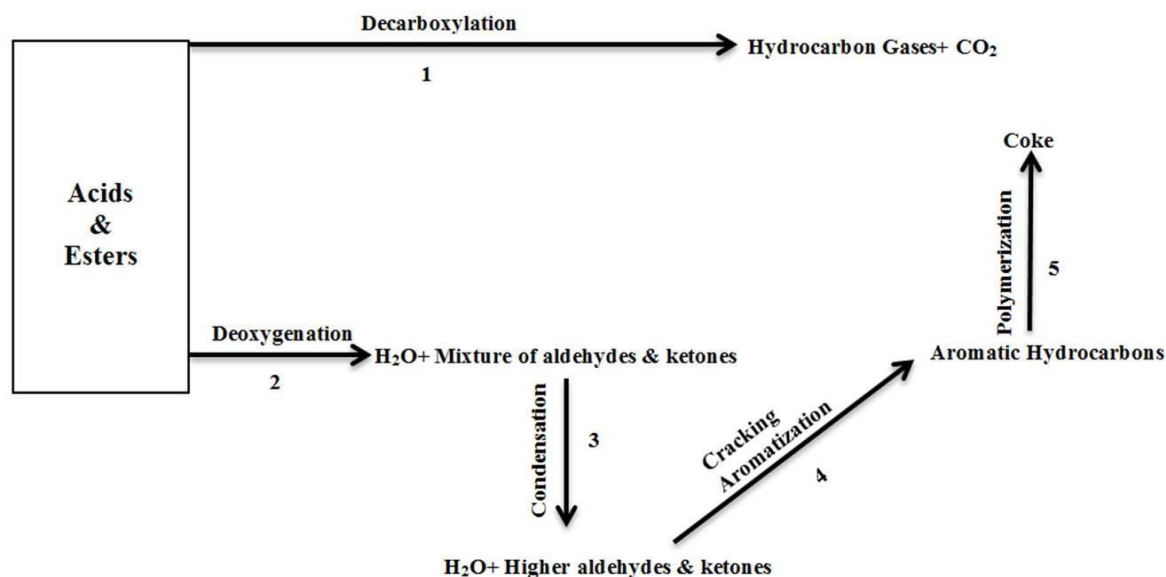


Figure 14. Proposed reaction pathway for the conversion of acids and esters [34]

In addition, the model compound used to study the alcohols reactivity was 4-Methylcyclohexanol. The assumed reaction pathway depicted in the scheme (Figure 15) shows the main reaction route (step 1-3). The alcohols dehydration was mentioned to be a major stage in ethanol reaction over zeolites. Dehydration as in (step 1) produced alkene and water, followed by cracking and aromatization to obtain alkylated benzenes (step 2). Following the formation of alkylated benzenes, the reaction scheme suggests polymerization reactions to form coke (step 3). The second route proceed through ring opening or cracking reactions to form hydrocarbon gases, straight-chain alcohols and CO (step 4) followed by cracking alcohols to obtain olefins, which will produce aromatic hydrocarbons (step 5).

The reactivity of ketones and aldehydes were also studied over HZSM-5 catalyst using cyclopentanone and 2-methylcyclopentanone as model compounds. The proposed reaction scheme shown in Figure 16 suggests that deoxygenation and decarbonylation are the starting reactions. The scheme also suggests that aromatic hydrocarbons and light paraffins can be produced through the sequence of steps (2-3) which includes oligomerization and cracking of the alkene or naphthene molecules formed via step 1, followed by aromatization reactions.

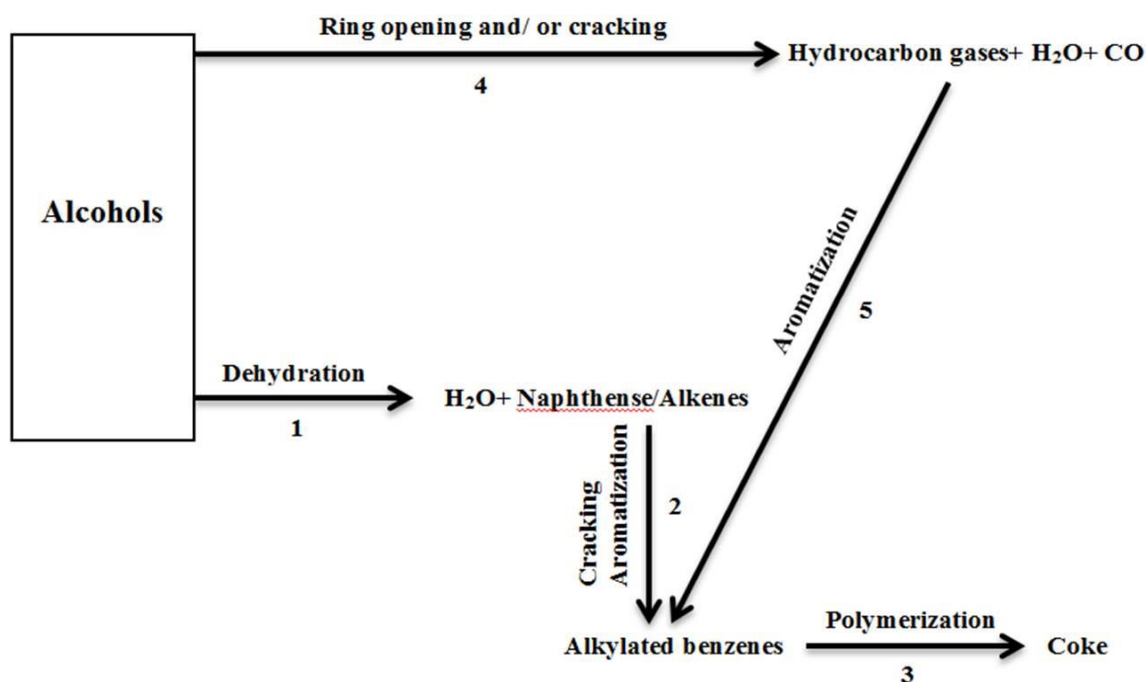


Figure 15. Proposed reaction pathway for the conversion of alcohols

The olefins formed in the scheme undergo a series of reactions to produce BTX (benzene, toluene and xylenes) and light paraffins. It is suggested also that coke formation happens via polymerization reactions (step 4) of the aromatic molecules formed from step 3. Decarbonylation (step 5) occurs through cracking of the ketone molecule forming carbon oxides and hydrocarbon gases. This scheme proposed that some of the hydrocarbon gases can produce aromatic hydrocarbons and paraffins via aromatization reactions (step 6).

Phenols and their derivatives considered as the most plentiful oxygenated compounds occur in the biomass derived oils. Therefore, reactivity of the phenolic components of pyrolysis oils over HZSM-5 must be studied. Figure 17 shows the reaction pathway proposed for the reaction of phenolic compounds. Isomerization of phenols depravities have been stated to be one of the major reactions of phenols over zeolite catalyst forming phenol isomers (step 1).

The scheme also suggests the reaction that includes the formation of olefins and hydrocarbon gases via cracking of alkyl groups attached to the phenol molecule (step 2), and the other reaction (step 3) involves an aromatization type reaction to obtain aromatics. The condensation reaction (step 4) mainly obtains coke, non-volatile residue and some water.

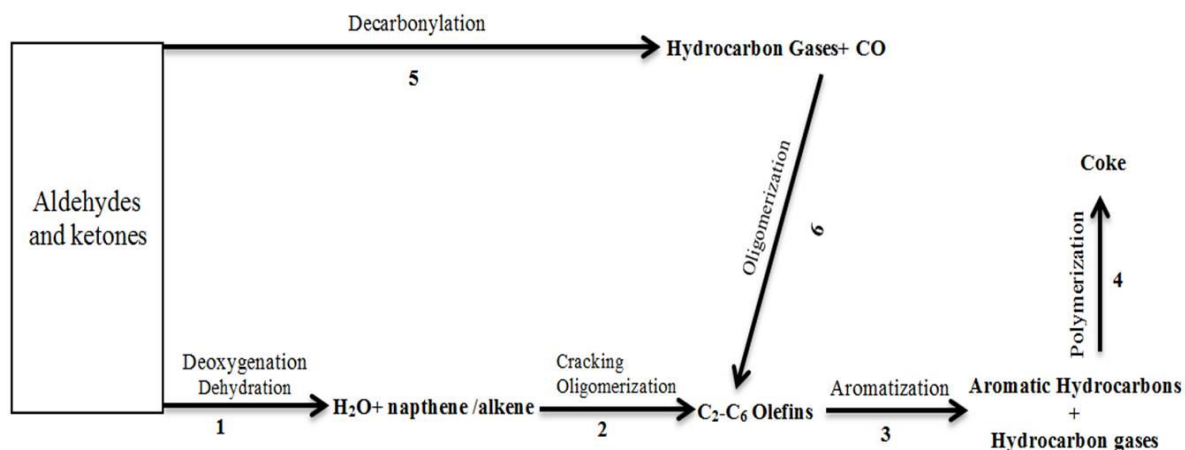


Figure 16. Proposed reaction pathway for the conversion of aldehydes and ketones [34]

The organic liquid product formed consists primarily of aromatics which are expected to be mainly achieved from deoxygenation (step 5) of phenols along with the removal of groups (such as methyl, hydroxyl and methoxy groups) in the aromatic rings with the zeolite catalyst. This proposes that the existing compounds of aromatic structure in the biomass-derived oils are more important for producing aromatic hydrocarbons over HZSM-5, meaning the pathway for aromatic production is possibly a direct deoxygenation of phenolics to aromatics.

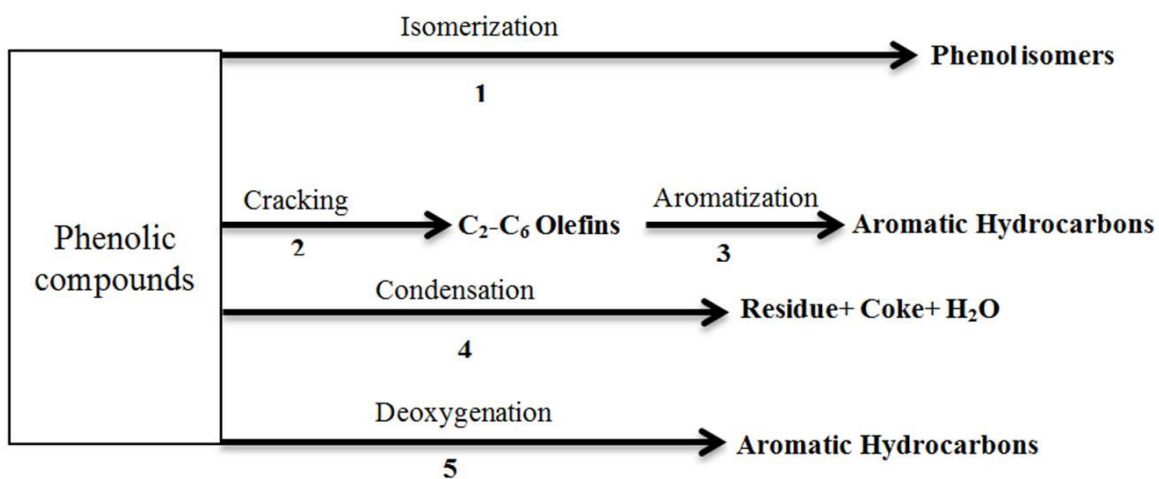


Figure 17. Proposed reaction pathway for the conversion of phenols

2.2 Prospect of catalytic upgrading of pyrolysis oils to gasoline

Upgrading pyrolysis oils to transport fuel, i.e. gasoline is still a technology in its starting point with respect to zeolite cracking and hydrodeoxygenation. Zeolite cracking seems an attractive route from a process point of view; its process conditions are attractive, in terms of independence of hydrogen use and the low operating pressure and this could make it capable to be industrially implemented. However, the coke formed during the process causes a deactivation problem, which gives the zeolite an insufficient lifetime. Additional concern is that zeolite cracking is unable to achieve high deoxygenation degrees [29]. It can be concluded that, zeolite cracking is still far from commercial application since it produces low yield of product with insufficient quality to deal with the demands of fuels. This is in agreement with Adjaye et al. [35, 62] who addressed concern on the low yield of hydrocarbons with the high formation of carbon. As a result, better approaches have been extensively studied to develop economically feasible routes for producing gasoline, which can be produced with prices equivalent to the conventional one.

In the following section we discussed the most promising routes for producing gasoline hydrocarbons through upgrading biomass derived-oils, i.e., catalytic fast pyrolysis (CFP), hydrodeoxygenation (HDO) and integrated hydro-pyrolysis and hydroconversion process (IH²).

2.2.1 Catalytic fast pyrolysis (CFP)

Catalytic fast pyrolysis (CFP) is one of the promising methods that used for producing gasoline range aromatics directly from the conversion of solid biomass. Catalytic fast pyrolysis includes the biomass pyrolysis in the presence of zeolites such as HZSM-5, which has been known to be the most effective catalyst for converting biomass derived oils to aromatic hydrocarbons, having a high selectivity for benzene, toluene, and xylenes. The CFP comprises a high heating rate of biomass about 500 °C s⁻¹ with intermediate temperatures that can be ranged from 400 °C to 600 °C. CFP has significant advantages over other conversion approaches; these advantages including (1) the solid biomass is converted to aromatic gasoline directly in a single reactor, where all the desired chemistry occurred in (2) using cheap silica–alumina catalyst (3) water is not required in this process (4) the treatment of biomass is very simple (grinding and drying), (5) CFP can be used with a variety of biomass feedstocks and the process can be performed in a fluidized bed reactor which is used today in a commercially scale in petroleum industry. Moreover, CFP produces aromatics, i.e., benzene, toluene, xylenes, and propylene which can fit as feedstocks into the petrochemicals industry. It is noteworthy that the reactions occur during catalytic fast pyrolysis are very

complicated. The reactions involve a homogeneous thermal decomposition of the biomass to smaller oxygenated species, which they are then dehydrated and diffuse into the pores of the zeolite catalyst, where they undertake a series of reactions, i.e., decarbonylation, dehydration and oligomerization to produce aromatic hydrocarbons, CO₂, CO, and water at the active sites. The main challenges with catalytic fast pyrolysis are the development of stable and active catalysts that can deal with a huge variation of decomposition intermediates from biomass; and also avoiding undesired coke, which can be formed during the reactions [87-89].

Several researchers studied the catalytic fast pyrolysis of biomass using the HZSM-5 catalyst. Pattiya et al. [90] studied the CFP of cassava rhizome using a fixed bed micro reactor. The influence of catalysts on pyrolysis products was noticed over the yields of gasoline aromatic hydrocarbons, lignin-derived compounds, phenols, carbonyls and acetic acid. The production of aromatic hydrocarbons and reduced oxygenated lignin derivatives indicated an improvement of the pyrolysis oil heating value and viscosity. In addition to direct conversion of cassava, Olazar et al. [91] have studied the flash pyrolysis of pine sawdust in a conical spouted-bed reactor based on a HZSM-5 zeolite. This reactor behaves well hydrodynamically for catalytic pyrolysis of biomass residues. High yields of aromatic hydrocarbons were reported in this study. More recently, high yields of gasoline aromatics have been produced directly from pine wood sawdust and furan performing catalytic fast pyrolysis in a continuous fluidized bed reactor which contains zeolite catalyst [89]. Figure 18 shows schematic of the fluidized bed reactor system.

2.2.2 Hydrodeoxygenation (HDO)

Hydrodeoxygenation is considered as an effective method for upgrading pyrolysis oils leading to hydrocarbons. The process of hydrodeoxygenation has recently received a considerable attention and seems a promising route for the production of biogasoline through upgrading of pyrolysis oils, and here it is seen that hydrogen is a requirement for the upgrading as it can contribute positively to deoxygenate the pyrolysis oil. However, challenges still occur in the field. The main challenges of this process are (1) achieving a high oxygen degree (2) lowering the consumption of hydrogen (3) considering the cost of catalysts by performing an appropriate and careful design; in addition, the requirement of reaction conditions (high temperatures and pressures) should be considered in order to bring this process closer to industrial utilisation.

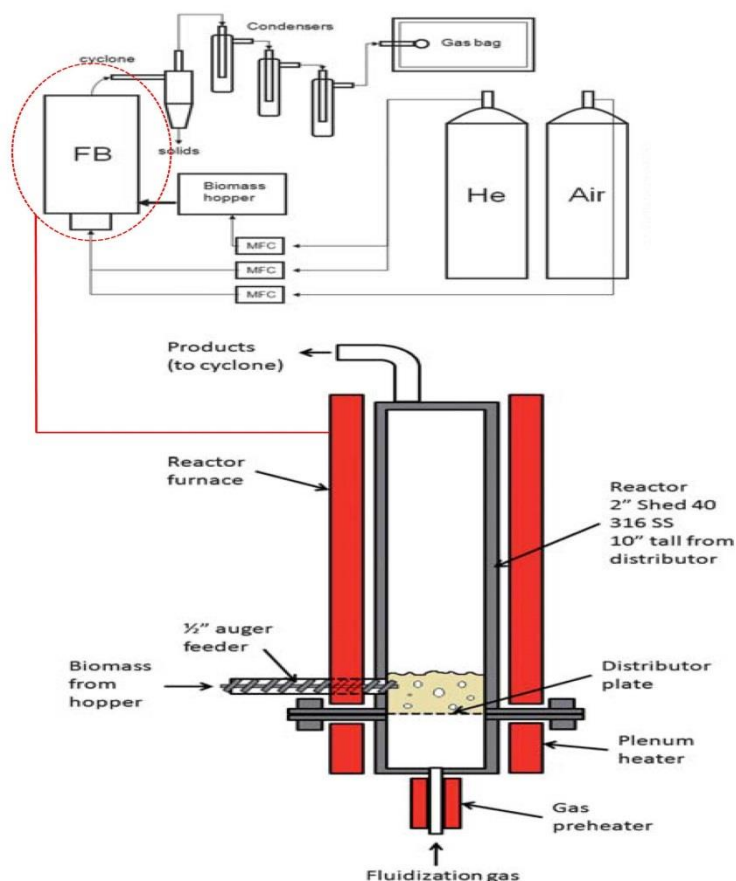


Figure 18. Experimental setup of the fluidized bed reactor system [89]

Therefore, further research on the design of HDO catalytic systems is needed to turn the process of HDO into economically feasible and compatible with current infrastructure [29, 92].

The prospect of upgrading pyrolysis oils should not be seen only in a laboratory scale, but also in an industrial one; so far HDO process to some extent has been assessed in industrial scale, clarifying the unit operations used in the process when going from biomass to fuel. Figure 19 depicted an outline of HDO process shows overall production route from biomass to fuels, i.e., gasoline, kerosene, diesel and fuel oil. The production process is classified into two sections: flash pyrolysis and biorefining. The pyrolysis section involves the pre-treatment of biomass (grinding and drying), which is required to ensure the sufficient heating during the fast pyrolysis. The pyrolysis process occurs in a fluid bed reactor system using a heating source of hot sand, which is subsequently removed using a cyclone and the vapour of biomass move to the condenser. The incondensable gases are separated from the liquids (oil) and the residual solids. The oil and

residual solids are filtered and then the pyrolysis oil sent to another processing site. The incondensable gases are reused with other hydrocarbons for heating up the sand for the pyrolysis. The production of pyrolysis oil has to take place at plants located near the biomass source in order to minimize the costs of transportation and the pyrolysis oils should supply a central biorefinery for the final production of the fuel as shown in Figure 19. The biorefinery section involves thermal treatment, HDO and distillation process. The pyrolysis oil fed to the system and incorporates a thermal treatment (without catalyst) carried out at 200 °C -300 °C. This process can be carried out with and without hydrogen to speed the reaction and stabilizing some of the reactive compounds in the pyrolysis oil and thereby lesser the carbon formation in the HDO process. The HDO synthesis is started after the thermal treatment to produce the upgraded pyrolysis oil which is processed by distillation to fractionate heavy and light oil. The fraction of heavy oil is further processed via hydrotreating and joined with the light oil fraction. Eventually, the light oil is distilled to produce gasoline and other fuels such as diesel, kerosene and fuel oils.

The U. S. Department of Energy made a relatively new economic study considering the entire process steps equivalent to Figure 19. The total cost from the process of treating biomass to gasoline was estimated for gasoline to be around 0.54 \$/l, as compare to 0.73 \$/l form that of crude oil, not including marketing, distribution, and taxes.

2.2.3 Integrated hydrolysis and hydroconversion process (IH²)

As seen in the last two approaches for upgrading pyrolysis oil to gasoline, several drawbacks associated with the upgrading processes occurred. Compared to these processes, which employ biomass to create transport fuels, a better approach of the biomass conversion is to develop a direct route for gasoline production with a high yield and quality, and can be easily transported and compete with the conventional gasoline. This can be achieved by demonstrating a new, economical technology.

A recent project was demonstrated using integrated hydrolysis and hydroconversion (IH²) [93]; the hydrolysis and hydroconversion processes were carried out in pressurized hydrogen for the direct conversion of biomass into gasoline and diesel. The gasoline and diesel from IH² contain very low oxygen content (< 1%), low total acid number (TAN < 1) and are compatible with petroleum based gasoline and diesel. Furthermore the gasoline from IH² is in high quality.

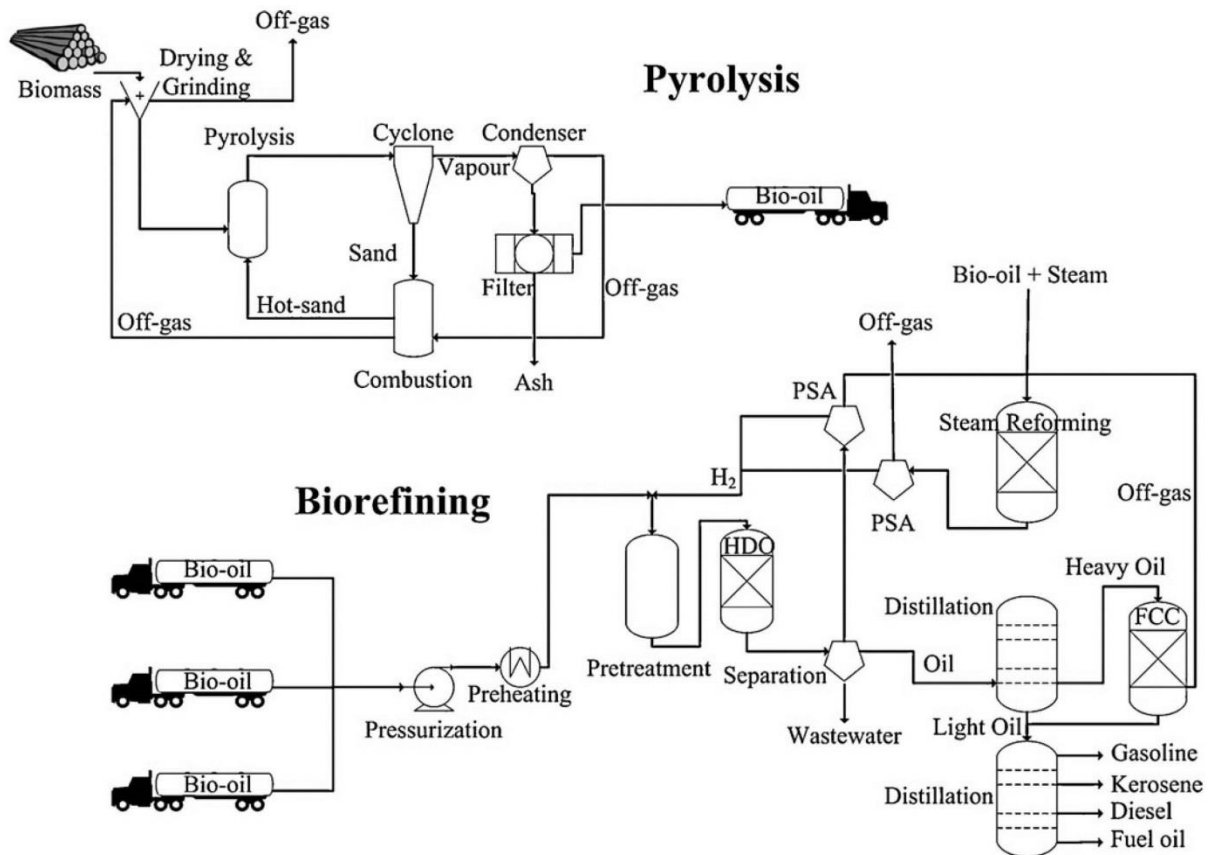


Figure 19. HDO process illustrating the overall production route from biomass to fuels, i.e., gasoline, kerosene, diesel and fuel oil [29]

IH² technology could utilize a variety of biomass resources to create gasoline and diesel, sufficient in quality and quantity to significantly reduce the dependence on crude oil. The commercialization of this process is expected to decrease the GHG emissions of U.S from transportation fuels by 90%.

The flow chart of the IH² process is depicted in Figure 20. The process consists of a fluidized-bed reactor for hydrolysis, where the biomass is converted into liquid and gas (vapor) in pressurized hydrogen, followed by a hydroconversion step where the vapour directed from the hydrolysis stage is treated by removing oxygen and produce gasoline and diesel products. The light gas (C₁-C₃) produced in the hydroconversion stage is separated and sent to an integrated steam reformer where the H² required for IH² process is produced. Therefore, it can be concluded that IH² process has significant advantages over the other upgrading routes (1) the process is self-sufficient as the required hydrogen internally produced, (2) generate plenty of light gases (C₁-C₃) within the process used in generating all the required hydrogen, (3) a direct production of gasoline and diesel with low oxygen content, TAN and high quality, (4) the operating and capital costs are lower than other

upgrading technologies, which give better economics ensuring a quick commercialization, (5) a variety of feedstocks, i.e., corn stover, wood, algae etc., can be utilized and converted to gasoline and diesel fuels.

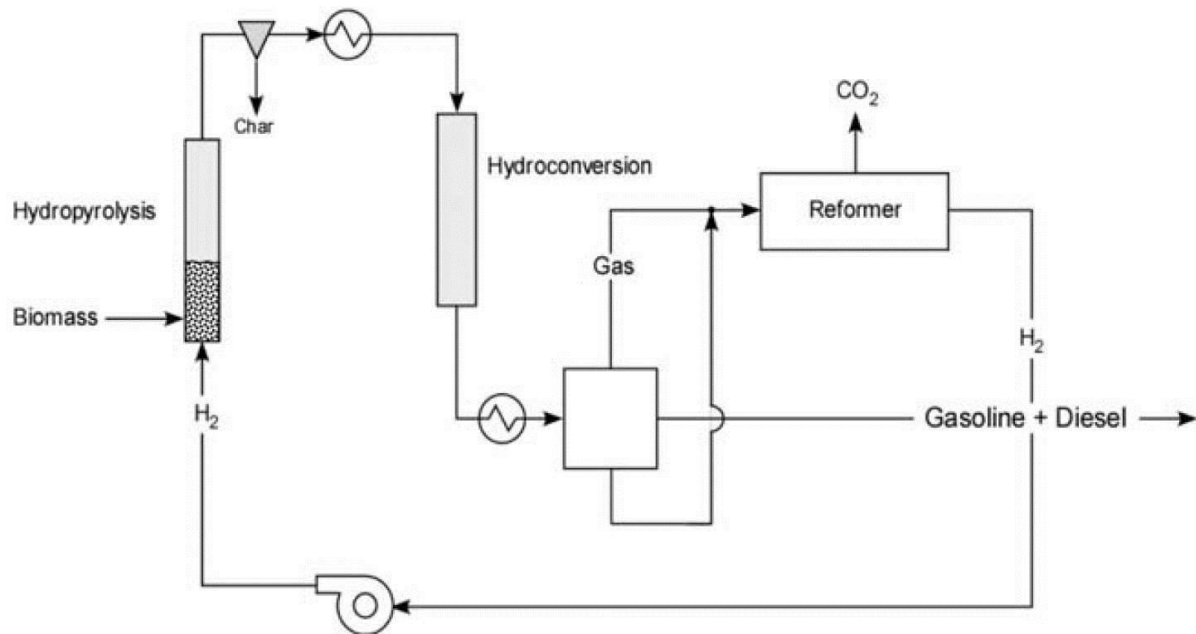


Figure 20. Overall process flow of the IH² system [93]

3. Objectives

The main objective of this thesis is to study the viability of upgrading wood derived oil with its fractions to generate biogasoline, particularly the aromatic portion which has potential fuel applications due to its high octane rating appropriate for blending gasoline.

This thesis has four objectives including:

1. Study the effect of a commercial zeolite catalyst on the conversion of three fractions obtained from rubberwood pyrolysis liquids to generate gasoline aromatics.
2. Study effect of temperature, catalyst weight and the N₂ flowrate on the yield of OLP and the percentage of gasoline aromatics in OLP.
3. Optimize the operating conditions to maximize the yield of OLP and the percentage of gasoline aromatics.
4. Gain a fundamental understanding of the optimal conditions with the use of a nanocrystalline zeolite.

4. Results and discussion

4.1 Fractionation and characterisation of the pyrolysis liquids derived from rubberwood

The purpose of fractionation and characterisation of the pyrolysis liquids in this section is to gain a fundamental understanding of the isolated fractions in terms of their potentiality to be used as feedstock for producing fuels or other valuable chemicals.

In this section, a crude pyrolysis liquid derived from rubberwood was collected from Phatthalung Province and treated to reduce water using evaporation, obtaining a viscous liquid (can be named as pyrolysis oil). The liquid was fractionated into light and heavy fractions using a conventional vacuum distillation as shown in Figure 21. Fractionation has shown to be a suitable technique to evaluate the entire pyrolysis liquid regarding the physiochemical characteristics of its fractions.

As investigated in this work, the light fraction had higher water content and stronger acidity compared to the heavy fraction and pyrolysis liquid which had a relatively low acidity and low water content. The light fraction's heating value was lower than those of the pyrolysis liquid and its heavy fraction. The heavy fraction's heating value was almost double that of the light fraction. In addition, the thermal behaviours were obtained indicating that the light fraction had the highest rate of decomposition and the lowest residual yield, contrary to the heavy fraction which had a slow weight loss over a wide range of temperatures, and it had the highest residual yield. Table 3 shows the physical characterization of the pyrolysis oil, light fraction and heavy fraction.

Table 3. Physical characteristics of the pyrolysis oil, light fraction and heavy fraction

Fractions	Appearance	Heating value (MJ/kg)		Water content (% w/w)	pH value
		GHV	NHV		
Pyrolysis oil	Light black	22	21	30	3.72
Light fraction	Dark yellow	14	12	60	2.67
Heavy fraction	Dark black	28	27	1.5	4.50

GHV : Gross heating value or higher heating value.
NHV : Net heating value.

The chemical composition of the pyrolysis liquid, its light fraction, and its heavy fraction were experimentally determined and categorized into different groups according to their chemical structures (Figure 22). The light fraction was dominated by acetic acid and the heavy fraction was mainly composed phenolic compounds. The results of this study demonstrated that the pyrolysis liquid produced during the process of charcoal production has the potential for more extensive and beneficial use. For instance, the light fraction, which has high acetic acid and water contents, can be used as a feedstock for producing pure acetic acid, whereas the heavy fraction can be directed to further processing and upgrading for use as a fuel. It also could be used as the raw material for producing a number of valuable chemicals (such as phenol, phenolic derivatives, resins etc.) which could be more attractive and beneficial than using it to make fuels.

More detailed results and discussion of this section are clarified on the publication as attached in Appendix A.

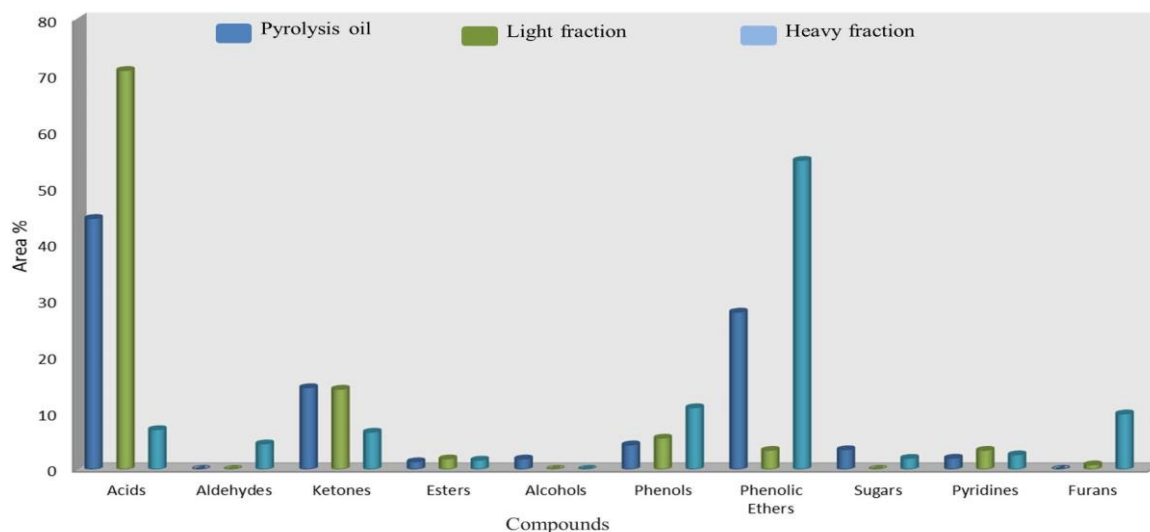


Figure 22. Distributions and classification of the components

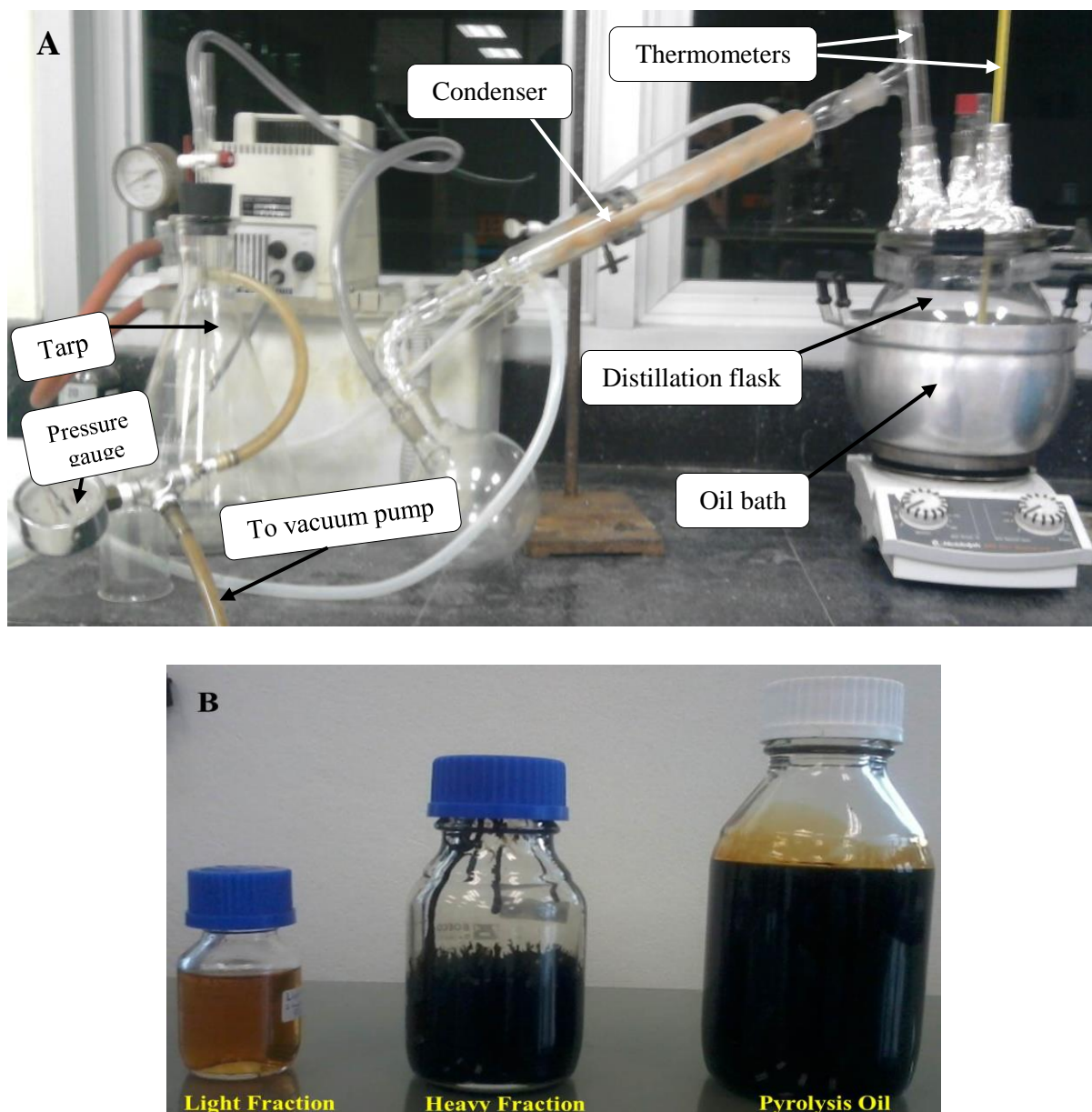


Figure 21. A) Conventional vacuum distillation assembly showing, B) Three fractions derived from the crude pyrolysis liquid

4.2 Catalytic cracking of pyrolysis oil derived from rubberwood to produce gasoline-range aromatics

This study intends to upgrade the first fraction (pyrolysis oil) to generate gasoline-range aromatics, i.e., benzene, toluene, ethylbenzene, and xylenes (BTEX), using a commercial HZSM-5 catalyst in a dual reactor (Figure 23). By investigating the effects of reaction temperature, catalyst weight, and nitrogen flow rate, it was demonstrated that the gasoline aromatics can be generated from the oil achieving a concentration approaching 27 wt% in the organic liquid product (OLP), as the OLP achieved a maximum yield of 13.6

wt%. Furthermore, experiments were conducted at the simulated optimum conditions to validate their accuracy. It was found that the yield of OLP was 15 wt% compared to the 13.6 wt% simulated value, and the percentage of gasoline aromatics was 30 wt% compared to 27 wt%. More discussion of this part has been written in the publication attached in Appendix B.

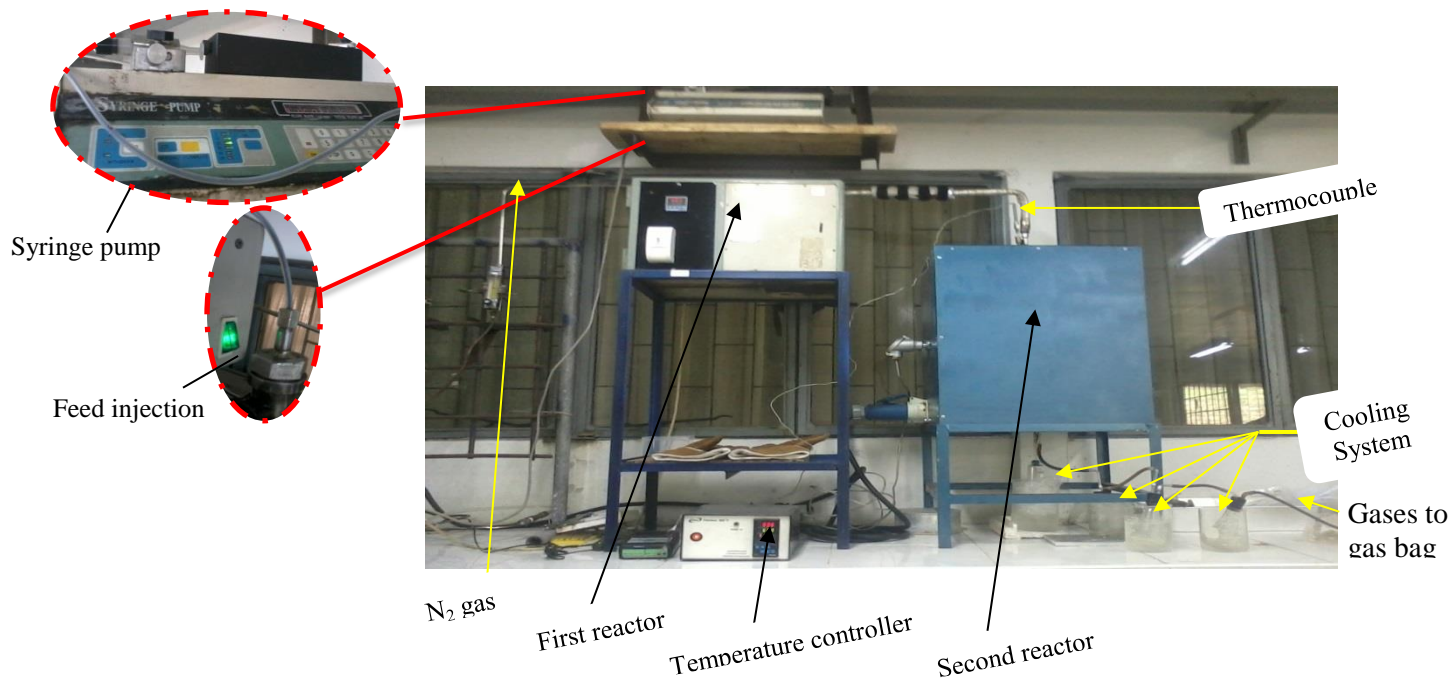


Figure 23. Dual reactor setup

The following points are not included into the attached paper (Appendix B). Therefore, they will be briefly addressed in this section.

4.2.1 Characterization of the commercial zeolite catalyst

The HZSM-5 catalyst used in the current study was prepared by calcining the $\text{NH}_4\text{-ZSM-5}$ form to remove the ammonia. Calcination was performed at 550 °C for 5 h in a stream of nitrogen. Three methods were used to identify and characterize the structure and composition of the catalyst. These methods are X-ray diffraction analysis, scanning electron microscopy and infrared spectroscopy.

4.2.1.1 X-Ray Diffraction (XRD) Analysis

XRD is used to fingerprint the zeolite catalyst. The structure and composition were identified using XRD; X'Pert MPD, PHILIPS, and crystal size was estimated by using Sherrer's equation. (Calculation of crystal size was mentioned in Appendix G). It was found that the crystal size of the commercial catalyst is 59 nm.

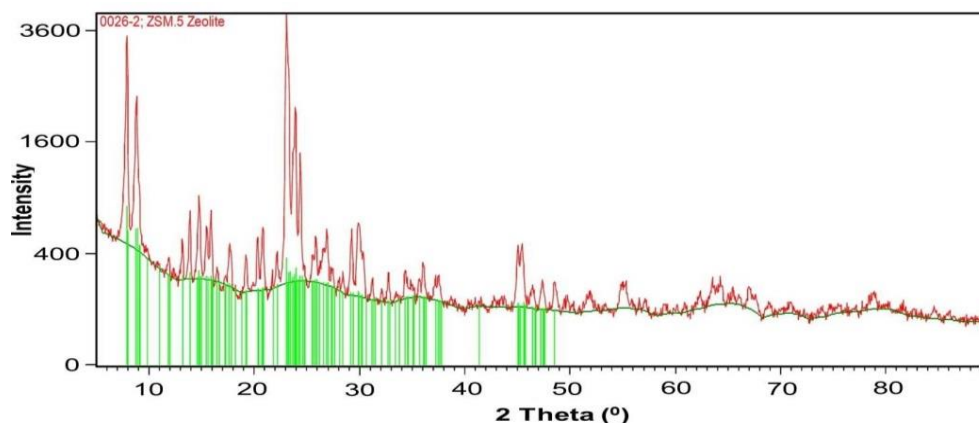


Figure 24. XRD pattern of HZSM-5 catalyst

4.2.1.2 Scanning Electron Microscopy (SEM)

The SEM was used to characterise the morphology of the particle and is taken for directly measuring the particle size. The morphology and particle sizes were identified from the (SEM) image taken with a JSM-5800 LV, JEOL, as depicted in Figure 25. The particle sizes here are the aggregations of crystal sizes which ranged approximately from 0.05 μm to 0.13 μm .

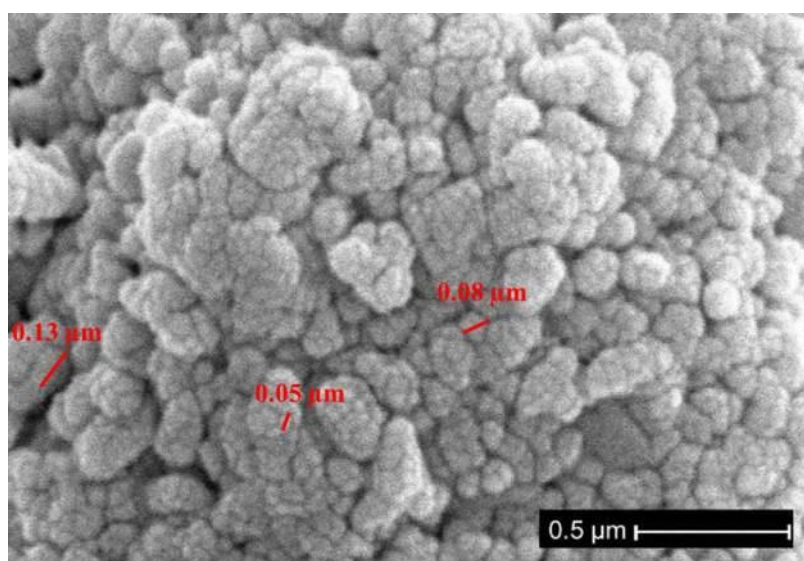


Figure 25. SEM image for HZSM-5 catalyst

4.2.1.3 Fourier-Transform Infrared (FTIR)

The FTIR spectra were collected using (EQUINOX 55, Bruker, Germany) FTIR spectroscopy, using in house method (WI-RES-FTIR-001). The spectra wave number covered a range from 4,000 to 400 cm^{-1} . The pellets of potassium bromide (KBr) were

prepared and tested in the FTIR spectrometer. The Brønsted and Lewis acid sites of the catalyst were determined using pyridine as a probe molecule. Figure 26 shows FTIR of adsorbed pyridine, which identifies the acid sites. As shown in the Figure, the catalyst displayed bands at 1490 cm^{-1} due to the pyridine associated with both Brønsted and Lewis acid sites. The exhibited bands at 1445 cm^{-1} was attributed due the weakly Lewis bound pyridine and that of 1545 cm^{-1} was assigned to pyridinium ion adsorbed on Brønsted acid sites [94].

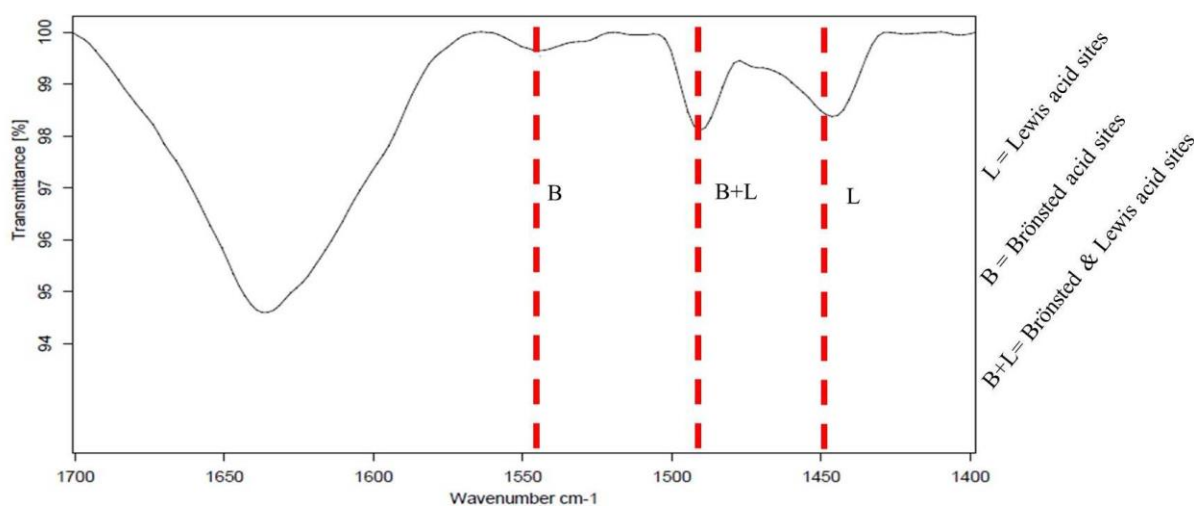
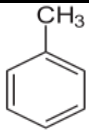
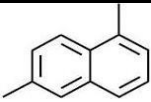
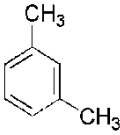
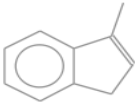
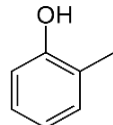
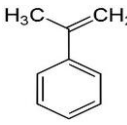
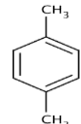
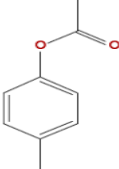
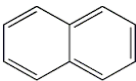
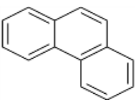
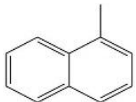
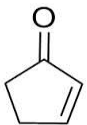
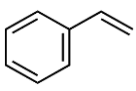
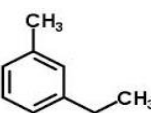
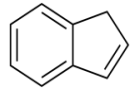
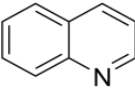
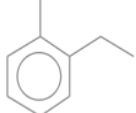
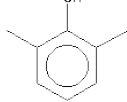


Figure 26. FFT-IR spectra of pyridine adsorbed in a commercial HZSM-5 after pyridine adsorption and evacuation at $150\text{ }^{\circ}\text{C}$

4.2.2 Chemical composition of the OLP identified by GC-MS

The chemical compositions shown in Tables 4 and 5 were identified by GCMS for the OLP produced in the optimum condition of (1) the highest OLP yield and (2) the highest percentage of gasoline aromatics respectively. As shown in the tables, it was found that other deoxygenated aromatic compounds were produced beside the BTEX. The former compounds are potentially interesting as they have high octane ratings [95]; Appendix E. As depicted in Table 4, the deoxygenated aromatics generated are dominated in the OLP and are more than those in Table 5. The OLP was produced in the optimum condition of $595\text{ }^{\circ}\text{C}$ temperatures, 5 gram of catalyst and mL/min N_2 flow rate. These conditions are capable to deoxygenate more compounds to form aromatic compounds. In contrast, the OLP produced at the condition of the highest OLP yield, i.e., $511\text{ }^{\circ}\text{C}$ temperature, 3.2 gram catalyst and 3 mL/min N_2 rate gained lower aromatic compounds but higher yield of OLP.

Table 4. Chemical composition at the optimum condition of the highest percentage of gasoline fraction

Compounds	Structure	Area %	Compounds	Structure	Area %
Toluene		5.90	Naphthalene, 1,6-dimethyl-		1.12
m-Xylene		5.17	1H-Indene, 3-methyl-		1.07
Phenol, 2-methyl-		4.46	Benzene, (1-methylethenyl)-		1.05
p-Xylene		4.40	Acetic acid, 4-methylphenyl ester		1.02
Naphthalene		4.00	Phenanthrene		0.96
Naphthalene, 1-methyl-		3.90	2-Cyclopenten-1-one		0.95
Styrene		3.50	Benzene, 1-ethyl-3-methyl-		0.94
Inden		3.48	Quinoline		0.84
Benzene, 1-ethenyl-2-methyl-		3.35	Phenol, 2,6-dimethyl-		0.77

4.2.3 Thermal cracking of the pyrolysis oil

The conversion of pyrolysis oil was investigated independently without the catalyst. It was observed that the yield of OLP and the gasoline aromatics in OLP derived from the thermal cracking of the pyrolysis oil are quite different from that of catalytic

cracking of pyrolysis oil using the zeolite catalyst as shown in Table 6. The increased OLP yield and aromatics with adding zeolite catalyst is the major difference. The thermal cracking of pyrolysis oil generated only small amount of aromatics and low yield of OLP.

From the results, it can be suggested that the thermal cracking is dominated by the decomposition of the bulky compounds to lighter ones. In contrast, the catalytic cracking and deoxygenation can convert the oxygenates of pyrolysis oil to aromatics (BTEX) using zeolite catalyst.

Table 5. Chemical composition at the optimum condition of the highest OLP yield

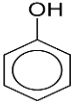
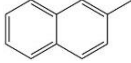
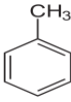
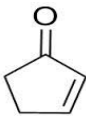
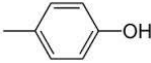
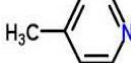
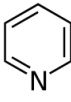
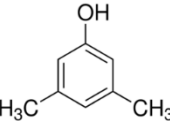
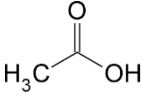
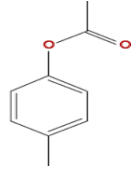
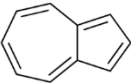
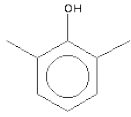
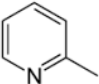
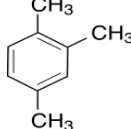
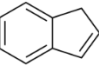
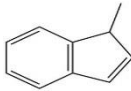
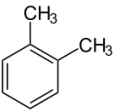
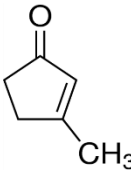

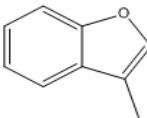
Compounds	Structure	Area %	Compounds	Structure	Area %
Phenol		14.9 4	Naphthalene, 2-methyl-		0.86
Toluene		6.85	Cyclopentenone		0.85
Phenol, 4-methyl-		5.77	Pyridine, 4-methyl-		0.69
Pyridine		4.67	Phenol, 3,5-dimethyl-		0.67
Acetic acid		3.52	Acetic acid, 4-methylphenyl ester		0.66
Cyclopentacycloheptene		3.10	Phenol, 2,6-dimethyl-		0.55
Pyridine, 2-methyl-		2.54	Benzene, 1,2,4-trimethyl		0.55
Inden		2.48	1H-Indene, 1-methyl-		0.53
Benzene, 1,2-dimethyl-		2.33	2-Cyclopenten-1-one, 3-methyl-		0.50
Triphenylene		1.97	3-Methylbenzofuran		0.49

Table 6. Comparison between thermal and catalytic cracking of the pyrolysis oil using three different conditions

Experimental design			Results			
Temperature °C	Catalyst g	N ₂ flow rate mL/min	OLP yield		Percentage of gasoline aromatics in OLP	
			Catalytic	Thermal	Catalytic	Thermal
400	3	10	11.07		0.57	
400	-	10		0.50		0.087
500	3	6.5	13.33		18.06	
500	-	6.5		1.65		1.00
600	3	3.0	11.40		22.02	
600	-	3.0		3.50		2.80

4.3 Catalytic conversion of pyrolysis tar to produce green gasoline-range aromatics

In this part, another fraction (pyrolysis tar) was also upgraded to generate gasoline-range aromatics, i.e., benzene, toluene, ethylbenzene, and xylenes (BTEX). The pyrolysis tar was isolated by decantation from the crude pyrolysis liquid after being settled for a period of time. The gasoline aromatics were generated from the pyrolysis tar through catalytic cracking using the HZSM-5 catalyst. By analysing the effects of reaction temperature, catalyst weight, and nitrogen flow rate, it was verified that the gasoline-range aromatics can be generated from the pyrolysis tar attaining a concentration approaching 54 wt% in the organic liquid product (OLP), as the OLP achieved a maximum yield of 28.33 wt%. The details of this part are written in the publication as attached in Appendix C.

The following points are not included into the attached paper (Appendix C). Therefore, they will be briefly addressed in this section.

4.3.1 Chemical composition of the organic liquid products identified by GC–MS

Pyrolysis tar can be regarded as an aromatic source (Table 1 in Appendix C) which can be more adaptable to produce gasoline range aromatics. As expected, the pyrolysis tar produced more aromatics than the pyrolysis oil as can be seen in Tables 7 and 8. The chemical compositions shown in Tables are determined by GCMS for the OLP produced in the optimum condition of (1) the highest OLP yield and (2) the highest percentage of gasoline aromatics respectively. As depicted in Table 7, the aromatic compounds has less percentage of oxygenates, i.e, benzofurans, 3-Methyl-benzofuran, 1,4,5-Trimethylnaphthalene, xylenol, phenol, methylantracene, naphthol that those in Table 8. However, the OLP analysed in

Table 8 has higher yield. The results of GCMS indicated that in addition to the deoxygenated aromatics compounds which can be used as high octane fuel additives in gasoline, the oxygenates could also be used as chemicals in other applications such as resin industry. More discussion on the conditions and conversion of pyrolysis tar to aromatics were explained in the attached publication (Appendix C).

4.3.2 Thermal cracking of the pyrolysis tar

An investigation was also performed for the conversion of pyrolysis tar separately without the catalyst. It can be seen that the OLP yield and the aromatics in OLP derived from the thermal cracking are also different to a great extent from the catalytic cracking with the zeolite catalyst Table 9.

Table 7. Chemical composition at the optimum condition of the highest percentage of gasoline fraction

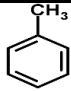
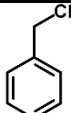
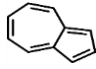
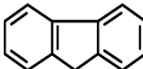
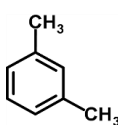
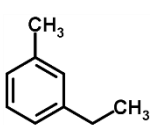
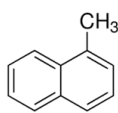
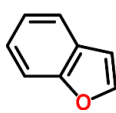
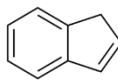
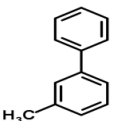
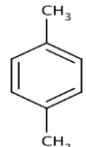
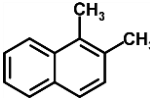
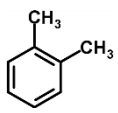
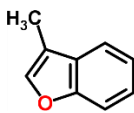
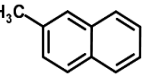
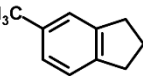
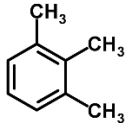
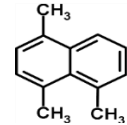
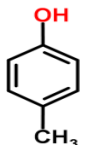
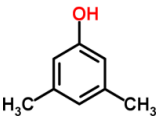
Compounds	Structure	Area %	Compounds	Structure	Area %
Toluene		22.3	Ethylbenzene		0.57
Azulene		8.43	Fluorene		0.55
m-Xylene		7.78	m-Ethyltoluene		0.54
1-Methylnaphthalene		7.68	Benzofuran		0.46
1H-Indene		4.27	3-Methylbiphenyl		0.46
p-Xylene		3.65	1,2-dimethyl naphthalene		0.40
o-Xylene		3.53	3-Methyl-benzofuran		0.40
2-Methylnaphthalene		3.01	5-Methylindan		0.34
1,2,3-Trimethylbenzene		2.74	1,4,5-Trimethylnaphthalene		0.34
p-Cresol		2.47	3,5-Xylenol		0.32

Table 8. Chemical composition at the optimum condition of the highest OLP yield

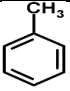
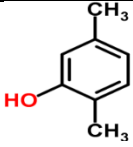
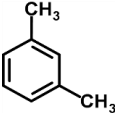
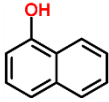
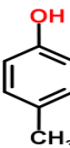
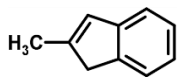
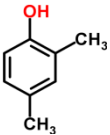
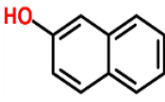
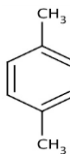
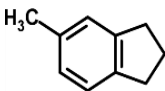
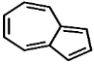
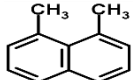
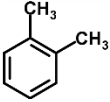
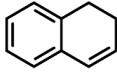
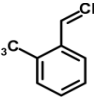
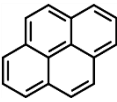
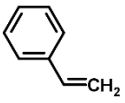
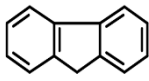
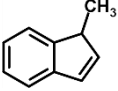
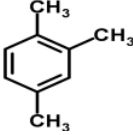
Compounds	Structure	Area %	Compounds	Structure	Area %
Toluene		25.76	2,5-Xylenol		0.55
m-Xylene		7	1-Naphthol		0.53
o-Cresol		6	2-Methyl-1H-indene		0.48
2,4-Xylenol		4	2-Naphthol		0.42
p-Xylene		4	5-Methylindan		0.39
Azulene		3.97	1,8-Dimethylnaphthalene		0.38
o-Xylene		3.91	1,2-Dihydronaphthalene		0.35
o-Methylstyrene		2.90	Pyrene		0.35
Styrene		2.72	Fluorene		0.31
1-Methylindene		2.42	1,2,4-Trimethylbenzene		0.31

Table 9. Comparison between thermal and catalytic cracking of the pyrolysis tar using three different conditions

Experimental design			Results			
Temperature °C	Catalyst g	N ₂ flow rate mL/min	OLP yield		Percentage of gasoline aromatics in OLP	
			Catalytic	Thermal	Catalytic	Thermal
400	3	10	18.30		9.90	
400	-	10		0.45		0.18
500	3	6.5	27.50		41.53	
500	-	6.5		2.12		0.34
600	3	3.0	24.35		50.65	
600	-	3.0		3.80		1.50

4.4 Comparative study for catalytic conversion of pyrolysis oil and tar derived from rubberwood to produce green gasoline-range aromatics

The purpose of this study is to compare the conversion of pyrolysis oil and tar derived from rubberwood to gasoline-range aromatics. In this study the conversion was investigated in terms of product distribution and the concentration of gasoline aromatics in organic liquid products (OLPs). It has been shown that the OLP obtained from tar featured a higher concentration of gasoline aromatics, approaching 54 wt%, whereas the OLP from pyrolysis oil exhibited a lower concentration, about 27 wt%. On the other hand, the OLP obtained from tar featured greater yields, with a maximum value of 28.33 wt%, compared to the OLP from pyrolysis oil, which gave a maximum yield of 13.6 wt%. In assessing the conversion of pyrolysis oil and tar, from the findings it can be demonstrated that tar is much more attractive as a potential alternative feedstock for green gasoline, since it contained high concentrations of BTEX aromatics in the OLP. More detailed results and discussion of this section are clarified on the publication as attached in Appendix D.

4.5 Catalytic conversion of heavy fraction of the pyrolysis oil to generate gasoline-range aromatics

In this part, the heavy fraction of the pyrolysis oil was used to generate gasoline aromatics. The heavy fraction was isolated from the vacuum distillation of the pyrolysis oil that was derived from rubberwood. The obtained heavy fraction was a dark-

black and a high viscous liquid. It has a high heating value and low water content comparing with the light fraction and the pyrolysis oil. The detailed heavy fraction isolation procedure and the physiochemical properties were described in our previous paper (Appendix A). The experimental runs were performed under different temperatures, catalysts weights and N₂ flowrates, same as those designed in the previous papers (Appendix B, C and D). Also, the detailed description of the dual reactor system could be found in the same papers.

As the heavy fraction was very viscous, 5% of ethanol was added to the sample prior to feed in the reactor.

4.5.1 Product distribution

Six products were generated from catalytic cracking of the heavy fraction, i.e., OLP, an aqueous product, char, tar, coke, and non-condensable gases as provided in Table 10.

Significant amount of chars were produced in this fraction comparing with the pyrolysis oil and tar due to the thermal effect on the fraction components and also possibly due to the existence of some carbon in the fraction (this probably occurred during the distillation process). The yield of char ranged from about 29 to 35 wt % as shown in the Table, and there was a slight decrease in the char formation with the increase of temperature, due to secondary reactions occurring. In addition the aqueous products (water content from 75-78 wt%) also obtained high yields ranged from about 25 to 37 wt %, indicating that oxygen was removed in a water form. The OLP ranged from about 5-10 wt % over the experimental runs. The maximum yield of OLP was about 10 wt% observed at 400 °C with 5 grams of catalyst. In this fraction a very low yield of OLP was observed as compared to the previous fractions. It can be suggested that the heavy fraction contained many carbons; the rest are oxygenates (Table 4, Appendix A) and the added ethanol, therefore the obtained OLP was only produced from the reaction of oxygenates and ethanol.

Table 10. Overall product distribution (wt% of the feed) for the 15 experimental runs

Run	Factors			OLP	Aqueous	Char ^a	Residue ^b	gas	Unaccounted ^c
	Temp	catalyst	Gas flowrate	Products (wt%)					
1	400	1	6.5	5.0	28.6	33.3	13.3	3.7	16
2	400	3	3	9.2	25.4	33.3	12	4.3	15.8
3	400	3	10	8.6	25.9	34.7	12	4.2	14.6
4	400	5	6.5	10.4	25.3	34.0	11.3	4.9	14.1
5	500	1	3	6.7	28.0	32.0	11.3	5.0	17.0
6	500	1	10	6.0	30.0	32.0	12	5.0	15.0
7	500	3	6.5	8.9	28.7	31.3	10.7	5.3	15.0
8	500	3	6.5	8.0	29.0	32.0	10.7	5.3	15.0
9	500	3	6.5	8.4	28.5	31.3	10	5.4	16.3
10	500	5	3	7.7	31.4	31.3	11.3	5.8	12.4
11	500	5	10	7.0	31.9	32.0	11.3	5.7	12.0
12	600	1	6.5	7.6	34.1	28.7	10.7	6.0	13.0
13	600	3	3	6.7	34.7	30.0	10	6.1	12.5
14	600	3	10	5.7	35.3	28.7	10.7	6.2	13.4
15	600	5	6.5	5.3	38.0	29.3	10	6.3	11.0

^a Char formed in the first reactor.

^b Residue is categorized as char and tar that were quantified in the second reactor.

^c The unaccounted part includes some liquids that were transferred from the first reactor via the tube to the second reactor and some tar deposits in the fitting.

4.5.2 Content of gasoline-range aromatics in OLP

As shown in Table 11, the percentage of gasoline aromatics in OLP ranged from about 1 to 43 wt%, with a maximum value of about 43 wt% at 500 °C, 5 g of catalyst and 3 mL/min of N₂ gas. As a known effect, the formation of aromatic compounds in this heavy fraction is attributed to the conversion of oxygenated compounds, principally substituted phenolic compounds and the ethanol which was added initially to the fraction before reaction by decarbonylation, cracking, dehydroxylation and decarboxylation reactions which are catalysed by HSZM-5's acid sides.

4.5.3 Optimization

The main interests in this study were OLP and the gasoline aromatics in the OLP; hereafter we reported results of the influences of the three variables on the OLP yield and the percentage of gasoline aromatics. We applied the response surface methodology (RSM) to predict the optimum values of the three variables. A mathematical model was developed based on the experimental design performed initially by Essential Regression software. Additionally, as can be seen in Figure 27 the values for OLP yield and gasoline aromatics were in good agreement with the experimental results, confirming the fitness of the model, as indicated by the determination coefficients (R^2) of 0.93 and 0.88 for the model's predictions of OLP yield and gasoline aromatics, respectively.

Table 11. Composition of gasoline aromatics in the OLP

<i>Runs</i>	Benzene	Toluene	Ethyl benzene	Xylenes^a	(gasoline aromatics)^b
	wt%				
1	0.00	0.20	0.23	0.57	1.00
2	1.81	6.49	0.55	4.99	13.84
3	0.30	2.03	0.68	7.15	10.16
4	11.57	0.71	0.62	1.53	14.43
5	0.47	1.58	0.08	0.65	2.78
6	0.00	0.098	0.05	1.56	1.71
7	6.26	15.17	0.15	11.42	33.00
8	10.32	17.34	0.53	3.89	32.08
9	0.65	4.62	0.00	27.42	32.69
10	0.40	22.13	2.84	17.34	42.71
11	0.95	22.51	0.49	16.23	40.18
12	0.11	1.53	0.14	0.01	1.79
13	0.15	6.49	4.91	0.011	11.56
14	0.026	4.55	5.86	0.003	10.44
15	0.01	15.58	0.48	5.54	21.61

^a Xylenes= *p. xylene*, *m. xylene*, *o. xylene*

^b Summation of BTEX

The reaction conditions were optimized, and the results showed that the maximum yield of OLP was about 11 wt% for a temperature of 400 °C and a catalyst weight of 5 g. Correspondingly, the maximum percentage of gasoline aromatics was about 38 wt%, obtained at 600 °C and a catalyst weight of 5 g. The interaction effects of the significant variables on the OLP yield and percentage of gasoline aromatics are displayed in the three-dimensional (3D) response surfaces and their corresponding 2-D contours as shown in Figure 28. The response surface was performed to get the optimal levels of the parameter of the maximum OLP response and maximum percentage of gasoline aromatics at the highest point of the surface.

Figure 28 (A) shows the mutual effects of the catalyst weight and temperature on the yield of OLP. The highest yield of OLP was achieved at around 5 g of catalyst and 400 °C, and then decreased gradually to almost 5 wt% with the increase of the catalyst until 1 g at the same temperature. This might be occurred due to fewer cracking of the heavy fraction. In addition to that, the mutual effects of the catalyst weight and temperature on the percentage of aromatics were illustrated in Figure 28 (B). This Figure indicates that a small drop in aromatics percentage happened with the decrease of catalyst weight from 5 g to 3 g; yet a high decrease of aromatic percentage was occurred at a very low weight of the catalyst.

It was observed that some values of aromatics percentage placed beyond the independent variables as shown in Figure 28 (B). This indicates that an additional improvement of the conditions is needed.

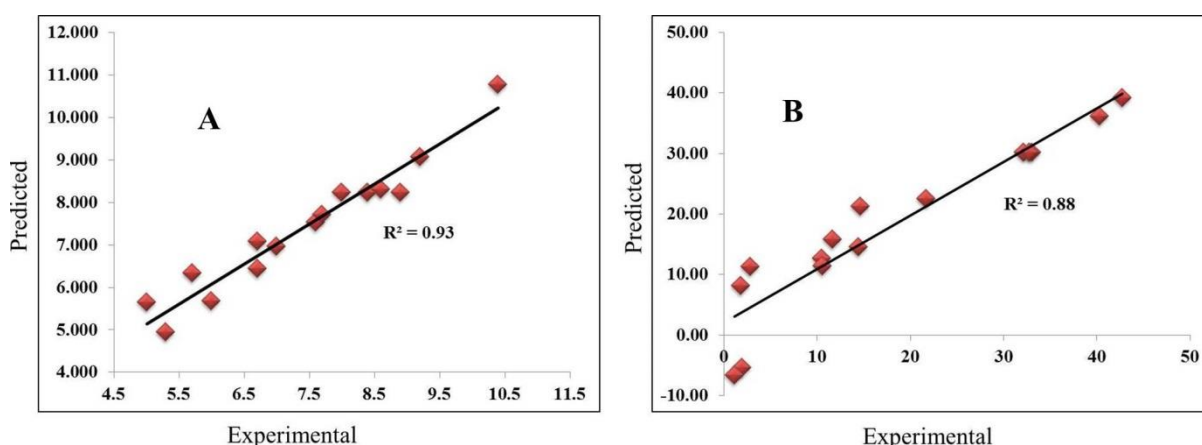


Figure 27. Experimental results versus predicted values of (A) OLP yield and (B) gasoline aromatics (%) in OLP

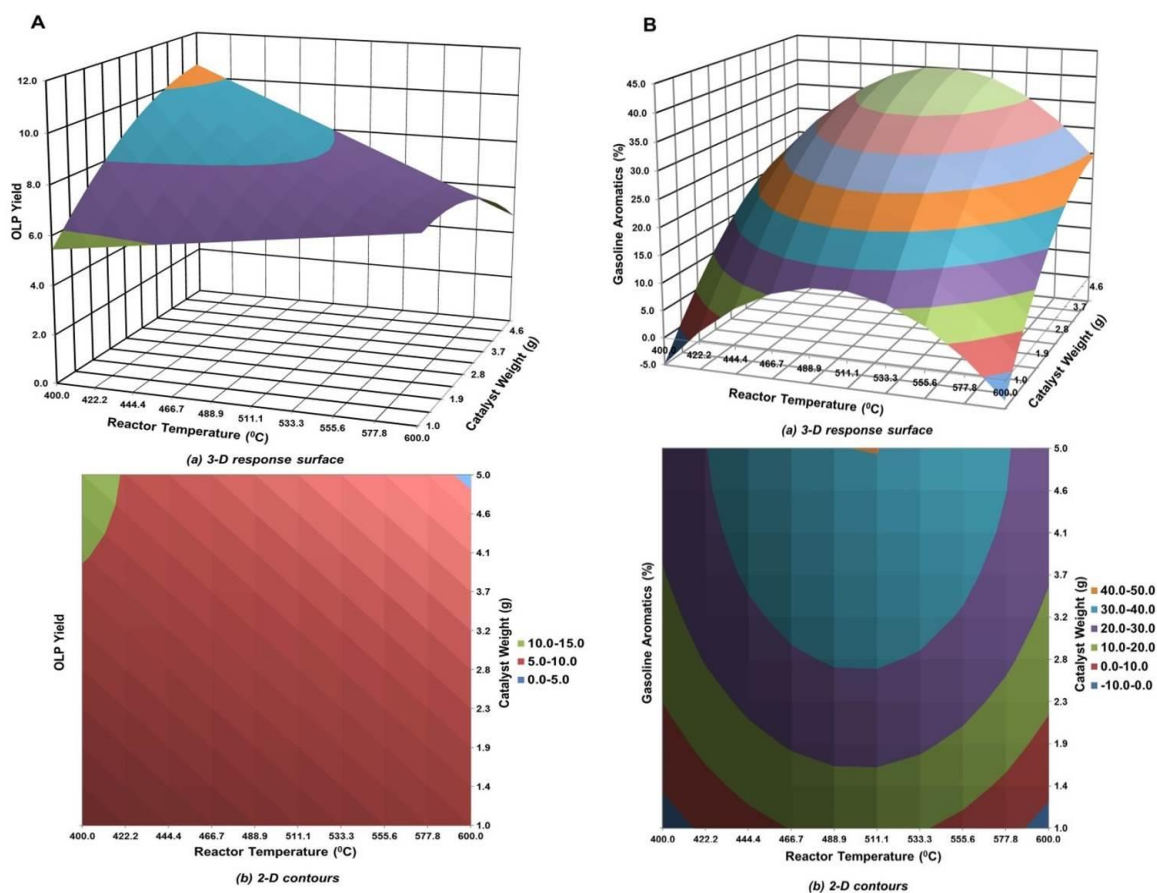


Figure 28. Surface plot of: (A) OLP yield and (B) gasoline aromatics (%) in OLP as functions of catalyst weight and reactor temperature

The validation of the predicted results was performed by conducting experimental runs with the optimum conditions, as shown in Table 12. The OLP yield was found to be 13 wt%, whereas the predicted value was 11 wt%. In a corresponding manner, the actual percentage of gasoline aromatics was about 49 wt% compared to the predicted value of 38 wt%. The compositions of aromatics in OLPs were identified as listed in Table 12. It was found that a remarkable concentration of toluene about 21wt% was formed and there was a low concentration of ethylbenzene about 21wt%. Furthermore, it was observed that the benzene concentration was about 8 wt%, somewhat less than those of toluene and xylenes, possibly due to the easy alkylation of benzene on the acidic HSZM-5 catalyst.

Table 12. Predicted and experimental results at optimum conditions

	Predicted	Experiment	Optimum conditions		
			Temperature (°C)	Catalyst weight (g)	N ₂ flow rate (mL/min)
OLP yield (wt%)	11	13	400	5	5
Percentage of gasoline aromatics (wt%)	38	49	600	5	-

Table 13. Gasoline aromatics content in OLP at optimum conditions

	wt%
Benzene	8.33
Toluene	21.00
Ethylbenzene	0.50
Xylenes	19.50
Total	49.30

4.6 Catalytic conversion of the three fractions over prepared nanocrystalline HZSM-5 zeolite and compared with the commercial catalyst

It has been known that zeolites have potential catalytic applications for different molecular transformations due to their porosity, shape-selectivity and tunable acidity. Among these, the ZSM-5 zeolite of MFI structural type has been successfully exploited for producing hydrocarbons not only from petroleum but also from different types of biomass feedstocks. It has the advantage of shape selectivity which is appropriate for generating range aromatics such as toluene, benzene, and xylenes). Extending zeolite's applications, latest researches are focused on the catalyst development for conversion of biomass into different hydrocarbons. As it is known, porosity is considered a vital property of ZSM-5 that enables the adsorption–desorption and diffusion behavior of the molecules. Accordingly, recent studies expose the advantage of decreasing the zeolite crystal size for the conversion of ethanol, where the additional porosity created in the nano crystal size delivers stage for greater diffusion properties [96].

In this study the catalytic conversion of the three fractions, i.e., pyrolysis oil, heavy fraction and pyrolysis tar was carried out using nanocrystalline HZSM-5zeolite prepared following the method reported by Van Grieken et al [80]. The procedure is summarized as shown in

Figure 29. In addition, the characterization of the catalyst was performed using X-ray diffraction analysis, scanning electron microscopy and infrared spectroscopy as explained below:

4.6.1 X-Ray Diffraction (XRD) Analysis

XRD is used to fingerprint the nanocrystalline zeolite catalyst. The structure and composition were identified using XRD; X'Pert MPD, PHILIPS, and crystal size was estimated by using Sherrer's equation. (Calculation of crystal size was mentioned in Appendix G). It was found that the crystal size of the nanocrystalline catalyst is 45 nm.

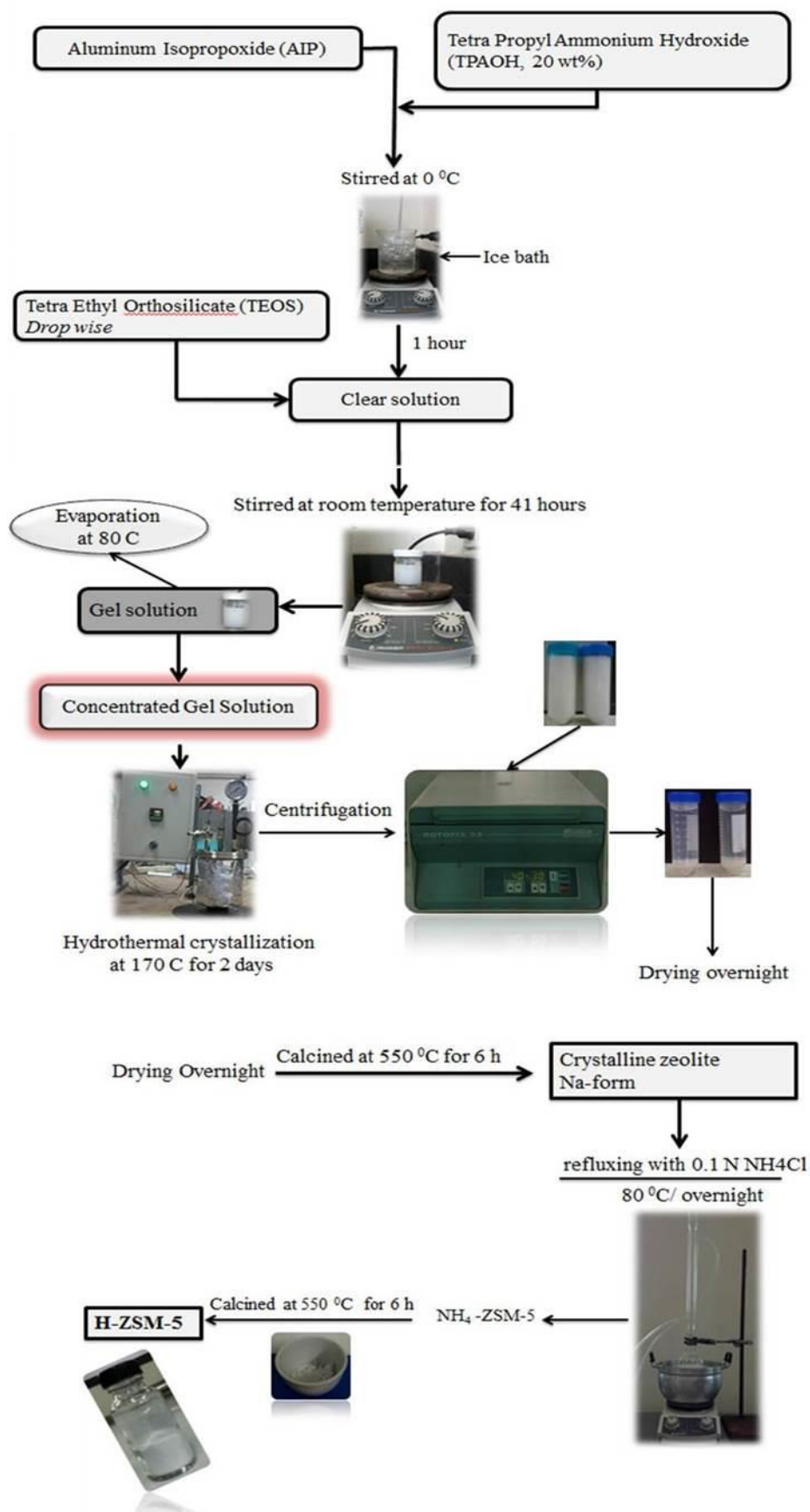


Figure 29. Preparation of nanocrystalline H-ZSM-5 using hydrothermal method

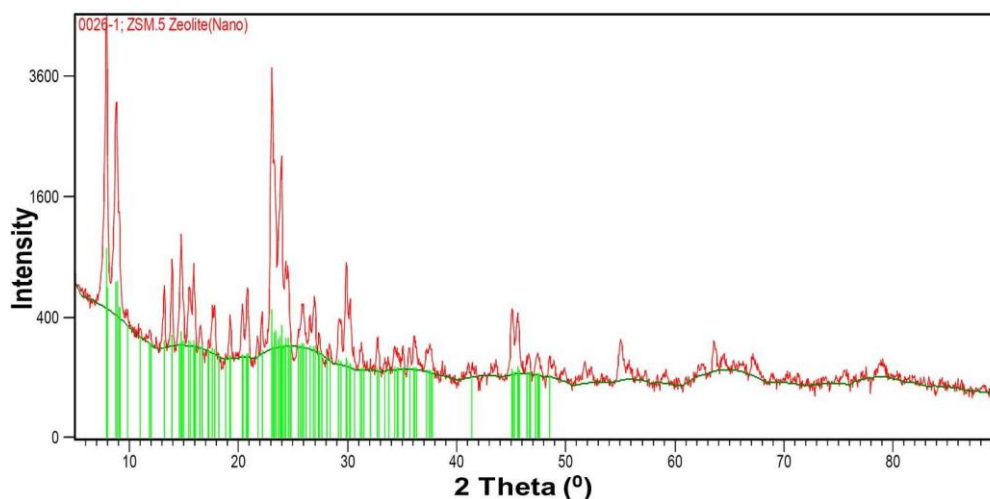


Figure 30. XRD pattern of nanocrystalline HZSM-5

4.6.2 Scanning Electron Microscopy (SEM)

The SEM was used to characterise the morphology of the particle and is taken for directly measuring the particle sizes which ranged approximately from 0.1 μm to 0.2 μm as shown Figure 31. The particle sizes and morphology were identified from the (SEM) image taken with a JSM-5800 LV, JEOL, as depicted in Figure 31.

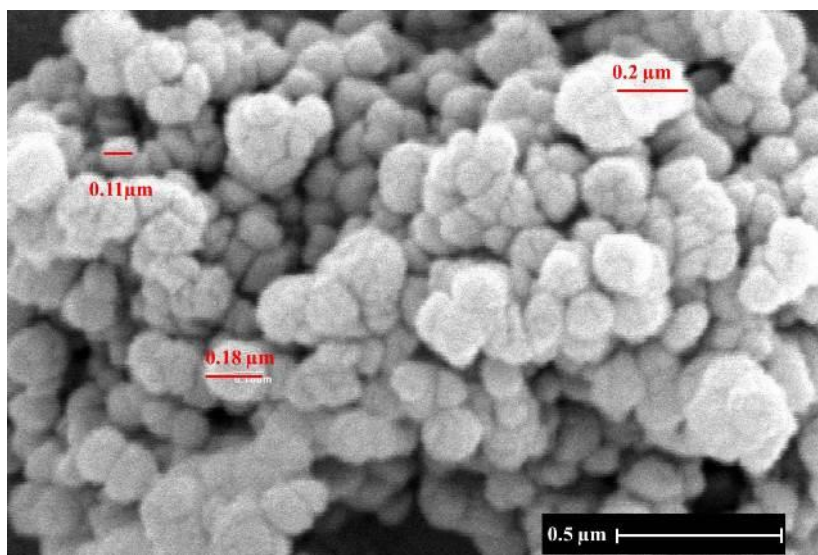


Figure 31. SEM image for nanocrystalline HZSM-5

4.6.3 Fourier-Transform Infrared (FTIR)

The FTIR spectra were collected using (EQUINOX 55, Bruker, Germany) FTIR spectroscopy, using in house method (WI-RES-FTIR-001). The spectra wave number covered a range from 4,000 to 400 cm^{-1} . The pellets of potassium bromide (KBr) were prepared and tested in the FTIR spectrometer. The Brønsted and Lewis acid sites of the catalyst were determined using pyridine as a probe molecule. Figure 32 shows FTIR of adsorbed pyridine, which identifies the acid sites.

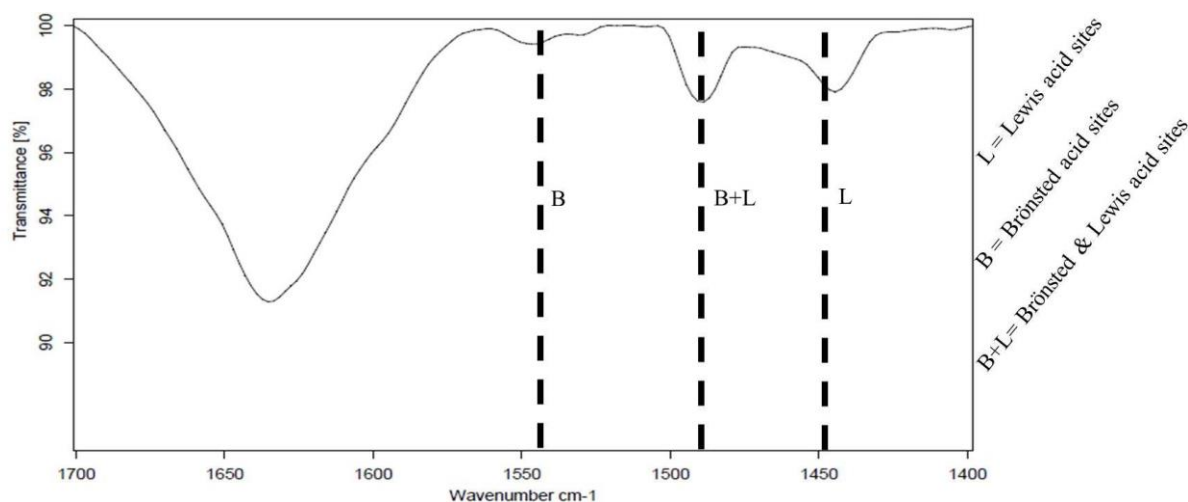


Figure 32. FFT-IR spectra of pyridine adsorbed in a nanocrystalline HZSM-5 after pyridine adsorption and evacuation at 150 °C

The main findings from the conversion of the three fractions were compared and described with the ordinary commercial catalyst.

The conversion of the three fractions using nano catalyst was conducted in the dual reactor with the same optimal conditions of each fraction, i.e., temperature, catalyst weight and N_2 flowrate.

4.6.4 OLP yields and the percentages of aromatics

The compositions of the OLPs, particularly (BTEX) aromatics were analysed by GC-FID, and Table 14 shows the distributions of the aromatic hydrocarbons for each fraction comparing with those produced by using the commercial catalyst. The identified aromatics indicated that the contents were dominated by toluene in both catalysts and had low amount of ethylbenzene.

The effect of the optimal operating parameters on the OLP yields and percentages of aromatics, are listed in Table 15. It was found that the OLPs obtained from the

three fractions exhibited higher yields with the nano catalyst, whereas the ordinary catalyst exhibited little lower yields. Correspondingly, the nano catalyst displayed higher aromatic percentages of 33 wt%, 51 wt% and 51.26 wt% for the pyrolysis oil, heavy fraction and tar respectively, while the aromatics percentages on the commercial catalyst were little lower as shown in Table 15.

The prepared nanocrystalline HZSM-5 zeolite showed a smaller crystal size as compared to the commercial catalyst, indicating that the nano catalyst would gain a higher additional surface area. This surface area is an important characteristic of the catalyst which promotes the diffusion behaviour of the molecules. As a result the nano catalyst in this study showed a higher performance producing higher yield of OLPS and higher concentration of aromatics in OLPs as depicted in Table 14, 15.

Table 14. Compositions of BTEX aromatics in the OLP for the three fractions using prepared nanocrystalline and commercial catalysts

Aromatics (wt%)	Pyrolysis oil		Heavy fraction		Pyrolysis tar	
	NC	CC	NC	CC	NC	CC
Benzene	4.19	5.16	6.18	8.33	6.92	8.15
Toluene	15.43	14.42	33.80	21.09	32.39	22.69
Ethylbenzene	1.13	0.58	1.06	0.55	2.26	4.03
Xylenes	11.81	9.84	9.59	19.52	9.69	13.25
NC: Prepared nanocatalyst						
CC: Commercial catalyst						

Table 15. Experimental results at optimum conditions for the three fractions using prepared nanocrystalline and commercial catalysts

	Pyrolysis oil		Heavy fraction		Pyrolysis tar	
	NC	CC	NC	CC	NC	CC
OLP yield (wt%)	16.47	15.00	15.00	13.00	27.00	25.25
Percentage of aromatics (wt%)	33.00	30.00	51.00	49.00	51.26	48.00
NC: prepared nanocatalyst						
CC: Commercial catalyst						

4.6.5 Chemical composition of the organic liquid products identified by GC–MS

The chemical composition of the OLPs was characterized using GC/MS and the relative percentage area of the compound was calculated. It was found that a large amount of deoxygenated aromatics were determined showing 81.59 % from total detected area of 89.54 % and the rest of compounds were phenolic compounds as in Table 16 for the pyrolysis oil's OLP analysed at the highest percentage of gasoline fraction. The OLP from heavy fraction showed 73.29 % of deoxygenated aromatics from total detected area of 88.96 % as in Table 17. The OPL from pyrolysis tar has the highest aromatics concentration of about 85 % from total area of about 90 % with a less amount of oxygenated compound with about 5% as in Table 18. On the other hand, the relative percentages of the deoxygenated compounds in the light OLPs yields were little lower as shown in Tables 19, 20 and 21.

Interestingly, the aromatic content from the three fractions using nano catalyst was higher than those produced by the ordinary catalyst. These aromatics are much in toluene and xylenes with small amount of ethylbenzene and benzene which makes the OLPs appropriate for gasoline applications.

Table 16. OLP composition of the pyrolysis oil at the optimum condition of the highest percentage of gasoline fraction

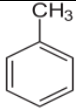
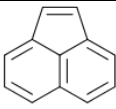
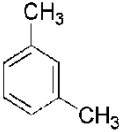
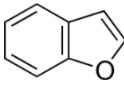
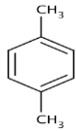
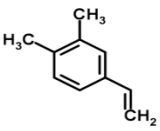
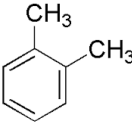
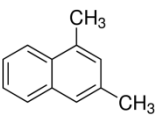
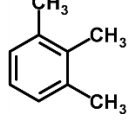
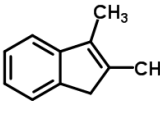
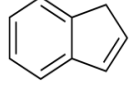
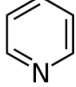
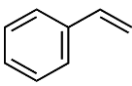
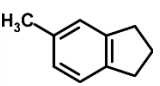
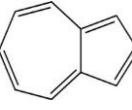
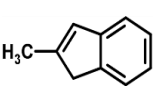
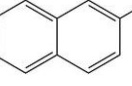
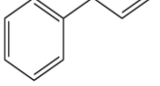
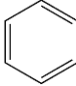
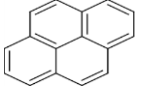
Compounds	Structure	Area %	Compounds	Structure	Area %
Toluene		13.58	Acenaphthylene		0.99
m-Xylene		10.06	Benzofuran		0.93
p-Xylene		6.35	3,4-Dimethylstyrene		0.86
o-Xylene		6.12	1,3-dimethyl naphthalene		0.84
1,2,3-trimethylbenzene		4.73	2,3-Dimethyl-1H-indene		0.64
Inden		4.04	Pyridine		0.58
Styrene		3.73	5-Methylindan		0.57
Azulene		3.56	2-Methyl-1H-indene		0.57
2-Methylnaphthalene		3.45	Propenylbenzene		0.48
Benzene		3.20	Pyrene		0.43

Table 17. OLP composition of the heavy fraction at the optimum condition of the highest percentage of gasoline fraction

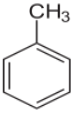
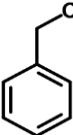
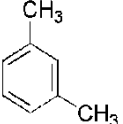
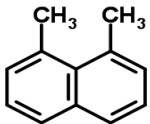
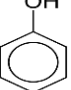
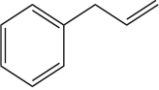
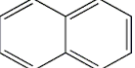
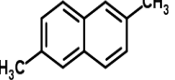
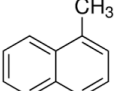
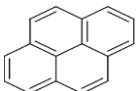
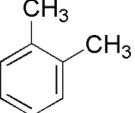
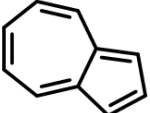
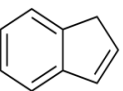
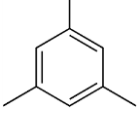
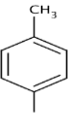
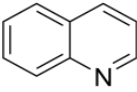
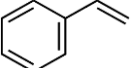
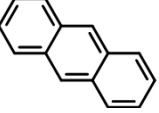
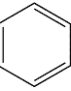
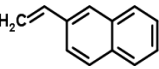
Compounds	Structure	Area %	Compounds	Structure	Area %
Toluene		15.04	Ethylbenzene		0.93
m-Xylene		7.23	1,8-Dimethylnaphthalene		0.88
Phenol		6.22	Propenylbenzene		0.83
Naphthalene		5.01	2,6-Dimethylnaphthalene		0.73
1-Methylnaphthalene		4.4	Pyrene		0.71
o-Xylene		4.34	Azulene		0.67
Inden		4.24	1,3,5-Trimethylbenzene		0.62
p-Xylene		3.79	Quinoline		0.57
Styrene		3.63	Anthracin		0.57
Benzene		3.0	2-Vinylnaphthalene		0.55

Table 18. OLP composition of the pyrolysis tar at the optimum condition of the highest percentage of gasoline fraction

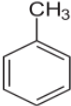
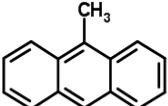
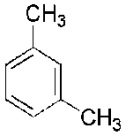
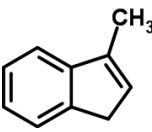
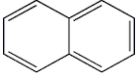
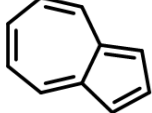
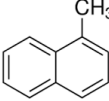
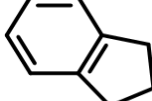
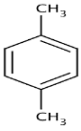
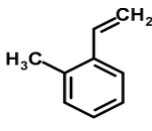
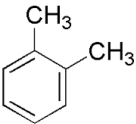
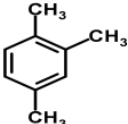
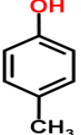
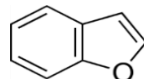
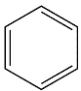
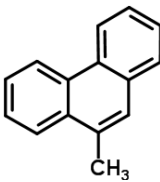
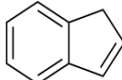
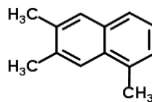
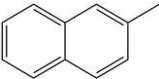
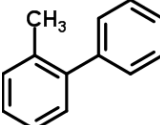
Compounds	Structure	Area %	Compounds	Structure	Area %
Toluene		10.64	9-Methylanthracene		1.32
m-Xylene		6.12	3-Methylindene		1.31
Naphthalene		5.61	Azulene		1.23
1-Methylnaphthalene		4.33	Indane		1.14
p-Xylene		4.19	o-Methylstyrene		1.1
o-Xylene		4.18	1,2,4-Trimethylbenzene		1.02
p-Cresol		3.5	Benzofuran		0.98
Benzene		3.43	9-Methylphenanthrene		0.86
Inden		2.98	2,3,5-Trimethylnaphthalene		0.79
2-Methylnaphthalene		2.7	2-Methylbiphenyl		0.79

Table 19. OLP composition of the pyrolysis oil at the optimum condition of the highest OLP yield

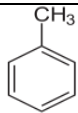
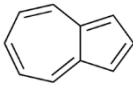
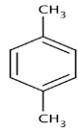
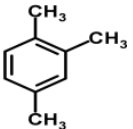
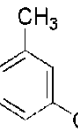
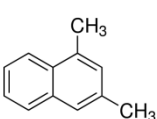
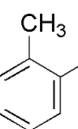
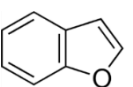
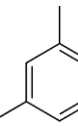
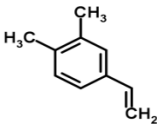
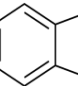
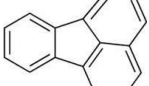
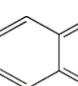
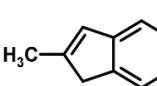
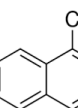
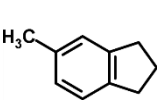
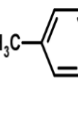
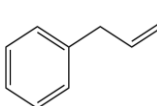
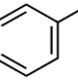
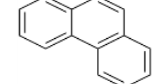
Compounds	Structure	Area %	Compounds	Structure	Area %
Toluene		12.15	Cyclopentacycloheptene		1.15
P-xylene		8.68	1,2,4-Trimethylbenzene		1.09
m-Xylene		5.37	1,3-dimethyl naphthalene		0.97
o-Xylene		5.01	Benzofuran		0.96
1,3,5-trimethylbenzene		4.29	3,4-Dimethylstyrene		0.95
Inden		4.07	Fluoranthene		0.86
Naphthalene		4.07	2-Methyl-1H-indene		0.79
1-Methylnaphthalene		4.01	5-Methylindan		0.75
m-Methylstyrene		3.93	Propenylbenzene		0.52
Styrene		3.62	Phenanthren		0.50

Table 20. OLP composition of the heavy fraction at the optimum condition of the highest OLP yield

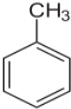
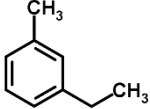
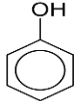
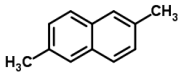
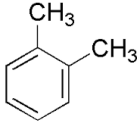
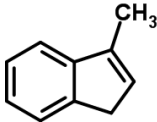
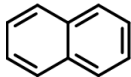
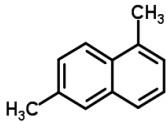
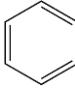
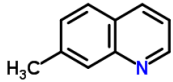
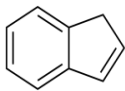
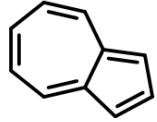
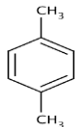
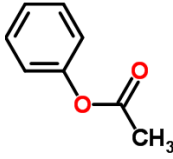
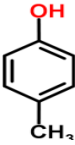
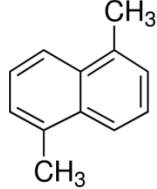
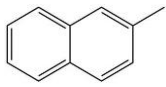
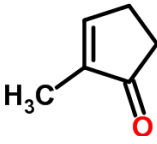
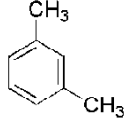
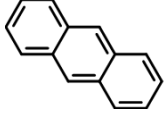
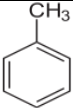
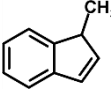
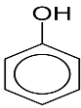
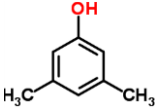
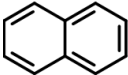
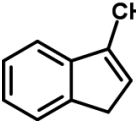
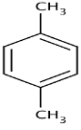
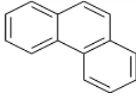
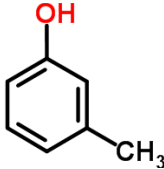
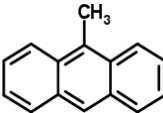
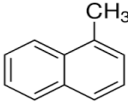
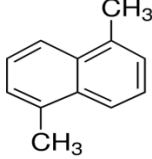
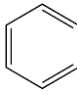
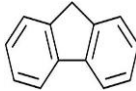
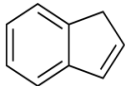
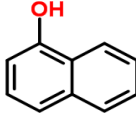
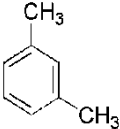
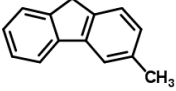
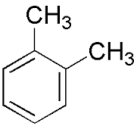
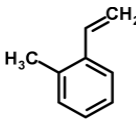
Compounds	Structure	Area %	Compounds	Structure	Area %
Toluene		21.14	m-Ethyltoluene		0.61
Phenol		9.5	2,6-Dimethylnaphthalene		0.60
o-Xylene		5.99	3-Methylindene		0.58
Naphthalene		4.62	1,6-Dimethylnaphthalene		0.55
Benzene		4.10	7-Methylquinoline		0.52
Inden		3.73	Azulene		0.51
p-Xylene		3.32	Phenyl acetate		0.46
p-Cresol		3.18	1,5-Dimethylnaphthalene		0.44
2-Methylnaphthalene		3.07	2-Methyl-2-cyclopentenone		0.44
m-Xylene		2.76	Anthracin		0.42

Table 21. OLP composition of the pyrolysis tar at the optimum condition of the highest OLP yield

Compounds	Structure	Area %	Compounds	Structure	Area %
Toluene		22.07	1-Methylindene		0.93
Phenol		9.03	3,5-Xylenol		0.81
Naphthalene		6.02	3-Methylindene		0.78
p-Xylene		5.35	Phenanthren		0.75
m-Cresol		4.96	9-Methylanthracene		0.75
1-Methylnaphthalene		4.38	1,5-Dimethylnaphthalene		0.71
Benzene		3.7	Fluorene		0.70
Inden		3.64	1-Naphthol		0.67
m-Xylene		2.81	3-Methyl-9H-fluorene		0.51
o-Xylene		2.46	o-Methylstyrene		0.5

4.6.6 The elemental compositions (CHN-O) of the organic liquid products

The biomass derived oils have high oxygen contents which result in a different elemental composition from that of petroleum. The petroleum hydrocarbons have very low oxygen contents of less than 0.06 [97].

In our study, the described results of the chemical composition were further demonstrated with the elemental analysis, which was needed to characterize the three fractions before and after upgrading and to determine the carbon, hydrogen, nitrogen and sulphur contents. The CHNOS of all the samples (pyrolysis oil, heavy fraction, pyrolysis tar and the OLPs from the three fractions) were directly analysed using a CHNS/O Analyzer, Flash EA 1112 Series, Thermo Quest. The data shown in Appendix K displayed the carbon, hydrogen and oxygen contents of the fractions before and after upgrading.

The upgrading process which is performed via catalytic cracking reduces the oxygen content of the pyrolysis oils and thereby can enhance some properties such miscibility, which makes the upgraded oil (OLP) miscible with other hydrocarbons. Also, can reduce the oxygen content which leads to increase the heating value of the upgraded oil (OLP).

The oxygenated compounds of OLPs in Tables 16, 17 and 18 were significantly decreased as compared to those from the fractions before upgrading as shown in Table 2, 4 Appendix A and Table 1 Appendix C. This was confirmed accordingly by the CHNO analysis as shown in Figure 33, where the three fractions, i.e, pyrolysis oil, heavy fraction and pyrolysis tar have underwent a significant oxygen removal when using the nano catalyst. The Figure shows approximate elemental compositions of the upgraded fractions (OLPs) with the nano catalyst and the commercial catalyst comparing with the fractions before upgrading. Form the Figure, it can be seen that the total weight percent of the elements is not equal to 100%. This might be attributed to the weight of chlorine element which was not considered in the elemental analysis (Appendix F).

A crucial deference between the two catalysts is that nano catalyst showed a higher decrease of oxygen about 2 wt%, 4 wt% and 3.5 wt% for the upgraded pyrolysis oil, heavy fraction and tar respectively, whereas the commercial catalyst exhibited about 15 wt%, 16 wt% and 5 wt% for the pyrolysis oil, heavy fraction and tar respectively as shown in Figure 34.

The removal of oxygen occurred due to the effect of zeolite catalysts which were able to decrease oxygen content of the pyrolysis oil, heavy fraction and pyrolysis tar. The oxygen removal happened via different reactions such as cracking, decarboxylation,

decarbonylation and hydrogenation. The Oxygen was removed from the oxygenated compounds as water, CO₂ and CO.

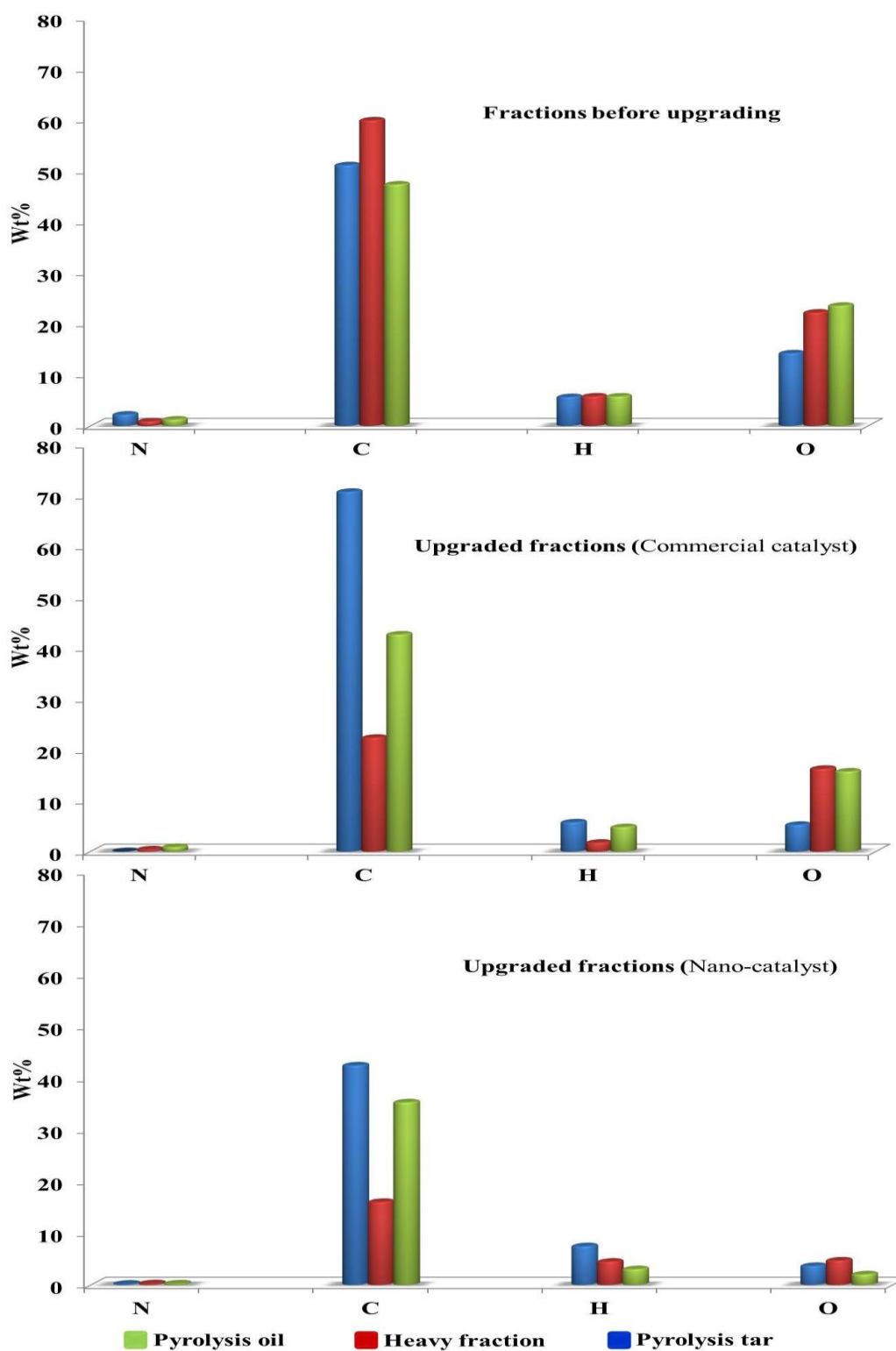


Figure 33. Elemental composition of the three fractions upgraded with nano-catalyst and ordinary catalyst compared the same fractions before upgrading

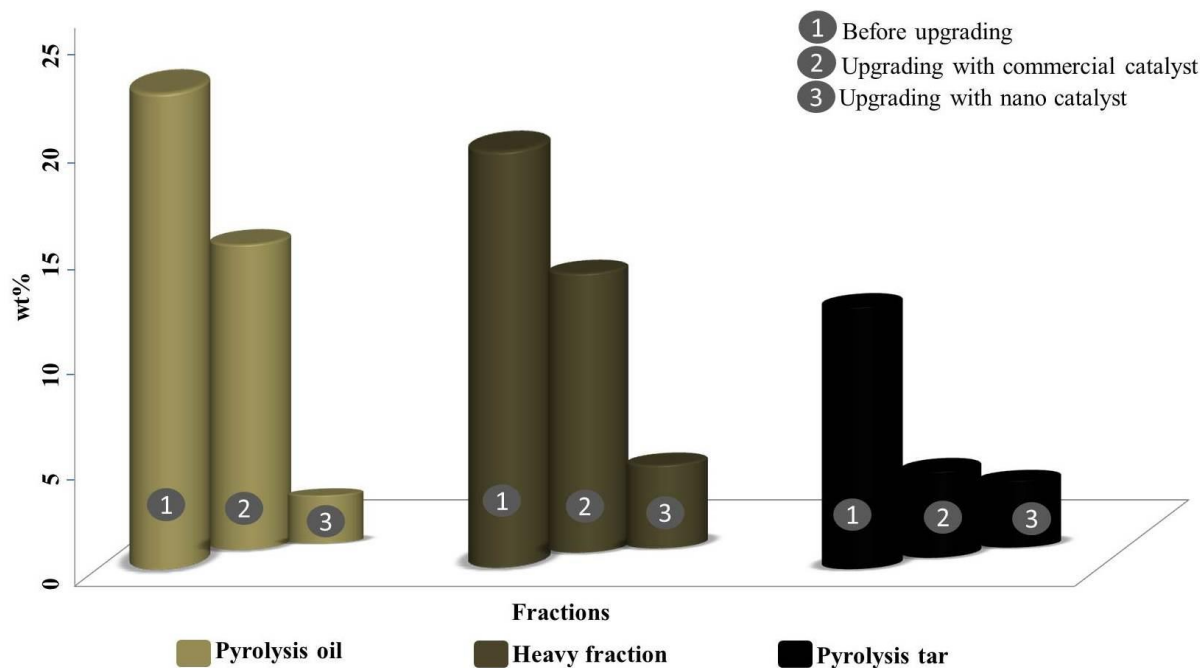


Figure 34. Oxygen content of the three fractions upgraded with nano-catalyst and ordinary catalyst compared the same fractions before upgrading

5. Concluding remarks

5.1 Conclusions

The combination of biomass pyrolysis and catalytic upgrading of the biomass derived oils is a prospective route to biofuels. The upgrading process using zeolite catalysts has been the key focus of the thesis in this study.

A crude pyrolysis liquid derived from rubberwood was obtained from Phatthalung province. The pyrolysis liquid included aqueous phase and settled tar. The settled tar was separated by decantation and kept in a refrigerator overnight to remove the rest of water. Additionally, the aqueous portion was treated to remove water by evaporation and the concentrated liquid was then named pyrolysis oil. The pyrolysis oil itself was fractionated into two fractions, i.e., light fraction and heavy fraction by a conventional vacuum distillation. The isolation of tar, pyrolysis oil, heavy fraction and light fraction has shown to be useful for assessing the whole pyrolysis liquid regarding physiochemical characteristics of its fractions. The four fractions were physiochemically characterized showing that the light fraction had a very high water content and acetic acid; therefore it was ignored from the upgrading experiments. However, it was suggested that light fraction can be used as a feedstock for producing pure acetic acid, whereas the pyrolysis oil, tar and heavy fraction can be directed to further upgrading process for use as fuels.

The pyrolysis oil was catalytically upgraded using a commercial HZSM-5 catalyst to generate BTEX gasoline aromatics with concentration approaching 30 wt% in the OLP. A 15 wt% maximum value of OLP was obtained at 511 °C, 3.2 g of catalyst, and an N₂, while a 30 wt% maximum percent of gasoline aromatics was obtained at 595 °C, 5 g of catalyst, and an N₂ flow rate of 3 mL/min.

The pyrolysis tar was also upgraded using a commercial HZSM-5 catalyst. The maximum yield of OLP was about 28.33 wt%, achieved at 536 °C and a catalyst weight of 3.5 g. The OLP exhibited a higher percentage of BTEX aromatics with a maximum value of about 54 wt%, obtained at 575 °C with a catalyst weight of 5 g.

The residual heavy fraction was diluted first with 5% ethanol due to its high viscosity. The mixture was upgraded with the commercial catalyst producing a very low yield of OLP compared to the previous fractions approaching 11 wt% achieved at 400 °C and a catalyst weight of 5 g. However, the maximum value of BTEX aromatics was about 38 wt%, obtained at 600 °C and a catalyst weight of 5 g.

Apart from the BTEX aromatics determined in the OLPs, it was found that other aromatic compounds were produced having high octane ratings such as naphthalene, methyl-naphthalene, indan, etc. On the other hand, it was observed that side products were also generated during the process, including char, aqueous liquid, coke, tar and gases. Among the side products, the bio-char seems the most important product, as it can be processed further for use as an adsorbent in a variety of applications.

The pyrolysis oil, tar and heavy fraction were converted over a prepared nanocrystalline HZSM-5 zeolite to OLPs approaching different concentrations of aromatics. The experiments were conducted at the same optimal conditions of the commercial catalysts experiments for each fraction. Our findings demonstrated that the OLPs obtained from the three fractions exhibited higher yields for the nano catalyst, whereas the ordinary catalyst exhibited little lower yields. Correspondingly, the nano catalyst displayed higher aromatic percentages of about 33 wt%, 51 wt% and 51.26 wt% for the pyrolysis oil, heavy fraction and tar respectively, while the aromatics percentages on the commercial catalyst were little lower, i.e., 30 wt%, 49 wt% and 48 wt% for the pyrolysis oil, heavy fraction and tar respectively. In addition, the CHNO analysis of the OLPs obtained by using the nano catalyst showed a high decrease of oxygen about 2 wt%, 4 wt% and 3.5 wt% for the upgraded pyrolysis oil, heavy fraction and tar respectively, whereas the commercial catalyst exhibited about 15 wt%, 16 wt% and 5 wt% for the pyrolysis oil, heavy fraction and tar respectively.

Overall, in evaluating the conversion of pyrolysis oil, tar and heavy fraction to generate gasoline aromatics, the pyrolysis tar showed higher yield of OLP (28.33 wt%) and higher concentration of aromatics in OLP (54 wt%) among the two fractions. Therefore, it can be concluded that pyrolysis tar showed significant potential for use in producing gasoline, since it contained high concentrations of BTEX components in the OLP.

5.2 Suggestions and future work

1. The separation of pyrolysis oils fractions by conventional vacuum distillation seems not efficient due to the high temperature and long residence time which affect the thermos-sensitive pyrolysis oil. For this reason it is recommend using molecular distillation which is usually used for the distillation of thermally unstable materials.
2. By using a dual reactor system, char formation has been mentioned to be higher in the first reactor and some losses of liquids were observed in the connecting tubes and fittings. For this reason it is recommended that one fixed bed reactor (under specific conditions such as decreasing the feed flowrate) can be used.
3. The process of catalytic cracking produced low yields of OLPs. Hydroxygenation in this case is favourable as it can produce higher yield of OLP, however the cost of hydrogen should be considered.
4. Using zeolite catalyst in a nano particle size is recommended nowadays due to their high porosity which facilitates the adsorption–desorption and diffusion behavior of the molecules. However, the synthesis of producing nano catalyst should be changed from bottom-up method to top-down due to the high cost of the former method.

6. References

- [1] Breheny, Michael. The compact city and transport energy consumption. *Transactions of the institute of British Geographers* (1995): 81-101.
- [2] Dresselhaus, M. S., and I. L. Thomas. Alternative energy technologies. *Nature* 414, (2001): 332-337.
- [3] Sorrell, Steve, Jamie Speirs, Roger Bentley, Adam Brandt, and Richard Miller. Global oil depletion: A review of the evidence. *Energy Policy* 38, (2010): 5290-5295.
- [4] Balat, Mustafa. Production of bioethanol from lignocellulosic materials via the biochemical pathway: a review. *Energy conversion and management* 52, (2011): 858-875.
- [5] Asif, Muhammad, and Tariq Muneer. Energy supply, its demand and security issues for developed and emerging economies. *Renewable and Sustainable Energy Reviews* 11, (2007): 1388-1413.
- [6] Demirbas, M. Fatih, Mustafa Balat, and Havva Balat. Potential contribution of biomass to the sustainable energy development. *Energy Conversion and Management* 50, (2009):1746-1760.
- [7] Cherubini, Francesco. The biorefinery concept: using biomass instead of oil for producing energy and chemicals. *Energy Conversion and Management* 51, (2010): 1412-1421.
- [8] IEA (International Energy Agency). Bioenergy project development & biomass supply, [accessed February, 2009].
<http://www.iea.org/publications/freepublications/publication/biomass.pdf>
- [9] Roedl, Anne. Production and energetic utilization of wood from short rotation coppice—a life cycle assessment. *The International Journal of Life Cycle Assessment* 15, (2010): 567-578.
- [10] Charles, Michael B., Rachel Ryan, Neal Ryan, and Richard Oloruntoba. Public policy and biofuels: The way forward? *Energy Policy* 35, (2007): 5737-5746.
- [11] Mojović, Ljiljana, Dušanka Pejin, Olgica Grujić, Siniša Markov, Jelena Pejin, Marica Rakin, Maja Vukašinović, Svetlana Nikolić, and Dragiša Savić. Progress in the production of bioethanol on starch-based feedstocks. *Chemical Industry and Chemical Engineering Quarterly* 15, (2009): 211-226.
- [12] Carriquiry, Miguel A., Xiaodong Du, and Govinda R. Timilsina. Second generation biofuels: economics and policies. *Energy Policy* 39, (2011): 4222-4234.

- [13] Göransson, Kristina, Ulf Söderlind, Jie He, and Wennan Zhang. Review of syngas production via biomass DFBGs. *Renewable and Sustainable Energy Reviews* 15, (2011): 482-492.
- [14] Keil, Frerich J. Methanol-to-hydrocarbons: process technology. *Microporous and Mesoporous Materials* 29, (1999): 49-66.
- [15] Damartzis, T., and A. Zabaniotou. Thermochemical conversion of biomass to second generation biofuels through integrated process design—A review. *Renewable and Sustainable Energy Reviews* 15, (2011): 366-378.
- [16] Holmgren, J., R. Marinangeli, P. Nair, D. Elliott, and R. Bain. Consider Upgrading Pyrolysis Oils Into Renewable Fuels. *Hydrocarbon Processing* 87, (2008).
- [17] Grange, Paul, E. Laurent, R. Maggi, A. Centeno, and Bernard Delmon. Hydrotreatment of pyrolysis oils from biomass: reactivity of the various categories of oxygenated compounds and preliminary techno-economical study. *Catalysis today* 29, (1996): 297-301.
- [18] Rogers, J. G., and John G. Brammer. Analysis of transport costs for energy crops for use in biomass pyrolysis plant networks. *Biomass and Bioenergy* 33, (2009): 1367-1375.
- [19] Perego, Carlo, and Aldo Bosetti. Biomass to fuels: The role of zeolite and mesoporous materials. *Microporous and Mesoporous Materials* 144, (2011): 28-39.
- [20] Mohan, Dinesh, Charles U. Pittman, and Philip H. Steele. Pyrolysis of wood/biomass for bio-oil: a critical review. *Energy & Fuels* 20, (2006): 848-889.
- [21] Stevens, Christian. *Thermochemical processing of biomass: conversion into fuels, chemicals and power*. Edited by Robert C. Brown. John Wiley & Sons, 2011.
- [22] Elliott, Douglas C. Historical developments in hydroprocessing bio-oils. *Energy & Fuels* 21, (2007): 1792-1815.
- [23] Elliott, D. C., E. G. Baker, D. Beckman, Y. Solantausta, V. Tolenhiemo, S. B. Gevert, C. Hörnell, A. Östman, and B. Kjellström. Technoeconomic assessment of direct biomass liquefaction to transportation fuels. *Biomass* 22, (1990): 251-269.
- [24] Zhang, Qi, Jie Chang, Tiejun Wang, and Ying Xu. Review of biomass pyrolysis oil properties and upgrading research. *Energy conversion and management* 48, (2007): 87-92.
- [25] Czernik, Stefan, and A. V. Bridgwater. Overview of applications of biomass fast pyrolysis oil. *Energy & Fuels* 18, (2004): 590-598.

- [26] Mudge, L. K., E. G. Baker, M. D. Brown, and W. A. Wilcox. "Catalytic destruction of tars in biomass-derived gases. In *Research in Thermochemical Biomass Conversion*, pp. 1141-1155. Springer Netherlands, 1988.
- [27] Huber, George W., and Avelino Corma. Synergies between Bio-and Oil Refineries for the Production of Fuels from Biomass. *Angewandte Chemie International Edition* 46, (2007): 7184-7201.
- [28] Vitolo, S., B. Bresci, M. Seggiani, and M. G. Gallo. Catalytic upgrading of pyrolytic oils over HZSM-5 zeolite: behaviour of the catalyst when used in repeated upgrading–regenerating cycles. *Fuel* 80, (2001): 17-26.
- [29] Mortensen, Peter Mølgaard, J-D. Grunwaldt, Peter Arendt Jensen, K. G. Knudsen, and Anker Degn Jensen. A review of catalytic upgrading of bio-oil to engine fuels. *Applied Catalysis A: General* 407, (2011): 1-19.
- [30] Jacobson, Kathlene, Kalpana C. Maheria, and Ajay Kumar Dalai. Bio-oil valorization: a review. *Renewable and Sustainable Energy Reviews* 23 (2013): 91-106.
- [31] Bridgwater, A. V., D. Meier, and D. Radlein. An overview of fast pyrolysis of biomass. *Organic Geochemistry* 30, (1999): 1479-1493.
- [32] Saidi, Majid, Fereshteh Samimi, Dornaz Karimipourfard, Tarit Nimmanwudipong, Bruce C. Gates, and Mohammad Reza Rahimpour. Upgrading of lignin-derived bio-oils by catalytic hydrodeoxygenation. *Energy & Environmental Science* 7, (2014): 103-129.
- [33] Vispute, Tushar P., Huiyan Zhang, Aimaro Sanna, Rui Xiao, and George W. Huber. Renewable chemical commodity feedstocks from integrated catalytic processing of pyrolysis oils. *Science* 330, (2010): 1222-1227.
- [34] Adjaye, John D., and N. N. Bakhshi. Catalytic conversion of a biomass-derived oil to fuels and chemicals I: model compound studies and reaction pathways. *Biomass and Bioenergy* 8, (1995): 131-149.
- [35] Adjaye, J. D., and N. N. Bakhshi. Production of hydrocarbons by catalytic upgrading of a fast pyrolysis bio-oil. Part II: Comparative catalyst performance and reaction pathways. *Fuel Processing Technology* 45, (1995): 185-202.
- [36] Wildschut, Jelle, Farchad H. Mahfud, Robbie H. Venderbosch, and Hero J. Heeres. Hydrotreatment of fast pyrolysis oil using heterogeneous noble-metal catalysts. *Industrial & engineering chemistry research* 48, (2009): 10324-10334.

- [37] Elliott, DOUGLAS C., and E. G. Baker. *Upgrading biomass liquefaction products through hydrodeoxygenation*. No. PNL-SA-11891; CONF-840509-1. Pacific Northwest Lab., Richland, WA (USA), 1984.
- [38] Bridgwater, A. V. Production of high grade fuels and chemicals from catalytic pyrolysis of biomass. *Catalysis today* 29, (1996): 285-295.
- [39] Bridgwater, A. V. Catalysis in thermal biomass conversion. *Applied Catalysis A: General* 116, (1994): 5-47.
- [40] Venderbosch, R. H., A. R. Ardiyanti, J. Wildschut, A. Oasmaa, and H. J. Heeres. Stabilization of biomass-derived pyrolysis oils. *Journal of chemical technology and biotechnology* 85, (2010): 674-686.
- [41] Elliott, Douglas C., Todd R. Hart, Gary G. Neuenschwander, Leslie J. Rotness, and Alan H. Zacher. Catalytic hydroprocessing of biomass fast pyrolysis bio-oil to produce hydrocarbon products. *Environmental progress & sustainable energy* 28, (2009): 441-449.
- [42] de Miguel Mercader, F., M. J. Groeneveld, S. R. A. Kersten, N. W. J. Way, C. J. Schaverien, and J. A. Hogendoorn. Production of advanced biofuels: Co-processing of upgraded pyrolysis oil in standard refinery units. *Applied Catalysis B: Environmental* 96, (2010): 57-66.
- [43] Daudin, Antoine, Laurent Bournay, and Thierry Chapus. Method of converting effluents of renewable origin into fuel of excellent quality by using a molybdenum-based catalyst. U.S. Patent 8,546,626, issued October 1, 2013.
- [44] McCall, Michael J., Timothy A. Brandvold, and Douglas C. Elliott. *Fuel and fuel blending components from biomass derived pyrolysis oil*. No. 8,329,969. PNNL (Pacific Northwest National Laboratory (PNNL), Richland, WA (United States)), 2012.
- [45] Kwon, Kyung C., Howard Mayfield, Ted Marolla, Bob Nichols, and Mike Mashburn. Catalytic deoxygenation of liquid biomass for hydrocarbon fuels. *Renewable Energy* 36, (2011): 907-915.
- [46] Gutierrez, A., R. K. Kaila, M. L. Honkela, R. Slioor, and A. O. I. Krause. Hydrodeoxygenation of guaiacol on noble metal catalysts. *Catalysis today* 147, (2009): 239-246.
- [47] Pham, Trung T., Lance L. Lobban, Daniel E. Resasco, and Richard G. Mallinson. Hydrogenation and hydrodeoxygenation of 2-methyl-2-pentenal on supported metal catalysts. *Journal of Catalysis* 266, (2009): 9-14.

- [48] Yakovlev, V. A., S. A. Khromova, O. V. Sherstyuk, V. O. Dundich, D. Yu Ermakov, V. M. Novopashina, M. Yu Lebedev, O. Bulavchenko, and V. N. Parmon. Development of new catalytic systems for upgraded bio-fuels production from bio-crude-oil and biodiesel. *Catalysis Today* 144, (2009): 362-366.
- [49] Mendes, M. J., O. A. A. Santos, E. Jordão, and A. M. Silva. Hydrogenation of oleic acid over ruthenium catalysts. *Applied Catalysis A: General* 217, (2001): 253-262.
- [50] Stakheev, A. Yu, and L. M. Kustov. Effects of the support on the morphology and electronic properties of supported metal clusters: modern concepts and progress in 1990s. *Applied Catalysis A: General* 188, (1999): 3-35.
- [51] Mortensen, Peter Mølgaard, Anker Degn Jensen, Jan-Dierk Grunwaldt, and Peter Arendt Jensen. Catalytic Conversion of Bio-oil to Fuel for Transportation. (2013). PhD diss., Technical University of Denmark Danmarks Tekniske Universitet, Risø National Laboratory for Sustainable Energy Risø Nationallaboratoriet for Bæredygtig Energi.
- [52] Olcese, Roberto N., Jessica François, M. M. Bettahar, Dominique Petitjean, and Anthony Dufour. Hydrodeoxygenation of guaiacol, a surrogate of lignin pyrolysis vapors, over iron based catalysts: Kinetics and modeling of the lignin to aromatics integrated process. *Energy & Fuels* 27, (2013): 975-984.
- [53] Gutierrez, A., R. K. Kaila, M. L. Honkela, R. Slioor, and A. O. I. Krause. Hydrodeoxygenation of guaiacol on noble metal catalysts. *Catalysis today* 147, (2009): 239-246.
- [54] Furimsky, Edward. Catalytic hydrodeoxygenation. *Applied Catalysis A: General* 199, (2000): 147-190.
- [55] Zhao, H. Y., D. Li, P. Bui, and S. T. Oyama. Hydrodeoxygenation of guaiacol as model compound for pyrolysis oil on transition metal phosphide hydroprocessing catalysts. *Applied Catalysis A: General* 391, (2011): 305-310.
- [56] Ghampson, I. T., C. Sepúlveda, R. Garcia, B. G. Frederick, M. C. Wheeler, N. Escalona, and W. J. DeSisto. Guaiacol transformation over unsupported molybdenum-based nitride catalysts. *Applied Catalysis A: General* 413 (2012): 78-84.
- [57] Ghampson, I. Tyrone, Catherine Sepúlveda, Rafael Garcia, Ljubisa R. Radovic, JL García Fierro, William J. DeSisto, and Nestor Escalona. Hydrodeoxygenation of guaiacol over carbon-supported molybdenum nitride catalysts: Effects of nitriding methods and support properties. *Applied Catalysis A: General* 439 (2012): 111-124.

- [58] Romero, Y., F. Richard, and S. Brunet. Hydrodeoxygenation of 2-ethylphenol as a model compound of bio-crude over sulfided Mo-based catalysts: Promoting effect and reaction mechanism. *Applied Catalysis B: Environmental* 98, (2010): 213-223.
- [59] Bridgwater, Anthony V. Review of fast pyrolysis of biomass and product upgrading. *Biomass and bioenergy* 38 (2012): 68-94.
- [60] Furimsky, Edward, and Franklin E. Massoth. Deactivation of hydroprocessing catalysts. *Catalysis Today* 52, (1999): 381-495.
- [61] Adjaye, John Deheer. Catalytic conversion of biomass-derived oils to fuels and chemicals. (1993). PhD thesis. University of Saskatchewan.
- [62] Adjaye, John D., and N. N. Bakhshi. Production of hydrocarbons by catalytic upgrading of a fast pyrolysis bio-oil. Part I: Conversion over various catalysts. *Fuel Processing Technology* 45, (1995): 161-183.
- [63] Baldauf, W., U. Balfanz, and M. Rupp. Upgrading of flash pyrolysis oil and utilization in refineries. *Biomass and Bioenergy* 7, (1994): 237-244.
- [64] Sharma, R. K., and N. N. Bakhshi. Upgrading of wood-derived bio-oil over HZSM-5. *Bioresource technology* 35, (1991): 57-66.
- [65] Huber, George W., Sara Iborra, and Avelino Corma. Synthesis of transportation fuels from biomass: chemistry, catalysts, and engineering. *Chemical reviews* 106, (2006): 4044-4098.
- [66] Niwa, Miki, Naonobu Katada, and Kazu Okumura. *Characterization and design of zeolite catalysts: Solid acidity, shape selectivity and loading properties*. Vol. 141. Springer Science & Business Media, 2010.
- [67] Xu, Ruren, Wenqin Pang, Jihong Yu, Qisheng Huo, and Jiesheng Chen. *Chemistry of zeolites and related porous materials: synthesis and structure*. John Wiley & Sons, 2009.
- [68] Yu, Jihong, and Ruren Xu. Insight into the construction of open-framework aluminophosphates. *Chemical Society Reviews* 35, (2006): 593-604.
- [69] Auerbach, Scott M., Kathleen A. Carrado, and Prabir K. Dutta. *Handbook of zeolite science and technology*. CRC press, 2003.
- [70] Weisz, P. B., and V. J. Frilette. Intracrystalline and molecular-shape-selective catalysis by zeolite salts. *The Journal of Physical Chemistry* 64, (1960): 382-382.
- [71] Csicsery, Sigmund M. Shape-selective catalysis in zeolites. *Zeolites* 4, (1984): 202-213.

- [72] Roduner, Emil. Understanding catalysis. *Chemical Society Reviews* 43, (2014): 8226-8239.
- [73] Derouane, E. G., Jacques C. Vadrine, R. Ramos Pinto, P. M. Borges, L. Costa, M. A. N. D. A. Lemos, F. Lemos, and F. Ramôa Ribeiro. The acidity of zeolites: Concepts, measurements and relation to catalysis: A review on experimental and theoretical methods for the study of zeolite acidity. *Catalysis Reviews* 55, (2013): 454-515.
- [74] Kondo, Junko N., Ryoko Nishitani, Eisuke Yoda, Toshiyuki Yokoi, Takashi Tatsumi, and Kazunari Domen. A comparative IR characterization of acidic sites on HY zeolite by pyridine and CO probes with silica–alumina and γ -alumina references. *Physical Chemistry Chemical Physics* 12, (2010): 11576-11586.
- [75] Van der Gaag, Frederik J. ZSM-5 type zeolites: Synthesis and use in gasphase reactions with ammonia. (1987) PhD diss., TU Delft, Delft University of Technology.
- [76] Mravec, D., E. Streshtikova, and J. Ilavsky. Preparation of synthetic zeolite ZSM-5. *Chemical Papers* 41, (1987): 335-41.
- [77] Cusumano, J.A., et al., Chapter 9 - Inorganic Chemistry, in *Catalysis in Coal Conversion*. 1978, Academic Press. p. 100-120.
- [78] Larlus, O., S. Mintova, and T. Bein. Environmental syntheses of nanosized zeolites with high yield and monomodal particle size distribution. *Microporous and mesoporous materials* 96, no. 1 (2006): 405-412.
- [79] Larsen, Sarah C. Nanocrystalline zeolites and zeolite structures: synthesis, characterization, and applications. *The Journal of Physical Chemistry C* 111, (2007): 18464-18474.
- [80] M.A. Cambor, A. Corma, A. Misud, J. Perez-Pariente, S. Valencia, in: H. Chon, S.-K. Ihm, Y.S. Uh (Eds.), *Stud. Surf. Sci. Catal, Progress in Zeolite and Microporous Materials*, 105A, Elsevier, Amsterdam, 1997, p. 341.
- [81] Van Grieken, R., J. L. Sotelo, J. M. Menendez, and J. A. Melero. Anomalous crystallization mechanism in the synthesis of nanocrystalline ZSM-5. *Microporous and Mesoporous Materials* 39, (2000): 135-147.
- [82] Treacy, Michael MJ, and John B. Higgins. *Collection of Simulated XRD Powder Patterns for Zeolites Fifth (5th) Revised Edition*. Elsevier, 2007.
- [83] Huang, Jun, Wei Long, Pradeep K. Agrawal, and Christopher W. Jones. Effects of acidity on the conversion of the model bio-oil ketone cyclopentanone on H- Y zeolites. *The Journal of Physical Chemistry C* 113, (2009): 16702-16710.

- [84] Guo, Xiaoya, Yong Zheng, Baohua Zhang, and Jinyang Chen. Analysis of coke precursor on catalyst and study on regeneration of catalyst in upgrading of bio-oil. *Biomass and bioenergy* 33, (2009): 1469-1473.
- [85] Vitolo, S., B. Bresci, M. Seggiani, and M. G. Gallo. Catalytic upgrading of pyrolytic oils over HZSM-5 zeolite: behaviour of the catalyst when used in repeated upgrading–regenerating cycles. *Fuel* 80, (2001): 17-26.
- [86] Gayubo, Ana G., Andrés T. Aguayo, Alaitz Atutxa, Roberto Aguado, and Javier Bilbao. Transformation of oxygenate components of biomass pyrolysis oil on a HZSM-5 zeolite. I. Alcohols and phenols. *Industrial & Engineering Chemistry Research* 43, (2004): 2610-2618.
- [87] Liu, Changjun, Huamin Wang, Ayman M. Karim, Junming Sun, and Yong Wang. Catalytic fast pyrolysis of lignocellulosic biomass. *Chemical Society Reviews* 43, (2014): 7594-7623.
- [88] Carlson, Torren R., Tushar P. Vispute, and George W. Huber. Green gasoline by catalytic fast pyrolysis of solid biomass derived compounds. *Chem Sus Chem* 1, (2008): 397-400.
- [89] Carlson, Torren R., Yu-Ting Cheng, Jungho Jae, and George W. Huber. Production of green aromatics and olefins by catalytic fast pyrolysis of wood sawdust. *Energy & Environmental Science* 4, (2011): 145-161.
- [90] Pattiya, Adisak, James O. Titiloye, and Anthony V. Bridgwater. Fast pyrolysis of cassava rhizome in the presence of catalysts. *Journal of Analytical and Applied Pyrolysis* 81, (2008): 72-79.
- [91] Olazar, Martin, Roberto Aguado, Javier Bilbao, and Astrid Barona. Pyrolysis of sawdust in a conical spouted-bed reactor with a HZSM-5 catalyst. *AIChE Journal* 46, (2000): 1025-1033.
- [92] De, Sudipta, Basudeb Saha, and Rafael Luque. Hydrodeoxygenation processes: Advances on catalytic transformations of biomass-derived platform chemicals into hydrocarbon fuels. *Bioresource Technology* 178 (2015): 108-118.
- [93] Marker, Terry L., Larry G. Felix, Martin B. Linck, Michael J. Roberts, Pedro Ortiz-Toral, and Jim Wangerow. Integrated hydrolysis and hydroconversion (IH²®) for the direct production of gasoline and diesel fuels or blending components from biomass, Part 2: continuous testing. *Environmental Progress & Sustainable Energy* 33, (2014): 762-768.

- [94] Taufiqurrahmi, N., Mohamed, A. R., & Bhatia, S. Nanocrystalline zeolite beta and zeolite Y as catalysts in used palm oil cracking for the production of biofuel. *Journal of Nanoparticle Research*, 13, (2011): 3177-3189.
- [95] Ghosh, Prasenjeet, Karlton J. Hickey, and Stephen B. Jaffe. Development of a detailed gasoline composition-based octane model. *Industrial & engineering chemistry research* 45, (2006): 337-345.
- [96] Viswanadham, Nagabhatla, Sandeep K. Saxena, Jitendra Kumar, Peta Sreenivasulu, and Devaki Nandan. Catalytic performance of nano crystalline H-ZSM-5 in ethanol to gasoline (ETG) reaction. *Fuel* 95 (2012): 298-304.
- [97] Wang, Chao, Zhankui Du, Jingxue Pan, Jinhua Li, and Zhengyu Yang. Direct conversion of biomass to bio-petroleum at low temperature. *Journal of Analytical and Applied Pyrolysis* 78, (2007): 438-444.

7. Appendices

Appendix A

Characterisation of liquid derived from pyrolysis process of charcoal production in south of Thailand



Characterisation of Liquid Derived from Pyrolysis Process of Charcoal Production in South of Thailand

Abdulrahim Saad and S.B. Ratanwilai

Department of Chemical Engineering, Faculty of Engineering,
 Prince of Songkla University, Hat Yai, Songkhla 90112, Thailand

Received: April 10, 2014; Accepted in Revised Form: June 6, 2014

Abstract: Pyrolysis liquid obtained from local suppliers in Phatthalung Province, Thailand was separated in conventional vacuum distillation into light and heavy fractions. The physiochemical characteristics and thermal behaviour of the fractionated pyrolysis liquid were investigated. It was found that light fraction had higher water content and stronger acidity than heavy fraction and pyrolysis liquid. The heating value of light fraction was lower than those of the pyrolysis liquid and heavy fraction. The heating value of heavy portion was almost double that of the light fraction. The thermal behaviours of the pyrolysis liquid and the two fractions were determined. The light fraction had the highest decomposition rate and the lowest residual yield; in contrast to heavy fraction had slow weight loss through a wide range of temperatures and it had the highest residual yield. The chemical composition of the pyrolysis liquid and the two fractions were analysed by GC-MS. The chemical distribution differed for the fractions and the pyrolysis liquid. The light fraction was dominated by acetic acid and the heavy fraction was mainly composed phenolic compounds.

Key words: Pyrolysis liquid • Vacuum distillation • Light fraction • Heavy fraction • Physiochemical characterization

INTRODUCTION

Biomass represents a potential alternative source of energy to replace fossil fuels. It has attracted great attention as a renewable energy source after the global oil crisis in 1970s [1, 2]. In addition, biomass is considered the only current sustainable source to produce energy-related products, including electricity, heat and valuable chemicals, such as resins, flavourings and other materials [3, 4]. Furthermore, biomass is an environmentally-friendly candidate because it contains a low content of sulphur [5, 6].

The pyrolysis of biomass has been used for ages to produce charcoal and currently the slow-pyrolysis process is widely used for producing so-called biochar [7, 8]. However, extensive attention has been focused recently on fast pyrolysis to obtain pyrolysis liquid (pyrolysis oil) [9]. Pyrolysis oil is a complex, oxygenated compound with a wide range of boiling temperatures

that contains nearly 400 known compounds, primarily of phenolic compounds, organic acids, aldehydes, ketones, esters and water [10, 11].

Currently, pyrolysis oil has attracted considerable interest due to its several applications in industry. Although it has been proven to be a promising alternative to petroleum fuels, it also has potential for use in producing value-added chemicals for the pharmaceutical, food and paint industries [2, 12].

The pyrolysis oil mixture is quite complex and there has been significant interest in studying its chemical composition and thermal behaviour. Hence, its chemical and physical properties have been extensively discussed in literature [13-15].

A great deal of work has been done on fractionation and characterization of pyrolysis oil and different methods and techniques have been used. Garcia-Perez *et al.* [16] used different solvents to fractionate pyrolysis oil into six fractions, which were characterized by GC-MS,

Corresponding Author: Abdulrahim Saad, Department of Chemical Engineering, Faculty of Engineering,
 Prince of Songkla University, Hat Yai, Songkhla 90112, Thailand.
 Tel: +66874755690, E-mail: abdorahim@hotmail.com

Please cite this article as: Saad A. and S.B. Ratanwilai, 2014. Characterisation of liquid derived from pyrolysis process of charcoal production in south of Thailand. Iranica Journal of Energy and Environment, 5(2):184-191.

thermogravimetric techniques (TG) and gel permeation chromatography (GPC). A similar investigation was conducted by Sipila *et al.* [17] and they have reported the physiochemical properties and fuel characteristics of the water-soluble and water-insoluble fractions of flash pyrolysis oil. They also compared the properties and characteristics of these two fractions with those of the whole pyrolysis oil.

Apart from solvent extraction techniques, Wang, *et al.* [18-20] used molecular distillation techniques to separate pyrolysis oil into several fractions using different operational parameters and then studied the physiochemical characteristics of the fractions.

To a great extent, Thailand is an agriculture-based country and it has the potential for producing energy from biomass equivalent to about 25-30% of its primary energy needs; in addition, rubber wood is regarded as one of the most important sources of biomass and it is planted extensively in the peninsular area in southern Thailand [21]. Rubber wood has been utilised to a great extent by local farmers and small plants to produce charcoal, which is carried in conventional, slow-pyrolysis process. The pyrolysis liquid, called 'wood vinegar' locally, is produced as a by-product from the production of charcoal and it is used extensively by farmers in growing and protecting plants as well as to improve the quality of the soil [22].

To the best of our knowledge, few studies have been conducted on the physiochemical properties of pyrolysis liquid produced from the slow pyrolysis of wood in the process of charcoal production. Most of the studies focused on the fast pyrolysis oil; hence, the purpose of our work was to use vacuum distillation to separate the liquid produced by the slow pyrolysis of wood into fractions and then determine the chemical and physical properties of the fractions.

Pyrolysis liquid was collected from different producers in Phatthalung, one of the southern provinces in Thailand and conventional vacuum distillation was conducted to fractionate the liquid into two fractions.

The pyrolysis liquid and its fractions were analysed using GC-MS. The physical properties of the pyrolysis liquid and its two fractions were investigated, including heating value, pH, colour and thermal stability.

MATERIALS AND METHODS

Crude Pyrolysis Liquid: The crude pyrolysis liquid was obtained from local suppliers in Phatthalung Province. The suppliers produced the liquid as a by-product from the slow pyrolysis of wood in the process of making charcoal. The biomass source they used for making charcoal was mainly rubber wood. First, the crude pyrolysis liquid was treated to reduce water and remove the fine particles using evaporation and filtration, respectively.

Pyrolysis Liquid Fractionation: After the crude pyrolysis liquid was treated as described, the treated liquid was fractionated into two fractions. The fractionation was conducted in a conventional, vacuum-distillation facility at 60-70°C and 60-10 mmHg. The fractions collected from the distillation process were labelled as the light fraction (LF) and the heavy fraction (HF). The LF, which contained the light components, was vaporized, condensed and collected at room temperature. The HF, which contained the heavy components, could not be vaporized and collected as a residual fraction.

GC-MS Analyses: The compounds in the pyrolysis liquid and its fractions were identified with a Trace GC Ultra/ISQMST equipped with a capillary column of 30 m long \times 0.25 mm \times 0.25 μ m film thickness. The oven temperature was programmed to increase from 35 to 245°C. The data were acquired with Xcalibur software using the Wiley mass spectra library's.

Thermogravimetric Analysis and Physical Characteristics: The physical properties were measured to determine heating value, pH, water content

Table 1: Analysis methods and instruments used for physical characterisation

Physical Property	Method and Instrument
Heating value	CHNS/O Analyser, Flash EA 1112 Series Automatic calculation of GHV (Gross Heat Value) and NHV (Net Heat Value) using Eager 300 software.
pH	pH meter Water content Coulometric Karl Fischer titration method First, the sample was diluted with methanol and then analysed using a Karl Fischer titrator. A mass balance was used to determine the water content of the sample.
Appearance	Visual observation

and appearance of the pyrolysis liquid, light and heavy fractions. They were analysed according to the methods listed in Table 1. Thermogravimetry (TG) and Derivative Thermogravimetric (DTG) profiles of the pyrolysis liquid, light fraction and heavy fraction were assessed by a thermogravimetric analyser (Perkin Elmer TGA 7). The conditions were controlled under a nitrogen purge gas at temperatures ranging from 50 to 1000°C with a heating rate of 10°C/min.

RESULTS AND DISCUSSION

GC-MS Characterization of the Pyrolysis Liquid and its Fractions:

Several compounds were identified by the GC-MS analyses. The total ion chromatogram of the pyrolysis liquid in Figure 1 and Table 2 show the top 20 compounds of the pyrolysis liquid. Acetic acid had the highest concentration and it was followed by a group of abundant phenolic compounds. Among the phenolic compounds, syringol was the most abundant and it was followed by ketones, pyridines, sugars and acids in that order. Generally, the chemical composition was almost in agreement with that reported by Branca *et al.* [23] for pyrolysis liquid. In addition, Noor *et al.* conducted similar work using slow pyrolysis of cassava wastes for biochar production [8].

Figure 2 shows the GC-MS total ion chromatograms of the two fractions obtained from the vacuum distillation of the pyrolysis liquid. It was obvious that the distributions of the components differed in the two fractions and in the pyrolysis liquid. As illustrated in Figure 3, the compounds in the fractions were classified into different groups, such as acids, esters, phenols and ketones, according to their chemical structures.

Table 3 shows that the light fraction was dominated by acetic acid, followed by acetol. Some phenols were partially distilled during the distillation process and they were present in trace amounts in the light fraction, although the rest of the phenolic compounds were not present. Table 4 shows that the heavy fraction was composed mainly of 2, 6-dimethoxyphenol, followed by high-molecular weight phenols, ketones, pyridines, sugar and some acids.

Furthermore, it was noted that more compounds were detected in the two fractions than in the pyrolysis liquid due to thermal cracking process of conventional distillation that had a long residence time and a relatively

high temperature. As a result, the thermo-sensitive pyrolysis liquid was not completely vaporized and as a result, some compounds reacted, producing additional compounds [24].

Physical Characteristics of the Pyrolysis Liquid and its Fractions:

Table 5 presents the principal physical properties of the pyrolysis liquid and its fractions.

The pyrolysis liquid was a light-black liquid with a 30% water content, a pH value of 3.72 and a heating value of about 21 MJ/kg. The light fraction, which had good fluidity, was dark yellow with a high water content of 60%; in contrary, the heavy fraction had poor fluidity, was dark black with a relatively low water content of 1.5%. Moreover, the heating value of the light fraction was much lower than that of the heavy fraction. The heating value heavy fraction was almost double that of the light fraction. Earlier work has proven that the heating value depends mostly on the chemical composition and the water content [5]. In addition, it was noted that the light fraction had the lowest pH value due to its content of acids, particularly acetic acid, which had the highest concentration among all of the components in the light fraction.

Thermogravimetric Analysis:

In our study, we used thermogravimetric analysis (TGA) to investigate the thermal stability of the pyrolysis liquid and its fractions. The results of TGA were useful in studying and predicting the properties of the pyrolysis liquid and its fractions. Figure 4 shows the thermal behaviour of the pyrolysis liquid and its fractions at a heating rate of 10°C/min. The pyrolysis liquid was evaporated and decomposed over the temperature range of 25-1004°C; it had its maximum weight loss at 120°C (DGT plot) and its final residue yield at 1004°C was 2%. However, the light fraction, which had the highest rate of decomposition, evaporated mostly in the range of 25-186°C; its maximum weight loss occurred at 161°C (DGT plot) due to the release of water vapour (moisture content was 60%) and compounds that had low boiling points. The yield of the final residue was 0.1% at 1004°C. The heavy fraction had a different thermal behaviour from the light fraction. It had slow weight loss over a wide range of temperatures, *i.e.*, 35-110°C, due to the presence of compounds with higher boiling points and it had its maximum weight loss at 227°C (DGT plot). The yield of the final residue was 20% at 110°C.

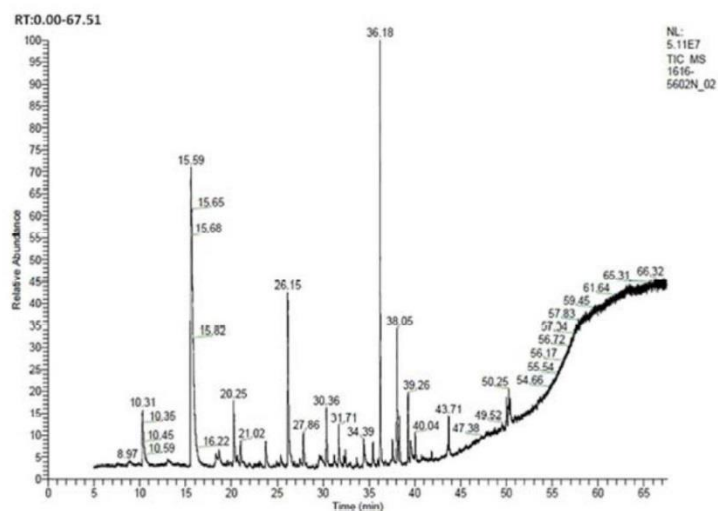


Fig. 1: Total ion GC-MS chromatograms of the pyrolysis liquid

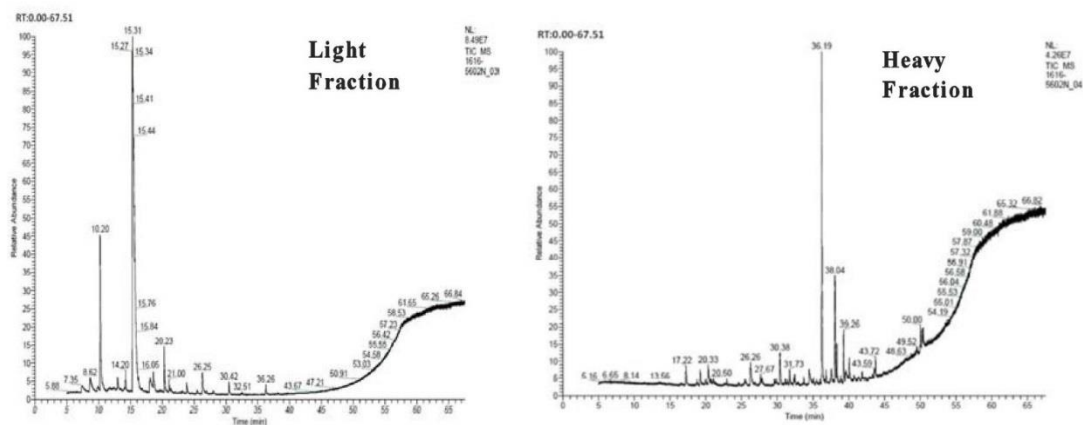


Fig. 2: Total ion GC-MS chromatograms of the two fractions obtained from the pyrolysis liquid using conventional vacuum distillation at 60-70°C and 60-10 mmHg

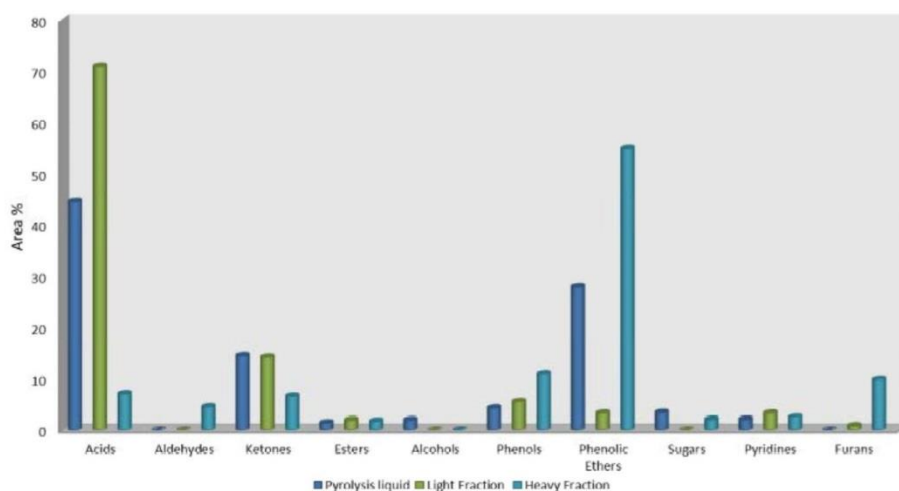


Fig. 3: Chemical distribution of the pyrolysis liquid and its two fractions

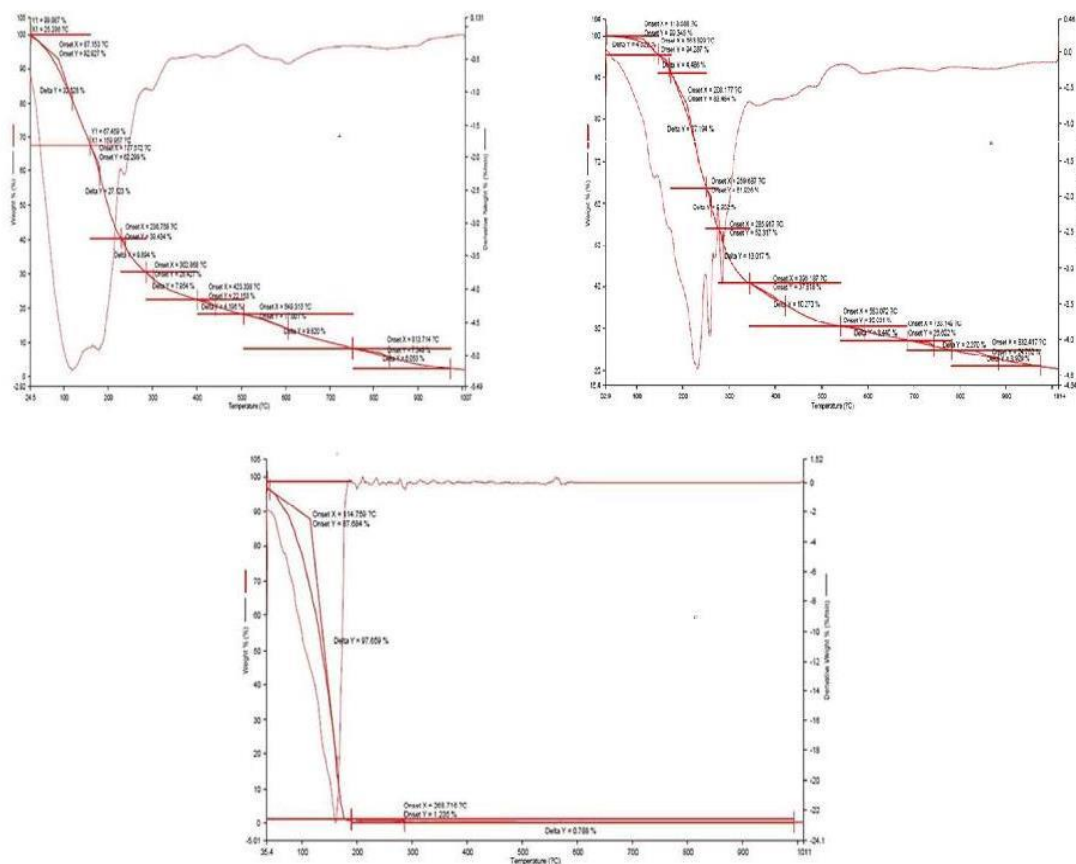


Fig. 4: TG and DTG at a heating rate of 10°C/min for (A) pyrolysis liquid, (B) heavy fraction and (C) light fraction

Table 2: Main chemical composition of the pyrolysis liquid identified by GC-MS

Composition	MW	Formula	Peak area % ^a
1 Acetic acid	60	C ₂ H ₄ O ₂	37.30
2 Syringol	154	C ₈ H ₁₀ O ₃	15.27
3 Corylon	112	C ₈ H ₈ O ₂	9.85
4 4-Methoxy-3-(methoxymethyl)phenol	168	C ₉ H ₁₂ O ₃	4.89
5 Acetol	74	C ₃ H ₆ O ₂	4.66
6 4-Chlorobutyric acid	122	C ₄ H ₇ ClO ₂	3.53
7 Phenol	94	C ₆ H ₆ O	2.43
8 2,6-Dihydroxy-4-methoxyacetophenone	182	C ₉ H ₁₀ O ₄	2.31
9 Butyryl oxide	158	C ₈ H ₁₄ O ₃	2.19
10 Anhydro - sugar	132	C ₅ H ₈ O ₄	1.96
11 3-Pyridinol	95	C ₅ H ₅ NO	1.87
12 3,4,8-Trimethyl-2-none-1-ol	182	C ₁₂ H ₂₂ O	1.84
13 Syringyl acetone	126	C ₇ H ₁₀ O ₂	1.47
14 Ethyl cyclopentenolone	180	C ₁₀ H ₁₂ O ₃	1.81
15 1-(4-Hydroxy-3-methoxyphenyl)acetone	166	C ₁₀ H ₁₄ O ₂	1.70
16 p-Butoxyphenol	210	C ₁₁ H ₁₆ O ₄	1.55
17 3,4-Anhydro-d-galactosan	144	C ₆ H ₆ O ₄	1.39
18 Levulinic acid	116	C ₅ H ₈ O ₃	1.35
19 à-Furanone	84	C ₄ H ₄ O ₂	1.35
20 2-hydroxy-4-6-dimethoxy acetophenone	196	C ₁₀ H ₁₂ O ₄	1.28

The composition of the pyrolysis liquid estimated by the peak area% of GC-MS

Table 3: Main chemical composition of the light fraction identified by GC-MS

	Composition	Mw	Formula	Peak area % ^a
1	Acetic acid	60	C ₂ H ₄ O ₂	67.96
2	Syringol	154	C ₈ H ₁₀ O ₃	0.48
3	Corylon	112	C ₆ H ₈ O ₂	1.88
4	4-Methoxy-3-(methoxymethyl)phenol	168	C ₉ H ₁₂ O ₃	2.9
5	Acetol	74	C ₃ H ₆ O ₂	11.36
6	4-Chlorobutyric acid	122	C ₄ H ₇ ClO ₂	2.88
7	Phenol	94	C ₆ H ₆ O	0.73
8	Pyridine, 4-methyl	93	C ₆ H ₇ N	2.67
9	Hydrazine, n-propionyl-N-methyl-	102	C ₆ H ₁₀ N ₂ O	1.99
10	Trimethylorthoacetate	120	C ₇ H ₁₂ O ₃	1.11
11	1-Hydroxy-2-butanone	88	C ₄ H ₈ O ₂	1.08
12	4-Hydroxybut-2-enoic acid lactone	84	C ₄ H ₆ O ₂	0.8
13	2-Hydroxyethyl acetate	104	C ₆ H ₈ O ₃	0.74
14	3,5-Dimethylpyridine	107	C ₇ H ₉ N	0.37
15	Pyridine	79	C ₅ H ₇ N	0.34
16	1,3,5-Trimethyl-2-octadecylcyclohexane	378	C ₂₃ H ₅₄	0.26

The composition of the light fraction estimated by the peak area% of GC-MS

Table 4: Main chemical composition of the heavy fraction identified by GC-MS

	Composition	Mw	Formula	Peak area % ^a
1	Syringol	154	C ₈ H ₁₀ O ₃	34.22
2	Corylon	112	C ₆ H ₈ O ₂	4.47
3	4-Methoxy-3-(methoxymethyl)phenol	168	C ₉ H ₁₂ O ₃	11.52
4	4-Chlorobutyric acid	122	C ₄ H ₇ ClO ₂	3.44
5	Phenol	94	C ₆ H ₆ O	3.9
6	2,6-Dihydroxy-4-methoxyacetophenone	182	C ₉ H ₁₀ O ₄	5.58
7	Butyryl oxide	158	C ₈ H ₁₄ O ₃	2.61
8	Anhydro- sugar	132	C ₇ H ₈ O ₄	1.76
9	3-Pyridinol	95	C ₅ H ₅ NO	2.75
10	3,4,8-Trimethyl-2-none-1-ol	182	C ₁₂ H ₂₂ O	4.18
11	Syringyl acetone	126	C ₇ H ₁₀ O ₂	2.4
12	Tetrahydro-2-methyl-2-Furanol	102	C ₅ H ₁₀ O ₂	3.66
13	1,4-Benzenediol	110	C ₆ H ₆ O ₂	3.6
14	3,4,5-Trimethoxybenzaldehyde	196	C ₁₀ H ₁₂ O ₄	3.51
15	Dihydro-5-(hydroxymethyl)-2(3h)-furanone	116	C ₅ H ₈ O ₃	2.91
16	Tetrahydrofuran, 2-hexyl-	102	C ₇ H ₁₀ O ₂	2.31
17	Butanoic acid, butyl-1,1-d2 ester	144	C ₈ H ₁₄ D ₂ O ₂	1.53
18	m-Cresol	108	C ₇ H ₈ O	1.21

The composition of the heavy fraction estimated by the peak area % of GC-MS

Table 5: Physical properties of pyrolysis liquid and its fractions

Sample	Appearance	Heating value (MJ/kg)		Water content (% w/w)	pH value
		GHV	NHV		
Pyrolysis liquid	Light black	22	21	30	3.72
Light fraction	Dark yellow	14	12	60	2.67
Heavy fraction	Dark black	28	27	1.5	4.50

CONCLUSIONS

Vacuum distillation was used to fractionate a woody pyrolysis liquid obtained from local suppliers in Phatthalung Province. Fractionation has shown to be a useful technique to assess the whole pyrolysis liquid with respect to physiochemical characteristics of its

fractions. The compositions of the pyrolysis liquid, its light fraction and its heavy fraction were experimentally determined and classified into different groups according to their chemical structures. It was obvious that the chemical compositions of the pyrolysis liquid and its two fractions were all different. The light fraction had high water content and strong acidity;

however, the pyrolysis liquid and its heavy fraction had relatively low acidity and low water content. The heating value of the light fraction was lower than those of the pyrolysis liquid and its heavy fraction, whereas the heavy fraction's heating value was almost double that of the light fraction. The thermal behaviour results that were obtained indicated that the light fraction had the highest rate of decomposition and the lowest residual yield; in contrast, the heavy fraction had a slow weight loss over a wide range of temperatures and it had the highest residual yield.

The results of this study demonstrated that the pyrolysis liquid produced during the process of charcoal production has the potential for more extensive and beneficial use. For instance, the light fraction, which has high acetic acid and water contents, can be used as a feedstock for producing pure acetic acid, whereas the heavy fraction can be directed to further processing and upgrading for use as a fuel. It also could be used as the raw material for producing a number of valuable chemicals, which could be more attractive and beneficial than using it to make fuels.

ACKNOWLEDGEMENTS

The authors are thankful for the financial support granted from graduate school of Prince of Songkla University and very grateful to the scientists of scientific equipment centre, who performed some of the analysis, reported in this paper.

REFERENCES

- Demirbas, A., 2007. Progress and recent trends in biofuels. *Progress in energy and combustion science*, 33(1): 1-18.
- Bridgwater, A.V. and G. Grassi, 1991. *Biomass pyrolysis liquids: upgrading and utilisation*. Springer.
- Huber, G.W., S. Iborra and A. Coma, 2006. Synthesis of transportation fuels from biomass: chemistry, catalysts and engineering. *Chemical reviews*, 106(9): 4044-4098.
- Dodds, D.R. and R.A. Gross, 2007. Chemicals from biomass. *Science*, 318(5854): 1250-1251.
- Jenkins, B., L. Baxter, T. Miles Jr and T. Miles, 1998. Combustion properties of biomass. *Fuel Processing Technology*, 54(1): 17-46.
- Patel, B. and B. Gami, 2012. Biomass Characterization and its Use as Solid Fuel for Combustion. *Iranica Journal of Energy and Environment*, 3: 123-128.
- Noor, N.M., A. Shariff and N. Abdullah, 2012. Slow Pyrolysis of Cassava Wastes for Biochar Production and Characterization. *Iranica Journal of Energy and Environment*, 3(5): 60-65.
- Bridgwater, A. and G. Peacocke, 2000. Fast pyrolysis processes for biomass. *Renewable and Sustainable Energy Reviews*, 4(1): 1-73.
- Mohan, D., C.U. Pittman and P.H. Steele, 2006. Pyrolysis of wood/biomass for bio-oil: a critical review. *Energy and Fuels*, 20(3): 848-889.
- Czernik, S. and A. Bridgwater, 2004. Overview of applications of biomass fast pyrolysis oil. *Energy and Fuels*, 18(2): 590-598.
- Chiaramonti, D., A. Oasmaa and Y. Solantausta, 2007. Power generation using fast pyrolysis liquids from biomass. *Renewable and Sustainable Energy Reviews*, 11(6): 1056-1086.
- Elliott, D.C., Analysis and comparison of biomass pyrolysis/gasification condensates: Final report, 1986, Pacific Northwest Lab., Richland, W.A. (USA).
- Peacocke, G., P. Russell, J. Jenkins and A. Bridgwater, 1994. Physical properties of flash pyrolysis liquids. *Biomass and Bioenergy*, 7(1): 169-177.
- Oasmaa, A. and P. Koponen, 1997. Physical characterisation of biomass-based pyrolysis liquids: Espoo.
- Garcia-Perez, M., A. Chaala, H. Pakdel, D. Kretschmer and C. Roy, 2007. Characterization of bio-oils in chemical families. *Biomass and Bioenergy*, 31(4): 222-242.
- Sipilä, K., E. Kuoppala, L. Fagernäs and A. Oasmaa, 1998. Characterization of biomass-based flash pyrolysis oils. *Biomass and Bioenergy*, 14(2): 103-113.
- Guo, X., S. Wang, Z. Guo, Q. Liu, Z. Luo and K. Cen, 2010. Pyrolysis characteristics of bio-oil fractions separated by molecular distillation. *Applied Energy*, 87(9): 2892-2898.
- Guo, Z., S. Wang, Y. Gu, G. Xu, X. Li and Z. Luo, 2010. Separation characteristics of biomass pyrolysis oil in molecular distillation. *Separation and Purification Technology*, 76(1): 52-57.
- Wang, S., Y. Gu, Q. Liu, Y. Yao, Z. Guo, Z. Luo and K. Cen, 2009. Separation of bio-oil by molecular distillation. *Fuel Processing Technology*, 90(5): 738-745.
- Krukanont, P. and S. Prasertsan, 2004. Geographical distribution of biomass and potential sites of rubber wood fired power plants in Southern Thailand. *Biomass and Bioenergy*, 26(1): 47-59.

22. Chalermnan, Y. and S. Peerapan, 2010. Wood-vinegar: by-product from rural charcoal kiln and its roles in plant protection. *Asian Journal of Food and Agro-Industry*, 2: 189-195.
23. Branca, C., P. Giudicianni and C. Di Blasi, 2003. GC/MS characterization of liquids generated from low-temperature pyrolysis of wood. *Industrial and Engineering Chemistry Research*, 42(14): 3190-3202.
24. Bridgewater, A.V., 2004. Biomass fast pyrolysis. *Thermal Science*, 8(2): 21-50.

Appendix B

Catalytic cracking of pyrolysis oil derived from rubberwood to produce green gasoline components

Catalytic Cracking of Pyrolysis Oil Derived from Rubberwood to Produce Green Gasoline Components

Abdulrahim Saad, Sukritthira Ratanawilai*, and Chakrit Tongurai

An attempt was made to generate gasoline-range aromatics from pyrolysis oil derived from rubberwood. Catalytic cracking of the pyrolysis oil was conducted using an HZSM-5 catalyst in a dual reactor. The effects of reaction temperature, catalyst weight, and nitrogen flow rate were investigated to determine the yield of organic liquid product (OLP) and the percentage of gasoline aromatics in the OLP. The results showed that the maximum OLP yield was about 13.6 wt%, which was achieved at 511 °C, a catalyst weight of 3.2 g, and an N₂ flow rate of 3 mL/min. The maximum percentage of gasoline aromatics was about 27 wt%, which was obtained at 595 °C, a catalyst weight of 5 g, and an N₂ flow rate of 3 mL/min. Although the yield of gasoline aromatics was low, the expected components were detected in the OLP, including benzene, toluene, ethyl benzene, and xylenes (BTEX). These findings demonstrated that green gasoline aromatics can be produced from rubberwood pyrolysis oil via zeolite cracking.

Keywords: Pyrolysis oil; Zeolite cracking; Organic liquid product (OLP); Green gasoline-range aromatics

Contact information: Department of Chemical Engineering, Faculty of Engineering, Prince of Songkla University, Had Yai, Songkhla, 90112, Thailand; * Corresponding author: sukritthira.b@psu.ac.th

INTRODUCTION

Biomass represents a potential alternative source of energy, which is an important complement to fossil fuels. As such, it attracted significant attention as a renewable source of energy after the global oil crisis of the 1970s (Demirbas 2007; Lucia 2008; Demirbas *et al.* 2009). In addition, biomass currently is considered to be the only sustainable source that can be used to produce energy-related products, including electricity, heat, and valuable chemicals such as resins, flavorings, and other materials (Huber *et al.* 2006; Dodds and Gross 2007).

The first generation of biofuels were primarily bioethanol and biodiesel made from sugar, starch, and vegetable oil. To date, such biofuels have been widely produced across several countries and continents, notably Brazil, South America, Europe, and the United States (Charles *et al.* 2007; Mojoviä *et al.* 2009); however, they have been produced from food-grade biomass, which could lead to critical concerns related to food security (Gronowska *et al.* 2009). Therefore, it is very important to be able to produce biofuels from non-food resources such as ligno-cellulosic materials: wood chips, switch grasses and most importantly agricultural wastes, such as sugarcane bagasse, corn stover and rice straw.

Pyrolysis oils derived from wood-based biomass are one of the most promising renewable fuels. They are environmentally-friendly candidates because they contain a low content of sulfur compared to fossil-derived oils (Czernik and Bridgwater 2004). Recently, extensive attention has been focused on the technology of fast pyrolysis rather than slow pyrolysis, as the former produces high yield of pyrolysis oil with low water content in a

short residence time; however, this technology is still not fully developed regarding its commercial applications. Correspondingly, the slow pyrolysis technology produces a low yield of oil with high water content in a long residence time; however, this technology is known to have been practiced for ages to enhance char production (Bridgwater and Peacocke 2000; Stevens and Brown 2011). Fast pyrolysis process, nonetheless, seems to be superior for the preparation of biofuel.

Pyrolysis oil has attracted considerable interest due to its many applications in industry. Even though pyrolysis oil has been shown to be an alternative to petroleum fuels, it also has potential for use in producing value-added chemicals for the pharmaceutical, food, and paint industries (Bridgwater and Grassi 1991; Chiaramonti *et al.* 2007). However, the direct substitution of pyrolysis oil for petroleum and other chemicals might be limited due to its thermal instability, high viscosity, and high oxygen content (Czernik and Bridgwater 2004; Mohan *et al.* 2006). As a result, before the pyrolysis oil can be used, an upgrading process is required to improve its quality by reducing the oxygen content (Zhang *et al.* 2007). Catalytic cracking and hydrotreating are two routes that have been used to upgrade the oil. The latter (named hydro-deoxygenation) is a deoxygenation process performed under high pressure of hydrogen; it has been studied recently for upgrading liquefied biomass obtained with the low-temperature liquefaction, which is a promising thermochemical route that uses less energy as compared to the pyrolysis technology. Related studies regarding the hydro-deoxygenation of liquefied biomass were reported by Grilc *et al.* (2014, 2015). The hydro-deoxygenation process, therefore, is considered as a vital process in the upgrading of biomass, perhaps even more so than cracking. However, catalytic cracking might be preferred because it has some significant advantages, *i.e.*, it does not require hydrogen, operates at atmospheric pressure, and has a lower operating cost (Huber and Corma 2007). Consequently, the zeolite cracking of pyrolysis oils to fuels and chemicals using HZSM-5 zeolite catalysts, which promote deoxygenation reactions, has attracted significant attention in recent years (Vitolo *et al.* 2001).

Presently, the concern of producing green gasoline, particularly gasoline-range aromatics from pyrolysis oil, has aroused attention. Previous studies have demonstrated that gasoline-range hydrocarbons can be produced from pyrolysis oil by catalytic cracking over HZSM-5 catalyst. Adjaye and Bakhshi (1995b,c) conducted extensive studies of the conversion of pyrolysis oil derived from maplewood to liquid products that had high concentrations of gasoline-range hydrocarbons. In their study, different zeolite catalysts were investigated for their relative performance in upgrading the pyrolysis oil, and the results showed that HZSM-5 was the most effective catalyst and gave a high yield of gasoline hydrocarbons, principally made up of BTEX aromatics.

A similar study was reported by Vitolo *et al.* (1999), who attempted to upgrade different pyrolysis oils derived from oak, pine, and a mixture of both using HZSM-5 and H-Y zeolites. Their findings showed that an HZSM-5 catalyst could be used to upgrade the pyrolysis oil and produce clear, separable oil, whereas the H-Y zeolites produced a single phase of aqueous liquid. The oils obtained by upgrading oak-derived pyrolysis oil at a different temperatures using HZSM-5, contained an elevated percentage of aromatics, including benzene, toluene, ethylbenzene, xylenes, and trimethylbenzenes. Furthermore, the upgraded oils showed a higher degree of deoxygenation with a quite high heating value and a good combustibility. The upgrading of pyrolysis oil derived from rice husk was investigated by Wang *et al.* (2013). They outlined a unique technique to produce high-quality gasoline rich with aromatic hydrocarbons by using a distilled fraction of the

pyrolysis oil with ethanol and investigated their co-cracking behaviour using the HZSM-5 catalyst.

Recently, Bi and co-workers (2013) explored an innovative cracking technique based on the residual heavy fraction (tar) of pyrolysis oil derived from straw stalks; with their technique they could increase the efficiency and selectivity of producing aromatics by passing an electric current through the catalytic reactor. The current promoted the deoxygenation and cracking reactions efficiently, giving higher yield of aromatics (mainly consisted of BTEX) as compared to those produced by the conventional catalytic conversion without current. Interestingly, it was found that, among the catalysts used in the study, HZSM-5 was the most effective and obtained the highest yield of aromatic hydrocarbons.

The rubber tree is widely planted in southern Thailand (Krukanont and Prasertsan 2004) and has been utilized to a great extent for charcoal production using the slow-pyrolysis process. The pyrolysis liquid is obtained as a by-product during the manufacture of charcoal, and it is used extensively in plant growth and protection, particularly in pesticide applications (Tiilikkala *et al.* 2010).

It would be highly desirable to get more exploitation to the pyrolysis liquid, as it will clearly add value to the production of charcoal. To the best of the authors' knowledge, pyrolysis liquid derived as a by-product from rubberwood has received limited attention, and no study has been conducted to upgrade it to gasoline-range aromatics or organic liquid product (OLP). Thus in this work, the catalytic conversion of pyrolysis liquid after treatment was investigated, and its viability for producing gasoline-range aromatics was studied.

In this paper, catalytic cracking of rubberwood-derived oil over HZSM-5 catalyst was conducted in a dual-reaction system. The effect of operating conditions on the yield of OLP and the percentage of gasoline aromatics in the OLP was investigated. The optimum operating conditions were analyzed using design of experiments (DOE) and response surface methodology (RSM).

EXPERIMENTAL

Materials

Preparation and characterization of pyrolysis oil

Crude pyrolysis liquid was treated to reduce water by evaporation. The concentrated liquid was then labelled as pyrolysis oil (Saad and Ratanwilia 2014). The concentrated liquid produced in the evaporation process was labelled as pyrolysis oil. Table 1 gives important characteristics of pyrolysis oil, such as water content, specific gravity, heating value, pH, and elemental content. The table also identifies the instruments used in analysis.

The chemical composition was identified using a gas chromatography mass spectrometry system (Trace GC Ultra/ISQMST) equipped with a capillary column of 30 m long \times 0.25 mm \times 0.25 μ m film thickness. The GC oven temperature was kept at 35 °C for 5 min, and programmed to increase from 35 to 245 °C at the rate of 4 °C/min. The data was acquired with Xcalibur software using the Wiley mass spectra library. Table 2 shows the chemical composition of the pyrolysis oil.

Table 1. Physical Characteristics and Elemental Analysis of Pyrolysis Oil

	Typical Value	Instrument
Water content (wt%)	30.00	Coulometric Karl Fischer titrator, Mettler Toledo DL 39, Taiwan.
Specific gravity	1.22	Specific Gravity Bottle.
Gross heating value (MJ/kg)	22.00	CHNS/O Analyzer, Flash EA 1112 Series, Thermo Quest, Italy.
Net heating value (MJ/kg)	21.00	<i>Automatic calculation of GHV (Gross Heat Value) and NHV (Net Heat Value) using Eager 300 software.</i>
pH	3.72	Docu-pH ⁺ meter, Sartorius Mechatronics, Germany.
Elemental composition (wt%)		CHNS/O Analyzer, Flash EA 1112 Series, Thermo Quest, Italy.
C	47.37	
H	5.78	
O	23.58	
N	1.26	

The conducted tests underwent duplicate runs to determine repeatability. The experimental error was less than 3.5%

Table 2. Chemical Composition of the Pyrolysis Oil Identified by GC-MS

	Composition	MW	Formula	Peak area % ^a
1	Acetic acid	60	C ₂ H ₄ O ₂	32.65
2	Syringol	154	C ₈ H ₁₀ O ₃	13.36
3	Corylon	112	C ₆ H ₈ O ₂	8.62
4	4-Methoxy-3-(methoxymethyl)phenol	168	C ₉ H ₁₂ O ₃	4.28
5	Acetol	74	C ₃ H ₆ O ₂	4.08
6	4-Chlorobutyric acid	122	C ₄ H ₇ ClO ₂	3.09
7	Phenol	94	C ₆ H ₆ O	2.13
8	2,6-Dihydroxy-4-methoxyacetophenone	182	C ₉ H ₁₀ O ₄	2.02
9	Butyryl oxide	158	C ₈ H ₁₄ O ₃	1.91
10	Anhydro sugar	132	C ₅ H ₈ O ₄	1.72
11	3-Pyridinol	95	C ₅ H ₅ NO	1.64
12	3,4,8-Trimethyl-2-none-1-ol	182	C ₁₂ H ₂₂ O	1.61
13	Syringyl acetone	126	C ₇ H ₁₀ O ₂	1.29
14	Ethyl cyclo pentenolone	180	C ₁₀ H ₁₂ O ₃	1.59
15	1-(4-Hydroxy-3-methoxyphenyl)acetone	166	C ₁₀ H ₁₄ O ₂	1.49
16	p-Butoxyphenol	210	C ₁₁ H ₁₄ O ₄	1.36
17	3,4-Anhydro-d-galactosan	144	C ₆ H ₈ O ₄	1.22
18	Levulinic acid	116	C ₅ H ₈ O ₃	1.18
19	à-Furanone	84	C ₄ H ₄ O ₂	1.18
20	2-hydroxy-4 6-dimethoxy acetophenone	196	C ₁₀ H ₁₂ O ₄	1.13
21	^b Unidentified			12.45

^a The composition of the pyrolysis oil was estimated by the peak area % of GC-MS
^b Determined by difference

Preparation and characterization of the catalyst

NH₄-ZSM-5 zeolite (CBV 3024E) was provided by Zeolyst International (USA) as a fine powder. Its surface area and SiO₂/Al₂O₃ ratio were 405 m²/g and 30, respectively. The HZSM-5 catalyst was prepared by removing the ammonia from NH₄-ZSM-5 by calcination at 550 °C for 5 h in a stream of nitrogen to obtain the protonic form, with stronger acid sites. The structure and composition of the catalyst were identified by an X-

ray diffraction (XRD; X'Pert MPD, PHILIPS), and the XRD patterns were found to be similar to the standard HZSM-5 zeolite reported by Treacy and Higgins (2007), as given in Fig. 1. The morphology and particle sizes were determined from the scanning electron microscopy (SEM) image taken with a JSM-5800 LV, JEOL, as shown in Fig 2.

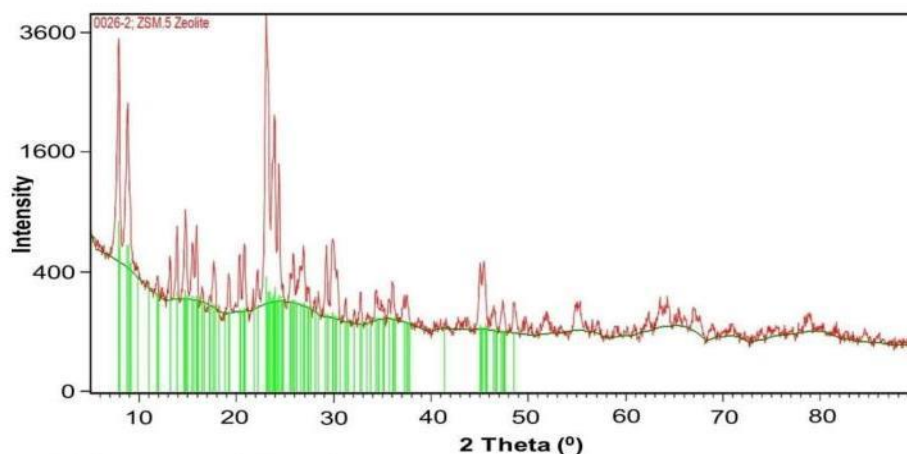


Fig. 1. XRD pattern of HZSM-5 catalyst

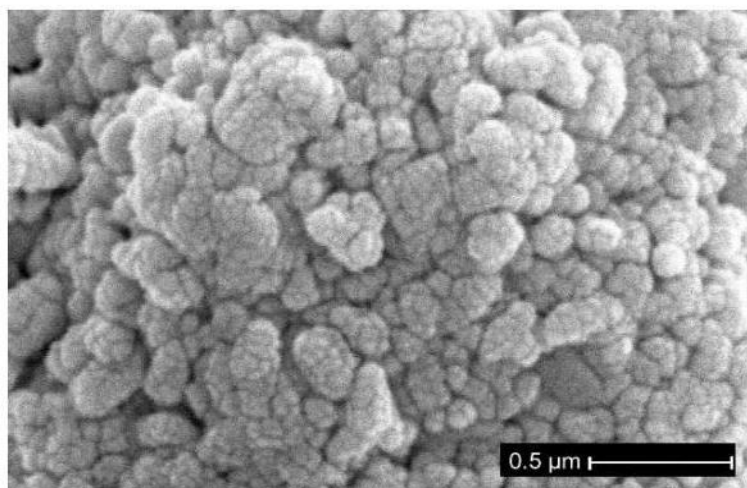


Fig. 2. SEM image for HZSM-5 catalyst

Methods

Experimental setup and procedure

The pyrolysis oil was cracked in a dual-reaction system without any catalyst in the first reactor, followed by a second fixed bed reactor loaded with HZSM-5 catalyst, as shown in Fig. 3. The reactors were stainless steel tubes with an inner diameter of 30 mm and lengths of 250 and 350 mm for the first and second reactors, respectively. The two reactors were placed coaxially in the furnaces. The dual reactor operation was studied previously (Sharma *et al.* 1993; Srinivas *et al.* 2000) in order to reduce coke formation during the process. It was found to be effective in enhancing the catalyst life by minimizing coking, hence reducing the frequency of catalyst regeneration. The experimental runs were conducted at atmospheric pressure in the dual reactor system, which was operated in the

temperature range of 400 to 600 °C with a catalyst weight of 1 to 5 g and a nitrogen flow rate of 3 to 10 mL/min.

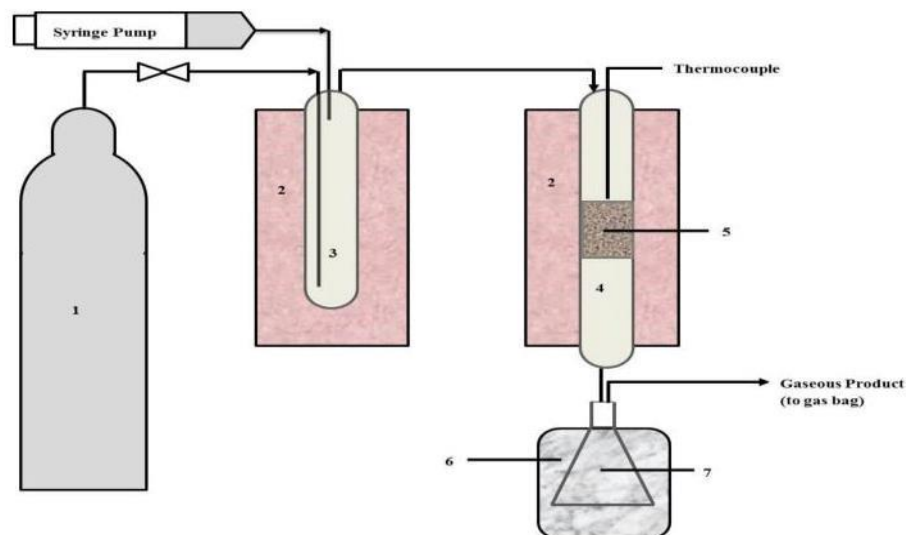


Fig. 3. Dual reactor setup showing (1) nitrogen cylinder, (2) furnace, (3) first reactor, (4) second reactor, (5) catalyst bed, (6) ice batch, (7) receiving flask

In a typical run, the second reactor was loaded with catalyst that was held on a plug of glass wool. The catalyst was weighed, and the values are provided in Table 3. Then, both reactors were heated in a stream of nitrogen until the desired temperature was attained, after which a syringe pump was used to introduce 15 g of pyrolysis oil into the first reactor at the rate of 1.4 g/min. The oil entered the first reactor together with the nitrogen carrier gas at different flow rates, as shown in Table 3. The oil was thermally cracked, and a significant amount of char was formed and deposited in the reactor. Then, the oil vapor flowed through the second reactor, passing the catalyst bed where the catalytic cracking of the oil vapor occurred. Some char was formed above the catalyst bed due to the thermal effect at the reactor's temperature. The products from the second reactor were cooled (collected in an ice-cooled flask) and separated into liquid and gaseous products. The liquid product was obtained in the form of immiscible layers, *i.e.*, an organic layer and an aqueous layer. The organic layer, *i.e.*, the OLP, was drawn off from the aqueous layer with a syringe. The amounts of OLP and aqueous liquid were determined by the difference in weight of the liquid product before and after the aqueous and organic layers were separated. In addition, the uncondensed gaseous product was collected in a gas bag, and its weight was estimated by the difference in weight of the bag before and after removing the gas, excluding the amount of N₂. Each experimental run lasted for about 1.30 h, because it was observed that the formation of products decreased significantly after 1.30 h for all runs.

After each run, the char formed in the first reactor was removed and weighed. The spent catalyst, tar, and the char deposited above the catalyst bed were removed from the second reactor. The inner surface of the reactor and the catalyst were washed with methanol to remove the tar. The washed catalyst was later dried at 100 °C overnight and then heated in air at 550 °C for 5 h in order to determine the weight of coke, which was determined by the difference in the weight of the catalyst before and after heating.

In addition, the yields of OLP, aqueous liquid, char, and gas relative to the total amount of pyrolysis oil feed were determined using the following relationship,

$$\text{Yield (wt\%)} = (P \times 100) / \text{pyrolysis oil fed (15 g)} \quad (1)$$

where P is the number of grams of product, *i.e.*, OLP, aqueous liquid, char, or gas.

Analysis of the liquid product

The liquid product included a separable oil layer (OLP) and an aqueous product. In this study, the product of interest was the gasoline fraction formed in the OLP, particularly gasoline-range aromatics, *i.e.*, benzene, toluene, ethylbenzene, and xylenes (BTEX), which were anticipated to have higher octane ratings (Diebold and Scahill 1988). Thus, only the gasoline hydrocarbons of BTEX were identified using gas chromatography (GC). The GC was equipped with a 30-m long, fused-silica capillary column and a flame ionization detector (FID). The oven temperature was programmed to increase from 40 to 250 °C. The identities of the peaks were determined by using BTEX standards, and the quantities were determined from a calibration curve that had been developed using the BTEX standard.

The aqueous product contained 78 to 85 wt% water, as determined by Karl Fischer titration, and it was expected to contain some water-soluble organic components, such as carboxylic acids, alcohols, and phenols. Then, a pH meter was used to attain the pH values, which ranged from 2.90 to 3.65.

Table 3. Experimental Design Matrix and Results

Runs	Experimental design			Experimental Results	
	Temperature °C	Catalyst g	N ₂ flow rate mL/min	OLP yield	Percentage of gasoline aromatics in OLP
1	400	1	6.5	5.80	0.34
2	400	3	3.0	11.27	0.62
3	400	3	10	11.07	0.57
4	400	5	6.5	11.33	1.43
5	500	1	3.0	12.13	6.69
6	500	1	10	12.00	6.48
7	500	3	6.5	13.20	17.11
8	500	3	6.5	13.13	17.25
9	500	3	6.5	13.33	18.06
10	500	5	3.0	12.47	23.81
11	500	5	10	12.33	23.10
12	600	1	6.5	12.27	6.71
13	600	3	3.0	11.53	26.41
14	600	3	10	11.40	22.02
15	600	5	6.5	10.00	19.95

The experiments were performed in duplicate (except the central points) for reproducibility check. The errors were found to be <3% in all the runs

Experimental Design and Response Surface Methodology

Response surface methodology (RSM) is one of the techniques used for designing experiments and developing an adequate mathematical model to predict the optimal values of independent variables (Cornell 1990; Clarke and Kempson 1997; Montgomery 2001).

In this study, the experiments were designed using Essential Regression and Experimental Design software. Three factors, *i.e.*, temperature (°C), the catalyst's weight

(g), and the flow rate of N₂ (mL/min), were chosen as the independent variables that would affect the catalytic cracking of the pyrolysis oil. The ranges of these factors included three levels, *i.e.*, low, central, and high. 15 experimental runs were designed using Box-Behnken with three center points as shown in Table 3.

Since OLP and gasoline aromatics were the most desired products, the experiments were conducted to determine two quantities (responses) as shown in Table 3, *i.e.*, the yield of OLP and the percentage of gasoline aromatics in the OLP. The model used for predicting OLP yield and percentage of aromatics is a quadratic equation as represented by,

$$Y = b_0 + b_1T + b_2C + b_3G + b_4T^2 + b_5C^2 + b_6G^2 + b_7TC + b_8TG + b_9CG \quad (2)$$

where Y is the predicted response; $b_0, b_1, b_2, b_3, b_4, b_5, b_6, b_7, b_8,$ and b_9 are the regression coefficients; and $T, C,$ and G are the coded independent variables for temperature, catalyst's weight and N₂ flow rate, respectively. In order to determine the optimum operating conditions, the response surface analysis was performed by utilizing Essential Regression software to maximize the yield of OLP and the percentage of gasoline aromatics.

RESULTS AND DISCUSSION

Product Distribution

The cracking process generated six products: OLP, an aqueous product, char, tar, coke, and non-condensable gases. Table 4 provides the overall product distribution for each run. It was observed that a significant amount of char was formed in the first reactor, and a small amount of char was formed above the catalyst bed in the second reactor. These observations imply that the formation of char occurred due to the thermal effect on the unstable components of the pyrolysis oil, more to the point, because of polymerization and condensation reactions, which form large molecules that are insoluble and infusible. Nevertheless, as shown in Table 4 (the yield of char ranged from about 18 to 22 wt % over the 15 runs), there was a slight decrease in the formation of char with the increase of temperature, probably due to secondary reactions occurring such as gasification. A similar observation concerning the formation of char during the cracking of pyrolysis oil, and the effect of temperature on char formation was reported by Adjaye and Bakhshi (1995b). The aqueous product contained 78 to 81 wt% water, indicating that some oxygen was removed in the form of water (Adjaye and Bakhshi 1995c). The amount of aqueous product ranged from about 36 to 53 wt %.

It was important to investigate the distribution of OLP yield, which ranged from about 6 to 13 wt% over the experimental runs. At 400 °C (runs 1-4), it was noted that the yield values were low, but they began to increase at 500 °C (runs 5-9) and reached a maximum of about 13 wt%. It was observed that the OLP decreased when the temperature was increased from 500 to 600 °C (runs 10-15). Adjaye and Bakhshi (1995b) and Bi *et al.* (2013) reported similar observations during the upgrading of pyrolysis oil and tar by HZSM-5 catalyst. They stated that the yield of OLP decreased as the temperature increased, meaning that a higher temperature led to the additional cracking of OLP, forming more gaseous products.

Table 4. Overall Product Distribution (wt% of the feed) for 15 Experimental Runs

Runs	Products					
	Aqueous Liquid	Organic Liquid Product	Char ^a	Residue ^b	Gas	Unaccounted
	wt%					
1	38.33	5.80	22.00	13.20	4.07	16.60
2	36.33	11.27	22.13	12.33	4.33	13.60
3	36.20	11.07	22.00	12.47	4.53	13.73
4	38.00	11.33	22.00	11.20	5.2	12.27
5	40.00	12.13	19.80	10.93	5.33	11.80
6	39.33	12.00	19.00	11.00	5.53	13.13
7	45.00	13.20	19.20	10.47	5.67	6.47
8	45.40	13.13	19.13	10.47	5.67	6.20
9	44.93	13.33	19.20	10.00	5.73	6.80
10	46.53	12.47	19.80	9.87	6.07	5.27
11	45.33	12.33	18.87	9.80	6.2	7.47
12	46.67	12.27	17.67	9.80	6.33	7.27
13	51.33	11.53	17.80	9.67	6.47	3.20
14	50.00	11.40	17.67	9.53	6.53	4.87
15	53.33	10.00	17.73	9.33	6.67	2.93

^a Char formed in the first reactor
^b Residue is categorized as char and tar that were quantified in the second reactor
All the experiments were repeated in duplicate (except the central points) showing a good reproducibility with low experiment errors (1–5 %)

The major oxygenated compounds in the pyrolysis oil (Table 2) were acids, phenolic compounds, ketones, esters, aldehydes, and a few others. It is important to state that the conversion of most of these oxygenated compounds to OLP over the HZSM-5 catalyst was an indication of its ability to remove oxygen through complex reactions, such as deoxygenation, cracking, cyclization, aromatization, isomerization and polymerization reactions (Adjaye and Bakhshi 1995a; Valle *et al.* 2010; Gong *et al.* 2011; Mentzel and Holm 2011). The low yield of OLP (about 6 to 13 wt%) might be attributed to the high water content of the sample (30%) and the char formation (about 18 to 22 wt%). In addition, the yield of gas increased slightly with the reaction temperature and catalyst, showing a highest value of about 7 wt% at 600 °C, 5 g of catalyst and, 6.5 mL/min of N₂ gas. The lowest value was 4 wt% achieved at 400 °C, 1 g of catalyst, and 6.5 mL/min of N₂ gas.

Content of Gasoline-Range Aromatics in OLP

The composition of OLP, particularly gasoline-range aromatics (BTEX), was of prime interest. Gasoline aromatics were analyzed by GC-FID, and Table 5 shows their distributions for the experimental runs.

It was found that the percentage of gasoline aromatics in OLP for all runs ranged from about 0.34 to 26 wt%, with a maximum value of about 26 wt% at 600 °C, 3 g of catalyst and 3 mL/min of N₂ gas. The formation of aromatic hydrocarbons in OLP supported the hypothesis that the oxygenated compounds, particularly substituted phenols, in the pyrolysis oil can be converted into aromatic hydrocarbons by dehydroxylation, decarbonylation, and decarboxylation with the HZSM-5 catalyst (Carlson *et al.* 2009; Valle *et al.* 2010; Zhao *et al.* 2010; Cheng and Huber 2011). In addition, as the pyrolysis oil contained some acids, alcohols, aldehydes, ketones and esters, it was suggested that during

the conversion of these compounds, olefins were formed as intermediate products, and they underwent a variety of further reactions to yield aromatic hydrocarbons (Adjaye and Bakhshi 1995a). It was noted that the percentage of gasoline aromatics increased slightly, from 0.34 wt% to 1.43 wt%, as the amount of catalyst used was increased at a reaction temperature of 400 °C. Similarly, at 500 °C, the percentage of gasoline aromatics increased significantly, from about 7 wt% to 24 wt%. There was a dramatic increase of gasoline aromatics at 600 °C when 3 g of catalyst were used instead of 1 g. However, a slight decrease was noted when 5 g of catalyst were used due to the secondary conversion of the aromatics. In general, by considering the effect of catalysts on the formation of aromatics, it can be seen that the decrease of catalyst (the feed rate of pyrolysis oil was fixed) generally minimizes the reactants residence time in the catalyst bed, as a result deoxygenation and cracking reactions will decrease. Regarding the effect of temperature on the aromatics distribution, it was noteworthy to observe that, with increasing reaction temperature (at fixed amounts of 1g, 3 g and 5 g of catalyst), the formation of aromatics remarkably increased; therefore, it can be suggested that higher temperature enhances further elimination of groups from the primary heavier aromatics (such as demethylation of xylenes) to form mostly toluene and further to benzene. However, with increasing temperature from 500 °C to 600 °C at 5 g of catalyst, the aromatics slightly decreased from about 23 wt% to 20 wt% as a result of the secondary cracking of the aromatics. Likewise, in terms of selectivity, increasing the catalyst and temperature contributed effectively to increasing the aromatics selectivity. Furthermore, it is suggested that the presence of HZSM-5 catalyst which exhibit shape selectivity, enhances the formation of toluene, xylenes and substituted benzenes in the OLP. Related observations and detailed proposals of the reaction pathways were studied previously (Adjaye and Bakhshi 1995a; Li *et al.* 2012; Zhu *et al.* 2013).

Table 5. Composition of Gasoline Aromatics in the OLP

Runs	OLP yield	Benzene	Toluene	Ethyl benzene	Xylenes ^a	(gasoline aromatics) ^b
		wt%				
1	5.80	0.06	0.14	0.12	0.02	0.34
2	11.27	0.10	0.32	0.18	0.02	0.62
3	11.07	0.13	0.25	0.17	0.02	0.57
4	11.33	0.30	0.97	Trace	0.16	1.43
5	12.13	0.75	2.49	Trace	3.45	6.69
6	12.00	0.63	2.08	Trace	3.77	6.48
7	13.20	2.20	7.03	0.07	7.81	17.11
8	13.13	3.12	10.23	0.95	2.95	17.25
9	13.33	2.88	10.07	1.70	3.41	18.06
10	12.47	3.65	16.10	0.72	3.34	23.81
11	12.33	3.31	15.49	0.73	3.57	23.10
12	12.27	1.32	2.86	0.85	1.68	6.71
13	11.53	6.47	16.86	0.70	2.38	26.41
14	11.40	6.14	13.47	0.00	2.41	22.02
15	10.00	0.00	8.66	0.38	10.91	19.95

^a Xylenes= p. xylene, m. xylene, o. xylene
^b Summation of BTEX
The experiments were conducted in duplicate (except the central points) to check their reproducibility. The errors were found to be <3%

The percentage of gasoline aromatics generated in this study was about the same as that obtained by Park *et al.* (2010) for the catalytic upgrading of pyrolytic vapors derived from the sawdust of radiata pine.

Optimization

The main interests in this work were OLP and gasoline aromatics in the OLP; hence, the results of the investigation are reported for the effects of three variables on the yield of OLP and the percentage of gasoline aromatics. RSM was used to predict the optimum values of the three variables. A mathematical model was developed based on the experimental design performed initially by Essential Regression software, as listed in Table 3. The experimental data was used to develop a quadratic regression model to predict the OLP yield and the aromatic percentage in OLP as a function of the three parameters including temperature (T , °C), catalyst's weight (C , g), and N_2 flow rate (G , mL/min), which was given by:

$$Y_{\text{OLP}} = -60.92 + 0.250T + 6.962C - 0.301G - 0.00021T^2 + 0.01959C^2 + 0.01959G^2 - 0.00975TC \quad (3)$$

$$Y_{\text{Aromatics}} = -183.03 + 0.700T - 0.00065T^2 - 0.932C^2 + 0.01716TC - 0.00043TG \quad (4)$$

The analysis of variance (ANOVA) summarized in Table 6, demonstrated that the models were highly significant at 95% confidence level, with high F-Value and very low F-significance. The regression coefficients and P-values were also shown; the latter were used to check the significance of each coefficient. From the significance test, it was found that temperature (T) and catalyst's weight (C) were the most significant factors (p-values <0.05) affecting the OLP yield and the aromatics percentage in OLP. Additionally, as can be seen in Fig. 4, the values predicted for OLP and gasoline aromatics by the mathematical model were in good agreement with the experimental results, confirming the fitness of the model. From the figure, the model's results fit well with the experimental results, as indicated by the determination coefficients (R^2) of 0.926 and 0.906 for the model's predictions of OLP yield and gasoline aromatics, respectively.

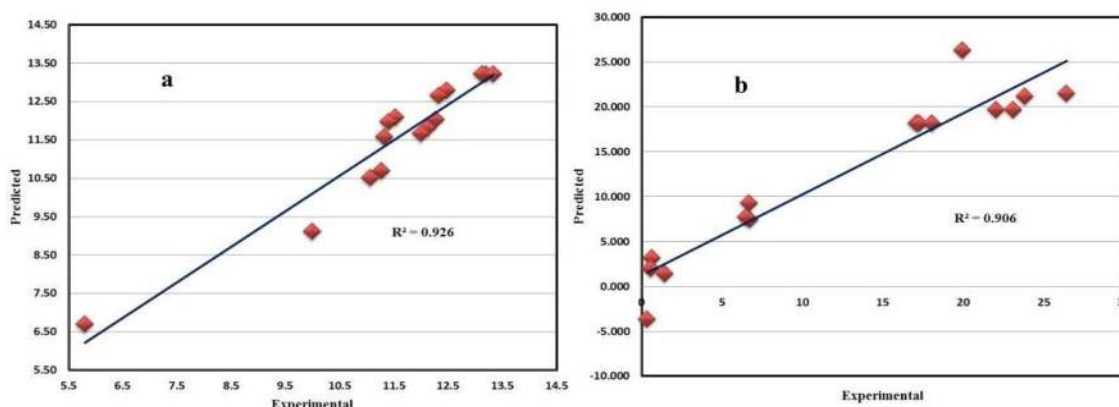


Fig. 4. Experimental results versus predicted values of (a) OLP yield and (b) gasoline aromatics (%) in OLP

Table 6. Analysis of Variance (ANOVA) for Quadratic Models

Source	Coefficient	P-value	Std Error	SS ^a	MS ^b	F-value	F-Significance	df ^c
Yield of OLP model								
b0	-60.92	0.00145	10.98					
b1	0.250	0.00083	0.04056					
b2	6.962	0.00082	1.125					
b3	-0.301	0.677	0.689					
b4	-0.00021	0.00162	3.94E-05					
b5	-0.307	0.02080	0.09862					
b6	0.01959	0.565	0.03220					
b7	-0.00975	0.00213	0.00190					
b8	5E-05	0.965	0.00108					
Regression				43.30	5.412	9.420	0.00677	8
Residual				3.447	0.575			6
LOF Error				3.427	0.857	83.174	0.01192	4
Pure Error				0.0206	0.0103			2
Total				46.74				14
Percentage of aromatics in OLP model								
b0	-183.03	0.00385	47.41					
b1	0.700	0.00542	0.192					
b2	-0.00065	0.00756	0.000192					
b3	-0.932	0.04863	0.409					
b4	0.01716	0.00737	0.00499					
b5	-0.00043	0.571	0.00074					
Regression				1187.8	237.57	17.30	0.000222	5
Residual				123.56	13.73			9
LOF Error				123.03	17.58	66.821	0.01482	7
Pure Error				0.526	0.263			2
Total				1311.4				14
^a SS= Sum of squares ^b MS= Mean squares ^c df= Degree of freedom Confidence level= 95%								

Essential Regression software was used to optimize the conditions, and the results showed that the maximum value of OLP yield was about 13.6 wt% for a temperature of 511 °C, a catalyst weight of 3.2 g, and an N₂ flow rate of 3 mL/min. Correspondingly, the maximum percentage of gasoline aromatics was about 27 wt%, which was obtained at 595 °C, a catalyst weight of 5 g, and an N₂ flow rate of 3 mL/min.

The three-dimensional (3D) response surfaces and their corresponding 2-D contours in Fig. 5, display the interaction effects of the most significant variables (temperature and catalyst weight) on the OLP yield and percentage of gasoline aromatics in OLP. The response surface can be used to determine the optimum levels of the parameters for the maximum response of OLP yield and aromatics percentage at the highest point of the surface. Fig. 5(A) shows the mutual effects of the temperature and catalyst weight on the OLP yield. The highest OLP yield was obtained at around 3 g of catalyst and decreased gradually to about 9 wt% with further increase of catalysts to about 5 g. However, there was a significant decrease in the OLP yield when the catalyst weight further decreased from 3 g to 1 g. This might be occurred due to less cracking of the pyrolysis oil. Also a highest OLP yield, i.e., about 13 wt%, was achieved at around 511 °C, then gradually dropped to about 11 wt% with increasing temperature to 600 °C due to an increased rate of cracking reactions, forming smaller compounds; however, an obvious

decrease of OLP yield was observed on lower temperatures as the cracking reactions do not take place efficiently at the lower temperatures. On the other hand, the mutual effects of the temperature and catalyst weight on the aromatics percentage were depicted in Fig. 5(B). This figure implies that a slight decrease in aromatics percentage occurred when the catalyst weight decreased from 5 g to about 3 g; however a significant drop of aromatics percentage was achieved at very low amount of catalysts. This can be explained by the impact of catalyst's acid sites, which are critical for maximizing aromatic percentage. So, as the amount of catalyst decreased (less acid sites), the formation of aromatics decreased. Likewise, the increase of coke deposition will lead to a blockage of the active sites, hence a decrease in the aromatics formation. Moreover, the aromatics percentage increased with increasing temperature, showing highest values at a temperature range of around 500 to 600 °C and thereafter decreased significantly at lower temperatures. The higher temperatures are usually required to thoroughly enhance deoxygenation reactions, to increase the aromatic formation.

The results from of the response surface in Fig. 5(B) show that some values of aromatics percentage (optimum) lay beyond the independent variables, which indicate the need for further improved conditions.

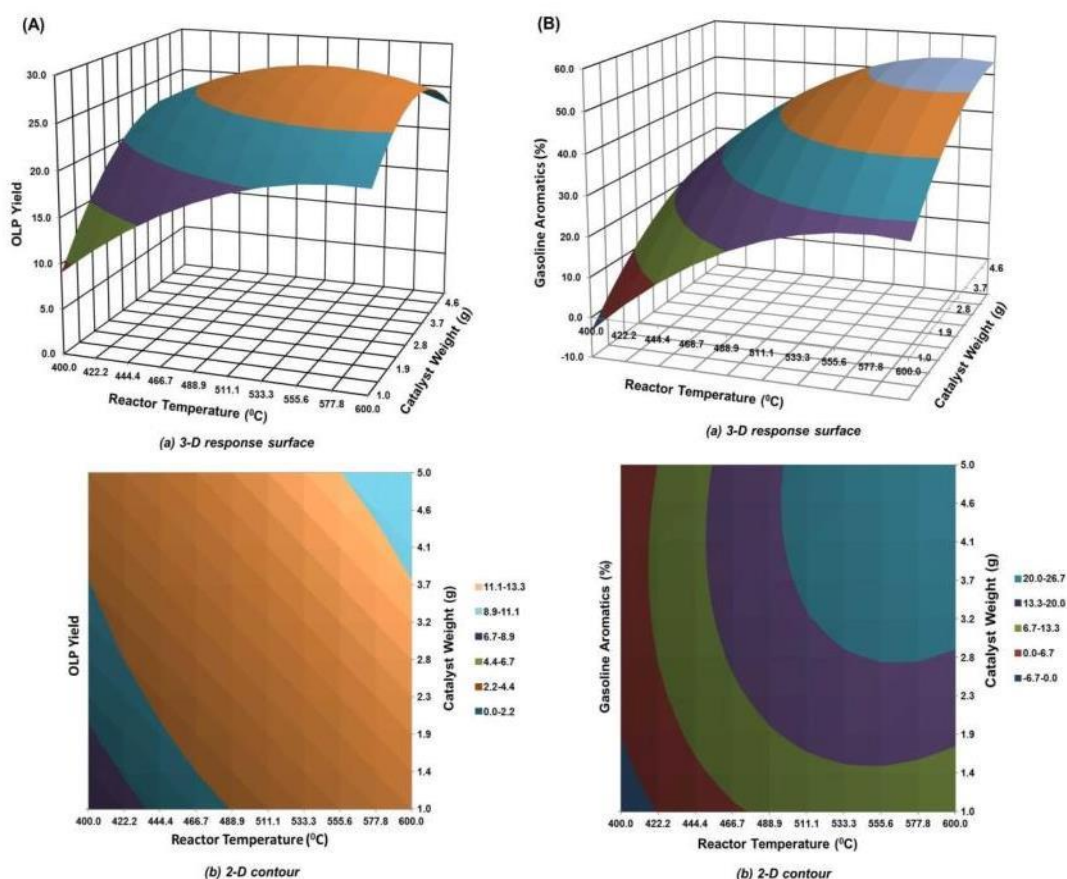


Fig. 5. Surface plot of: (A) OLP yield and (B) gasoline aromatics (%) in OLP as functions of catalyst weight and reactor temperature

The choice of the examined independent variables with their ranges seem appropriate with this process; however, the reduction of the feed rate (1.4 g/min) is most

likely needed, as it would probably enhance the catalyst cracking reactivity, hence increasing the aromatic concentration, which will therefore get the optimum values in the examined ranges.

The predicted results were validated by conducting experiments with the optimum conditions, as presented in Table 7. The yield of OLP was 15 wt%, whereas the predicted value was 13.6 wt%. The percentage of gasoline aromatics was 30 wt% compared to the predicted value of 27 wt%. The content of gasoline aromatics in OLP was identified, indicating that the content was dominated by toluene and that it had a very low percentage of ethylbenzene (Table 8). Furthermore, it was observed that the benzene concentration was somewhat less than the concentrations of toluene and xylenes, which indicated that benzene can be alkylated easily on the HSZM-5 catalyst due to its acidity (Chang *et al.* 1979; Bridgwater and Kuester 1988).

The BTEX are desirable chemicals that can be used as high octane gasoline additives. However, from environmental and safety viewpoints, benzene is not preferred due to its toxicity. As can be seen in Table 8, high amount of benzene was obtained in OLP, which is far from meeting gasoline specifications in the USA and Europe (Gibbs *et al.* 2009; Swick *et al.* 2014). Consequently, it would have to be recovered from toluene, xylenes, and ethylbenzene and used for chemicals production. Interestingly, BTEX also serve as important aromatic platforms, and they can provide feedstocks for producing a variety of chemicals, especially in the petrochemical industry.

Table 7. Predicted and Experimental Results at Optimum Conditions

	Predicted	Experiment	Optimum conditions		
			Temperature (°C)	Catalyst weight (g)	N ₂ flow rate (mL/min)
OLP yield (wt%)	13.6	15	511	3.2	3
Percentage of gasoline aromatics (wt%)	27	30	595	5	3

The values of the experimental results are average of duplicate trials with error <3

Table 8. Gasoline Aromatics Content in OLP at Optimum Conditions

	wt%
Benzene	5.16
Toluene	14.42
Ethylbenzene	0.58
Xylenes	9.84
Total	30.00

The values are average of duplicate trials with error <3

CONCLUSIONS

1. It was demonstrated that gasoline aromatics were generated from rubberwood-derived oil with concentration approaching 27 wt% in the OLP.
2. Temperature and catalyst weight were identified as the most significant factors affecting the OLP yield and the aromatics percentage in OLP. The model was adequate

for predicting the OLP yield and the percent of aromatics in OLP at less than 5% error. From RSM, a maximum value of 13.6 wt% of the OLP yield was obtained at 511 °C, 3.2 g of catalyst, and an N₂ flow rate of 3 mL/min, whereas the maximum percent of gasoline aromatics in the OLP. In other words, about 27 wt%, was achieved at 595 °C, 5 g of catalyst, and an N₂ flow rate of 3 mL/min.

3. Experiments were conducted at the optimum conditions in order to verify the accuracy of the simulated optimum conditions. The OLP yield was 15 wt% as compared to simulated value of 13.6 wt% (9.3% error). The percentage of gasoline aromatics was 30 wt% compared to simulated value of 27 wt% (10% error).
4. Among the side products, the bio-char seems the most important product, as it can be processed further for use as an adsorbent in a variety of applications.
5. It can be concluded that pyrolysis liquid obtained as a by-product of the production of charcoal from rubberwood has significant potential for use in producing gasoline since it contains BTEX components in the OLP.

ACKNOWLEDGMENTS

We sincerely acknowledge the graduate school of Prince of Songkla University for the financial support for this study. The authors express their gratitude to the scientists of the scientific equipment center, who performed some of the tests reported in this paper.

REFERENCES CITED

- Adjaye, J. D., and Bakhshi, N. N. (1995a). "Catalytic conversion of a biomass-derived oil to fuels and chemicals I: Model compound studies and reaction pathways," *Biomass. Bioenerg.* 8(3), 131-149. DOI: 10.1016/0961-9534(95)00018-3
- Adjaye, J. D., and Bakhshi, N. N. (1995b). "Production of hydrocarbons by catalytic upgrading of a fast pyrolysis bio-oil. Part I: Conversion over various catalysts," *Fuel. Process. Technol.* 45(3), 161-183. DOI: 10.1016/0378-3820(95)00034-5
- Adjaye, J. D., and Bakhshi, N. N. (1995c). "Production of hydrocarbons by catalytic upgrading of a fast pyrolysis bio-oil. Part II: Comparative catalyst performance and reaction pathways," *Fuel. Process. Technol.* 45(3), 185-202. DOI: 10.1016/0378-3820(95)00040-E
- Bi, P., Yuan, Y., Fan, M., Jiang, P., Zhai, Q., and Li, Q. (2013). "Production of aromatics through current-enhanced catalytic conversion of bio-oil tar," *Bioresour. Technol.* 136(0), 222-229. DOI: 10.1016/j.biortech.2013.02.100
- Bridgwater, A. V., and Grassi, G. (1991). *Biomass Pyrolysis Liquids: Upgrading and Utilization*, Elsevier Applied Science, London. DOI: 10.1007/978-94-011-3844-4
- Bridgwater, A. V., and Kuester, J. L. (1988). *Research in Thermochemical Biomass Conversion*, Elsevier Applied Science, London. DOI: 10.1007/978-94-009-2737-7
- Bridgwater, A. V., and Peacocke, G. V. C. (2000). "Fast pyrolysis processes for biomass," *Renew. Sust. Ener. Rev.* 4(1), 1-73. DOI: 10.1016/S1364-0321(99)00007-6

- Carlson, T., Tompsett, G., Conner, W., and Huber, G. (2009). "Aromatic production from catalytic fast pyrolysis of biomass-derived feedstocks," *Top. Catal.* 52(3), 241-252. DOI: 10.1007/s11244-008-9160-6
- Chang, C. D., Lang, W. H., and Smith, R. L. (1979). "The conversion of methanol and other O-compounds to hydrocarbons over zeolite catalysts: II. Pressure effects," *J. Catal.* 56(2), 169-173. DOI: 10.1016/0021-9517(79)90103-9
- Charles, M. B., Ryan, R., Ryan, N., and Oloruntoba, R. (2007). "Public policy and biofuels: The way forward?" *Energy Policy* 35(11), 5737-5746. DOI: 10.1016/j.enpol.2007.06.008
- Cheng, Y.-T., and Huber, G. W. (2011). "Chemistry of furan conversion into aromatics and olefins over HZSM-5: A model biomass conversion reaction," *ACS Catal.* 1(6), 611-628. DOI: 10.1021/cs200103j
- Chiaramonti, D., Oasmaa, A., and Solantausta, Y. (2007). "Power generation using fast pyrolysis liquids from biomass," *Renew. Sust. Energ. Rev.* 11(6), 1056-1086. DOI: 10.1016/j.rser.2005.07.008
- Clarke, G. M., and Kempson, R. E. (1997). *Introduction to the Design and Analysis of Experiments*, Arnold, London. DOI: 10.1002/(SICI)1097-0258(20000330)19:6<882::AID-SIM288>3.0.CO;2-5
- Cornell, J. A. (1990). *How to Apply Response Surface Methodology*, American Society for Quality Control, Statistics Division, ASQC, Milwaukee, Wisconsin.
- Czernik, S., and Bridgwater, A. V. (2004). "Overview of applications of biomass fast pyrolysis oil," *Energy Fuels* 18(2), 590-598. DOI: 10.1021/ef034067u
- Demirbas, A. (2007). "Progress and recent trends in biofuels," *Prog. Energ. Combust.* 33(1), 1-18. DOI: 10.1016/j.peccs.2006.06.001
- Demirbas, M. F., Balat, M., and Balat, H. (2009). "Potential contribution of biomass to the sustainable energy development," *Energ. Convers. Manage.* 50(7), 1746-1760. DOI: 10.1016/j.enconman.2009.03.013
- Diebold, J., and Scahill, J. (1988). "Biomass to gasoline (BTG): Upgrading pyrolytic vapours to aromatic gasoline with zeolite catalysts at atmospheric pressure," in: *Pyrolysis Oils from Biomass: Producing, Analyzing and Upgrading*, E.J. Soltes and T.A Milne (Eds.), ACS Symposium Series 376, 264-276. DOI: 10.1021/bk-1988-0376.ch023
- Dodds, D. R., and Gross, R. A. (2007). "Chemicals from biomass," *Science* 318(5854), 1250-1251. DOI: 10.1126/science.1146356
- Gibbs, L., Anderson, B., Barnes, K., Engeler, G., Freel, J., Horn, J., and Ingham, M. (2009). *Motor Gasolines Technical Review*, Chevron Products Company, San Ramon.
- Gong, F., Yang, Z., Hong, C., Huang, W., Ning, S., Zhang, Z., Xu, Y., and Li, Q. (2011). "Selective conversion of bio-oil to light olefins: Controlling catalytic cracking for maximum olefins," *Bioresource. Technol.* 102(19), 9247-9254. DOI: 10.1016/j.biortech.2011.07.009
- Grilc, M., Likozar, B., and Levec, J. (2014). "Hydrodeoxygenation and hydrocracking of solvolysed lignocellulosic biomass by oxide, reduced and sulphide form of NiMo, Ni, Mo and Pd catalysts," *Appl. Catal. B-Environ.* 150-151, 275-287. DOI: 10.1016/j.apcatb.2013.12.030
- Grilc, M., Likozar, B., and Levec, J. (2014). "Hydrotreatment of solvolytically liquefied lignocellulosic biomass over NiMo/Al₂O₃ catalyst: Reaction mechanism, hydrodeoxygenation kinetics and mass transfer model based on FTIR," *Biomass. Bioenerg.* 63, 300-312. DOI: 10.1016/j.biombioe.2014.02.014

- Grilc, M., Veryasov, G., Likozar, B., Jesih, A., and Levec, J. (2015). "Hydrodeoxygenation of solvolysed lignocellulosic biomass by unsupported MoS₂, MoO₂, Mo₂C and WS₂ catalysts," *Appl. Catal. B-Environ.* 163, 467-477. DOI: 10.1016/j.apcatb.2014.08.032
- Gronowska, M., Joshi, S., and MacLean, H. L. (2009). "A review of US and Canadian biomass supply studies," *BioResources* 4(1), 341-369.
- Huber, G. W., and Corma, A. (2007). "Synergies between bio- and oil refineries for the production of fuels from biomass," *Angew. Chem. Int. Ed.* 46(38), 7184-7201. DOI: 10.1002/anie.200604504
- Huber, G. W., Iborra, S., and Corma, A. (2006). "Synthesis of transportation fuels from biomass: Chemistry, catalysts, and engineering," *Chem. Rev.* 106(9), 4044-4098. DOI: 10.1021/cr068360d
- Krukanont, P., and Prasertsan, S. (2004). "Geographical distribution of biomass and potential sites of rubber wood fired power plants in Southern Thailand," *Biomass. Bioenerg.* 26(1), 47-59. DOI: 10.1016/S0961-9534(03)00060-6
- Li, X., Su, L., Wang, Y., Yu, Y., Wang, C., Li, X., and Wang, Z. (2012). "Catalytic fast pyrolysis of kraft lignin with HZSM-5 zeolite for producing aromatic hydrocarbons," *Front. Environ. Sci. Eng.* 6(3), 295-303. DOI: 10.1007/s11783-012-0410-2
- Lucia, L. A. (2008). "Lignocellulosic biomass: A potential feedstock to replace petroleum," *BioResources* 3(4), 981-982.
- Mentzel, U. V., and Holm, M. S. (2011). "Utilization of biomass: Conversion of model compounds to hydrocarbons over zeolite H-ZSM-5," *Appl. Catal. A-Gen.* 396(1-2), 59-67. DOI: 10.1016/j.apcata.2011.01.040
- Mohan, D., Pittman, C. U., and Steele, P. H. (2006). "Pyrolysis of wood/biomass for bio-oil: A critical review," *Energy Fuels* 20(3), 848-889. DOI: 10.1021/ef0502397
- Mojoviä, L., Pejin, D. A., Grujiä, O., Markov, S. A., Pejin, J., Rakin, M., Vukaä;inovä, M., Nikoliä, S., and Saviä, D. A. (2009). "Progress in the production of bioethanol on starch-based feedstocks," *Chem. Ind. Chem. Eng. Q.* 15(4), 211-226. DOI: 10.2298/CICEQ0904211M
- Montgomery, D. C. (2001). *Design and Analysis of Experiments*, 5th Ed., John Wiley & Sons., New York. DOI: 10.1002/qre.458
- Park, H. J., Heo, H. S., Jeon, J.-K., Kim, J., Ryoo, R., Jeong, K.-E., and Park, Y.-K. (2010). "Highly valuable chemicals production from catalytic upgrading of radiata pine sawdust-derived pyrolytic vapors over mesoporous MFI zeolites," *Appl. Catal. B-Environ.* 95(3-4), 365-373. DOI: 10.1016/j.apcatb.2010.01.015
- Saad, A., and Ratanwilai, S. B. (2014). "Characterisation of liquid derived from pyrolysis process of charcoal production in south of Thailand," *Iranica Journal of Energy and Environment* 5(2), 184-191. DOI: 10.5829/idosi.ijee.2014.05.02.10
- Sharma, R. K., and Bakhshi, N. N. (1993). "Catalytic conversion of fast pyrolysis oil to hydrocarbon fuels over HZSM-5 in a dual reactor system," *Biomass Bioenergy* 5(6), 445-455. DOI: 10.1016/0961-9534(93)90040-B
- Srinivas, S. T., Dalai, A. K., and Bakhshi, N. N. (2000). "Thermal and catalytic upgrading of a biomass-derived oil in a dual reaction system," *The Canadian Journal of Chemical Engineering* 78(2), 343-354. DOI: 10.1002/cjce.5450780209
- Stevens, C., and Brown, R. C. (2011). "Fast pyrolysis," in: *Thermochemical Processing of Biomass: Conversion into Fuels, Chemicals and Power*, (Vol. 12). R. C. Brown (Ed.), John Wiley & Sons. DOI: 10.1002/9781119990840.ch5

- Swick, D., et al. (2014). "Gasoline risk management: A compendium of regulations, standards, and industry practices," *Regul. Toxicol. Pharm.* 70(2, Supplement), S80-S92. DOI: 10.1016/j.yrtph.2014.06.022
- Tiilikkala, K., Fagernäs, L., and Tiilikkala, J. (2010). "History and use of wood pyrolysis liquids as biocide and plant protection product," *The Open Agriculture Journal* 4(Special Issue# 002), 111-118. DOI: 10.2174/1874331501004010111
- Treacy, M. M. J., and Higgins, J. B. (2007). *Collection of Simulated XRD Powder Patterns for Zeolites*, Fifth Revised Edition, Elsevier.
- Valle, B., Gayubo, A. G., Aguayo, A. T., Olazar, M., and Bilbao, J. (2010). "Selective production of aromatics by crude bio-oil valorization with a nickel-modified HZSM-5 zeolite catalyst," *Energy Fuels* 24(3), 2060-2070. DOI: 10.1021/ef901231j
- Valle, B., Gayubo, A. G., Alonso, A., Aguayo, A. T., and Bilbao, J. (2010). "Hydrothermally stable HZSM-5 zeolite catalysts for the transformation of crude bio-oil into hydrocarbons," *Appl. Catal. B-Environ.* 100(1-2), 318-327. DOI: 10.1016/j.apcatb.2010.08.008
- Vitolo, S., Bresci, B., Seggiani, M., and Gallo, M. G. (2001). "Catalytic upgrading of pyrolytic oils over HZSM-5 zeolite: Behaviour of the catalyst when used in repeated upgrading-regenerating cycles," *Fuel* 80(1), 17-26. DOI: 10.1016/S0016-2361(00)00063-6
- Vitolo, S., Seggiani, M., Frediani, P., Ambrosini, G., and Politi, L. (1999). "Catalytic upgrading of pyrolytic oils to fuel over different zeolites," *Fuel* 78(10), 1147-1159. DOI: 10.1016/S0016-2361(99)00045-9
- Wang, S., Cai, Q., Wang, X., Zhang, L., Wang, Y., and Luo, Z. (2013). "Biogasoline production from the co-cracking of the distilled fraction of bio-oil and ethanol," *Energy Fuels* 28(1), 115-122. DOI: 10.1021/ef4012615
- Zhang, Q., Chang, J., Wang, T., and Xu, Y. (2007). "Review of biomass pyrolysis oil properties and upgrading research," *Energ. Convers. Manage.* 48(1), 87-92. DOI: 10.1016/j.enconman.2006.05.010
- Zhao, Y., Deng, L., Liao, B., Fu, Y., and Guo, Q.-X. (2010). "Aromatics production via catalytic pyrolysis of pyrolytic lignins from bio-oil," *Energy Fuels* 24(10), 5735-5740. DOI: 10.1021/ef100896q
- Zhu, J., Wang, J., and Li, Q. (2013). "Transformation of bio-oil into BTX by bio-oil catalytic cracking," *Chin. J. Chem. Phys.* 26(4), 477-483. DOI: 10.1063/1674-0068/26/04/477-483

Article submitted: October 8, 2014; Peer review completed: February 22, 2015;

Revisions received and accepted: April 6, 2015; Published: April 15, 2015.

DOI: 10.15376/biores.10.2.3224-3241

Appendix C

Catalytic conversion of pyrolysis tar to produce green gasoline-range aromatics



2015 International Conference on Alternative Energy in Developing Countries and Emerging Economies

Catalytic Conversion of Pyrolysis Tar to Produce Green Gasoline-Range Aromatics

Abdulrahim Saad^{a*}, Sukritthira Ratanawilai^a, Chakrit Tongurai^a

^a*Department of Chemical Engineering, Faculty of Engineering, Prince of Songkla University, Had Yai, Songkhla, 90112, Thailand*

Abstract

Pyrolysis oils derived from wood biomass attracted the attention of many researchers due to their potential as a source of sulfur-free environmentally-friendly fuel. In this study, we attempted to generate gasoline-range aromatics from pyrolysis tar derived from rubber wood. Catalytic cracking of the pyrolysis tar was conducted using an HZSM-5 catalyst in a dual reactor. The effects of reaction temperatures (400-600 °C), catalyst weights (1-5 g), and nitrogen flow rates (3-10 mL/min) were investigated to determine their effects on the yield of organic liquid product (OLP) and the percentage of gasoline aromatics in the OLP. The maximum OLP yield was about 28.33 wt%, achieved at 536 °C and a catalyst weight of 3.5 g. The maximum percentage of gasoline aromatics was about 54 wt%, obtained at 575 °C with a catalyst weight of 5 g. Though, the yield of gasoline aromatics was low, the anticipated components, i.e., benzene, toluene, ethylbenzene, and xylenes (BTEX), were detected in the OLP proving that green gasoline aromatics can be produced from rubber wood pyrolysis tar via zeolite cracking

© 2015 The Authors. Published by Elsevier Ltd. This is an open access article under the CC BY-NC-ND license (<http://creativecommons.org/licenses/by-nc-nd/4.0/>).

Peer-review under responsibility of the Organizing Committee of 2015 AEDCEE

Keywords: Pyrolysis tar, zeolite cracking, organic liquid product (OLP), green gasoline-range aromatics

1. Introduction

With the global oil crisis of the 1970s and the greenhouse effect, there is increasing interest in exploring renewable energy resources to replace conventional fossil fuels. Biomass, one possible source of renewable energy, is a CO₂-neutral resource; as a result, significant attention has been paid to biomass as an alternative to petroleum fuels [1, 2].

Present-day pyrolysis oil has attracted considerable interest, particularly in fuel production, making it the most suitable material to compete with non-renewable fuel resources [3-4]. Direct substitution of pyrolysis oil for petroleum, however, might be limited due to pyrolysis oil's thermal

* Corresponding author. Tel.: +66-874-755690; fax: +66-74-558833.
 E-mail address: abdorahim@hotmail.com

instability, high viscosity, and high oxygen content [5]. As a result, an upgrading process is required to reduce its oxygen content. The upgrading process essentially involves the conversion of oxygen-rich compounds into hydrocarbons that are consistent with traditional fuels. Catalytic cracking and hydrotreating are two routes that have been used to upgrade the pyrolysis oil. However, catalytic cracking is favoured; it can be performed at atmospheric pressure and no hydrogen is required, which offer economic advantages over hydrodeoxygenation [3, 6]. Recently, the production of green gasoline, particularly gasoline-range aromatics from pyrolysis oils, has aroused attention. A handful of previous studies demonstrated that pyrolysis oil derived from different biomass sources could be converted to gasoline hydrocarbons by catalytic cracking over ZSM5 catalysts [7, 8, 9]; however, some related studies dealt with pyrolysis oil fractions, which can be easier to understand. Wang et al. [10] outlined the produce high-quality gasoline rich with aromatic hydrocarbons by using a distilled fraction of pyrolysis oil derived from rice husk. They revealed that the cracking behaviour of the distilled fraction can be enhanced by co-feeding ethanol while using the HZSM-5 catalyst. Recently, Bi and co-workers [11] used a residual distillation fraction of pyrolysis oil derived from straw stalks. The heavy fraction was transformed directly to higher yield of aromatics (mainly consisted of benzene, toluene, ethylbenzene, and xylenes; BTEX), by using HZSM-5 catalyst. Another study was conducted by Yan Zhao et al. [12], who produced a high yield of aromatic hydrocarbons from pyrolytic lignins (PLs) isolated from rice husk derived oil by performing a catalytic pyrolysis techniques using ZSM-5 catalyst.

The rubber tree is planted extensively in southern Thailand and is one of the country's leading economic crops. The rubber wood is utilized to a great extent by local farmers and small plants to produce charcoal via a slow pyrolysis process (carbonization) [13, 14]. The pyrolysis liquid is an unavoidable by-product obtained during the manufacture of charcoal; over time, the liquid is divided into aqueous and oily layers. The oily layer, more accurately called pyrolysis tar, is a sticky liquid mixture of different oxygenated compounds, primarily composed of phenols. The pyrolysis tar is normally removed from aqueous liquid because it contaminates plants and soil when sprayed on them. On the basis of compositions, pyrolysis tar has the capability to produce green gasoline rich with aromatic chemicals. Additionally, it can add value to the production of charcoal. To the best of authors' knowledge, pyrolysis tar as a by-product from charcoal production has received limited attention, and no study was conducted to upgrade it to gasoline-range aromatics or organic liquid product (OLP). Thus, this work was carried out with the aim of investigating the potential use of tar for producing green gasoline through catalytic cracking over an HZSM-5 catalyst in a dual reactor.

2. Materials and methods

2.1. Preparation and characterization of pyrolysis tar

Crude pyrolysis liquid was obtained from Phatthalung Province. The liquid had been settled for about two months; after that, the settled tar was separated by decantation. The separated tar was then kept in a refrigerator overnight to remove the rest of the water, which was separated by decantation. The chemical composition of the pyrolysis tar was determined by GC-MS analysis as shown in Table 1.

Table 1. Chemical Composition of the Pyrolysis Tar Identified by GC-MS

	Composition	MW	Formula	Peak area %
1	Syringol	154.00	C ₈ H ₁₀ O ₃	12.11
2	2, 6-Dihydroxy-4-methoxyacetophenone	182.17	C ₉ H ₁₀ O ₄	9.49
3	1,2,4-Trimethoxybenzene	168.19	C ₉ H ₁₂ O ₃	8.94
4	Creosol	138.16	C ₈ H ₁₀ O ₂	5.25
5	Guaiacol	124.13	C ₇ H ₈ O ₂	5.14
6	p-Ethylguaiacol	152.19	C ₉ H ₁₂ O ₂	4.89
7	o-Cresol	108.13	C ₇ H ₈ O	3.57
8	2,6-Dimethoxy-4-allylphenol	194.22	C ₁₁ H ₁₄ O ₃	3.43
9	p-Cresol	108.13	C ₇ H ₈ O	2.37
10	3,5-dimethylphenol	122.16	C ₈ H ₁₀ O	2.08
11	2-Methoxy-5-propylphenol	166.21	C ₁₀ H ₁₄ O ₂	1.79
12	Vanillyl methyl ketone	180.20	C ₁₀ H ₁₂ O ₃	0.88
13	Corylon	112.12	C ₆ H ₈ O ₂	0.87
14	2,5-Dimethylphenol	122.16	C ₈ H ₁₀ O	0.87
15	5-hydroxy-3-heptanone	130.18	C ₇ H ₁₄ O ₂	0.75
16	2,3-Dimethylphenol	122.16	C ₈ H ₁₀ O	0.65
17	Eugenol	164.20	C ₁₀ H ₁₂ O ₂	0.63
18	3,4,5-Trimethoxytoluene	182.21	C ₁₀ H ₁₄ O ₃	0.60
19	4-Methoxy-3-methylphenol	138.16	C ₈ H ₁₀ O ₂	0.56
20	3-Ethyl-2-hydroxy-2-cyclopenten-1-one	126.15	C ₇ H ₁₀ O ₂	0.54
21	3-Methyl-2-cyclopenten-1-one	96.12	C ₆ H ₈ O	0.51
22	Furfural	96.08	C ₅ H ₄ O ₂	0.48
23	3,4-Dimethoxytoluene	152.19	C ₉ H ₁₂ O ₂	0.42
24	2-Acetylfuran	110.11	C ₆ H ₈ O ₂	0.41
25	3,5-Dimethyl-2(5H)-furanone	112.12	C ₈ H ₈ O ₂	0.37
26	3-Ethyl-2-cyclopenten-1-one	110.15	C ₇ H ₁₀ O	0.35
27	2-methylcyclopentenone	96.12	C ₆ H ₈ O	0.33
28	2,3-Dimethoxytoluene	152.19	C ₉ H ₁₂ O ₂	0.33
29	5-Methyl-2-furfural	110.11	C ₆ H ₈ O ₂	0.28
30	Cyclopentenone	82.10	C ₅ H ₆ O	0.27
31	2,3-Dimethyl-2-cyclopenten-1-one	110.15	C ₇ H ₁₀ O	0.17
32	Unidentified			30.67

2.2. Preparation and characterization of the catalyst

NH₄-ZSM-5 zeolite (CBV 3024E) was purchased from Zeolyst International as a fine powder. Its surface area and SiO₂/Al₂O₃ ratio were 405 m²/g and 30, respectively. The HZSM-5 catalyst was prepared by removing the ammonia from NH₄-ZSM-5 by calcination at 550 °C for 5 h in a stream of nitrogen to obtain the HZSM-5 form prior to use. The structure of the catalyst was measured by X-ray diffraction (XRD; X'Pert MPD, PHILIPS). The morphology and particle sizes were determined from the scanning electron microscopy (SEM) image taken with a JSM-5800 LV, JEOL. Structure and morphology are depicted in Fig. 1.

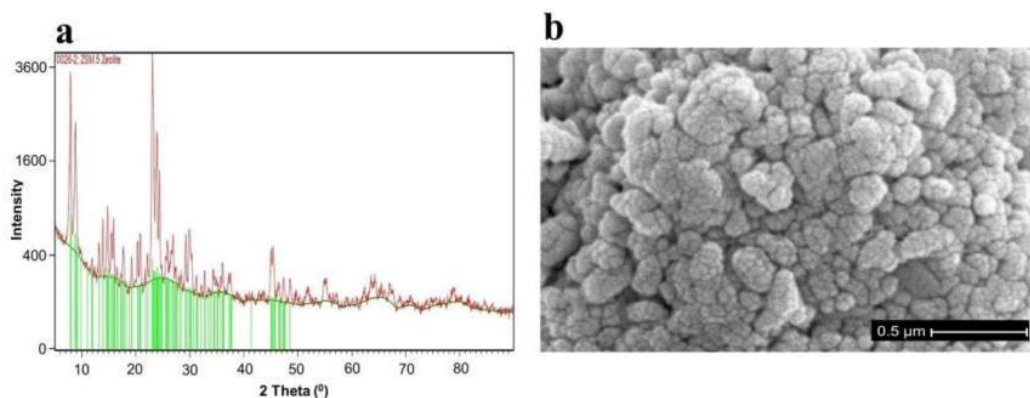


Fig. 1. (a) XRD pattern of HZSM-5 catalyst; (b) SEM image for HZSM-5 catalyst

2.3. Experimental setup and procedure

Catalytic cracking of pyrolysis tar was conducted in a dual reactor assembly without any catalyst in the first reactor, followed by a second fixed-bed reactor loaded with HZSM-5 catalyst, as depicted in Fig. 2. The reactors were cylindrical configurations made of stainless steel (i.d: 30 mm; length: 250 and 350 mm for the first and second reactors, respectively) and were placed coaxially in the furnaces. The experiments were operated at atmospheric pressure, a reaction temperature that varied from 400 to 600 °C, a catalyst weight of 1 to 5 g, and a nitrogen flow rate of 3 to 10 mL/min. In a typical experiment, the second reactor was loaded with catalyst that was held on a plug of glass wool. Before the reaction started, both reactors were heated in a nitrogen stream until the desired temperature was attained, after which a syringe pump was used to introduce 15 g of the feed (preheated pyrolysis tar) into the first reactor at the rate of 1.4 g/min, with different feeding rates of nitrogen serving as carrier gas. The products leaving the second reactor were condensed (collected in an ice-cooled flask) to separate the liquid and gaseous products. The liquid product was obtained in the form of immiscible layers, i.e., an organic layer and an aqueous layer. The organic layer, i.e., the OLP, was drawn off from the aqueous layer with a syringe. In addition, the uncondensed gaseous product was collected in a gas bag and its weight was obtained. The yields of products, i.e., OLP, aqueous liquid, char, and gas, relative to the total amount of the feed, were calculated using the following equation:

Yield (wt%) = $(P \times 100) / \text{feed}$ (15 g), where P is the number of grams of product, i.e., OLP, aqueous liquid, char, or gas.

2.4. Characterization of the liquid product

The liquid product included a separable oil layer (OLP) and an aqueous product. In this work, the product of interest was the gasoline fraction formed in the OLP, particularly gasoline-range aromatics, i.e., benzene, toluene, ethylbenzene, and xylenes (BTEX), which have higher octane ratings. Hence, only the gasoline hydrocarbons of BTEX were identified using gas chromatography (GC). The identities of the peaks were determined by using BTEX standards, and the quantities were determined from a calibration curve that had been developed using the BTEX standard. The aqueous product consisted mainly of water, as determined by Karl Fischer titration. It was anticipated that the aqueous products would contain some water-soluble organic components, such

as alcohols, carboxylic acids, and phenols. Then, a pH meter was used to attain the pH values, which ranged from 3.0 to 3.8.

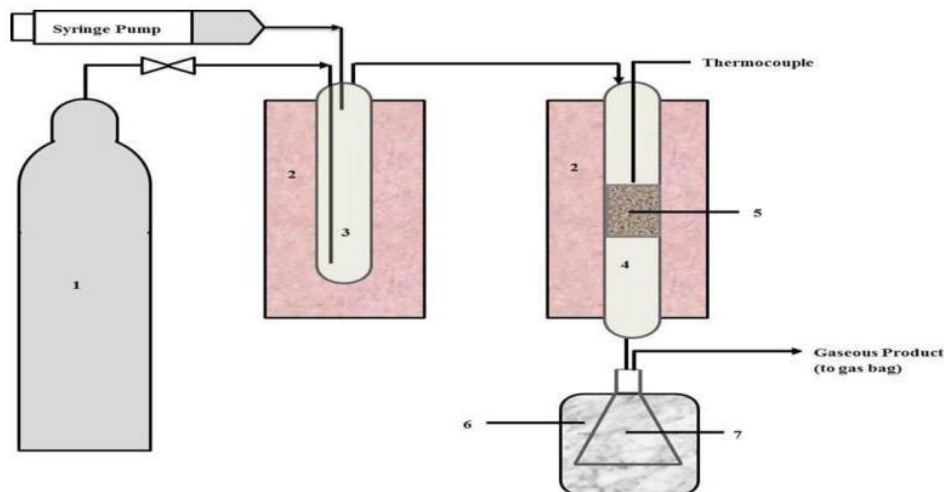


Fig. 2. Dual reactor setup showing (1) nitrogen cylinder, (2) furnace, (3) first reactor, (4) second reactor, (5) catalyst bed, (6) ice bath, (7) receiving flask

2.5. Experimental design

The Essential Regression and Experimental Design software was used to design the experiments. Three factors, i.e., temperature ($^{\circ}\text{C}$), the catalyst's weight (g), and the flow rate of N_2 (mL/min), were chosen as the independent variables that would affect the catalytic cracking of the pyrolysis oil.

Since OLP and gasoline aromatics were the most desired products, it was necessary to determine two quantities (responses) as shown in Table 2, i.e., the yield of OLP and the percentage of gasoline aromatics in the OLP.

Table 2. Experimental Design Matrix and Results

Runs	Experimental design			Experimental Results	
	Temperature $^{\circ}\text{C}$	Catalyst g	N_2 flow rate mL/min	OLP yield	Percentage of gasoline aromatics in OLP
1	400	1	6.5	10.00	2.01
2	400	3	3.0	18.45	10.10
3	400	3	10	18.30	9.90
4	400	5	6.5	20.28	29.83
5	500	1	3.0	15.13	20.88
6	500	1	10	14.98	20.00
7	500	3	6.5	27.31	40.77
8	500	3	6.5	27.50	41.53
9	500	3	6.5	26.90	42.00
10	500	5	3.0	25.00	49.41
11	500	5	10	24.80	48.29
12	600	1	6.5	22.65	24.28
13	600	3	3.0	24.40	52.25
14	600	3	10	24.35	50.65
15	600	5	6.5	22.00	45.21

3. Results and discussion

3.1. Product Distribution

Six products from catalytic cracking of pyrolysis tar were generated: OLP, an aqueous product, char, tar, coke, and non-condensable gases as provided in Table 3. It was observed that a significant amount of char was formed in the first reactor, and a small amount of char was formed above the catalyst bed in the second reactor, possibly due to the thermal effect on the unstable components of the tar. The yield of char ranged from about 20 to 24 wt % as shown in Table 3, and there was a slight decrease in the formation of char with the increase of temperature, probably due to secondary reactions occurring such as gasification. The yields of aqueous products ranged from about 25 to 33 wt % with water content ranged from 80-83 wt%, indicating that some oxygen was removed in the form of water [15]. It was essential to investigate the distributions of OLP, which ranged from about 10-27 wt % over the experimental runs. Low OLP yield was observed at 400 °C, while the maximum yield was about 27 wt% at 500 °C with 3 grams of catalyst. It was observed that there was a slight decrease in OLP when the temperature was increased from 500 to 600 °C, probably due to the additional conversion of OLP, forming more gaseous products. A similar observation was reported by Bi et al. [11]. As can be seen in Table 1, the major oxygenated compounds in the pyrolysis tar were phenolic compounds, ketones, esters, aldehydes, and a few others. Thus, it should be stated that the conversion of most of these oxygenated compounds to OLP over the HZSM-5 catalyst was an indication of its ability to remove oxygen through complex reactions, such as deoxygenation, cracking, cyclization, aromatization, isomerization and polymerization reactions [16, 17]. Furthermore, the yield of gas increased slightly with the reaction temperature and catalyst, showing a highest value of about 6.7 wt% at 600 °C, 5 g of catalyst and, 6.5 mL/min of N₂ gas. The lowest value was about 4 wt% attained at 400 °C, 1 g of catalyst, and 6.5 mL/min of N₂ gas.

Table 3. Overall Product Distribution (wt% of the feed) for 15 Experimental Runs

Runs	Products					
	Aqueous Liquid	Organic Liquid Product	Char ^a	Residue ^b	Gas	Unaccounted
	wt%					
1	30.00	10.00	24.00	14.00	4.11	17.89
2	25.37	18.45	23.50	13.50	4.45	14.73
3	25.30	18.30	23.00	13.30	4.50	15.60
4	25.00	20.28	23.30	13.10	5.32	13.00
5	28.30	15.13	22.62	13.00	5.35	15.60
6	28.30	14.98	22.00	13.10	5.48	16.14
7	27.00	27.31	22.54	13.00	5.70	4.45
8	26.50	27.50	22.50	12.80	5.68	5.02
9	26.20	26.90	22.60	12.80	5.77	5.73
10	29.84	25.00	22.60	12.91	6.10	3.55
11	30.00	24.80	22.00	12.87	6.15	4.18
12	31.00	22.65	20.00	12.30	6.34	7.71
13	32.66	24.40	20.30	12.00	6.44	4.20
14	32.51	24.35	20.00	12.00	6.60	4.54
15	33.00	22.00	20.00	11.89	6.70	6.41

^a Char formed in the first reactor
^b Residue is categorized as char and tar that were quantified in the second reactor

3.2. Content of Gasoline-Range Aromatics in OLP

As extremely desirable compounds, gasoline-range aromatics (BTEX) in OLP were selected as target compounds in our study. Gasoline aromatics were analyzed by GC-FID, and Fig. 3 shows their distributions for the experimental runs. From Table 2, the percentage of gasoline aromatics in OLP ranged from about 2 to 52 wt%, with a maximum value of about 52 wt% at 600 °C, 3 g of catalyst and 3 mL/min of N₂ gas. As a known effect, the formation of aromatic hydrocarbons is attributed to the conversion of oxygenated compounds, particularly substituted phenols, from biomass pyrolysis by cracking, dehydroxylation, decarbonylation, and decarboxylation reactions, which are catalysed by HSZM-5's acid sites [17-19].

It was noted that, at 400 °C, the gasoline aromatics increased slightly from 2.01 wt% to 29.83 wt%, coincident with the increase of catalyst. Similarly, at 500 °C, the percentage of gasoline aromatics increased significantly, from about 20.88 wt% to 49 wt%. The OLP achieved a dramatic increase of gasoline aromatics at 600 °C when 3 g of catalyst were used instead of 1 g; however, a slight drop occurred when 5 g of catalyst were used, possibly due to the secondary conversion of the aromatics [20]. The percentage of gasoline aromatics generated in this study was in a reasonable agreement with the results of Zhao et al. [12], who reported a 40 wt % of aromatics that can be generated from a pyrolytic when pyrolyzing 0.5 g at 600 °C using a 0.5 g of zeolite catalyst and 50 mL/min N₂.

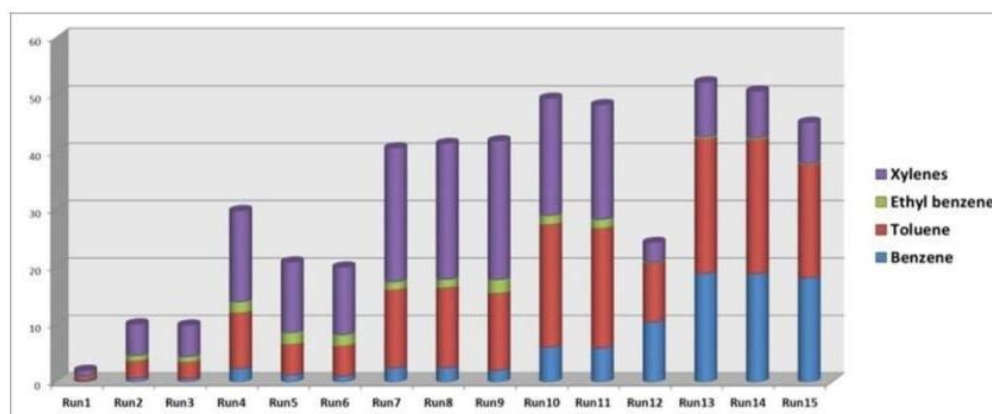


Fig. 3. Distributions of BTEX aromatics in the OLP

3.3. Optimization

The main targets in this study were OLP and gasoline aromatics in the OLP; hence, we reported the results of our investigation of influences of the three variables on the yield of OLP and the percentage of gasoline aromatics. Response surface methodology (RSM) was applied to predict the optimum values of the three variables. A mathematical model was developed based on the experimental design performed initially by Essential Regression software, as shown in Table 2. The table shows the values predicted for OLP yield and gasoline aromatics by the mathematical model were in good agreement with the experimental results, confirming the fitness of the model, as indicated by the determination coefficients (R^2) of 0.964 and 0.929 for the model's predictions of OLP yield and gasoline aromatics, respectively. The reaction conditions were optimized by applying Essential Regression software, and the results showed that the maximum value of OLP yield was about 28.33 wt% for a temperature of 536 °C and a catalyst weight of 3.5 g. Correspondingly, the maximum percentage of gasoline aromatics was about 54 wt%, obtained at

575 °C and a catalyst weight of 5 g. The three-dimensional (3D) response surfaces in Fig. 4, display the interaction effects of the significant variables (temperature and catalyst weight) on the OLP yield and percentage of gasoline aromatics in OLP.

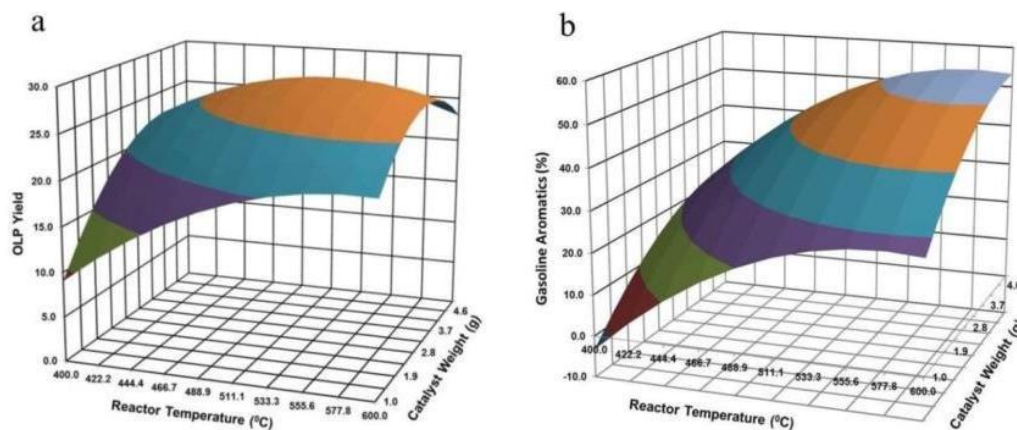


Fig. 4. Surface plot of: (a) OLP yield and (b) gasoline aromatics (%) in OLP as functions of catalyst weight and temperature

4. Conclusions

The gasoline aromatics were generated from rubber wood-derived tar through catalytic cracking using the HZSM-5 catalyst. From RSM, the maximum yield of OLP was about 28.33 wt%, achieved at 536 °C and a catalyst weight of 3.5 g, whereas the maximum percent of gasoline aromatics in the OLP, i.e., about 54 wt%, was obtained at 575 °C and a catalyst weight of 5 g. Side products also were obtained, including an aqueous liquid, tar, coke, gases, and, more importantly, char, which can be processed further for use as a sorbent. Overall, in assessing the conversion of pyrolysis tar derived from rubber wood to gasoline aromatics, it can be concluded that the pyrolysis tar has significant potential for use in producing gasoline since it contains BTEX components in the OLP.

Acknowledgments

The authors sincerely acknowledge the graduate school of Prince of Songkla University for the financial support for this study.

References

- [1] Demirbas, M.F., M. Balat, and H. Balat. Potential contribution of biomass to the sustainable energy development. *Energy Convers. Manage* 2009; **50**(7): 1746-1760.
- [2] Demirbas, A. Progress and recent trends in biofuels. *Prog. Energy Combust* 2007; **33**(1): 1-18.
- [3] Czernik, S. and A.V. Bridgwater. Overview of Applications of Biomass Fast Pyrolysis Oil. *Energy Fuels* 2004; **18**(2): 590-598.
- [4] Bridgwater, A. V., and Grassi, G. *Biomass pyrolysis liquids: Upgrading and utilization*, Elsevier Applied Science, London; 1991.
- [5] Mohan, D., C.U. Pittman, and P.H. Steele. Pyrolysis of Wood/Biomass for Bio-oil: A Critical Review. *Energy Fuels* 2006; **20**(3): 848-889.
- [6] Huber, G.W. and A. Corma. Synergies between Bio- and Oil Refineries for the Production of Fuels from Biomass. *Angew. Chem. Int. Ed* 2007; **46**(38): 7184-7201.

- [7] Zhang, Q., et al. Review of biomass pyrolysis oil properties and upgrading research. *Energ. Convers. Manage* 2007; **48**(1): 87-92.
- [8] Vitolo, S., et al. Catalytic upgrading of pyrolytic oils to fuel over different zeolites. *Fuel* 1999; **78**(10): 1147-1159.
- [9] Mortensen, P.M., et al. A review of catalytic upgrading of bio-oil to engine fuels. *Appl. Catal. A: General* 2011; **407**(2): 1-19.
- [10] Wang, S., et al. Biogasoline Production from the Co-cracking of the Distilled Fraction of Bio-oil and Ethanol. *Energy Fuels* 2013; **28**(1): 115-122.
- [11] Bi, P., et al. Production of aromatics through current-enhanced catalytic conversion of bio-oil tar. *Bioresource. Technol* 2013; **136**: 222-229.
- [12] Zhao, Y., et al. Aromatics Production via Catalytic Pyrolysis of Pyrolytic Lignins from Bio-Oil. *Energy Fuels* 2010; **24**(10): 5735-5740.
- [13] Krukanont, P. and S. Prasertsan. Geographical distribution of biomass and potential sites of rubber wood fired power plants in Southern Thailand. *Biomass. Bioenerg* 2004; **26**(1): 47-59.
- [14] Prasertsan, S. and B. Sajjakulnukit. Biomass and biogas energy in Thailand: Potential, opportunity and barriers. *Renewable Energy* 2006; **31**(5): 599-610.
- [15] Adjaye, J.D. and N.N. Bakhshi. Production of hydrocarbons by catalytic upgrading of a fast pyrolysis bio-oil. Part II: Comparative catalyst performance and reaction pathways. *Fuel. Process. Technol* 1995; **45**(3): 185-202.
- [16] Mentzel, U.V. and M.S. Holm. Utilization of biomass: Conversion of model compounds to hydrocarbons over zeolite H-ZSM-5. *Appl. Catal. A: General* 2011; **396**(1-2): 59-67.
- [17] Valle, B., et al. Hydrothermally stable HZSM-5 zeolite catalysts for the transformation of crude bio-oil into hydrocarbons. *Appl. Catal. B-Environ* 2010; **100**(1-2): 318-327.
- [18] Li, X., et al. Catalytic fast pyrolysis of Kraft lignin with HZSM-5 zeolite for producing aromatic hydrocarbons. *Front. Environ. Sci. Eng* 2012; **6**(3): 295-303.
- [19] Cheng, Y.-T. and G.W. Huber. Chemistry of Furan Conversion into Aromatics and Olefins over HZSM-5: A Model Biomass Conversion Reaction. *ACS Catalysis* 2011; **1**(6): 611-628.
- [20] Adjaye, J.D. and N.N. Bakhshi. Catalytic conversion of a biomass-derived oil to fuels and chemicals I: Model compound studies and reaction pathways. *Biomass. Bioenerg* 1995; **8**(3): 131-149.

Appendix D

Comparative study for catalytic conversion of pyrolysis oil and tar derived from rubberwood to produce green gasoline-range aromatics

Comparative Study for Catalytic Conversion of Pyrolysis Oil and Tar Derived from Rubberwood to Produce Green Gasoline-Range Aromatics

Abdulrahim Saad ^{a,*}, Sukritthira Ratanawilai ^a, and Chakrit Tongurai ^a

^a *Department of Chemical Engineering, Faculty of Engineering, Prince of Songkla University, Had Yai, Songkhla, Thailand*

**Corresponding author. Tel.: +66874755690; E-mail addresses: abdorahim@hotmail.com*

ABSTRACT

The conversion of biomass-derived oils to fuels may be a promising alternative to petroleum-based fuels. The aim of the study was to generate gasoline-range aromatics from pyrolysis oil (PO) and pyrolysis tar (PT) derived from rubberwood. In this study, we compared PO and PT conversion in terms of product distribution and the concentration of gasoline aromatics in organic liquid products (OLPs). Catalytic cracking of PO and PT was conducted under similar operating conditions, in a dual reactor using an HZSM-5 catalyst. The effects of reaction temperatures, catalyst weights, and nitrogen flow rates were investigated to determine their effects on the yields of OLPs and the percentages of gasoline aromatics in the OLPs. The OLP obtained from PT exhibited greater yields, with a maximum value of about 28.33 wt%, achieved at 536 °C with a catalyst weight of 3.5 g, compared to the OLP from PO, which gave a maximum yield of about 13.6 wt%, achieved at 511 °C with a catalyst weight of 3.2 g. The OLP obtained from PT had higher gasoline aromatics, with a maximum percentage of about 54 wt%, obtained at 575 °C with a catalyst weight of 5 g, while the OLP from PO had fewer aromatics, around 27 wt%, at 595 °C and a catalyst weight of 5 g. The findings of this study imply that PT is much more attractive as a potential alternative feedstock for green gasoline.

Keywords: Pyrolysis oil; Pyrolysis tar; Zeolite cracking; Organic liquid product (OLP); Green gasoline-range aromatics

1. Introduction

Declining exhaustible resources and increased demand for energy, as well as ecological considerations regarding fossil fuels, have led to the development of new and alternative energy sources. Biomass, a renewable source of energy, represents a potential source to replace fossil fuels. It is inexpensive, abundant, CO₂-neutral, and clean, with negligible nitrogen and sulphur content; hence, it attracted significant attention, particularly after the global oil crisis of the 1970s [1-3].

To meet the needs for alternative fuels, attention has turned to pyrolysis oils (POs) derived from biomass. The pyrolysis of biomass to produce oils is of growing interest and has the potential to be

35 economically viable in the future [4]. POs are flowing, viscous liquids with a dark brown colour that
36 are environmentally-friendly, as they are CO₂ neutral and contain a low content of sulphur compared
37 to fossil-derived oils [5, 6]. The chemical composition of POs is very complex, containing a wide
38 range of organic compounds and water. The direct use of POs as high-grade fuels might be limited
39 due to some inferior characteristics or undesirable properties, such as high viscosity, thermal
40 instability, poor heating value, and high oxygen content [7]. As a consequence, it is necessary to
41 improve the quality of POs by upgrading them before they can be used as fuels. The upgrading
42 process essentially involves the conversion of oxygen-rich compounds into hydrocarbons that are
43 consistent with traditional fuels [8]. Upgrading POs is accomplished by several techniques, such as
44 catalytic cracking, hydrodeoxygenation, and steam reforming. Among these techniques, catalytic
45 cracking is favoured; it can be performed at atmospheric pressure and no hydrogen is required, thus
46 reducing operating costs, which offer economic advantages over hydrodeoxygenation and steam
47 reforming [9]. Some studies on this upgrading technique have been reported in literature [6, 10-12];
48 related works by Valle et al., and Stephanidis et al. [13, 14] demonstrated that a variety of
49 hydrocarbons can be produced by the catalytic upgrading of POs when H-ZSM-5 zeolite is used as a
50 catalyst. The HZSM-5 zeolite is the most effective catalyst for the production of aromatic
51 hydrocarbons, because it promotes deoxygenation reactions due to its shape selectivity and strong
52 acidity [15-17].

53 Currently, the production of green gasoline, especially gasoline-range aromatics from PO, has
54 attracted considerable attention. Multiple studies investigated the viability of producing gasoline
55 hydrocarbons from POs derived from different biomass sources by catalytic cracking over ZSM5
56 catalysts [18-21]; however, some related studies dealt with PO fractions, which can be easier to
57 understand. Wang et al. [22] outlined a unique technique to produce high-quality gasoline rich with
58 aromatic hydrocarbons by using a distilled fraction of PO derived from rice husk. They revealed that
59 the cracking behaviour of the distilled PO fraction is significantly enhanced by co-feeding ethanol
60 while using the HZSM-5 catalyst. Bi and co-workers [23] used a residual distillation fraction of PO
61 derived from straw stalks. The heavy fraction was transformed directly to aromatic hydrocarbons

62 (benzene, toluene, and xylenes; BTX). Among the catalysts, HZSM-5 was the most effective and
63 obtained the highest yield of BTX aromatics.

64 Another study was conducted by Zhang et al. [24], who presented results on the aromatic
65 hydrocarbons produced from the catalytic pyrolysis of aspen lignin extracted using a butanol-based
66 organosolv process. They screened two different zeolite catalysts; HZSM-5 and HY, and found
67 HZSM-5 to be more effective than HY for the production of aromatic hydrocarbons.

68 More recently, there has been a study reported by Shen et al. [25], who investigated the viability of
69 generating gasoline aromatics from lignin precipitated from black-liquor. The black-liquor lignin was
70 pyrolyzed using five solid zeolite catalysts. Among them, HZSM-5 was the most effective catalyst in
71 promoting the yield of aromatic monomers.

72 The rubber tree is planted extensively in southern Thailand and is one of the country's leading
73 economic crops. The rubberwood is utilised to a great extent by local farmers and small plants to
74 produce charcoal via a slow pyrolysis process (carbonization) [26, 27]. The pyrolysis liquid is an
75 unavoidable by-product obtained during the manufacture of charcoal; over time, the liquid is divided
76 into aqueous and oily layers. The former (known as pyroligneous liquid), more accurately called
77 wood vinegar, is used extensively in agriculture for plant growth and protection, particularly in
78 pesticide applications [28]. The oily layer (pyrolysis tar; PT) is a sticky liquid that is also called
79 sedimentation tar. It is a multi-component mixture of different compounds, primarily composed of
80 phenols. The PT is normally removed from pyroligneous liquid because it contaminates plants and
81 soil when sprayed on them [29, 30]. Although the pyrolysis liquid (pyroligneous liquid and tar) is a
82 by-product discharged during the carbonization process, it would be highly desirable to utilise it, as it
83 might clearly improve the feasibility of charcoal production and add value.

84 In this paper, pyroligneous liquid, after vacuum concentration, was referred to as PO and the
85 sedimentation tar as PT. On the basis of their compositions, it was suggested that the two portions
86 have potential for use as a feedstock for producing green gasoline.

87 In the present study, we provide a comparative assessment on the catalytic conversion of the PO
88 and PT for the production of gasoline aromatic hydrocarbons. The primary objective of this study is to
89 make a comparison based on the product distributions; more importantly, OPL yields and the

90 concentrations of gasoline aromatics in OPLs as well. The conversion of PO to gasoline aromatics
91 was rarely considered for PT, and no study presented a comparison of both, particularly for those
92 derived from rubberwood.

93 In this paper, catalytic cracking of PO and PT over HZSM-5 catalyst was conducted under similar
94 conditions in dual-reaction system. The study investigated the effect of operating conditions on the
95 yields of OLPs and the percentages of gasoline aromatics in the OLPs. Design of experiments (DOE)
96 and response surface methodology (RSM) were used to analyse the optimum operating conditions.

97

98 **2. Materials and Methods**

99 *2.1 Materials*

100 Crude pyrolysis liquid was obtained from Phatthalung Province (in the southern part of Thailand).
101 The pyrolysis liquid included aqueous phase and settled tar. The liquid had settled for about two
102 months; after that, the settled tar was separated by decantation. The separated tar was then kept in a
103 refrigerator overnight to remove the rest of the water, which was separated by decantation.
104 Additionally, the aqueous portion of pyroligneous liquid was treated to remove water by evaporation.
105 The concentrated liquid was then named PO. The chemical compositions of PO and PT (Table 1)
106 were determined by GC-MS analysis and found to contain a diverse range of compounds, including,
107 principally, phenols as in the PT, and acetic acid in the PO. Other important characteristics of PO and
108 PT, such as water content, specific gravity, heating value, and elemental content, are presented in
109 Table 2.

110 **Table 1**
111 Main components of the pyrolysis oil and tar, identified by GC-MS

Pyrolysis tar					Pyrolysis oil				
No	Composition	MW	Formula	Peak area % ^a	No	MW	Formula	Peak area % ^a	
1	Syringol	154	C ₈ H ₁₀ O ₃	12.11	1	60	C ₂ H ₄ O ₂	32.65	
2	2, 6-Dihydroxy-4-methoxyacetophenone	182.17	C ₉ H ₁₀ O ₄	9.49	2	154	C ₈ H ₁₀ O ₃	13.36	
3	1,2,4-Trimethoxybenzene	168.19	C ₉ H ₁₂ O ₃	8.94	3	112	C ₆ H ₈ O ₂	8.62	
4	Creosol	138.16	C ₈ H ₁₀ O ₂	5.25	4	168	C ₉ H ₁₂ O ₃	4.28	
5	Guaiacol	124.13	C ₇ H ₈ O ₂	5.14	5	74	C ₃ H ₆ O ₂	4.08	
6	p-Ethylguaiacol	152.19	C ₉ H ₁₂ O ₂	4.89	6	122	C ₄ H ₇ ClO ₂	3.09	
7	o-Cresol	108.13	C ₇ H ₈ O	3.57	7	94	C ₆ H ₆ O	2.13	
8	2,6-Dimethoxy-4-allylphenol	194.22	C ₁₁ H ₁₄ O ₃	3.43	8	182	C ₉ H ₁₀ O ₄	2.02	
9	p-Cresol	108.13	C ₇ H ₈ O	2.37	9	158	C ₈ H ₁₄ O ₃	1.91	
10	3,5-dimethylphenol	122.16	C ₈ H ₁₀ O	2.08	10	132	C ₅ H ₈ O ₄	1.72	
11	2-Methoxy-5-propylphenol	166.21	C ₁₀ H ₁₄ O ₂	1.79	11	95	C ₅ H ₅ NO	1.64	
12	Vanillyl methyl ketone	180.20	C ₁₀ H ₁₂ O ₃	0.88	12	182	C ₁₂ H ₂₂ O	1.61	
13	Corylon	112.12	C ₆ H ₈ O ₂	0.87	13	126	C ₇ H ₁₀ O ₂	1.29	
14	2,5-Dimethylphenol	122.16	C ₈ H ₁₀ O	0.87	14	180	C ₁₀ H ₁₂ O ₃	1.59	
15	5-hydroxy-3-heptanone	130.18	C ₇ H ₁₄ O ₂	0.75	15	166	C ₁₀ H ₁₄ O ₂	1.49	
16	2,3-Dimethylphenol	122.16	C ₈ H ₁₀ O	0.65	16	210	C ₁₁ H ₁₄ O ₄	1.36	
17	Eugenol	164.20	C ₁₀ H ₁₂ O ₂	0.63	17	144	C ₆ H ₈ O ₄	1.22	
18	3,4,5-Trimethoxytoluene	182.21	C ₁₀ H ₁₄ O ₃	0.60	18	116	C ₅ H ₈ O ₃	1.18	
19	4-Methoxy-3-methylphenol	138.16	C ₈ H ₁₀ O ₂	0.56	19	84	C ₄ H ₄ O ₂	1.18	
20	3-Ethyl-2-hydroxy-2-cyclopenten-1-one	126.15	C ₇ H ₁₀ O ₂	0.54	20	196	C ₁₀ H ₁₂ O ₄	1.13	
21	3-Methyl-2-cyclopenten-1-one	96.12	C ₆ H ₈ O	0.51	21		^b Unidentified	12.45	
22	Furfural	96.08	C ₅ H ₄ O ₂	0.48					
23	3,4-Dimethoxytoluene	152.19	C ₉ H ₁₂ O ₂	0.42					
24	2-Acetylfuran	110.11	C ₆ H ₆ O ₂	0.41					
25	3,5-Dimethyl-2(SH)-furanone	112.12	C ₆ H ₈ O ₂	0.37					
26	3-Ethyl-2-cyclopenten-1-one	110.15	C ₇ H ₁₀ O	0.35					
27	2-methylcyclopentenone	96.12	C ₆ H ₈ O	0.33					
28	2,3-Dimethoxytoluene	152.19	C ₉ H ₁₂ O ₂	0.33					
29	5-Methyl-2-furfural	110.11	C ₆ H ₈ O ₂	0.28					
30	Methyl 3-furoate	126.11	C ₆ H ₆ O ₃	0.27					
31	Isopropylidencyclohexane	124.24	C ₈ H ₁₆	0.27					
32	Cyclopentenone	82.10	C ₅ H ₆ O	0.27					
33	2,3-Dimethyl-2-cyclopenten-1-one	110.15	C ₇ H ₁₀ O	0.17					
34	^b Unidentified			30.13					

112 ^a The composition of the pyrolysis oil and tar was estimated by the peak area % of GC-MS

113 ^b Determined by difference

114 **Table 2**
 115 Physical characteristics and elemental analysis of pyrolysis oil and tar

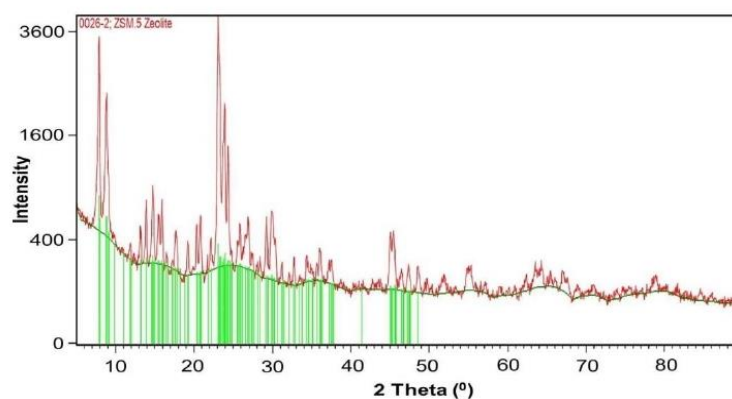
	Typical value		Instrument
	Pyrolysis oil	Pyrolysis tar	
Water content (wt%)	30.00	1.75	Coulometric Karl Fischer titrator, Mettler Toledo DL 39, Taiwan.
Specific gravity	1.22	1.31	Specific Gravity Bottle.
Gross heating value (MJ/kg)	22.00	35.19	CHNS/O Analyzer, Flash EA 1112 Series, Thermo Quest, Italy. <i>Automatic calculation of GHV (Gross Heat Value) and NHV (Net Heat Value) using Eager 300 software.</i>
pH	3.72	4.45	Docu-pH ⁺ meter, Sartorius Mechatronics, Germany.
Elemental composition (wt%)			CHNS/O Analyzer, Flash EA 1112 Series, Thermo Quest, Italy.
C	47.37	51.16	
H	5.78	5.67	
O	23.58	14.26	
N	1.26	2.24	

116

117 *2.2 Catalyst and characterizations*

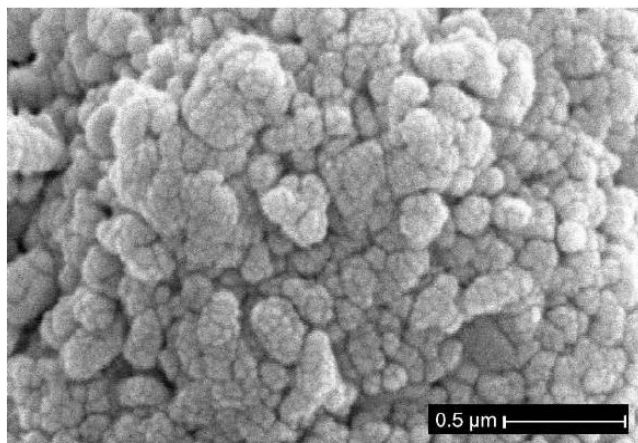
118 NH₄-ZSM-5 zeolite (CBV 3024E) was purchased from Zeolyst International as a fine powder. Its
 119 surface area and SiO₂/Al₂O₃ ratio were 405 m²/g and 30, respectively. NH₄-ZSM-5 was calcined in
 120 nitrogen atmosphere at 550 °C for 5 h to obtain the HZSM-5 form prior to use. The structure of the
 121 catalyst was measured by X-ray diffraction (XRD; X'Pert MPD, PHILIPS), and the XRD patterns
 122 were similar to the standard HZSM-5 zeolite reported by Treacy et al. [31], as depicted in Fig. 1. The
 123 morphology and particle sizes were determined from the scanning electron microscopy (SEM) image
 124 taken with a JSM-5800 LV, JEOL, as depicted in Fig 2.

125



126 **Fig. 1.** X-ray diffraction pattern of HZSM-5 catalyst
 127
 128

129



130
131
132 **Fig. 2.** Scanning electron microscopy image for HZSM-5 catalyst
133
134

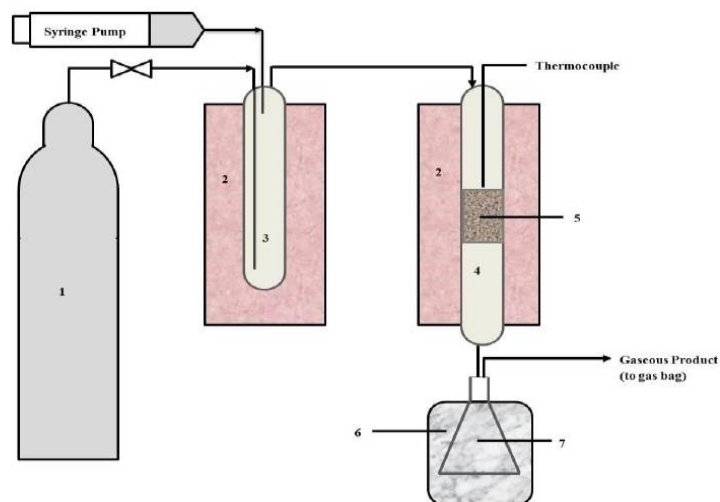
130
131
132
133
134

135 2.3 Experimental setup and procedure

136 Catalytic cracking of PO and PT was conducted under similar conditions in a dual reactor
137 assembly without any catalyst in the first reactor, followed by a second fixed-bed reactor loaded with
138 HZSM-5 catalyst, as shown in Fig. 3. The reactors were cylindrical configurations made of stainless
139 steel (i.d: 30 mm; length: 250 and 350 mm for the first and second reactors, respectively) and were
140 placed coaxially in the furnaces. The dual reactor operation was studied previously [32-35] and was
141 found to be effective in improving the catalyst life by reducing coke formation during the process,
142 hence minimizing the regularity of catalyst regeneration. The experiments were operated at
143 atmospheric pressure, a reaction temperature that varied from 400 to 600 °C, a catalyst weight of 1 to
144 5 g, and a nitrogen flow rate of 3 to 10 mL/min. In a typical experiment, the second reactor was
145 loaded with catalyst that was held by a plug of glass wool, placed on a supporting stainless steel mesh,
146 and positioned centrally within the reactor. Before the reaction started, both reactors were heated in a
147 nitrogen stream until the desired temperature was reached, after which 15 grams of the feed (PO or
148 preheated PT) was fed into the first reactor (1.4 g/min) by a syringe pump, with typical feeding rates
149 of nitrogen serving as carrier gas, with the values shown in Table 3. A significant amount of char was
150 formed in the reactor and the vapour, leaving the reactor subjected to the second fixed-bed reactor,
151 passing through the catalyst bed where the catalytic cracking of the vapour occurred. A small amount
152 of char also deposited above the catalyst bed.

153 The product mixture leaving the second reactor was condensed (collected in an ice-cooled flask),
 154 to separate the liquid and gaseous products. The liquid product consisted of aqueous and oil phases in
 155 the form of immiscible layers. The oil phase, i.e., the OLP, was drawn off from the aqueous layer with
 156 a syringe. The weights of OLP and aqueous liquid were obtained. Additionally, the gaseous product
 157 was collected in a gas bag and weighed by estimating the weight difference of the bag before and after
 158 removing the gas. Each run lasted for about 1.30 h and this time was selected based on preliminary
 159 experiments showing that the formation of products decreased significantly after 1.30 h for all runs.
 160 After each run, the spent catalyst, tar, and the char deposited above the catalyst bed were removed
 161 from the second reactor, while the char formed in the first reactor was removed and weighed. The
 162 spent catalyst and the inner surface of the reactor were washed with methanol to remove the tar. The
 163 washed catalyst was then dried overnight and heated in an air flow for 5 h at 550 °C to obtain the
 164 weight of coke, which was determined by the difference in the weight of the catalyst before and after
 165 heating. Furthermore, the yields of products, i.e., OLP, aqueous liquid, char, and gas, relative to the
 166 total amount of the feed, were calculated using the following equation:
 167 Yield (wt%)= (P x 100)/feed (15 g), where P is the number of grams of product, i.e., OLP, aqueous
 168 liquid, char, or gas.

169



170
 171
 172
 173
 174
 175

Fig. 3. Dual reactor setup showing (1) nitrogen cylinder, (2) furnace, (3) first reactor, (4) second reactor, (5) catalyst bed, (6) ice bath, and (7) receiving flask

176 2.4 Characterization of the liquid product

177 The liquid product consisted of an organic oily layer (the OLP) and an aqueous layer. In this
178 work, the product of interest was the gasoline fraction formed in the OLPs, particularly gasoline-range
179 aromatics, i.e., benzene, toluene, ethylbenzene, and xylenes (BTEX), which have higher octane
180 ratings [36]. Hence, only the gasoline hydrocarbons of BTEX were measured using gas
181 chromatography (GC). GC analysis was performed using a Hewlett–Packard 7890 Model gas
182 chromatograph equipped with a 30 m long \times 0.32 mm fused-silica capillary column and a flame
183 ionization detector (FID). The initial oven temperature was 40 °C, held for 5 min, and then
184 programmed from 40 to 250 °C at 5 C/min. Hydrogen was employed as a carrier gas at a constant
185 flow rate of 30 ml/min. The identities of the chromatographic peaks were identified by using pure
186 BTEX compounds, and the quantities were determined from a calibration curve that had been
187 developed using the BTEX standard. The aqueous products consisted mainly of water (about 78 to 85
188 wt% and 80 to 84 wt% for PO and PT, respectively), as measured by Karl Fischer titration. It was
189 anticipated that the aqueous products would contain some water-soluble organic components, such as
190 alcohols, carboxylic acids, and phenols. Then, the pH was obtained using a pH meter, giving values
191 that ranged from 2.90 to 3.65 and from 3.0 to 3.8 for PO and PT, respectively.

192 2.5 Experimental design

193 Response surface methodology (RSM) is a modern approach employed for designing experiments
194 and developing an adequate mathematical model to evaluate and predict the optimal values of the
195 output (response) [37]. In this study, Essential Regression and Experimental Design software was
196 used to design the experiments.

197 For the experimental design of the catalytic cracking of PO and PT, three factors, i.e., temperature
198 (°C), the catalyst's weight (g), and the flow rate of N₂ (mL/min), were chosen as the independent
199 variables that would most likely influence the catalytic cracking of the PO and PT. The low (-1),
200 central (0), and high (1) levels of all the independent variables were based on preliminary experiments
201 and previous studies [17, 19, 24]. The ranges of these factors are listed in Table 3. The matrix of the
202 experimental design and the results of the 15 runs are summarized in Table 3. The 15 experimental
203 runs were designed using Box-Behnken with three center points.

205 Since OLP and gasoline aromatics were the most desired products, it was necessary to determine two
 206 quantities (responses) as shown in Table 3, i.e., the yield of OLP and the percentage of gasoline
 207 aromatics in the OLP. The quadratic model used for predicting OLP yield and aromatics percentage in
 208 terms of coded variables is represented as Eq. (1).

$$209 \quad Y = b_0 + b_1T + b_2C + b_3G + b_4T^2 + b_5C^2 + b_6G^2 + b_7TC + b_8TG + b_9CG \quad (1).$$

211 Where Y is the predicted response; b_0 , b_1 , b_2 , b_3 , b_4 , b_5 , b_6 , b_7 , b_8 and b_9 are the regression
 212 coefficients; and T, C, and G are the coded independent variables for temperature, catalyst's weight
 213 and N_2 flow rate, respectively.

214 In order to make predictions and optimizations, the response surface analysis was accomplished by
 215 utilizing Essential Regression software to maximize the yield of OLP and the percentage of gasoline
 216 aromatics.

217
 218 **Table 3**
 219 Experimental design matrix and results

Runs	Experimental design			Experimental results			
	Temperature °C	Catalyst g	N_2 flow rate mL/min	OLP yield		Percentage of gasoline aromatics in OLP	
				Pyrolysis oil	Pyrolysis Tar	Pyrolysis oil	Pyrolysis Tar
1	400	1	6.5	5.80	10.00	0.34	2.01
2	400	3	3.0	11.27	18.45	0.62	10.10
3	400	3	10	11.07	18.30	0.57	9.90
4	400	5	6.5	11.33	20.28	1.43	29.83
5	500	1	3.0	12.13	15.13	6.69	20.88
6	500	1	10	12.00	14.98	6.48	20.00
7	500	3	6.5	13.20	27.31	17.11	40.77
8	500	3	6.5	13.13	27.50	17.25	41.53
9	500	3	6.5	13.33	26.90	18.06	42.00
10	500	5	3.0	12.47	25.00	23.81	49.41
11	500	5	10	12.33	24.80	23.10	48.29
12	600	1	6.5	12.27	22.65	6.71	24.28
13	600	3	3.0	11.53	24.40	26.41	52.25
14	600	3	10	11.40	24.35	22.02	50.65
15	600	5	6.5	10.00	22.00	19.95	45.21

220

221 3. Results and discussion

222 3.1 Pyrolysis oil (PO) and pyrolysis tar (PT) properties

223 Properties of PO and PT, including chemical compositions, water contents, pH, specific gravities,
 224 heating values, and elemental analyses, are presented in Tables 1 and 2. The results of GC-MS

225 analysis (Table 1) revealed that PO and PT are extremely complex mixtures of various oxygenated
226 compounds. The main components of the PT included phenolic compounds with a high percentage of
227 syringol, while the PO showed relatively lower contents of phenolic compounds than PT but a higher
228 acetic acid concentration, indicating that the PO was different from PT in terms of physical properties.
229 The physical characteristics and elemental analysis are shown in Table 2. The elemental C, H, N, and
230 O analysis showed that PT had higher carbon content (51%) than PO (47.37%); in contrast, the PO
231 showed higher oxygen content (23.58 %) than PT (14%). Additionally, hydrogen and nitrogen
232 contents did not show significant differences between PO and PT. Water content was higher in PO
233 (30%) than PT (1.75%). The pH value of the PT (4.45) was slightly higher than the PO (3.72), and the
234 specific gravities for PO and PT were 1.22 and 1.31, respectively. One of the most important
235 properties to characterize the POs is the heating value; the heating value of the PT (33.46 MJ/kg) was
236 higher than the PO (21.00 MJ/kg), implying that the PT has less oxygen content in its compounds.

237 3.2 Product distribution

238 Six products from catalytic cracking of PO and PT were generated: OLP, an aqueous product,
239 char, tar, coke, and non-condensable gases. The overall product distributions for each run are shown
240 in Table 4. As expected, significant amounts of chars were formed in the first reactor, and small
241 amounts of chars were formed above the catalyst bed in the second reactor. Generally, these
242 observations imply that the formation of chars is a function of the thermal effect on the unstable
243 components of the PO and PT; more to the point, due to condensation and polymerization reactions,
244 which form insoluble compounds of large molecules. However, there was a slight decrease in the
245 formation of chars with the increase of temperature, possibly due to additional reactions as shown in
246 Table 4. The char yields from PO (18-22 wt %) were slightly lower than those from PT (20-24 wt %).
247 The effect of temperature, formation and yields of chars during the cracking of PO and PT seem to be
248 reasonable, comparable to the studies of Yong et al. and Hyun et al. [38, 39].

249 The yields of aqueous products obtained from PO and PT did not vary greatly between them. The
250 amounts of aqueous products obtained from PO (78-81 wt% water content) ranged from 36 to 53 wt
251 %, whereas the amount obtained from PT (80-73 wt% water content) ranged from about 25 to 33 wt
252 %. This is reasonable, indicating that some oxygen was removed in the form of water [40]; however,

253 the aqueous products from PO showed higher yields due to the free water (30 wt %) before the
254 cracking process.

255 It was essential to investigate the distributions of OLP yields generated from the conversion of PO
256 and PT. The OLP yields from the conversion of PT were high (about 10-27 wt %), compared to about
257 6 to 13 wt% from that of PO for the cracking reactions performed between 400 °C-600 °C. The higher
258 yields produced from PT cracking could be due to the deoxygenation reactions of its low oxygen
259 content compounds. In contrast, the lower yields from PO were probably due to its high oxygen
260 content and high water content as well. Additionally, low OLP yields from both PO and PT were
261 observed at 400 °C, while the maximum yield obtained from PO was about 13 wt% at 500 °C with 3
262 grams of catalyst, lower than the yield from PT, which produced about 27 wt% at the same
263 conditions. It was observed that there was a slight decrease in OLPs when the temperature was
264 increased from 500 to 600 °C. Similar notes were reported by Wang et al. and Bi et al. [23, 41] during
265 the upgrading of tar and pyrolysis oil model compounds. They stated that the OLP yield decreased
266 with the increase of temperature due to the additional conversion of OLP, forming further gases.

267 As can be seen in Table 1, the major constituents of the PO and PT contained a wide range of
268 different oxygenated compounds, including phenols, acids, and a few others. Thus, it should be stated
269 that the conversion of such oxygenated compounds to OLP over the HZSM-5 catalyst was an
270 indication of the catalyst's ability to remove oxygen through complex reactions, such as
271 deoxygenation, cracking, cyclisation, aromatisation, isomerisation, and polymerisation reactions [32,
272 40, 42, 43]. In our study, the low yields of OLP from PO (about 6-13 wt%) and PT (about 10-27
273 wt%) might be attributed to the char formation (about 18-22 wt% and 20-24 wt% from PO and PT,
274 respectively). Regarding the values of OLP yields from the conversion of PO and PT, a typical
275 comparison cannot be made with other studies since the experimental conditions applied in this study
276 were different. Additionally, a comparison study of PO and PT derived from rubberwood has not been
277 studied for hydrocarbon production. Nevertheless, related studies by Zhu et al., Bi and co-workers
278 [23, 44] displayed the catalytic conversion of pyrolysis oil and its heavy fraction (tar) derived from
279 straw stalks. The yield of the organic liquid from PO was from 31-36 wt% when an upgrading process

280 was carried out at a temperature range of 500-600 °C, using 10 gram of the catalyst with 10 gram of
281 the PO. Likewise, the organic liquid from the heavy fraction (tar) exhibited a yield value ranged from
282 about 21-30 wt% when catalytic conversion was carried out at a temperature range of 400-600 °C, 10
283 g of the catalyst and 10 g of the tar fed with a 20 g/h N₂ as carrier gas.

284 Furthermore, the yields of gases from catalytic cracking of PO and PT were obtained. The yields
285 did not vary greatly between that of PO and PT, and these yields showed 4.07-6.67 wt% and 4.11-
286 6.70 wt % for PO and PT, respectively. As expected, the reaction performed at lower temperatures
287 resulted in a lower yield of gases. Inversely, the higher yields of gases were obtained at higher
288 temperatures.

294 **Table 4**
 295 Overall product distribution (wt% of the feed) for the 15 experimental runs

Runs	Products wt%											
	Aqueous Liquid		Organic Liquid Product		Char ^a		Residue ^b		Gas		Unaccounted	
	Pyrolysis oil	Pyrolysis tar	Pyrolysis oil	Pyrolysis tar	Pyrolysis oil	Pyrolysis tar	Pyrolysis oil	Pyrolysis tar	Pyrolysis oil	Pyrolysis tar	Pyrolysis oil	Pyrolysis tar
1	38.33	30.00	5.80	10.00	22.00	24.00	13.20	14.00	4.07	4.11	16.60	17.89
2	36.33	25.37	11.27	18.45	22.13	23.50	12.33	13.50	4.33	4.45	13.60	14.73
3	36.20	25.30	11.07	18.30	22.00	23.00	12.47	13.30	4.53	4.50	13.73	15.60
4	38.00	25.00	11.33	20.28	22.00	23.30	11.20	13.10	5.2	5.32	12.27	13.00
5	40.00	28.30	12.13	15.13	19.80	22.62	10.93	13.00	5.33	5.35	11.80	15.60
6	39.33	28.30	12.00	14.98	19.00	22.00	11.00	13.10	5.53	5.48	13.13	16.14
7	45.00	27.00	13.20	27.31	19.20	22.54	10.47	13.00	5.67	5.70	6.47	4.45
8	45.40	26.50	13.13	27.50	19.13	22.50	10.47	12.80	5.67	5.68	6.20	5.02
9	44.93	26.20	13.33	26.90	19.20	22.60	10.00	12.80	5.73	5.77	6.80	5.73
10	46.53	29.84	12.47	25.00	19.80	22.60	9.87	12.91	6.07	6.10	5.27	3.55
11	45.33	30.00	12.33	24.80	18.87	22.00	9.80	12.87	6.2	6.15	7.47	4.18
12	46.67	31.00	12.27	22.65	17.67	20.00	9.80	12.30	6.33	6.34	7.27	7.71
13	51.33	32.66	11.53	24.40	17.80	20.30	9.67	12.00	6.47	6.44	3.20	4.20
14	50.00	32.51	11.40	24.35	17.67	20.00	9.53	12.00	6.53	6.60	4.87	4.54
15	53.33	33.00	10.00	22.00	17.73	20.00	9.33	11.89	6.67	6.70	2.93	6.41

^a Char formed in the first reactor

^b Residue is categorized as char and tar that were quantified in the second reactor

296
297

298 *3.3 Content of gasoline-range aromatics in OLPs*

299 As extremely desirable compounds, gasoline-range aromatics (BTEX) in OLPs were selected as
300 target compounds in our study. The gasoline aromatics were analysed by GC-FID, and Table 5 shows
301 the aromatics distributions obtained from PO and PT among the experimental runs. The percentage of
302 gasoline aromatics in OLP from PO exhibited a range of about 0.34 to 26 wt%. Accordingly, the OLP
303 from PT attained a different percentage of gasoline aromatics that ranged from about 2 to 52 wt%.
304 The highest content of gasoline aromatics was obtained at 600 °C, 3 g of catalyst, and 3 mL/min of N₂
305 gas, with values of about 26 wt% and 52 wt% from PO and PT, respectively. As a known effect, the
306 formation of aromatic hydrocarbons in OLP is attributed to the conversion of oxygenated organic
307 compounds; particularly substituted phenols, from biomass pyrolysis by cracking, dehydroxylation,
308 decarbonylation, and decarboxylation reactions, which are catalysed by HSZM-5's acid sites [18, 20,
309 45-47]. Additionally, as PO and PT contained some light organics (acids, alcohols, aldehydes, ketones
310 and esters), it was proposed in earlier studies that olefins (C₂-C₆) formed as intermediate products
311 during the conversion of these compounds. The olefins then aromatize through a variety of reactions
312 to benzene and other aromatic hydrocarbons [48-51].

313 It was noted that, at 400 °C, the gasoline aromatics from PO increased slightly from 0.34 wt% to
314 1.43 wt%, coincident with the increase of catalyst; however, the gasoline aromatics from PT increased
315 from 2.01 wt% to 29.83 wt% in the same conditions, which is much higher than that from PO.
316 Similarly, at 500 °C, the percentage of gasoline aromatics obtained from PO increased significantly,
317 from about 7 wt% to 24 wt%, but that obtained from PT increased from 20.88 wt% to 49 wt%.
318 Interestingly, it was found that OLP from both PO and PT achieved a dramatic increase of gasoline
319 aromatics at 600 °C when 3 g of catalyst were used instead of 1 g; however, a slight drop occurred
320 when 5 g of catalyst were used, possibly due to the secondary conversion of the aromatics [25, 47,
321 51].

322 Generally, by considering the effect of catalysts on aromatics formation, it is interesting to note that
323 the decrease of catalyst decreases the deoxygenation and cracking reactions. This trend could be
324 attributed to the reduction of reactants residence time in the catalyst bed, noting that the feed rate of
325 pyrolysis oil was fixed. Respecting the effect of temperature on the aromatics distribution, it was

326 clearly observed that, increasing reaction temperature at fixed amounts of 1g, 3 g and 5 g of catalyst,
327 increased remarkably the formation of aromatics in OLPs; thus it can be suggested that at higher
328 temperatures, there would be a further elimination of groups from the primary heavier aromatics to
329 form mostly toluene and further to benzene. Though, as the temperature increased from 500 °C to 600
330 °C at 5 g of catalyst, the aromatics from PO slightly decreased from about 23 wt% to 20 wt%, and that
331 from PT also decreased from about 48 wt% to 45 wt% due to the secondary cracking of the aromatics.
332 Related observations and detailed proposals of the reaction pathways were studied previously [18, 25,
333 43, 45, 50, 52, 53].

334 To our knowledge, no study considering the disparity of PO and PT derived from rubberwood for
335 producing gasoline aromatics, thus no exact comparison could be made with previous studies.
336 However the study by Zhu et al., Bi and co-workers [23, 44] on the PO and heavy fraction (tar)
337 derived from straw stalks showed that the percentage of aromatics (BTEX) from PO was almost 30 %
338 for all the conducted temperatures ranged from 500-600 °C, and the aromatics (BTEX) from heavy
339 fraction (tar) exhibited values ranged from about 13-35 % at the temperatures ranged from 400-600
340 °C.

341 The results from our study indicate that the PT would produce more gasoline aromatics than PO,
342 which was expected due to the transformation of the high concentration of phenolics and other
343 oxygenated compounds in PT, compared to PO.

344 345 *3.4 Optimization*

346 The main targets in our study were OLP and gasoline aromatics in the OLPs; therefore, we
347 reported the results of our investigation of influences of the three variables on the yields of OLPs and
348 the percentages of gasoline aromatics. RSM was used to predict the optimum values of the three
349 variables. A mathematical model was developed based on the experimental design performed initially
350 by Essential Regression software, as shown in Table 3. The table shows the experimental results of
351 the OLP yields and the percentages of gasoline aromatics that were used to fit the model. Figs. 4 and 5
352 show that the values predicted for OLP and gasoline aromatics (for PO and PT) by the mathematical
353 model were in good agreement with the experimental results, confirming the fitness of the model.

354 From Fig. 4, the model's results fit well with the experimental results, as indicated by the
355 determination coefficients (R^2) of 0.926 and 0.906 for the model's predictions of OLP yield and
356 gasoline aromatics from PO, respectively. Correspondingly, determination coefficients (R^2) of 0.964
357 and 0.929 for the model's predictions of OLP yield and gasoline aromatics from PT, respectively,
358 were also attained, as shown in Fig. 5.

359 **Table 5**
 360 Composition of gasoline aromatics in the OLPs

Runs	Benzene wt%		Toluene wt%		Ethyl benzene wt%		Xylenes ^a wt%		(gasoline aromatics) ^b wt%	
	Pyrolysis Oil	Pyrolysis Tar	Pyrolysis Oil	Pyrolysis Tar	Pyrolysis Oil	Pyrolysis Tar	Pyrolysis Oil	Pyrolysis Tar	Pyrolysis Oil	Pyrolysis Tar
1	0.06	0.22	0.14	0.67	0.12	0.18	0.02	0.94	0.34	2.01
2	0.10	0.64	0.32	2.99	0.18	0.96	0.02	5.51	0.62	10.10
3	0.13	0.60	0.25	2.85	0.17	0.95	0.02	5.50	0.57	9.90
4	0.30	2.34	0.97	9.69	Trace	1.92	0.16	15.88	1.43	29.83
5	0.75	1.25	2.49	5.28	Trace	2.07	3.45	12.28	6.69	20.88
6	0.63	1.05	2.08	5.21	Trace	1.96	3.77	11.78	6.48	20.00
7	2.20	2.43	7.03	13.60	0.07	1.43	7.81	23.31	17.11	40.77
8	3.12	2.48	10.23	13.93	0.95	1.45	2.95	23.67	17.25	41.53
9	2.88	2.06	10.07	13.39	1.70	2.37	3.41	24.18	18.06	42.00
10	3.65	6.05	16.10	21.38	0.72	1.56	3.34	20.42	23.81	49.41
11	3.31	5.92	15.49	20.87	0.73	1.53	3.57	19.97	23.10	48.29
12	1.32	10.45	2.86	10.21	0.85	0.19	1.68	3.43	6.71	24.28
13	6.47	18.90	16.86	23.41	0.70	0.38	2.38	9.56	26.41	52.25
14	6.14	18.84	13.47	23.32	0.00	0.32	2.41	8.17	22.02	50.65
15	0.00	18.11	8.66	19.76	0.38	0.23	10.91	7.11	19.95	45.21

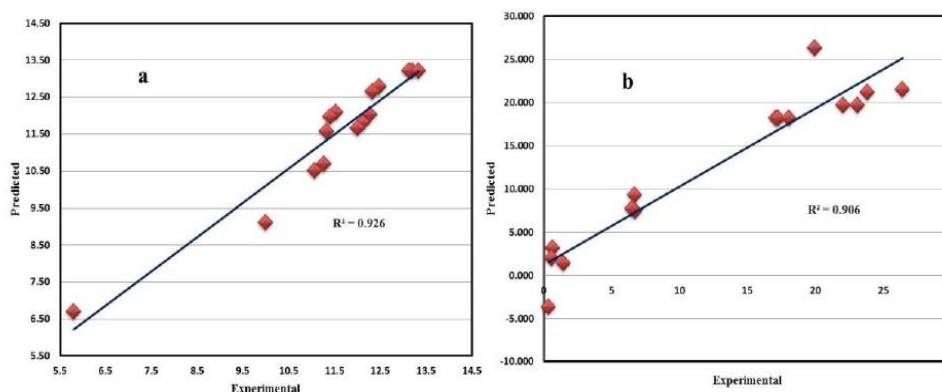
^a Xylenes= p. xylene, m. xylene, o. xylene

^b Summation of BTEX

361

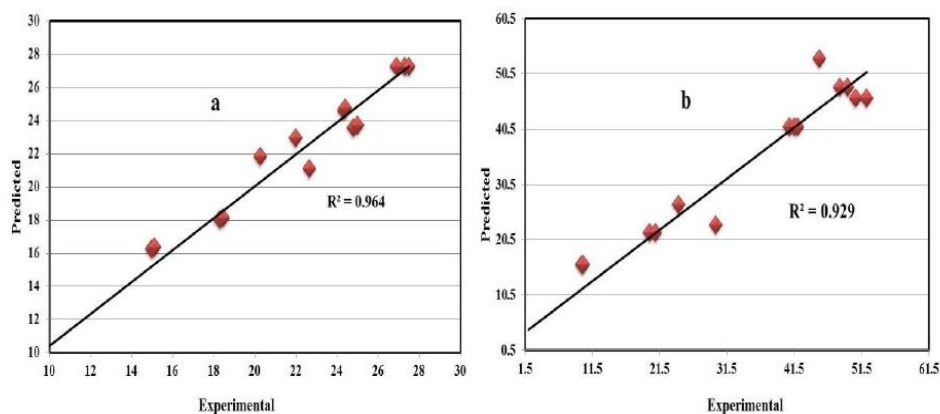
362

363



364

365 Fig. 4. Experimental results versus predicted values of (a) OLP yield and (b) gasoline aromatics (%) in OLP
 366 obtained from pyrolysis oil
 367
 368



369

370 Fig. 5. Experimental results versus predicted values of (a) OLP yield and (b) gasoline aromatics (%) in OLP
 371 obtained from pyrolysis tar
 372
 373

Essential Regression software was used to optimize the conditions, and the results showed that the maximum value of OLP yield obtained from PO was about 13.6 wt% for a temperature of 511 °C and a catalyst weight of 3.2 g, while the maximum value of OLP yield from PT was about 28.33 wt% for a temperature of 536 °C and a catalyst weight of 3.5 g. The results are depicted in the response surface graphs, Fig. 6, which shows the effect of the most significant variables (temperature and catalyst weight) for the optimum yields of OLP obtained from PO and PT. In addition, the maximum percentage of gasoline aromatics attained from PO was about 27 wt%, obtained at 595 °C and a catalyst weight of 5 g, whereas that attained from PT was about 54 wt%, obtained at 575 °C and a catalyst weight of 5 g. Fig. 7 shows the effects of the most significant variables, i.e., temperature and

382 the catalyst's weight, on the response surface graphs for the optimum percentages of gasoline
 383 aromatics in OLPs obtained from PO and PT.

384 The validation of the predicted results was performed by conducting experimental runs with the
 385 optimum conditions, as depicted in Table 6. The OLP yield from PO was found to be 15 wt%,
 386 whereas the predicted value was 13.6 wt%. In a corresponding manner, the OLP yield from PT was
 387 about 25.25 wt%, while the predicted value was about 28.33 wt%. The actual percentage of gasoline
 388 aromatics attained from PO was about 30 wt% compared to the predicted value of 27 wt%, and the
 389 actual percentage from PT was found to be 48 wt% compared to the predicted value of 54 wt%. The
 390 compositions of aromatics in OLPs were identified. As illustrated in Fig. 8, there was a remarkable
 391 concentration of toluene from about 22 wt% as for OLP from PT to about 14 % wt% as for OLP from
 392 PO. It can be seen in the figure that the contents of aromatics from both PO and PT have a very low
 393 concentration of ethylbenzene. Moreover, it was observed that the benzene concentration was about 5
 394 wt% and 8 wt% for the OLP from PO and PT, respectively. These values were somewhat less than
 395 those of toluene and xylenes, probably due to the easy alkylation of benzene on the acidic HSZM-5
 396 catalyst [54, 55]. However, benzene might not be preferred due to its toxicity, and the concentrations
 397 obtained in this study seem far from meeting gasoline specifications in the USA and Europe [56, 57].
 398 Accordingly, benzene would have to be recovered from xylenes, ethylbenzene and toluene and
 399 utilized in other chemical applications.

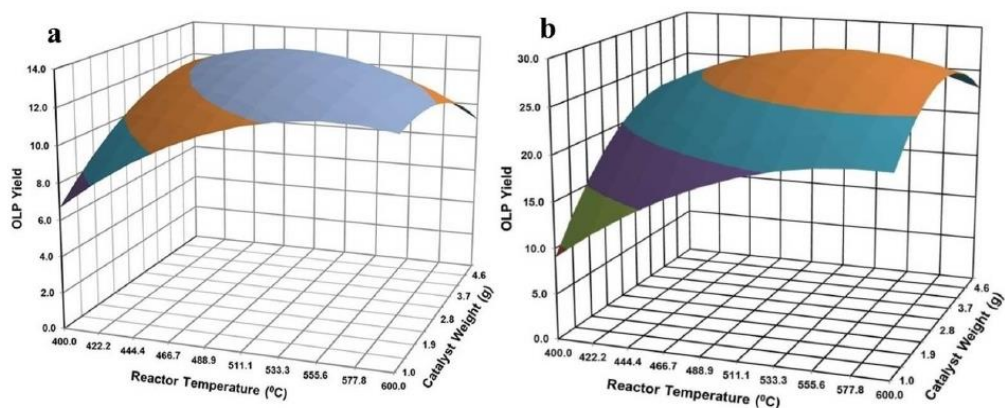
400
 401

402 **Table 6**
 403 Predicted and Experimental Results at Optimum Conditions

	OLP and gasoline aromatics from PO			
	Predicted	Experiment	Optimum conditions	
			Temperature (°C)	Catalyst weight (g)
OLP yield (wt%)	13.6	15	511	3.2
Percentage of gasoline aromatics (wt%)	27	30	595	5
	OLP and gasoline aromatics from PT			
OLP yield (wt%)	28.33	25.25	536	3.5
Percentage of gasoline aromatics (wt%)	54	48	575	5

404
 405
 406

407



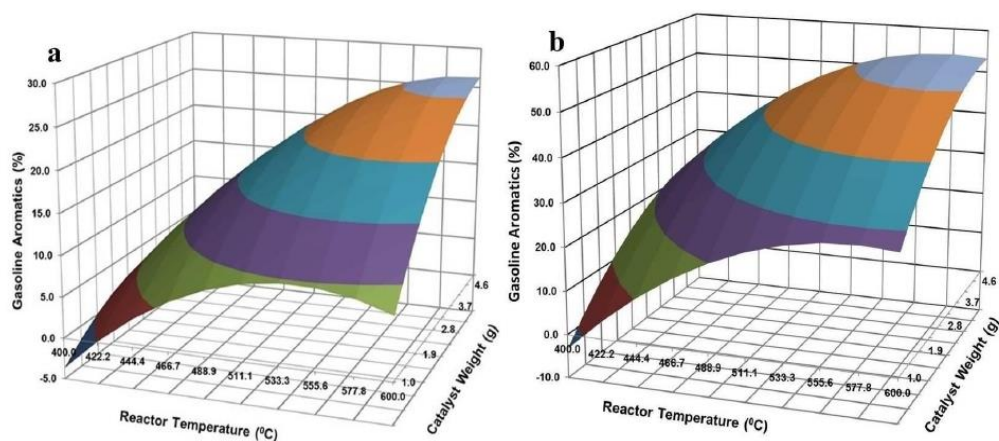
408

409

410

411

Fig. 6. Surface plot of OLP yield as a function of catalyst weight and reactor temperature-OLP from a) pyrolysis oil and b) pyrolysis tar

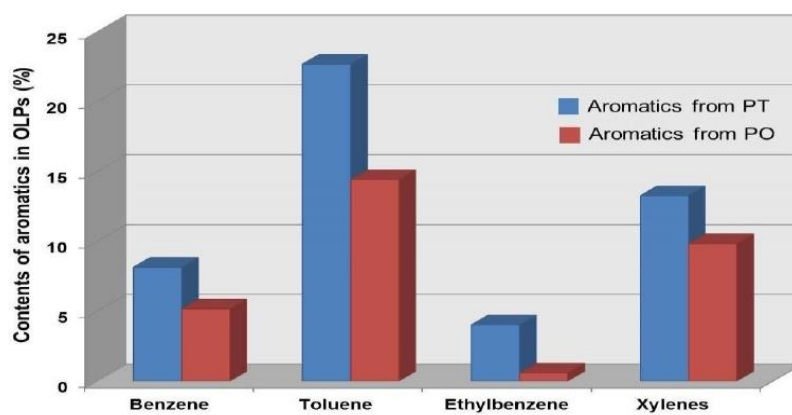


412

413

414

Fig. 7. Surface plot of gasoline aromatics (%) in OLP as a function of the catalyst's weight temperature - OLP from a) pyrolysis oil and b) pyrolysis tar



415

416

417

Fig. 8. Gasoline aromatics content in OLP form PT and PO at the optimum conditions

418 **4. Conclusions**

419 Our findings demonstrated that both PO and PT derived from rubberwood can be employed for
420 generating green gasoline rich with aromatics through catalytic cracking using the HZSM-5 catalyst.
421 The optimum conditions to maximize the OLP yields and the percentages of gasoline aromatics in the
422 OLPs were investigated; the maximum yield of OLP from PT was about 28.33 wt%, achieved at 536
423 °C and a catalyst weight of 3.5 g, which was significantly higher than that from PO (13.6 wt%),
424 achieved at 511 °C and a catalyst weight of 3.2 g. Additionally, the OLP from PT features a higher
425 concentration of gasoline aromatics, with a maximum percentage of about 54 wt%, obtained at 575 °C
426 and a catalyst weight of 5 g, whereas the OLP from PO exhibited a lower concentration of gasoline
427 aromatics, about 27 wt%, at 595 °C and a catalyst weight of 5 g. In addition, side products from both
428 PO and PT also were obtained, including an aqueous liquid, tar, coke, gases, and, more importantly,
429 char, which has been a major area of research interest, as it can be processed further for use as a
430 sorbent.

431 Overall, in assessing the conversion of PO and PT derived from rubberwood to generate gasoline
432 aromatics, the PT showed significant potential for use in producing gasoline, since it contained high
433 concentrations of BTEX components in the OLP. However, further research is needed to increase the
434 yield of gasoline aromatics and decrease the char formation.

435 436 **Acknowledgments**

437 This study was financially supported by the graduate school of Prince of Songkla University (No:
438 0919/2552). The authors also acknowledge the scientists of the scientific equipment center for
439 performing some of the tests reported in this paper.

440 441 **Reference**

442 [1] Lauri, Pekka, Petr Havlík, Georg Kindermann, Nicklas Forsell, Hannes Böttcher, and Michael
443 Obersteiner. Woody biomass energy potential in 2050. *Energy policy* 2014; 66: 19-31.

- 444 [2] Abbasi, Tasneem, and S. A. Abbasi. Biomass energy and the environmental impacts
445 associated with its production and utilization. *Renewable and Sustainable Energy Reviews*
446 2010; 14: 919-937.
- 447 [3] Fogassy, Gabriella, Nicolas Thegarid, Yves Schuurman, and Claude Mirodatos. From
448 biomass to bio-gasoline by FCC co-processing: effect of feed composition and catalyst
449 structure on product quality. *Energy & Environmental Science* 2011; 4: 5068-5076.
- 450 [4] Butler, Eoin, Ger Devlin, Dietrich Meier, and Kevin McDonnell. A review of recent
451 laboratory research and commercial developments in fast pyrolysis and upgrading. *Renewable*
452 *and Sustainable Energy Reviews* 2011; 15: 4171-4186.
- 453 [5] Bridgwater, Anthony V. Review of fast pyrolysis of biomass and product upgrading. *Biomass*
454 *and bioenergy* 2012; 38: 68-94.
- 455 [6] Jacobson, Kathlene, Kalpana C. Maheria, and Ajay Kumar Dalai. Bio-oil valorization: a
456 review. *Renewable and Sustainable Energy Reviews* 2013; 23: 91-106.
- 457 [7] Abnisa, Faisal, and Wan Mohd Ashri Wan Daud. A review on co-pyrolysis of biomass: an
458 optional technique to obtain a high-grade pyrolysis oil. *Energy Conversion and Management*
459 2014; 87: 71-85.
- 460 [8] Kanaujia, Pankaj K., Y. K. Sharma, M. O. Garg, Deependra Tripathi, and Raghuvir Singh.
461 Review of analytical strategies in the production and upgrading of bio-oils derived from
462 lignocellulosic biomass. *Journal of Analytical and Applied Pyrolysis* 2014; 105: 55-74.
- 463 [9] Graça, Inês, José M. Lopes, Henrique S. Cerqueira, and Maria F. Ribeiro. Bio-oils upgrading
464 for second generation biofuels. *Industrial & Engineering Chemistry Research* 2012; 52: 275-
465 287.
- 466 [10] De Miguel Mercader, Ferran, Michiel J. Groeneveld, Sascha RA Kersten, Christophe
467 Geantet, Guy Toussaint, Nico WJ Way, Colin J. Schaverien, and Kees JA Hogendoorn.
468 Hydrodeoxygenation of pyrolysis oil fractions: process understanding and quality
469 assessment through co-processing in refinery units. *Energy & Environmental Science* 2011;
470 4: 985-997.

- 471 [11] Mortensen, Peter Mølgaard, J-D. Grunwaldt, Peter Arendt Jensen, K. G. Knudsen, and Anker
472 Degn Jensen. A review of catalytic upgrading of bio-oil to engine fuels. *Applied Catalysis A:
473 General* 2011; 407: 1-19.
- 474 [12] Sharifzadeh, M., C. J. Richard, K. Liu, K. Hellgardt, D. Chadwick, and N. Shah. An
475 integrated process for biomass pyrolysis oil upgrading: A synergistic approach. *Biomass and
476 Bioenergy* 2015; 76: 108-117.
- 477 [13] Valle, Beatriz, Ana G. Gayubo, Ainhoa Alonso, Andrés T. Aguayo, and Javier Bilbao.
478 Hydrothermally stable HZSM-5 zeolite catalysts for the transformation of crude bio-oil into
479 hydrocarbons. *Applied Catalysis B: Environmental* 2010; 100: 318-327.
- 480 [14] Stephanidis, S., C. Nitsos, K. Kalogiannis, E. F. Iliopoulou, A. A. Lappas, and K. S.
481 Triantafyllidis. Catalytic upgrading of lignocellulosic biomass pyrolysis vapours: Effect of
482 hydrothermal pre-treatment of biomass. *Catalysis Today* 2011; 167: 37-45.
- 483 [15] Shun, Tan, Zhijun ZHANG, Sun Jianping, and W. A. N. G. Qingwen. Recent progress of
484 catalytic pyrolysis of biomass by HZSM-5. *Chinese Journal of Catalysis* 2013; 34: 641-650.
- 485 [16] Perego, Carlo, and Aldo Bosetti. Biomass to fuels: The role of zeolite and mesoporous
486 materials. *Microporous and Mesoporous Materials* 2011; 144: 28-39.
- 487 [17] Taarning, Esben, Christian M. Osmundsen, Xiaobo Yang, Bodil Voss, Simon I. Andersen,
488 and Claus H. Christensen. Zeolite-catalyzed biomass conversion to fuels and chemicals.
489 *Energy & Environmental Science* 2011; 4: 793-804.
- 490 [18] Rezaei, Pouya Sirous, Hoda Shafaghat, and Wan Mohd Ashri Wan Daud. Production of green
491 aromatics and olefins by catalytic cracking of oxygenate compounds derived from biomass
492 pyrolysis: A review. *Applied Catalysis A: General* 2014; 469: 490-511.
- 493 [19] Zhang, Zhaoxia, Peiyan Bi, Peiwen Jiang, Minghui Fan, Shumei Deng, Qi Zhai, and Quanxin
494 Li. Production of gasoline fraction from bio-oil under atmospheric conditions by an integrated
495 catalytic transformation process. *Energy* 2015; 90: 1922-1930.
- 496 [20] Zhang, Huiyan, Yu-Ting Cheng, Tushar P. Vispute, Rui Xiao, and George W. Huber.
497 Catalytic conversion of biomass-derived feedstocks into olefins and aromatics with ZSM-5:
498 the hydrogen to carbon effective ratio. *Energy & Environmental Science* 2011; 4: 2297-2307.

- 499 [21] Wang, Lu, Hanwu Lei, John Lee, Shulin Chen, Juming Tang, and Birgitte Ahring. Aromatic
500 hydrocarbons production from packed-bed catalysis coupled with microwave pyrolysis of
501 Douglas fir sawdust pellets. *RSC Advances* 2013; 3: 14609-14615.
- 502 [22] Wang, Shurong, Qinjie Cai, Xiangyu Wang, Li Zhang, Yurong Wang, and Zhongyang Luo.
503 Biogasoline production from the co-cracking of the distilled fraction of bio-oil and ethanol.
504 *Energy & Fuels* 2013; 28: 115-122.
- 505 [23] Bi, Peiyan, Yanni Yuan, Minghui Fan, Peiwen Jiang, Qi Zhai, and Quanxin Li. Production of
506 aromatics through current-enhanced catalytic conversion of bio-oil tar. *Bioresource*
507 *technology* 2013; 136: 222-229.
- 508 [24] Zhang, Min, Fernando LP Resende, and Alex Moutsoglou. Catalytic fast pyrolysis of aspen
509 lignin via Py-GC/MS. *Fuel* 2014; 116: 358-369.
- 510 [25] Shen, Dekui, Jing Zhao, Rui Xiao, and Sai Gu. Production of aromatic monomers from
511 catalytic pyrolysis of black-liquor lignin. *Journal of Analytical and Applied Pyrolysis* 2015;
512 111: 47-54.
- 513 [26] Phommexay, Phansamai, Chutamas Satasook, Paul Bates, Malcolm Pearch, and Sara
514 Bumrungsri. The impact of rubber plantations on the diversity and activity of understory
515 insectivorous bats in southern Thailand. *Biodiversity and Conservation* 2011; 20: 1441-1456.
- 516 [27] Prasertsan, S., and B. Sajjakulnukit. Biomass and biogas energy in Thailand: potential,
517 opportunity and barriers. *Renewable energy* 2006; 31: 599-610.
- 518 [28] Rahmat, Budy, Dwi Pangesti, Dedi Natawijaya, and Dedi Sufyadi. Generation of Wood-waste
519 Vinegar and its Effectiveness as a Plant Growth Regulator and Pest Insect Repellent.
520 *BioResources* 2014; 9: 6350-6360.
- 521 [29] Fagernäs, Leena, Eeva Kuoppala, Kari Tiilikkala, and Anja Oasmaa. Chemical composition
522 of birch wood slow pyrolysis products. *Energy & Fuels* 2012; 26: 1275-1283.
- 523 [30] Fagernäs, Leena, Eeva Kuoppala, and Pekka Simell. Polycyclic aromatic hydrocarbons in
524 birch wood slow pyrolysis products. *Energy & Fuels* 2012; 26: 6960-6970.
- 525 [31] Treacy, Michael MJ, and John B. Higgins. *Collection of Simulated XRD Powder Patterns for*
526 *Zeolites. Fifth Revised Edition. Elsevier* 2007.

- 527 [32] Ko, Chang Hyun, Sung Hoon Park, Jong-Ki Jeon, Dong Jin Suh, Kwang-Eun Jeong, and
528 Young-Kwon Park. Upgrading of biofuel by the catalytic deoxygenation of biomass. *Korean
529 Journal of Chemical Engineering* 2012; 29: 1657-1665.
- 530 [33] Aho, A., A. Tokarev, P. Backman, N. Kumar, K. Eränen, M. Hupa, B. Holmbom, T. Salmi,
531 and D. Yu Murzin. Catalytic pyrolysis of pine biomass over H-Beta zeolite in a dual-fluidized
532 bed reactor: effect of space velocity on the yield and composition of pyrolysis products.
533 *Topics in Catalysis* 2011; 54: 941-948.
- 534 [34] Güngör, Ahmet, Sermin Önenç, Suat Ucar, and Jale Yanik. Comparison between the “one-
535 step” and “two-step” catalytic pyrolysis of pine bark. *Journal of Analytical and Applied
536 Pyrolysis* 2012; 97: 39-48.
- 537 [35] Bulushev, Dmitri A., and Julian RH Ross. Catalysis for conversion of biomass to fuels via
538 pyrolysis and gasification: a review. *Catalysis Today* 2011; 171: 1-13.
- 539 [36] Mendes, Gisele, Helga G. Aleme, and Paulo JS Barbeira. Determination of octane numbers in
540 gasoline by distillation curves and partial least squares regression. *Fuel* 2012; 97: 131-136.
- 541 [37] Trinca, Luzia. *Designs and Analysis of Experiments, Volume 3: Special Designs and
542 Applications* edited by HINKELMANN, K. *Biometrics* 2012.
- 543 [38] Choi, Yong S., Kyong-Hwan Lee, Jing Zhang, Robert C. Brown, and Brent H. Shanks.
544 Manipulation of chemical species in bio-oil using in situ catalytic fast pyrolysis in both a
545 bench-scale fluidized bed pyrolyzer and micropyrolyzer. *Biomass and Bioenergy* 2015; 81:
546 256-264.
- 547 [39] Park, Hyun Ju, Jong-Ki Jeon, Dong Jin Suh, Young-Woong Suh, Hyeon Su Heo, and Young-
548 Kwon Park. Catalytic vapor cracking for improvement of bio-oil quality. *Catalysis surveys
549 from Asia* 2011; 15: 161-180.
- 550 [40] Kwon, Kyung C., Howard Mayfield, Ted Marolla, Bob Nichols, and Mike Mashburn.
551 Catalytic deoxygenation of liquid biomass for hydrocarbon fuels. *Renewable Energy* 2011;
552 36: 907-915.
- 553 [41] Wang, Shurong, Qinjie Cai, Junhao Chen, Li Zhang, Xiangyu Wang, and Chunjiang Yu.
554 Green aromatic hydrocarbon production from cocracking of a bio-oil model compound

- 555 mixture and ethanol over Ga₂O₃/HZSM-5. *Industrial & Engineering Chemistry Research*
556 2014; 53: 13935-13944.
- 557 [42] Gong, Feiyan, Zhi Yang, Chenggui Hong, Weiwei Huang, Shen Ning, Zhaoxia Zhang, Yong
558 Xu, and Quanxin Li. Selective conversion of bio-oil to light olefins: controlling catalytic
559 cracking for maximum olefins. *Bioresource technology* 2011; 102: 9247-9254.
- 560 [43] Mentzel, Uffe V., and Martin S. Holm. Utilization of biomass: Conversion of model
561 compounds to hydrocarbons over zeolite H-ZSM-5. *Applied Catalysis A: General* 2011; 396:
562 59-67.
- 563 [44] Zhu, Jiu-fang, Ji-cong Wang, and Quan-xin Li. Transformation of Bio-oil into BTX by Bio-
564 oil Catalytic Cracking. *Chinese Journal of Chemical Physics* 2013; 26: 477-483.
- 565 [45] Li, Xiangyu, Lu Su, Yujue Wang, Yanqing Yu, Chengwen Wang, Xiaoliang Li, and Zhihua
566 Wang. Catalytic fast pyrolysis of Kraft lignin with HZSM-5 zeolite for producing aromatic
567 hydrocarbons. *Frontiers of Environmental Science & Engineering* 2012; 6: 295-303.
- 568 [46] Cheng, Yu-Ting, and George W. Huber. Chemistry of furan conversion into aromatics and
569 olefins over HZSM-5: a model biomass conversion reaction. *ACS Catalysis* 2011; 1: 611-628.
- 570 [47] Zhao, Yan, Yao Fu, and Qing-Xiang Guo. Production of aromatic hydrocarbons through
571 catalytic pyrolysis of γ -valerolactone from biomass. *Bioresource technology* 2012; 114: 740-
572 744.
- 573 [48] Cheng, Yu-Ting, Jungho Jae, Jian Shi, Wei Fan, and George W. Huber. Production of
574 Renewable Aromatic Compounds by Catalytic Fast Pyrolysis of Lignocellulosic Biomass
575 with Bifunctional Ga/ZSM-5 Catalysts. *Angewandte Chemie* 2012; 124: 1416-1419.
- 576 [49] Wang, Shurong, Zuogang Guo, Qinjie Cai, and Long Guo. Catalytic conversion of carboxylic
577 acids in bio-oil for liquid hydrocarbons production. *Biomass and Bioenergy* 2012; 45: 138-
578 143.
- 579 [50] Mihalcik, David J., Charles A. Mullen, and Akwasi A. Boateng. Screening acidic zeolites for
580 catalytic fast pyrolysis of biomass and its components. *Journal of Analytical and Applied*
581 *Pyrolysis* 2011; 92: 224-232.

- 582 [51] Kim, Jae-Young, Jae Hoon Lee, Jeesu Park, Jeong Kwon Kim, Donghwan An, In Kyu Song,
583 and Joon Weon Choi. Catalytic pyrolysis of lignin over HZSM-5 catalysts: Effect of various
584 parameters on the production of aromatic hydrocarbon. *Journal of Analytical and Applied*
585 *Pyrolysis* 2015; 114: 273-280.
- 586 [52] Wang, Shurong, Qinjie Cai, Xiangyu Wang, Zuogang Guo, and Zhongyang Luo. Bio-gasoline
587 production from co-cracking of hydroxypropanone and ethanol. *Fuel Processing Technology*
588 2013; 111: 86-93.
- 589 [53] Ma, Zhiqiang, Ekaterina Troussard, and Jeroen A. van Bokhoven. Controlling the selectivity
590 to chemicals from lignin via catalytic fast pyrolysis. *Applied Catalysis A: General* 2012; 423:
591 130-136.
- 592 [54] Odedairo, T., and S. Al-Khattaf. Comparative study of zeolite catalyzed alkylation of benzene
593 with alcohols of different chain length: H-ZSM-5 versus mordenite. *Catalysis Today* 2013;
594 204: 73-84.
- 595 [55] Odedairo, T., and S. Al-Khattaf. Alkylation and transalkylation of alkylbenzenes in cymene
596 production over zeolite catalysts. *Chemical Engineering Journal* 2011; 167: 240-254.
- 597 [56] Swick, Derek, Andrew Jaques, J. C. Walker, and Herb Estreicher. Gasoline risk management:
598 A compendium of regulations, standards, and industry practices. *Regulatory Toxicology and*
599 *Pharmacology* 2014; 70: S80-S92.
- 600 [57] Keenan, J. J., S. Gaffney, S. A. Gross, C. J. Ronk, D. J. Paustenbach, D. Galbraith, and B. D.
601 Kerger. An evidence-based analysis of epidemiologic associations between lymphatic and
602 hematopoietic cancers and occupational exposure to gasoline. *Human & experimental*
603 *toxicology* 2013; 32: 1007-1027.

Appendix E

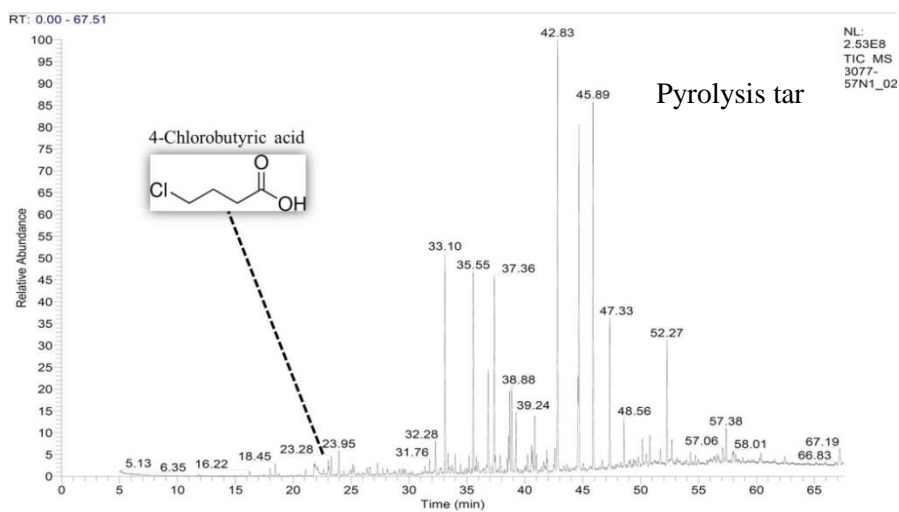
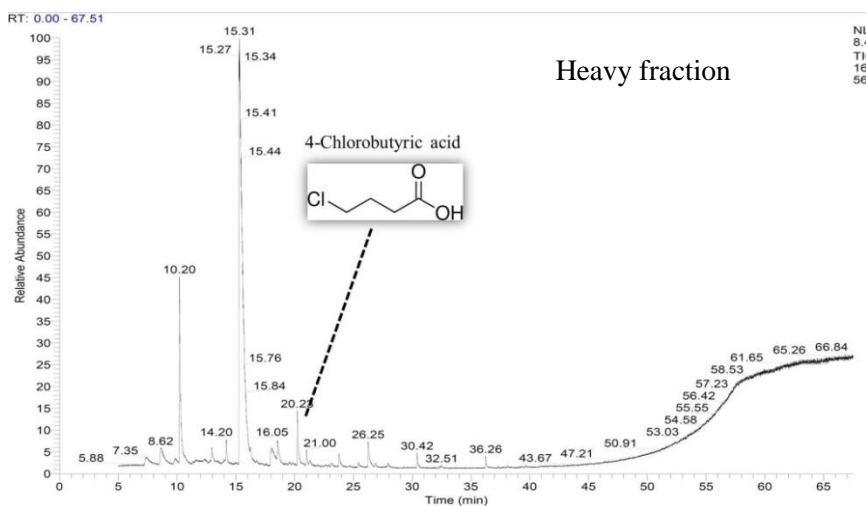
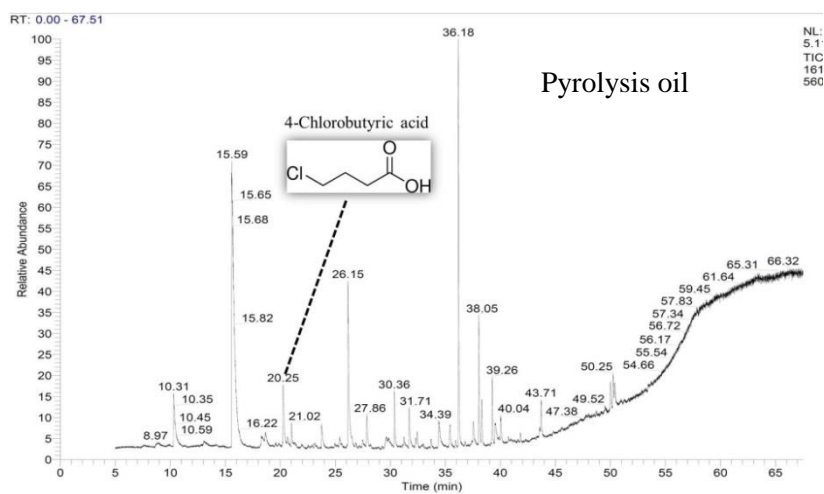
Research octane number (RON) and Motor octane number (MON) of pure compounds

Table 2. Various Lumps Considered in the Present Octane Model along with Their Pure-Component RONs and MONs

	RON	MON		RON	MON		RON	MON
Paraffins			Paraffins (cont'd.)			Aromatics (cont'd.)		
<i>n</i> -butane	94	89.6	<i>n</i> -undecane	-35	-35	C ₁₂ aromatics	102	90
isobutane	102	97.6	C ₁₁ monomethyl	5	5			
<i>n</i> -pentane	62	62.6	C ₁₁ dimethyls	35	35	Olefins/Cyclic Olefins		
<i>i</i> -pentane	92	90.3	C ₁₁ trimethyls	90	82	<i>n</i> -butenes	98.7	82.1
<i>n</i> -hexane	24.8	26	<i>n</i> -dodecane	-40	-40	<i>n</i> -pentenes	90	77.2
C ₆ monomethyls	76	73.9	C ₁₂ monomethyl	5	5	<i>i</i> -pentenes	103	82
2,2-dimethylbutane	91.8	93.4	C ₁₂ dimethyls	30	30	cyclopentene	93.3	69.7
2,3-dimethylbutane	105.8	94.3	C ₁₂ trimethyls	85	80	<i>n</i> -hexenes	90	80
<i>n</i> -heptane	0	0				<i>i</i> -hexenes	100	83
C ₇ monomethyls	52	52	Naphthenes			total C ₆ cyclic olefins	95	80
C ₇ dimethyls	93.76	90	cyclopentane	100	84.9	total C ₇ =	90	78
2,2,3-trimethylbutane	112.8	101.32	cyclohexane	82.5	77.2	total C ₈ =	90	77
<i>n</i> -octane	-15	-20	<i>m</i> -cyclopentane	91.3	80			
C ₈ monomethyls	25	32.3	C ₇ naphthenes	82.0	77	Oxygenates		
C ₈ dimethyls	69	74.5	C ₈ naphthenes	55	50	MTBE	115.2	97.2
C ₈ trimethyls	105	98.8	C ₉ naphthenes	35	30	TAME	115	98
<i>n</i> -nonane	-20	-20				EtOH	108	92.9
C ₉ monomethyls	15	22.3	Aromatics					
C ₉ dimethyls	50	60	benzene	102.7	105			
C ₉ trimethyls	100	93	toluene	118	103.5			
<i>n</i> -decane	-30	-30	C ₈ aromatics	112	105			
C ₁₀ monomethyls	10	10	C ₉ aromatics	110	101			
C ₁₀ dimethyls	40	40	C ₁₀ aromatics	109	98			
C ₁₀ trimethyls	95	87	C ₁₁ aromatics	105	94			

Appendix F

Chloride in the pyrolysis oil, tar and heavy fraction



Appendix G

Sherrer's equation used for estimating the crystal size

$$D = k \cdot \lambda / (\beta \cdot \cos \Theta)$$

D= the crystal size (nm), K= the crystal shape factor (0.9), Lambda =the wavelength of the X-ray (0.154059nm), Beta= the FWHM (The full-width-at-half- Maximum), Theta= the Bragg's angle.

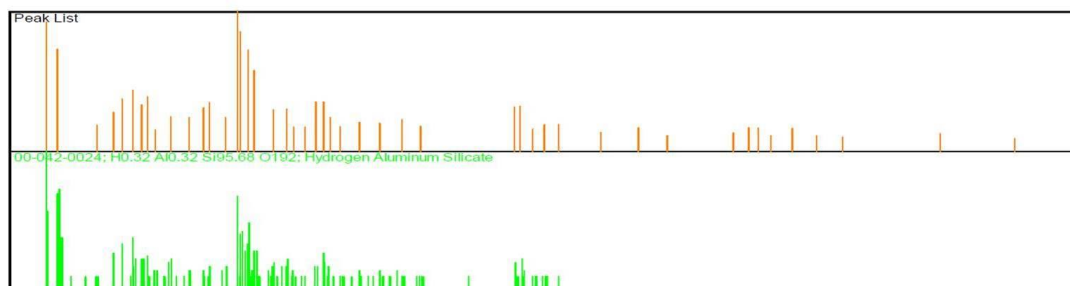
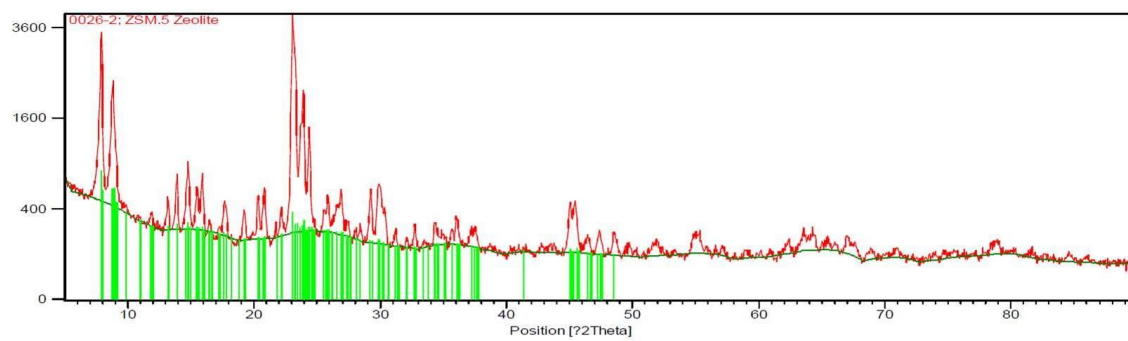
The values of FWHM (Beta) and Bragg's angle (Theta) were taken for the peaks in XRD patterns

1. Crystal size of the commercial catalyst

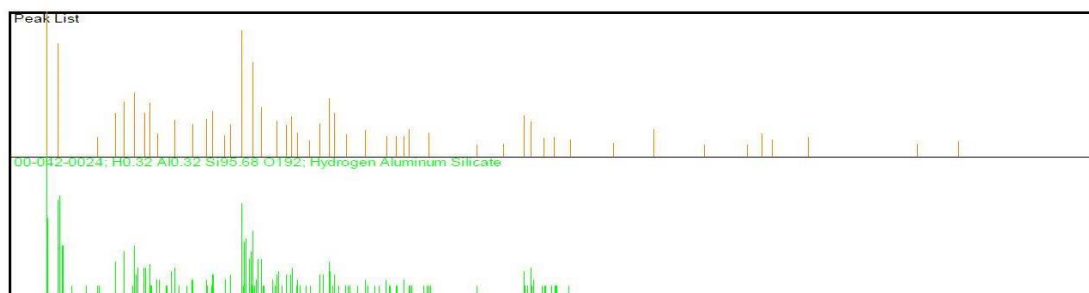
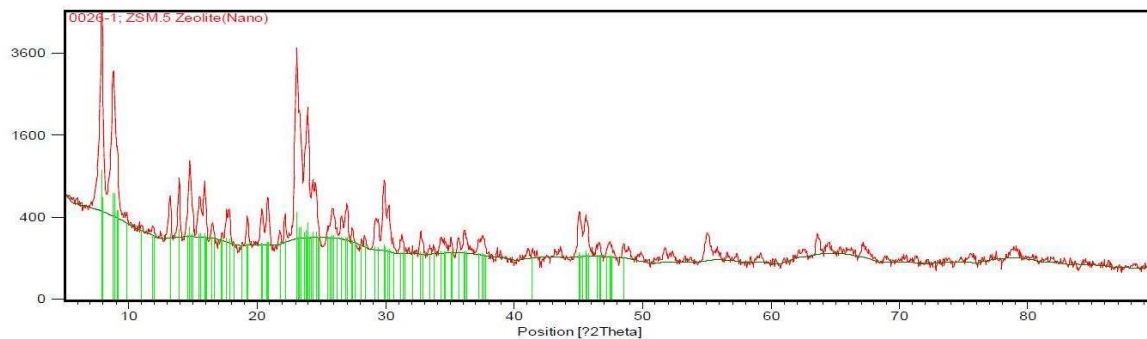
Sherrer' s Equation				
D = k*lambda/(beta * cos Theta)				
Peak 1	k	=	0.9	
	lambda	=	0.15406 nanometer	
	beta	=	0.1968 deg. 2 Theta ==>	0.0034 rad
	theta	=	23.0477 deg. 2 Theta ==>	0.2011 rad. Theta
	D1	=	41.2 nanometer	
Peak 2	k	=	0.9	
	lambda	=	0.15406 nanometer	
	beta	=	0.1476 deg. 2 Theta ==>	0.0026 rad
	theta	=	7.9162 deg. 2 Theta ==>	0.0691 rad. Theta
	D1	=	54.0 nanometer	
Peak 3	k	=	0.9	
	lambda	=	0.15406 nanometer	
	beta	=	0.0984 deg. 2 Theta ==>	0.0017 rad
	theta	=	23.2777 deg. 2 Theta ==>	0.2031 rad. Theta
	D1	=	82.4 nanometer	
Average of Crystal Size			59 nm	

2. Crystal size of the nano catalyst

Sherrer' s Equation				
D = k*lambda/(beta * cos Theta)				
Peak 1	k	=	0.9	
	lambda	=	0.1540598 nanometer	
	beta	=	0.1968 deg. 2 Theta ==>	0.0034 rad
	theta	=	7.9229 deg. 2 Theta ==>	0.0691 rad. Theta
	D1	=	40.5 nanometer	
Peak 2	k	=	0.9	
	lambda	=	0.1540598 nanometer	
	beta	=	0.1476 deg. 2 Theta ==>	0.0026 rad
	theta	=	23.0569 deg. 2 Theta ==>	0.2012 rad. Theta
	D1	=	54.9 nanometer	
Peak 3	k	=	0.9	
	lambda	=	0.1540598 nanometer	
	beta	=	0.1968 deg. 2 Theta ==>	0.0034 rad
	theta	=	8.81 deg. 2 Theta ==>	0.0769 rad. Theta
	D1	=	40.5 nanometer	
Average of Crystal Size			45 nm	



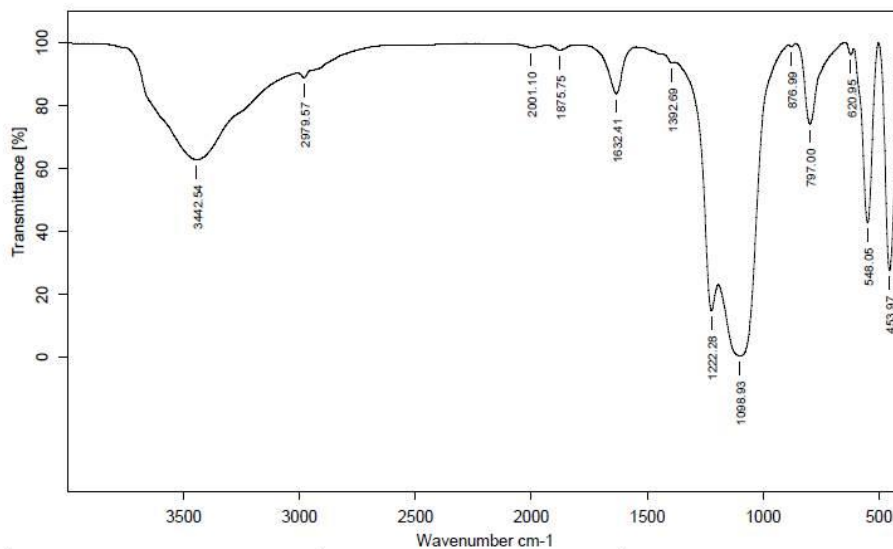
XRD pattern of HZSM-5 commercial catalyst



XRD pattern of HZSM-5 nano catalyst

Appendix H

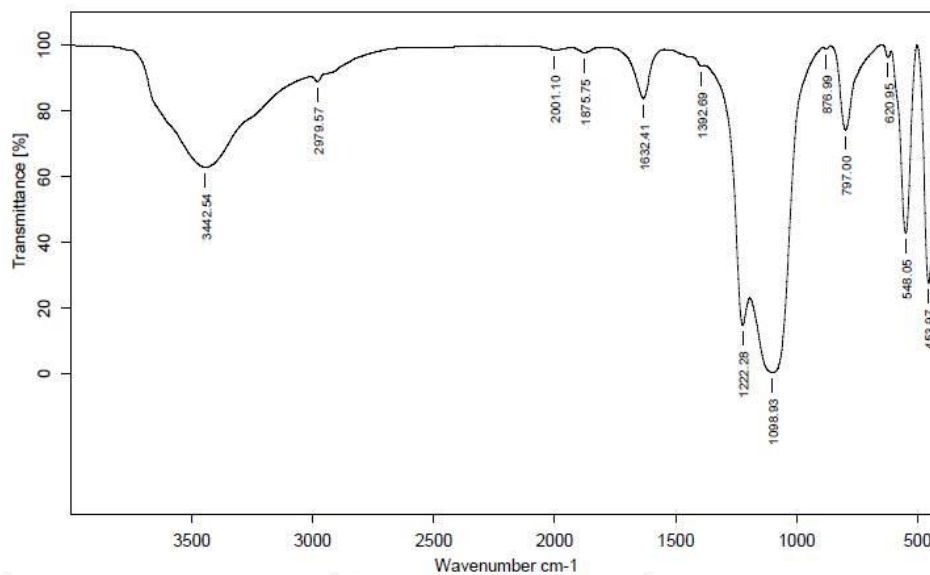
Fourier-Transform Infrared (FTIR)



Sample : H.ZSM.5		Frequency Range :4000-400 cm-1		Measured on : 30/01/2013	
File name:0426ABDULRAHIM	Resolution : 4	Instrument : EQUINOX55		Sample Scans : 32	
Customer :Abdulrahim	Zerofilling : 2	Acquisition Mode Double Sided,Forward-Backward			

FT-IR Spectroscopy

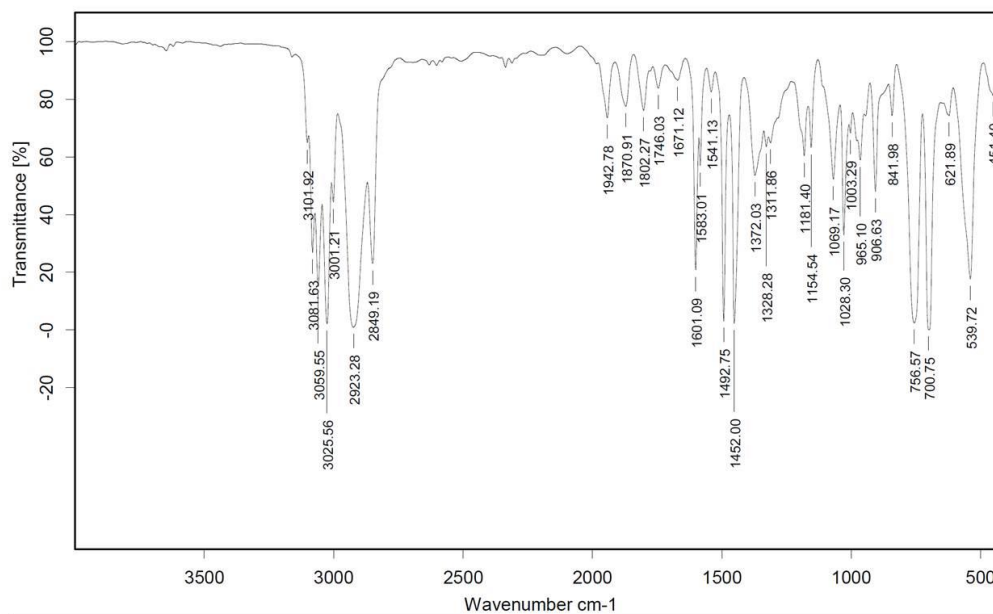
FT-IR spectra of pyridine adsorbed in a commercial HZSM-5 after pyridine adsorption and evacuation at 150 °C



Sample : H.ZSM.5		Frequency Range :4000-400 cm-1		Measured on : 30/01/2013	
File name:0426ABDULRAHIM	Resolution : 4	Instrument : EQUINOX55		Sample Scans : 32	
Customer :Abdulrahim	Zerofilling : 2	Acquisition Mode Double Sided,Forward-Backward			

FT-IR Spectroscopy

FT-IR spectra of pyridine adsorbed in a nanocrystalline HZSM-5 after pyridine adsorption and evacuation at 150 °C



Sample : std. PS	Frequency Range : 4000-400 cm-1	Measured on : 30/01/2013
File name:0426ABDULRAHIM	Resolution : 4	Instrument : EQUINOX55
Customer :Abdulrahim	Zerofilling : 2	Sample Scans : 32
Acquisition Mode Double Sided,Forward-Backward		

FT-IR Spectroscopy

Wavenumber Standards for FFT-IR Spectrometry

Appendix I

GC-FID analysis

GC-FID was used for identifying the chemical compositions of OLPs. The GC (Trace GC Ultra/ISQMST) equipped with a capillary column of 30 m long \times 0.25 mm \times 0.25 μ m film thickness. The temperature of oven was kept at 35 °C for 5 min. It was set to raise from 35 to 245 °C at a 4 °C/min rate.

Sample calculation for wt % of compounds

wt% calculation for the benzene formed in the OLP from pyrolysis oil at the optimum condition

1 μ l of the sample = 0.001 ml (density = 0.8 g/ mL)

0.001 ml * 0.8 g/ml = 0.0008 g = **0.8 mg**

From calibration curve, 16768.9 (Benzene Area) = 12469.64 ppm.

12469.64 ppm = 12469.64 mg/ L

12469.64 mg: 1000 ml

X mg : 0.001 ml

(X mg) Weight of benzene equivalent to 0.001 = 0.001 ml * 12469.64/1000

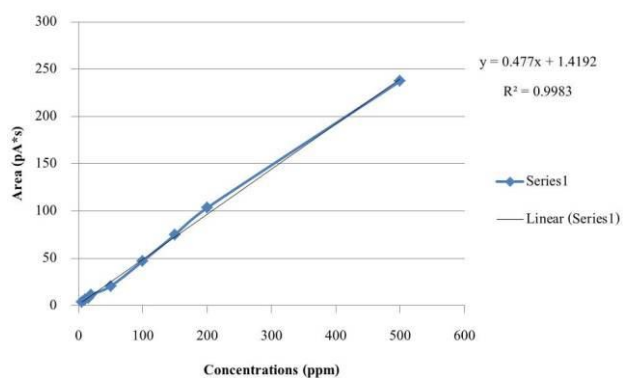
(X mg) Weight of benzene equivalent to 0.001 = 0.01246964 mg

wt% = 0.01246964 mg/ 0.8 mg *100= 1.558705 %

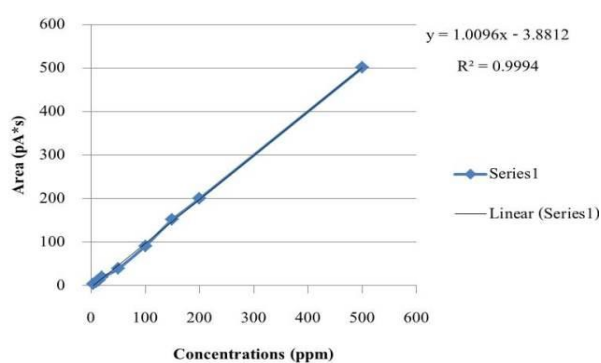
Dilution factor = 4.95

wt% =1.558705 %* 4.96 = 7.73 wt%

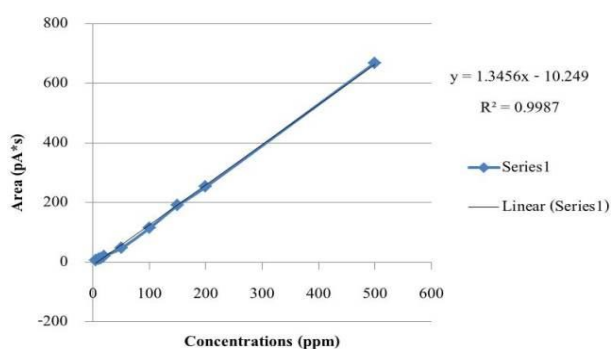
Pentene Calibration Curve



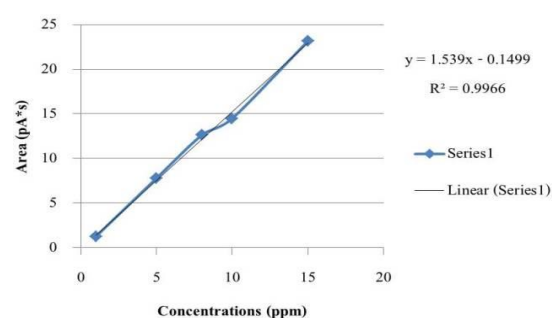
Isooctane Calibration Curve



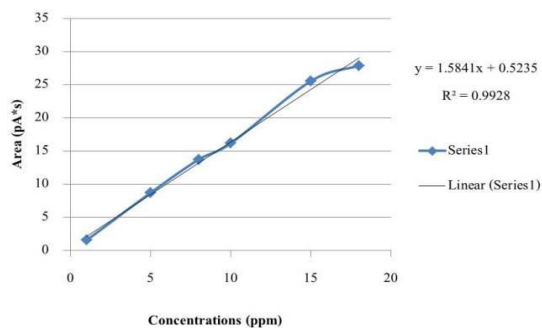
Benzene Calibration Curve



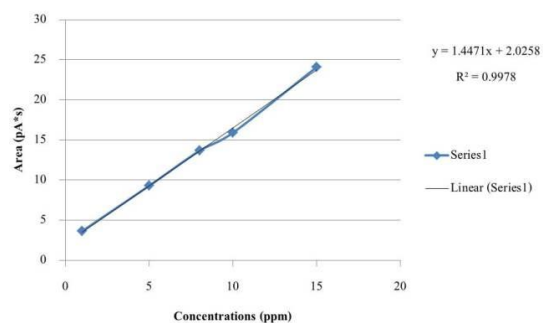
Touene Calibration Curve



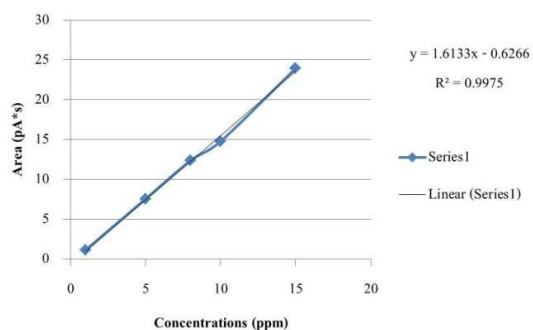
Ethylbenzene Calibration Curve



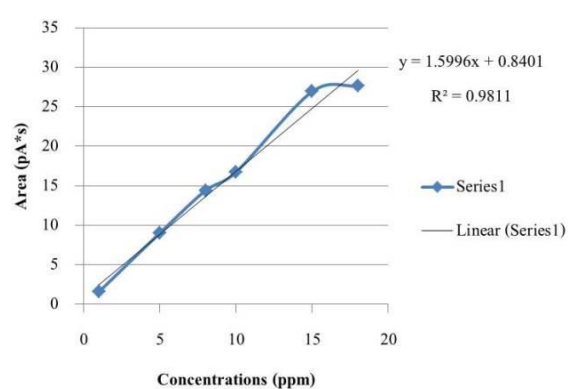
p-xylene Calibration Curve



m-xylene Calibration Curve



o-xylene Calibration Curve

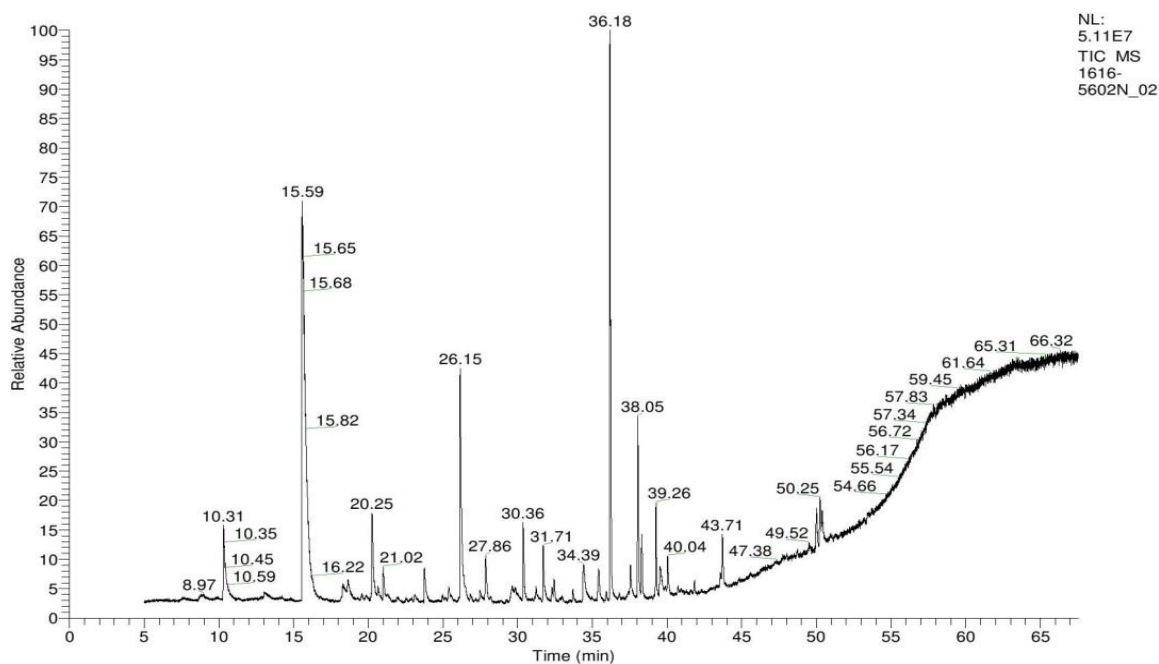


Appendix J

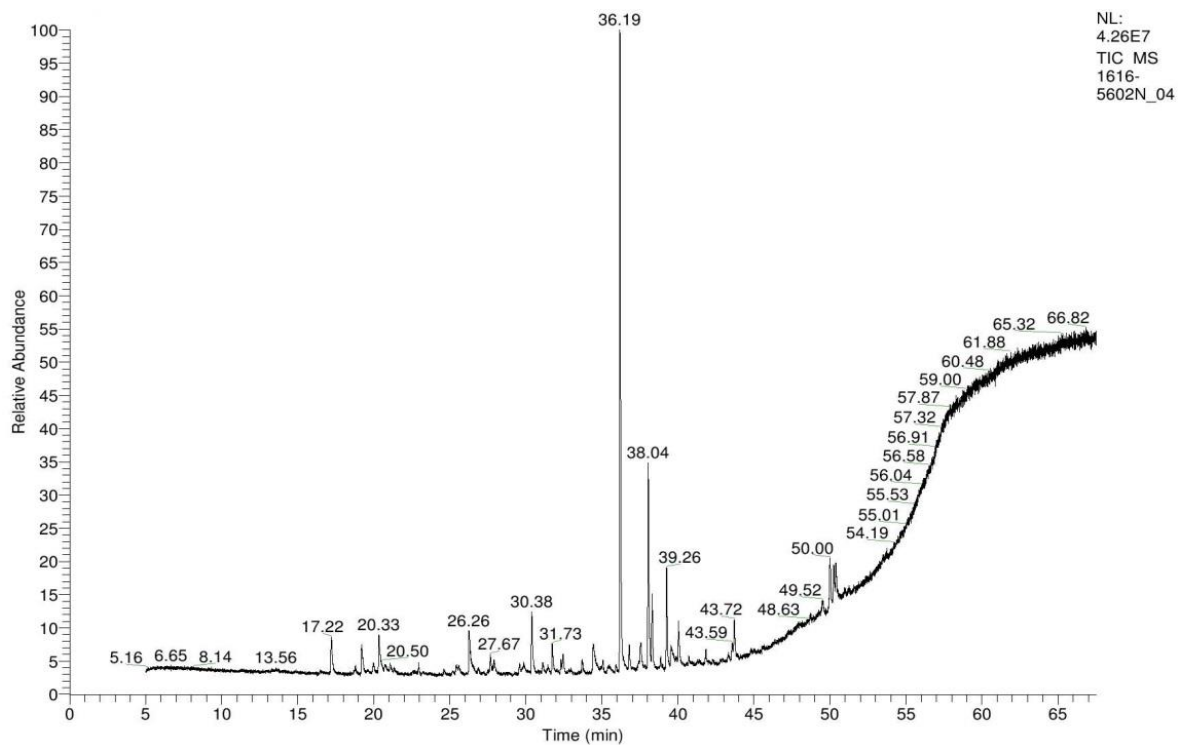
GC-MS analyses

Identification of chemical compounds of the three fractions before and after upgrading

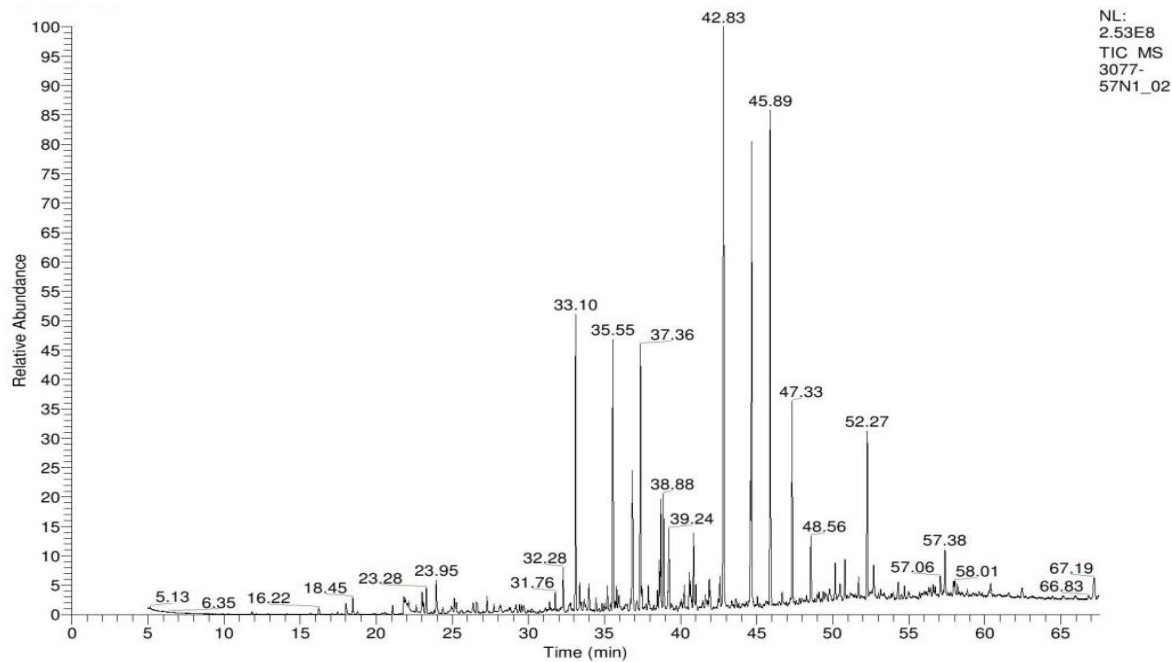
The compounds in the pyrolysis liquid and its fractions were identified with a Trace GC Ultra/ISQMST equipped with a capillary column of 30 m long \times 0.25 mm \times 0.25 μ m film thickness. The oven temperature was programmed to increase from 35 to 245 $^{\circ}$ C. The data were acquired with Xcalibur software using the Wiley mass spectra library's.



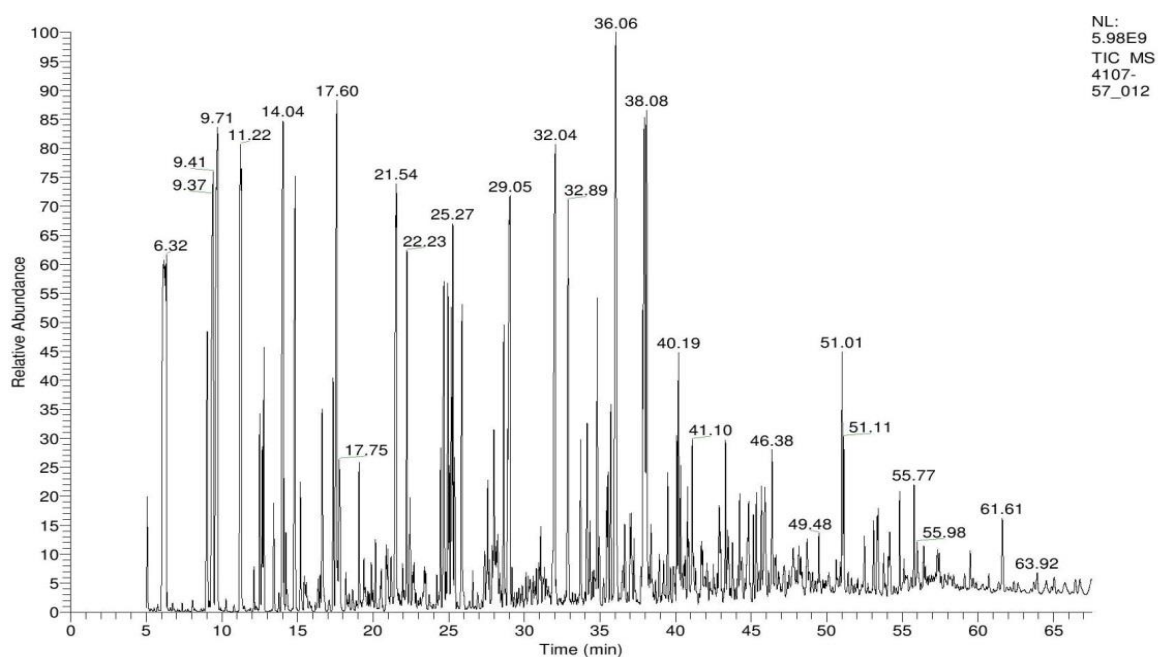
GC/MS chromatogram of pyrolysis oil



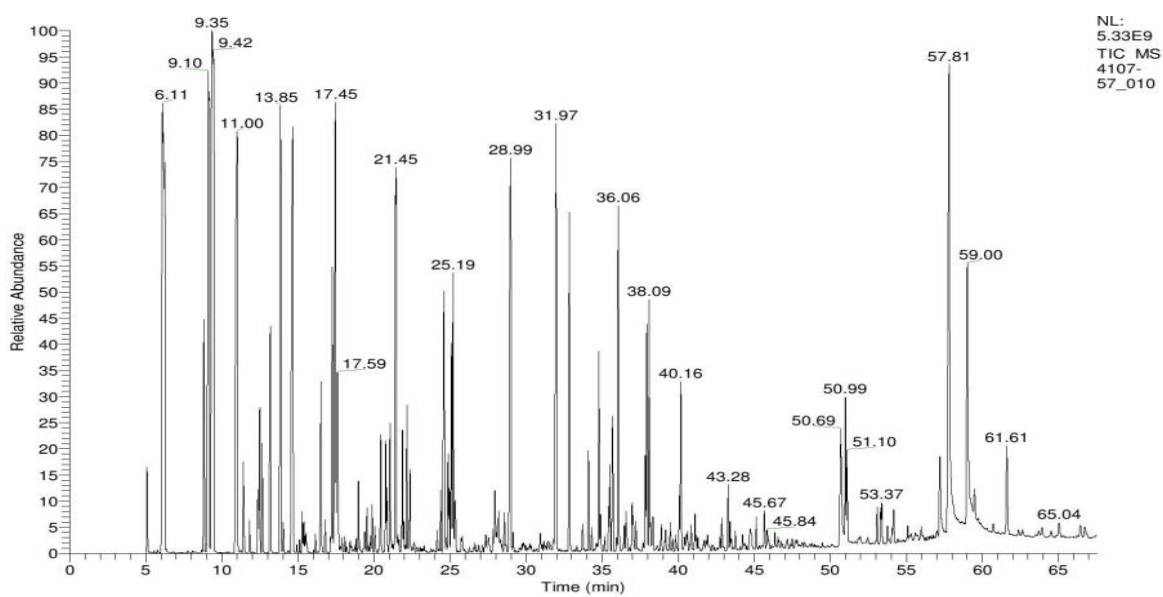
GC/MS chromatogram of heavy fraction



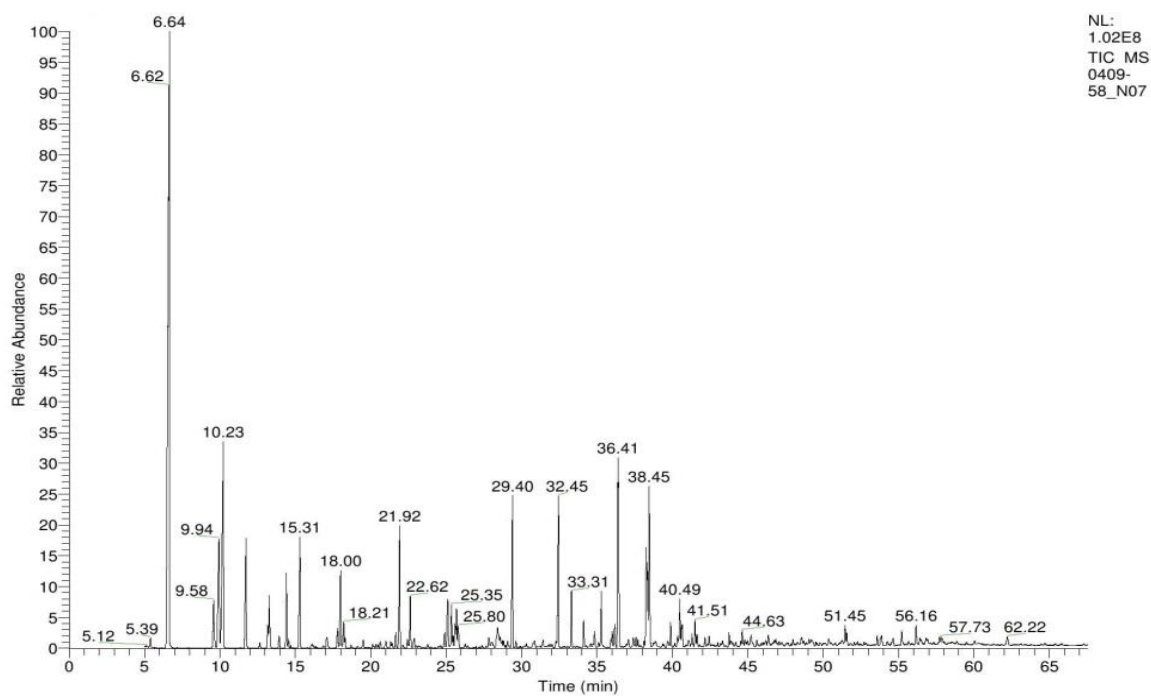
GC/MS chromatogram of pyrolysis tar



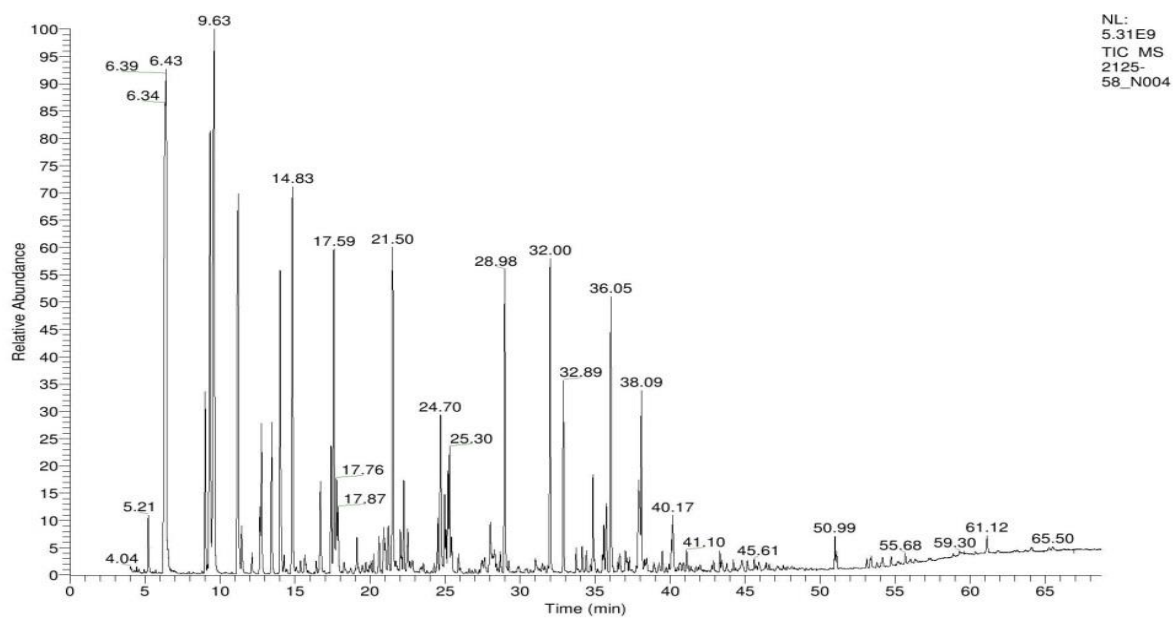
GC/MS chromatogram of OLP from pyrolysis oi using commercial catalyst



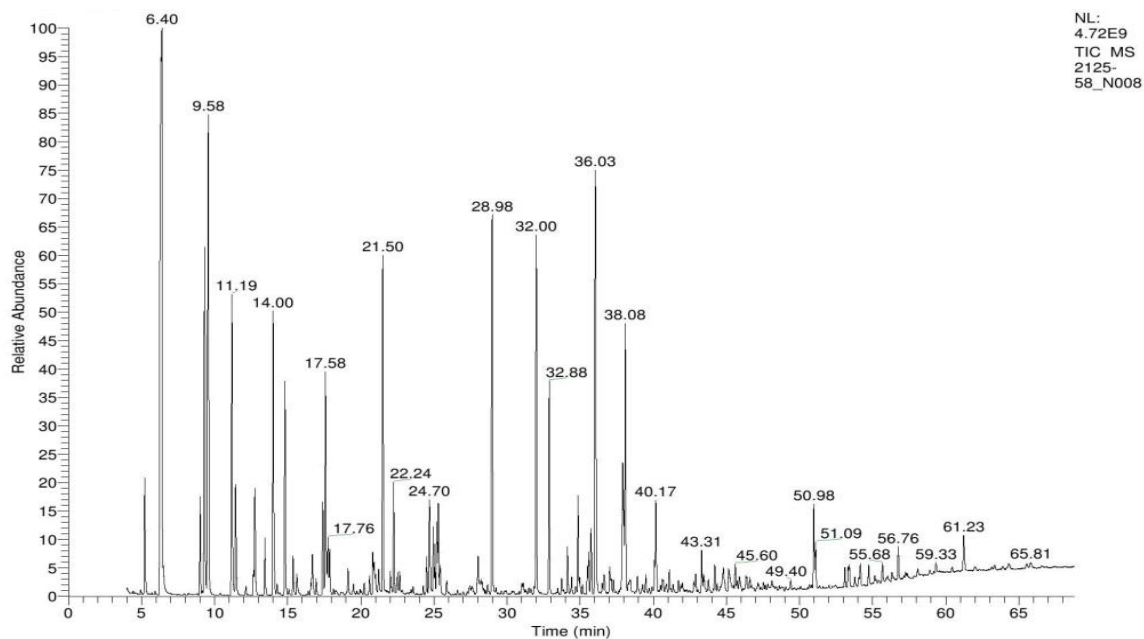
GC/MS chromatogram of OLP from heavy fraction using commercial catalyst



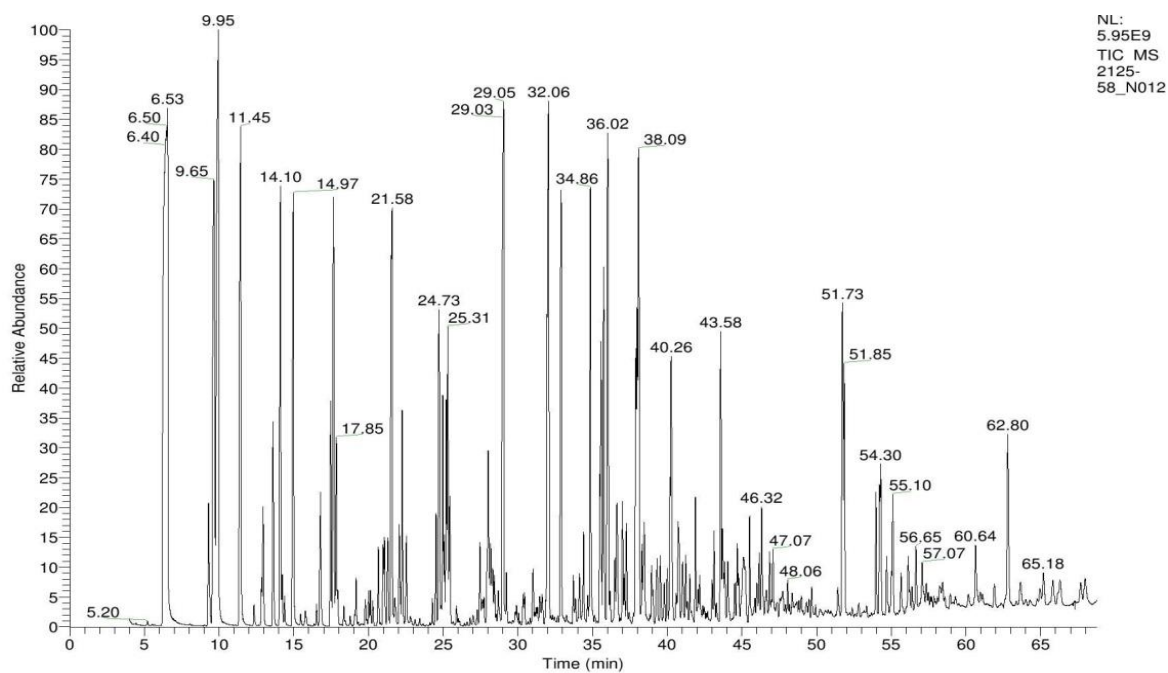
GC/MS chromatogram of OLP from pyrolysis tar using commercial catalyst



GC/MS chromatogram of OLP from pyrolysis oi using nano catalyst



GC/MS chromatogram of OLP from heavy fraction using com nanao merical catalyst



GC/MS chromatogram of OLP from pyrolysis tar using nono catalyst

Appendix K

CHN-O analyses

Test equipment: CHN-O analyser, CE instruments Flash EA 1112 Series, Thermo Quest, Italy.

Test technique: Dynamic Flash Combustion

Test condition:

For C H N			
Left furnace temperature	900 °C	Oven temperature	65 °C
Carrier flow	130 mL/ min	Reference flow	100 mL/min
Oxygen flow	250 mL/min		
For oxygen			
Right furnace temperature	1060 °C	Oven temperature	65 °C
Carrier flow	130 mL/min	Reference flow	100 mL/min

CHN-O analysis

1. For pyrolysis oil, heavy fraction and tar before upgrading

Elements %	Pyrolysis oil	Heavy fraction	Tar
N	1.26	0.90	2.24
C	47.37	59.95	51.16
H	5.78	5.80	5.67
O	23.58	22.25	14.26

2. For pyrolysis oil, heavy fraction and tar before upgrading (with commercial zeolite)

Elements %	Pyrolysis oil	Heavy fraction	Tar
N	0.93	0.46	Nil
C	42.68	22.40	70.72
H	4.84	1.79	5.79
O	15.77	16.31	5.30

3. For pyrolysis oil, heavy fraction and tar before upgrading (with nano zeolite)

Elements %	Pyrolysis oil	Heavy fraction	Tar
N	0.24	0.28	0.08
C	35.33	16.07	42.48
H	3.06	4.51	7.5
O	2.06	4.74	3.96

VITAE

Name Abdulrahim Khaled Saad
Student ID 5410130029
Educational Attainment

Degree	Name of Institution	Year of Graduation
B. Sc. In Chemical Technology	Al-Neelain University	2003
M. Sc. In Chemical Engineering	University of Gezira	2006

Scholarship Awards during Enrolment

Graduate School Scholarship, Graduate School, Prince of Songkla University, 2011-2014

Financial Support for Thesis, Graduate School, prince of Songkla University, 2013

Work – Position and Address (If Possible)

Researcher, Department of Chemical Industries. Industrial Research & Consultancy Center (IRCC). Ministry of Science & Technology. Sudan

List of Publication and Proceeding (If Possible)

Abdulrahim Saad, Sukritthira Ratanawilai. "Characterisation of liquid derived from pyrolysis process of charcoal production in south of Thailand." Iranica Journal of Energy and Environment, 2014, 5(2):184-191.

Abdulrahim Saad, Sukritthira Ratanawilai, and Chakrit Tongurai. "Catalytic Cracking of Pyrolysis Oil Derived from Rubberwood to Produce Green Gasoline Components." BioResources, 2015, 10 (2): 3224-3241.

Abdulrahim Saad, Sukritthira Ratanawilai, and Chakrit Tongurai. "Catalytic Conversion of Pyrolysis Tar to Produce Green Gasoline-range Aromatics." Energy

Procedia, 2015, 79: 471–479. International Conference on Alternative Energy in Developing Countries and Emerging Economies-May 2015.

Abdulrahim Saad, Sukritthira Ratanawilai, and Chakrit Tongurai. "Comparative Study for Catalytic Conversion of Pyrolysis Oil and Tar Derived from Rubberwood to Produce Green Gasoline-Range Aromatics." This manuscript has been submitted to the journal of "Biomass and Bioenergy", Elsevier.